EUROPEAN COMMISSION

Community Research

RAPHAEL

Contract Number: 516508 (FI6O)

European Data on HTR Fuel Characterization

(Deliverable D-BF1.2)

Authors : **K. Verfondern, FZJ**
in cooperation with P. Pohl, AVR GmbH

With the contribution from CEA (D. Roudil, C. Jegou, P. Bros)

Date of issue of this report : May 2007

Start date of project : **15/04/2005** Duration : **48 Months**

Project co-funded by the European Commission under the Euratom Research and Training Programme on Nuclear Energy within the Sixth Framework Programme (2002-2006)		
Dissemination Level		
PU	Public	
RE	Restricted to the partners of the RAPHAEL project	**X**
CO	Confidential, only for specific distribution list defined on this document	

Distribution list

Person and organisation name and/or group	Comments
E. BOGUSH (AREVA NP)	RAPHAEL-IP Organisation
B. CARLUEC (AREVA NP)	RAPHAEL-IP Organisation
W. VON LENZA (FZJ)	SP Leader
K. VERFONDERN (FZJ)	WP Contact , Task Leader
P. BROS (CEA)	WP Leader, Co-Author
J. FACHINGER (FZJ)	WP Contact
D. MILLINGTON (NNC)	WP Contact , Co-Author
P. VAN ISEGHEM (SCK – CEN)	WP Contact, Co-Author
F. CELLIER (AREVA NP)	WP Contact
T. ABRAM (BNFL)	WP Contact
D. ROUDIL (CEA)	WP Contact, Co-Author
C. JEGOU (CEA)	WP Contact, Co-Author
A. SNEYERS (SCK – CEN)	WP Contact
M.H. MOULINEY (AREVA NC)	WP Contact
H. BRÜCHER (FZJ)	WP Contact
V. CHAUVET (LGI)	PM

ReActor for Process heat, Hydrogen And ELectricity generation (RAPHAEL)		
Sub-project: SP-BF **Work package:** 1	**RAPHAEL document no:** RAPHAEL-0705-D-BF1.2	**Document type:** Deliverable
Issued by: FZJ **Internal no.:** VIP 0603-D-BF1.2-b		**Document status:** Final

Document title

European Data on HTR Fuel Characterization

Executive summary

Two High-Temperature Gas-Cooled Reactors were operated in Germany, the AVR in Jülich from 1967-1988 and the THTR-300 in Hamm-Uentrop from 1983-1988. The report describes the design of the spherical fuel element and the management of the spent fuel of these reactors. The reactor operation was accompanied by a comprehensive fuel development and qualification program, where the AVR served as test bed for mass fuel testing. It was completed by extensive postirradiation examination work. The total spent fuel from the two German HTGRs amounts to approximately 910,000 spheres with 32 % being from the AVR and 68 % from the THTR-300. The total activities for the year 2003 amount to $7.5*10^{16}$ Bq for the spent AVR fuel and $1.1*10^{17}$ Bq for the spent THTR fuel. The corresponding decay heat production is 6.2 kWt from all AVR fuel and 8.4 kWt from all THTR fuel. The final section describes studies conducted in the past and still on-going work which is related to the final disposal of German spent HTGR fuel.

French, Belgium and UK data complete this report.

Revisions

Rev.	Date	Short description	Author	WP Leader	SP Leader	Coordinator
00	01.03.2006	First issue	K. Verfondern FZJ	P. Bros CEA	W. von Lensa FZJ	E. Bogusch Areva NP
01	15.05.2007	Second issue	K. Verfondern FZJ	P. Bros CEA	W. von Lensa FZJ	E. Bogusch Areva NP

TABLE OF CONTENTS

LIST OF FIGURES

LIST OF TABLES

1 CONCEPTS OF HTGR SPENT FUEL TREATMENT IN EUROPE

From the worldwide seven High Temperature Gas-Cooled Reactors (HTGR) that have been or are being operated, three are located in Europe. The world's first HTGR was the Dragon Reactor Experiment (DRE) in Winfrith, UK, a joint project of the OECD countries. The other two European HTGRs were the AVR reactor in Jülich and the THTR-300 reactor in Hamm-Uentrop, both located in Germany.

Fabrication of particle fuel for these reactors on a larger scale was basically done in and by the respective countries. On the other hand, within the frame of R&D programs, fuel fabrication was also carried out in various other European countries, often crossing the borderlines to other countries, in insignificant amounts though. This was usually for testing and post-examination purposes within fuel qualification programs in other European (and US) nuclear research and irradiation facilities including those in Austria, Belgium, France, Germany, Italy, the Netherlands, Sweden, Switzerland, and the UK. This particular fuel, however, was mainly brought back to its origin countries after testing or mixed and stored together with other national radioactive waste.

There are various approaches in the European countries to deal with the spent fuel of HTGRs defined by the respective national standards and codes and, in principle, based upon the international set of guidelines issued by the IAEA. For the further management of the waste inventories (classification, disposal routes, etc.), the radiological characteristics and thermal output of the conditioned waste are decisive.

1.1 HTGR Spent Fuel in Belgium

In Belgium, the CEN/SCL and Belgonucleaire have studied in the past coated particle fuel to be used in LWRs, HTGRs, or fast reactors, mainly with regard to plutonium recycling. The work on HTGR fuel kernel production was carried out for the Dragon Reactor Experiment dealing with the preliminary production of UO_2 and $(U,Pu)O_2$ (containing up to 35 % PuO_2) particle kernels.

Late 1970s irradiation campaign of fuel needles in the GSB circuit in BR2 in cooperation with KFA.

Irradiation of coated particles in the MOPS series (MOI Particles Swept). Coated particles in graphite cylinders (20 mm dia., x mm long) were irradiated at 1200°C in the BR2 with measurement of fission product release.

In Belgium, spent HTGR fuel does not exist in significant quantities. But if it were existing, it would be classified as C waste (substantial amounts of beta and alpha emitters, heat production > 20 W/m^3) and it would be subjected to direct disposal.

1.2 HTGR Spent Fuel in France

In France, the CEA has carried out studies on HTGR particle fuel between 1968-1979 [Millet 2001, Chapelot 2001], mainly in collaboration with foreign partners (General Atomic, Dragon project, KFA – Jülich). This experience covers fuel technology [Millet 2001, Eichenbaum 2001], systems [Millet 2001], materials [Millet 2001] and reactor physics [Morier 1972, Marin 2000]. An extensive irradiation program was conducted in the SILOE, PEGASE, RAPSODIE and OSIRIS reactors to qualify the fuels fabricated by the CEA. About 50 million particles (free or in compacts and fuel blocks) were tested with online analysis and post-irradiation examinations. Studies on CEA fuels were also performed to examine fission product release or migration into the graphite matrix. These studies included experimental irradiation of uncoated kernels or defective particles in the PEGASE and SILOE reactors to determine the contamination induced on structural elements in the reactor, and its evolution in the case of gas flow variations using the irradiation facilities OSIRIS (Saclay), SILOE and SILOETTE (Grenoble), PEGASE, PEGGY, MARIUS, CESAR, RAPSODIE (Cadarache). Fuels used were high-enriched uranium-thorium including also fissile UCO and fertile ThO_2 particles.

Also France has no HTGR spent fuel and there are also no definite disposal solutions for certain categories of waste. Former activities with HTGR fuel were related to irradiation testing. With regard to the Very High Temperature Reactor (VHTR), R&D activities have been resumed recently with the goals to establish an industrial manufacturing process of coated particle fuel and to qualify it for VHTR relevant conditions. A first lab-scale fabrication facility for coated particles, GAIA, started operation in 2005 [Fonquernie 2004].

1.3 HTGR Spent Fuel in Germany

Since the end of the 1970s, the HTGR fuel strategy in Germany was guided by the need to meet non-proliferation aspects and to find a convincing publicly accepted spent fuel concept. The German reference spherical fuel element with its safety related properties has many positive features, which are effective not only during normal operation and during accidents, but also under conditions of intermediate storage and final disposal :

- Efficient use of uranium and in-situ generated plutonium in LEU fuel due to high burnup ;
- Isotopic composition of the spent fuel which is non-proliferation friendly ;
- TRISO coating of the fuel particles provides an effective long-term barrier against fission product transport and reduces the need for additional barriers ;
- Due to the low power density of the fuel, passive air cooling systems are sufficient from the beginning of intermediate storage ;
- Disposal techniques developed for medium active waste can be applied to spent HTGR fuel ;
- Homogeneous graphite matrix minimizes any spent fuel conditioning effort ;
- Corrosion resistance of both matrix graphite and particle coatings against repository relevant salt brines allows simple fuel disposal packaging concept ;

- Due to the small fuel sphere dimensions, small and easy-to-handle equipment can be used in intermediate and final storage.

For these reasons, the concept for HTGR spent fuel treatment, which was selected in January 1985, is presently the only accepted method of spent fuel management in Germany involving the two steps of :

1. intermediate dry storage in appropriate containers and facilities, and
2. transfer to a deep-mined salt dome repository for final disposal utilizing techniques of treatment similar to heat generating medium active waste.

But also an alternative option to the bore hole storage is in discussion: the storage in POLLUX containers for direct disposal.

In Germany, two high temperature reactors were operated, the AVR test reactor in Jülich and the prototype reactor THTR-300 in Hamm-Uentrop. Both were shut down in the meantime with all fuel removed from the reactor cores.

High burnup and high fast neutron fluence may have impact on the retention capability of the particle coatings. High burnup leads to kernel swelling and high inner gas pressures. A high fast neutron fluence leads to lattice damage in the coatings.

1.4 HTGR Spent Fuel in the UK

The United Kingdom has experience of the defueling and decommissioning of existing HTR waste due to operation of the Dragon Reactor Experiment (DRE). Dragon was the pioneering experimental reactor of the OECD High Temperature Reactor Project and was situated at Winfrith in the UK. The reactor was designed and built as a fuel and materials test facility and was the world's first high temperature reactor.

The UK scheme does not preempt the disposal route and relies on additional site-based conditions for acceptance.

2 MANAGEMENT OF SPENT HTGR FUEL

2.1 Spent Fuel from the AVR

2.1.1 Decommissioning of the AVR

The construction of the 46 MWt AVR reactor in Jülich was started in 1959. It obtained first criticality in August 1966 and began operation end of 1967. During the 21 years of operation with a time utilization factor average of 67.2 %, a thermal power production of 5117 GWh, and a

delivery of 1670 GWh of electricity were achieved. In the 1970s, the focus was on demonstrating reactor operation with the best ever time availability of 92 % in 1976. In the 1980s, the focus turned to more experiments designed and conducted by AVR and FZJ in cooperation with the German nuclear industry and various foreign partners. At the end of 1988, the reactor was permanently shut down. Application for the license for decommissioning was submitted in December 1987. Until the license was granted, the reactor was held at "zero-power operation".

Safestore decommissioning of the AVR began in 1994. It was split into two phases [Marnet 1997]:

1. Defueling of the reactor, dismantling of plant systems outside the reactor building;

2. Dismantling of components, alteration of components, installation and operation of new facilities for the state of safe enclosure as well as operation in the state of safe enclosure.

Originally a strategy for a complete removal was investigated consisting of a step-by-step dismantling, which allowed the plant to be transferred into a configuration of safe enclosure after either step [Marnet 1997].

In 2003, the AVR GmbH was taken over by the "Energiewerke Nord" (EWN) in Lubmin, Germany, and the decommissioning strategy was changed. In an agreement between the Federal Government and the State of NRW, it was decided to not only have a safe enclosure of the AVR reactor, but to have the site returned to green-field status by the year 2012. The plan is to lift the grouted reactor pressure vessel including all internals with a weight of some 2000 t as a whole out of the reactor building and store it in a separate building. The fuel is stored in CASTOR casks at an interim dry storage facility at FZJ.

2.1.2 AVR Fuel

The AVR was primarily used to test the HTGR concept, the fuel, and the components. Fueling of the first core loading started on July 14, 1966, with about 30,000 first core fuel elements, 70,000 moderator (graphite) balls, and 3000 absorber balls. In sum, more than 290,000 spherical fuel elements of 5 different types and 15 variants (carbide/oxide, BISO/TRISO, HEU/LEU) (see Tables 1 to 4 and Figs. 1 and 2) with more than 6 billion coated fuel particles plus about 80,000 graphite (moderator) balls were inserted into the core. Fuel element design also changed soon with reload charge 3 from machined graphite shells to pressed matrix materials (see Fig. 1).

Using high enriched mixed carbide/oxide fuel at the beginning, the reactor core was, since mid 1982, gradually converted to low enriched fuel. By the end of operation, a total of 2.4 million spheres were recycled in the core, some 180,400 fuel elements were removed from the core. Operating elements inserted to the core were distinguished between fuel elements, graphite moderator spheres, and boron spheres. From October 1971, boron and graphite spheres were no longer distinguished. The detailed fuel composition of the reactor core is indicated in Fig. 2. The composition of the reactor inventory of totally ~110,000 fuel spheres remaining in the reactor at the end of operation was about 50 % of HEU and 50 % LEU fuel [Pohl 2001].

Table 1: Fuel elements inserted in the AVR reactor [Pohl 2002]

Fuel variant	Reload charge number	Begin insertion	Number of fuel elements	Fuel kernel	Kernel diameter [µm]	U-235 enrichm. [%]	Fuel Composition			Coating	No. of cp per sphere
							U-235	U_{tot}	Th		
UCC	0	Jul 1966	30,155	$(Th,U)C_2$	200	93.0	1.00	1.075	4.87	HTI BISO	171,000
T	1-1	Oct 1968	4550	$(Th,U)C_2$	400	93.1	1.00	1.074	4.96	HTI BISO	23,700
	1-2	Aug 1973	2954								
GK	3	Apr 1969	17,770	$(Th,U)C_2$	400	93.0	1.00	1.075	4.94	HTI BISO	23,700
	4	Jul 1970	6210								
	5-1	Nov 1970	26,814								
GO-1	5-2	Dec 1971	39,662	$(Th,U)O_2$	400	92.3	1.00	1.083	4.96	HTI BISO	20,800
	7	Jan 1973									
	6-1	Oct 1973									
	12	Mar 1976	11,325								
	14	Nov 1976	9930								
GO-2	15	Feb 1981	6083	$(Th,U)O_2$	500	93.0	1.00	1.075	5	LTI TRISO	
	20	Oct 1985	11,850								
GO-3	18	Jul 1981	11,546	$(Th,U)O_2$	400	93.0	1.00	1.075	4.96	HTI BISO	20,800
GO-THTR (22 = KAHTER)	9	Sep 1974	5145	$(Th,U)O_2$	400	93.0	0.96	1.033	10.2	HTI BISO	38,600
	10	Dec 1974	10,022								
	11	Dec 1974	5000								
	22	Sep 1986	15,248								

GFB-1	8-1	May 1974	1440	UO_2 ThO_2	200 600	93.0 -	1.00 -	1.075 -	- 9.99	LTI BISO	24,500 10,100
GFB-2	8-2	May 1974	1610	UO_2 ThO_2	200 600	93.0 -	1.00 -	1.075 -	- 9.99	LTI TRISO LTI BISO	24,500 10,100
GFB-3	13-1	Dec 1977	6076	UC_2 ThO_2	200 500	93.0 -	1.00 -	1.075 -	- 5	LTI TRISO LTI BISO	
GFB-4	13-2	Jul 1980	5860	UC_2 ThO_2 + additives	200 530	93.0 -	1.00 -	1.075 -	- 5	LTI TRISO LTI BISO	27,100 8600
GFB-5	13-3	Dec 1977	5354	UCO ThO_2	200 500	93.0 -	0.93 -	1.00 -	- 4.814	LTI TRISO LTI TRISO	
GLE-1	6-2	Dec 1973	2400	UO_2	600	14.94 0.7	1.32 0.08	8.6 11.4	-	LTI BISO	8000 9500
GLE-3	19	Jul 1982	24,611	UO_2	502	9.82	1.00	10.2	-	LTI TRISO	16,400
GLE-4	21	Feb 1984	20,350	UO_2	502	16.76	1.00	6.0	-	LTI TRISO	9560
	21-2	Oct 1987	8740								
			Σ 290,705								

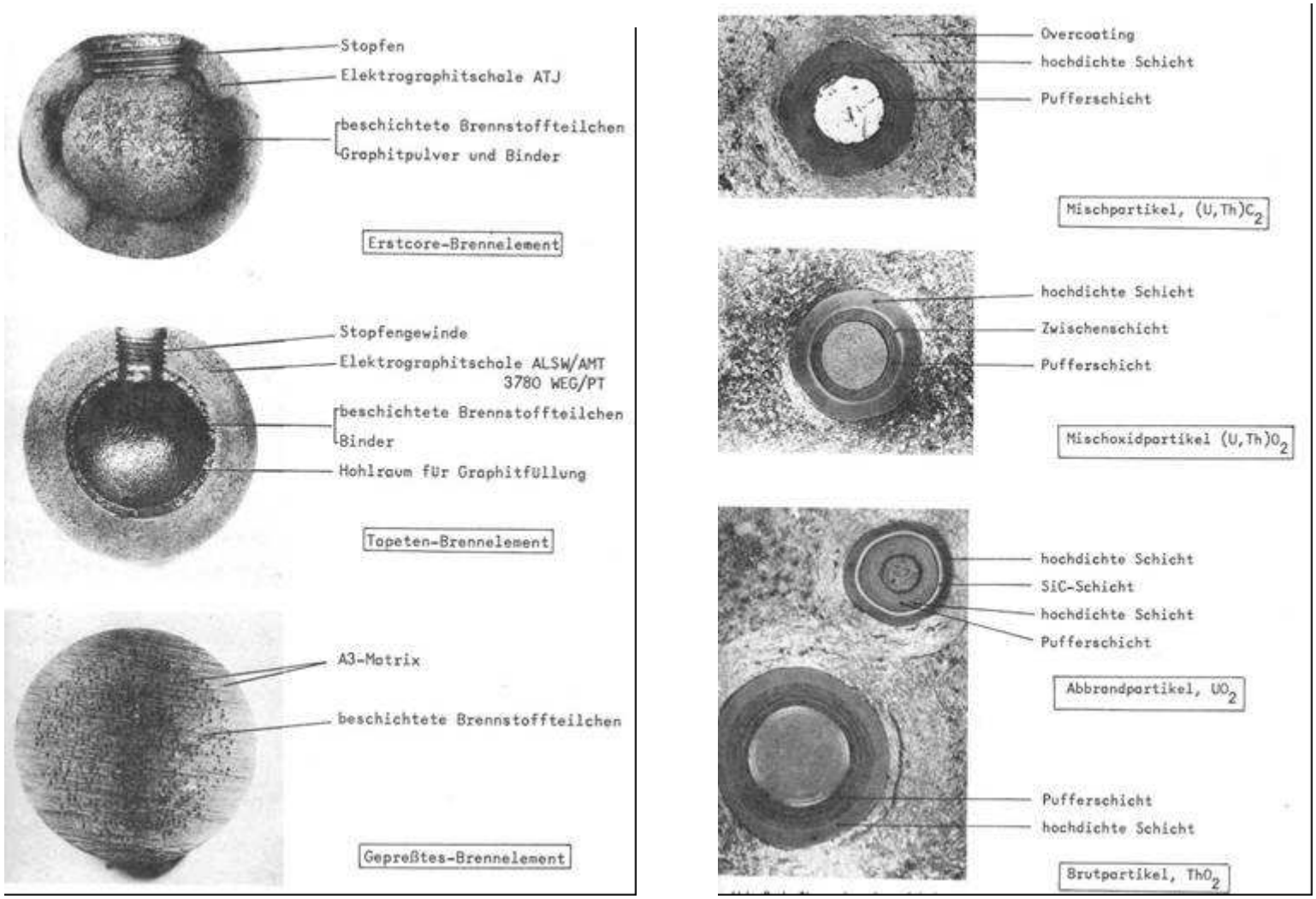

Figure 1: Types of fuel elements (left) and of coated particles used in the AVR [Wimmers 1977]

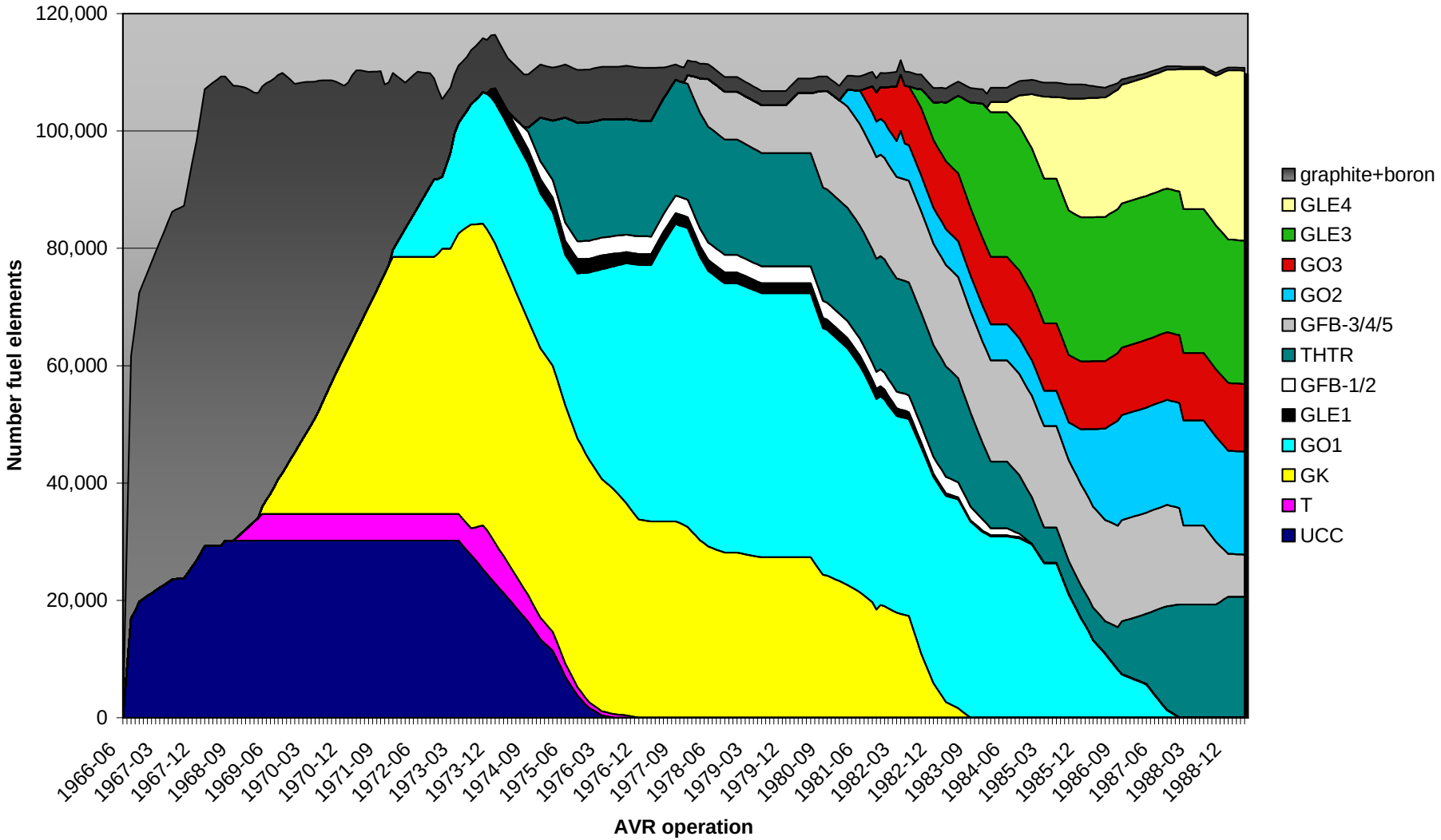

Figure 2 : Operational life history of different fuel element types in the AVR

AVR Fuel Element Types

(1) **UCC-type:** UCC elements consist of a hollow sphere made of electrographite with 10 mm wall thickness. Through a hole, the coated particles and a "matrix" called mixture of graphite powder, binder, and a graphite, which expands irreversibly at high temperatures (1450°C), were pressed in to fill the void. The hole was closed with a threading plug (see Fig. 1 top). This type fuel element had with 20 % the highest particle packing fraction.

(2) **Wall paper (T) type:** A similar design was developed by the German NUKEM company, also using a hollow sphere with 10 or 11 mm wall thickness. A mixture of coated particles and resin binder was introduced through a hole and was made by rotational movement to stick on the inside wall like a wall paper (3-4 particle layers). The remaining void was filled with a binder containing graphite powder.

(3) **Pressed type:** All following AVR reload charges (since 1969) consisted of NUKEM manufactured semi-isostatically pressed mixtures of particles with so-called "A3 standard" matrix material, 64 % natural graphite plus 16 % electrographite plus 20 % resin binder, in a 50 mm diameter sphere plus a fuel-free A3 standard zone of 5 mm thickness on the outside.

a. **GK** (= "gepresst karbidisch" = pressed carbide)
b. **GO-1** (= "gepresst oxidisch" = pressed oxide).
c. **GO-2** with high-enriched, mixed-oxide fuel like GO-1, but with a larger particle kernel and a TRISO coating.
d. **GO-3** with "noble BISO" coating, which reduced the heavy metal contamination.
e. **GO-THTR** with high-enriched, mixed-oxide fuel according to the THTR reference fuel design. Fuel elements of the same type used in the KAHTER critical formation were given to the AVR core after termination of that project.
f. **GFB** (= "gepresst feed breed") with both BISO and TRISO coating was produced to test the fissile / fertile application for the purpose of facilitating reprocessing.
g. **GLE-1** (= "gepresst low enriched") was fabricated to test LEU fuel with BISO coating. The fuel element with 20 g of heavy metal was designed for HTGR with an OTTO loading scheme. The very high fuel content of 1.4 g of U-235 was to raise the temperature load. It was the first – and remained the only – reload charge with a U-235 content very different from 1 g. Because of their poor performance, all 2400 spheres of this reload charge 6-2 were removed from the core as soon as possible.
h. **GLE-2** was similar to GLE-1, i.e., also 1.4 g of U-235, but the particle coatings contained an additional SiC interlayer. However, due to the large particle size (kernel diameter of 600 µm) and the high volume fraction (17,700 cp/sphere), many particles became defective already during the pressing process. Since more particles were expected to fail under operating conditions, the 2630 spheres designated as AVR reload charge 6-3 were rejected and have never gone into the AVR core.
i. **GLE-3** and **GLE-4**, the latest fuel production charges for the AVR, are closest to what was later considered the German reference HTGR fuel characterized by a very low level of free uranium in the fuel element.

AVR reload charge 2 was projected to be of T type (like reload 1), but later replaced in favor of reload charge 3 (GK). Also reload charge 16 projected as type **GLT** (= "gepresst low enriched two particle system") with 20 % enriched UCO, and reload charge 17 projected as variant **GO-2**, but with 20 g of heavy metal, were later replaced in favor of reload charge 18 (GO-3).

Table 2 lists the number of AVR fuel spheres with respect to specific design features.

Table 2 : AVR as test bed for different types of fuel [Pohl 2001]

Type of fuel	Number of fuel spheres
Fuel element design	
Shell type	37,700
Pressed type	253,000
of which A3-3 matrix*	135,300
A3-27 matrix*	117,700
Fuel design	
HEU, (Th,U)C_2	87,600
HEU, (Th,U)O_2	129,400
HEU, fissile/fertile	20,300
LEU, UO_2	53,400
Coating design	
BISO	202,900
TRISO	74,300
Mixed (fissile TRISO/fertile BISO)	13,500

* A3-3 is a matrix material consisting of natural graphite powder (72.0 %), electro graphite powder (18.0 %) and non-graphitized phenol resin binder coke (10.0 %). A3-27 is like A3-3 with slightly deviating component shares (71.2 %, 17.8 %, and 11.0 %, respectively), and with the resin binder being synthesized during matrix manufacture. A3-27 was used starting with AVR reload charge 14.

Distinction of the different fuel element types, apart from burnup measurements at discharge, could be made by weight measurements. Weight ranges of the single variants are indicated in Fig. 3. Another possibility to distinguish between the different fuel types is the pattern of grooves defined for the various pressed type fuel elements.

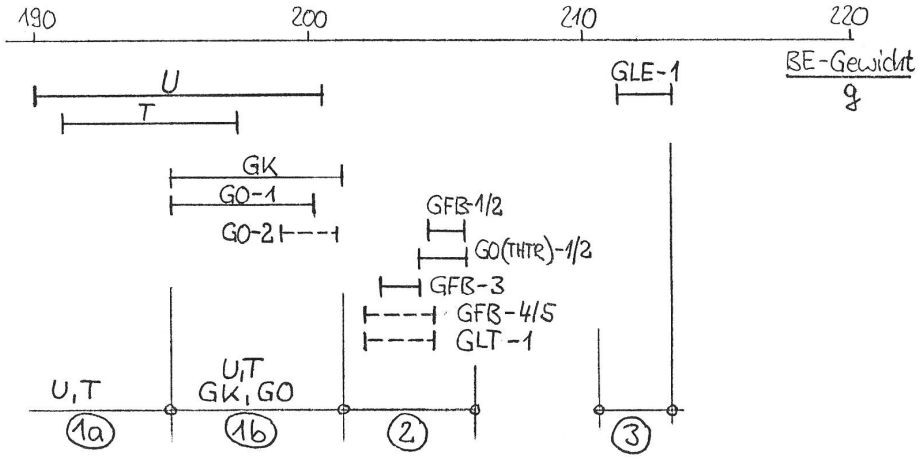

Figure 3 : Nominal weights of the different variants of AVR fuel spheres

2.1.3 Unloading of the AVR Fuel after Final Reactor Shutdown

Table 3 describes the fuel composition of the AVR after terminating the operation of the reactor end of 1988.

Table 3 : Fuel inventory of AVR at the end of operation [Pohl 2002]

AVR Fuel			Number of FE (rounded)
Type		Variant	
HEU	5 g Th	GO, GFB-3/4/5	39,300
	10 g Th	THTR	17,400
LEU	10 % enr	GLE-3	24,500
	16.7 % enr	GLE-4	29,000
		Total:	**110,200**

Defueling started in April 1994 with HEU fuel only. Due to the fact that a particular license was required for LEU fuel handling in the Hot Cells of FZJ, all LEU fuel identified was reshuffled back into the core. Selection was made by measurement of the U-232 isotope which is practically present in the thorium containing HEU fuel only. During operation, a perfect distinction by Pa-233 in the gamma scan was possible. The defueling process was interrupted after having discharged 35,000 HEU fuel elements with a HEU share in the circulated elements reduced to 17 %. After the LEU license was finally granted, defueling was resumed in March 1996. It was restricted at the beginning by the fact that upper limits for heavy metal and Pu-239 contents had to be obeyed. After obtaining the permission for considerably higher limits, unselective defueling could begin with still 63,000 spheres in the core [Pohl 1997]. The defueling was completed by middle of 1998.

The defueling process was accompanied by regular criticality measurements to ensure in-time countermeasures in case of too high a fuel concentration in the core center conceivably resulting from the fresher fuel of the outer zone displaced to the inside during defueling [Pohl 1997].

Table 4 lists the book balance of charged and discharged AVR fuel elements. The figure of “12” as the overall difference should not be taken too seriously due to the uncertainties in counting spheres in cases of misidentifying fuel types, broken spheres, or problems with the charging system. As a result of an inspection for residual fuel in the core, the equivalent of 197 fuel elements was said to be unretrievable [Pohl 2002]. It is an estimated upper limit of fuel loss in the core, but was considered by the regulator to be sufficiently low and safely enclosed to remain in the reactor during its interim storage. All lost fuel is classified as HEU fuel with originally 5 g of Th. Total heavy metal left in the core was calculated to be 486 g of uranium (including 71 g of U-235 and 24 g of U-233), 7.2 g of plutonium, and 1180 g of Th-232 [Pohl 2002].

Table 4 : Book balance of charged and discharged AVR fuel elements [Pohl 2002]

Fuel type	Fuel variant	Charged	Fraction of total fuel [%]	Charged	Discharged	Diff.
HEU, 5 g Th	UCC	30,155	10.4			
	T	7504	2.6			
	GK	50,794	17.5			
	GO	90,396	31.1			
	GFB-3/4/5	17,290	5.9			
		total:		196,139	201,945	-5806
10 g Th	GFB-1/2	3050	1.0			
	THTR	35,415	12.2			
		total:		38,465	32,978	5487
	All HEU		**80.7**	**234,604**	**234,923**	**-319**
LEU, 7 % enr	GLE-1	2400	0.8	2400	2327	73
10 % enr	GLE-3	24,611	8.5	24,611	24,412	199
16.7 % enr	GLE-4	29,090	10.0	29,090	29,031	59
	All LEU		**19.3**	**56,101**	**55,770**	**331**
		Total:	**100.0**	**290,705**	**290,693**	**12**

The book discharge deviations were corrected not until after final defueling. It was, however, known by sphere measurements before the KAHTER fuel loading that in the last years of operation, GLE-1 elements were no longer in the reactor, and that the number of the old HEU elements with 10 g of Th was only around 2000 (instead of over 5000 as in the book). Both was confirmed in the defueling process.

2.1.4 Spent Fuel Management for AVR

Steel cans with a capacity of 50 fuel spheres each were filled at the AVR site and transported to the Hot Cells at FZJ, where they were sealed and stored in a water pool serving as a buffer storage. The steel cans were then opened and the fuel from those, which did not indicate water penetration, was repacked into larger, dry storage canisters with a capacity of 950 balls (see Fig. 4 top) [Krumbach 2004]. Fuel elements which were found wet due to leaky sealings of the steel cans, were also given into the dry storage canisters, but then sealed with a particular leak-tight welding. The dry storage canisters are filled with helium of 0.1 MPa, their specified leak tightness is $< 10^{-2}$ Pa l/s. The employment of the 950 ball canisters was considered to ease the future repackaging step to the reference 400 l final disposal drums.

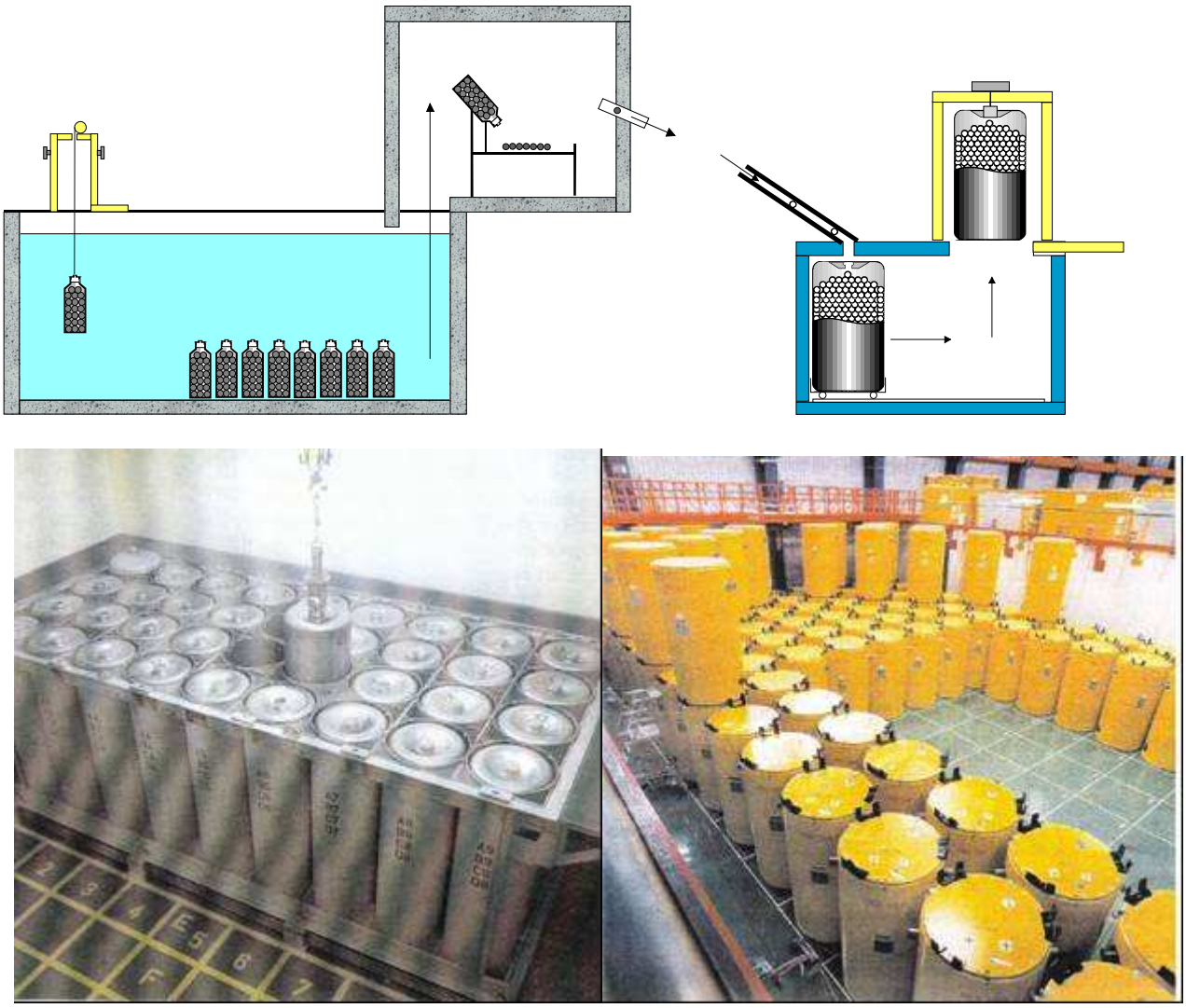

Figure 4 : AVR spent fuel management in the Hot Cells
at FZJ (top) AVR canister storage (bottom left), storage in CASTOR casks (bottom right)

For the intermediate storage, two concepts are being applied:

(i) canister storage behind a concrete shielding; or
(ii) storage directly in shielded containers.

A natural convection type, dry storage facility, which is operated since 1981 without any disturbance, took up 72 of the dry storage canisters in 36 positions up to now (see Fig. 4 bottom left). Heat removal designed for 7.2 kW is supported by an air venting system of 2000 Nm^3/h. According to the second concept, two of the canisters are inserted into a CASTOR THTR/AVR type storage cask closed by a double lid system. The CASTOR casks are stored at FZJ in the intermediate dry storage facility licensed to take up a total of 158 casks (see Fig. 4 bottom right). The maximum heat production of 15 kW (if completely filled) is passively removed by natural convection [Röllig 1987].

This procedure has been done for all fuel discharged during reactor operation and after reactor shutdown, which are approximately 290,000 fuel spheres in (presumably) 153 CASTOR casks. Last transport to the storage site was in August 2000. As of September 2004, the AVR container store contains 132 CASTOR casks with a total of 250,560 spheres and the dry storage facility contains 34 fuel canisters with a total of 32,264 spheres.

2.2 Spent Fuel from the THTR-300 Reactor

2.2.1 Decommissioning of the THTR-300

The concept of the "Thorium Hochtemperatur-Reaktor", THTR-300, in Hamm-Uentrop dates back to the end of the 1960s. The THTR-300 with a thermal power of 750 MW was operated for a total of 16,410 hours or an equivalent time of 423 days of operation at full load. Construction (1971 – 1983) and operation (1983 – 1988) of the reactor were characterized by various licensing-technical and political obstacles, which eventually ended up in the decision by the operator in September 1989 for decommissioning the reactor.

The decommissioning procedure is conducted in four consecutive steps [Schröder 1993]:

1. Shutdown operation; primary circuit depressurized; helium substituted for nitrogen; shutdown rods fully inserted and locked; removal of decay heat (< 20 kW) by natural convection and radiation;
2. Unloading the reactor and spent fuel storage as a prerequisite for safe enclosure; reactivity < 0.95 during unloading by addition of 7000 absorber balls; core inspection device for visual control of fuel-free state;
3. Establishment of safe enclosure; residual radioactivity sealed from environment and controlled; effective dose from release into environment < 0.1 mSv/yr; all buildings except for reactor hall, reactor building, and auxiliary building to be released from the validity of the Atomic Act;
4. Operation of passively "safe enclosure" over 30 years; largely no maintenance; monitoring the few remaining systems to be operated from adjacent fossil power plant.

Steps 2, 3, and 4 require a license according to the German Atomic Act.

The establishment of the configuration of safe enclosure was achieved in February 1997 (comparable to the IAEA passive SAFE STORAGE option). The operation of the safely enclosed plant will last for 30 years, before a complete dismantling may take place.

The association with a thorium high temperature reactor (THTR) was the reprocessing of the bred U-233. The development of economic reprocessing methods was initiated in 1966 leading to the so-called THOREX process scheme and the construction of a semi-technical facility called JUPITER. However, works on reprocessing of HTGR fuel were abandoned in 1985 and the option of interim storage over several decades with future final disposal favored [Merz 1993].

2.2.2 THTR Fuel

The THTR fuel concept was designed for a high-enriched uranium-thorium fuel cycle. The reference fuel particle consists of a homogeneous U-Th mixed oxide kernel of 406 µm diameter surrounded by a BISO coating composed of a low-density buffer layer, a gas-tight sealing layer, and a high-density isotropic outer HTI layer. Total particle diameter is about 760 µm. The spherical fuel element contains approx. 34,100 of those BISO coated fuel particles. The total heavy metal content amounts to 1.032 g of 93 % enriched uranium and 10.2 g of thorium per ball. The main characteristics of the THTR fuel are summarized in Table 5. Fuel fabrication took place from 1973 to 1980 for the initial core (380,000 spheres) and from 1980 to 1988 for reload (600,000 spheres).

Table 5 : Characteristics of the THTR initial core fuel
[Röllig 1991b, Rebmann 1988]

Coated particle	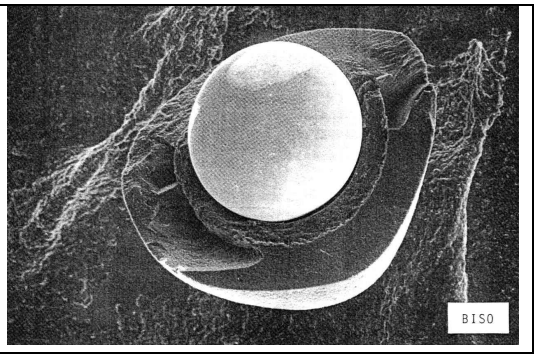
Particle Batch	
Kernel composition	$(Th,U)O_2$
Kernel density [kg/m^3]	9100
Kernel diameter [µm]	406 ± 10.6
Enrichment [U_{235} wt.%]	93 %
Coating thicknesses [µm]	
Buffer	77.4 ± 13.9
Sealing + HTI	100.0 ± 11
HTI	78.1 ± 9.4
Overcoating	~75
U-contamination of HTI	$(1.03 \pm 0.15)*10^{-3}$
Fuel element	
Type	
Diameter [mm]	60
Matrix material grade	A3-3
Density [kg/m^3]	1720
Weight [g]	204
Heavy metal loading [g/FE]	1.032 g of U + 10.2 g of Th
Number of coated particles per FE	~34,100
Volume packing fraction in fuel zone [%]	12
Free uranium	$(3.0 \pm 0.69)*10^{-4}$
Corrosion rate*) [mg/(cm^2 h)]	≤ 0.125 at 900°C ≤ 1.0 at 1000°C

*) in standardized atmosphere of 1 vol% H_2O in flowing helium at 900/1000°C and atmospheric pressure

The initial THTR core contained a total of 674,200 spherical elements, of which 358,200 (or 35 %) were fuel elements, 272,500 (40 %) were graphite elements, and 43,500 (7 %) were B and Hf doped absorber elements. During THTR operation, 1.3 million spheres were circulated, 235,000 of which were permanently removed and replaced by fresh fuel [Bäumer 1991]. At the time of termination of operation on September 1, 1989, a total of 704,426 operating elements were in the core and the loading facility [Knizia 2002]. From the core itself, approximately 670,000 operating elements (see Table 6) had to be finally removed from the core, 84 % of which were fuel elements. An at-reactor canister storage for spent THTR fuel was licensed in 1982. It received its first regular spent fuel in 1988.

Table 6 : Composition of THTR core
[Niephaus 2000]

Number of operating elements in the core at beginning of unloading process		
562,929		Fuel elements
76,130		Graphite elements
30,779		Absorber elements
Σ 669,838		Operating elements

In addition, the internal operating element storage contained about 240,000 operating elements.

2.2.3 Unloading of the THTR Fuel after Reactor Shutdown

Unloading of the THTR pebble bed core was initiated in December 1993 with a concept based on detailed calculations and tests with a core model. The unloading process was completed in October 1994 achieving the state of a “nuclear fuel free” reactor.

The unloading process is, in principle, similar to the discharging process during normal operation except for some process engineering modifications concerning the replacement of the helium gas by nitrogen and air as well as the reduced temperature in the depressurized reactor. Absolutely subcritical conditions during the unloading process were guaranteed by insertion of both reflector and in-core control rods and by the addition of 4200 absorber elements.

The unloading of the THTR pebble bed was monitored by means of the burnup measuring system, a graphite moderated 500 W “Solid Moderated Reactor” (SMR), where a reactivity effect was created when a fuel element was passing. Operating elements were sorted by this way and transferred to steel canisters each containing 2100 elements.

The flow pattern of the spheres during the unloading procedure was examined in experiments using a 1:2 core model showing that a central funnel is formed which leads to a mixture of fuel elements with different burnups [Bäumer 1991b].

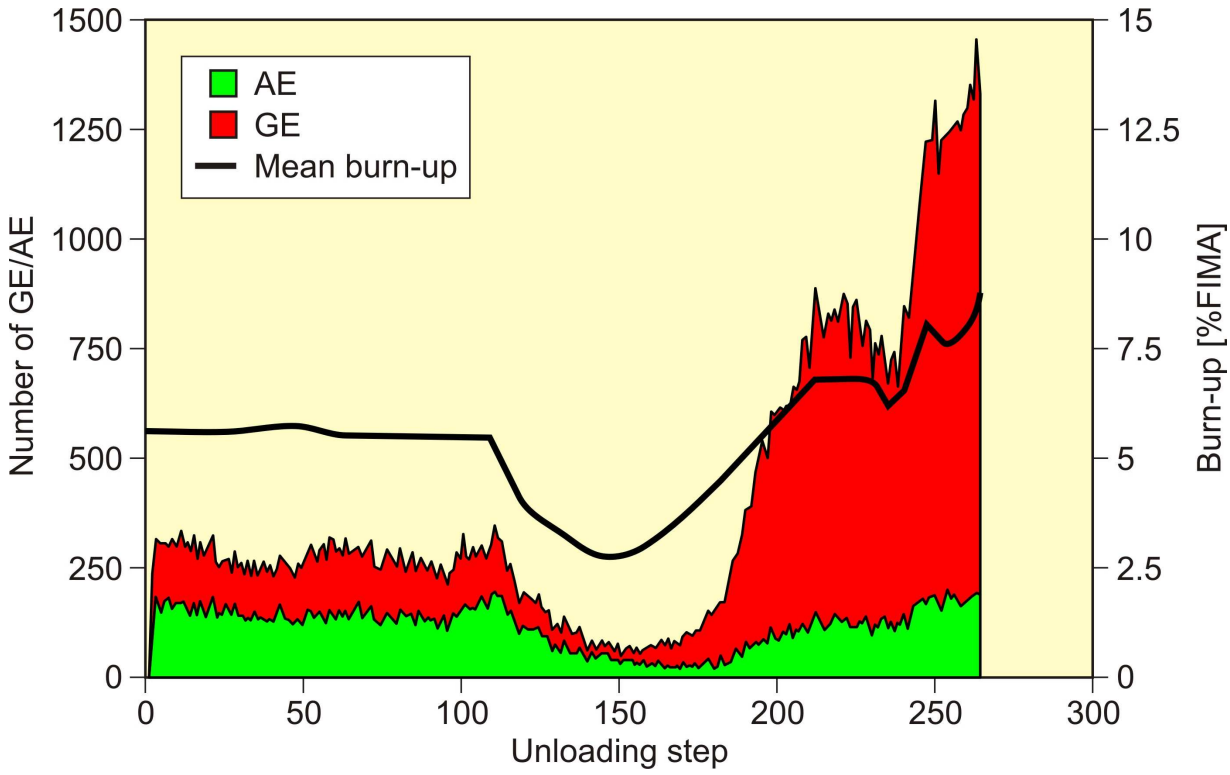

Figure 5 : Discharged absorber (AE) and graphite elements (GE) per unloading step (= 2100 fuel elements and mean burnup of fuel elements [Plätzer 1997]

The diagram in Fig. 5 shows the number of discharged absorber elements (AE) and graphite elements (GE), respectively, per each of the 268 "unloading steps", which corresponds to 2100 discharged fuel elements or one filled steel canister. Furthermore the mean burnup of the removed fuel elements is plotted exhibiting different phases during the unloading process. The minimum in burnup around unloading step 150 is due to fuel elements from the surface of the outer upper core with a low-irradiation history, whereas the later increase in burnup is from highly irradiated fuel from the bottom edge of the core [Plätzer 1997].

The efficiency of the selection process was about 97 %, meaning that from the total of about 300,000 graphite elements and 43,500 absorber balls, approximately 3 % have gone with the fuel elements into the fuel canisters [Niephaus 2000].

Between start and end of plant operation, ten containers were filled with about 17,000 damaged operating elements mainly due to control rod operation, four more were filled until the end of fuel unloading.

The inventory of fissile material remaining in the core after completion of the unloading process was estimated to be 0.976 kg, significantly lower than the required value of 2.5 kg.

2.2.4 Spent Fuel Management for the THTR-300

All fuel canisters were stored for 1-2 yrs in a reactor spent fuel store with 72 storing positions for three canisters each plus 9 more positions for high active waste (see Fig. 6). Shielding is given by concrete walls of 1.9 m thickness. The store is designed for a heat removal of 232 kW which is realized by a forced convection cooling [Röllig 1987].

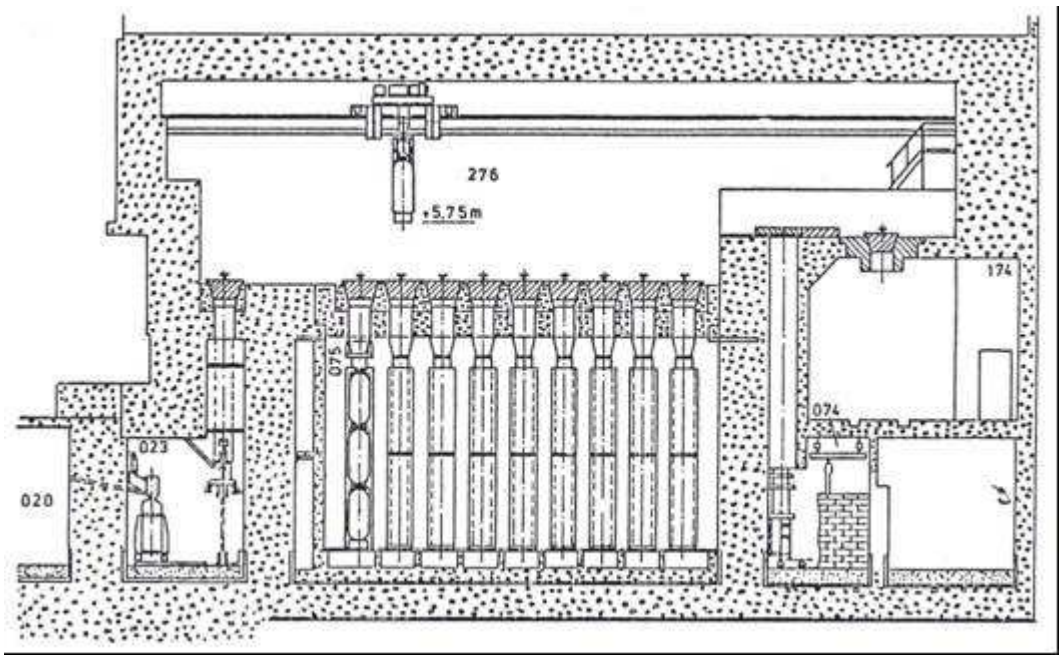

Figure 6 : THTR-300 store for spent fuel
[Röllig 1987]

For the next step of storage and transport of the fuel elements to an external interim store, respective casks of the CASTOR THTR/AVR type have been used with one CASTOR to contain one fuel canister with approximately 2100 fuel elements.

Maximum burnup per fuel element container was about 8.8 % FIMA, maximum decay heat per fuel element container was about 100 W, both values significantly lower than the design values. Neutron dose rates at the loaded transport and storage cask were shown to be less than 1 µSv/h.

The storage license for the casks in the interim storage site Ahaus (BZA) was issued in 1992. Special six-axle railway wagons were available to carry three casks each. By April 1995, a total number of approximately 620,000 spent fuel elements had been transported in 306 CASTOR casks in 57 shipments from the THTR site to the BZA. A schematic of the complete spent fuel management is shown in Fig. 7 top.

The THTR fuel will remain in the intermediate storage until a final disposal site is available, with the repository Gorleben representing a candidate site. In contrast, the graphite and absorber elements, because of their low radioactivity and heat generation, will possibly go to the repository

Konrad [Schröder 1993]. The fuel would then be repackaged from the CASTOR casks to 400 l waste containers with a capacity of 1500-1800 fuel elements to be disposed in a bore hole field.

All still unused fresh fuel elements, at the time of final shutdown a total of 362,348 spheres, was sold back to the manufacturing company NUKEM, which then shipped the fuel to UKAEA in Dounreay for reprocessing [Dietrich 2006].

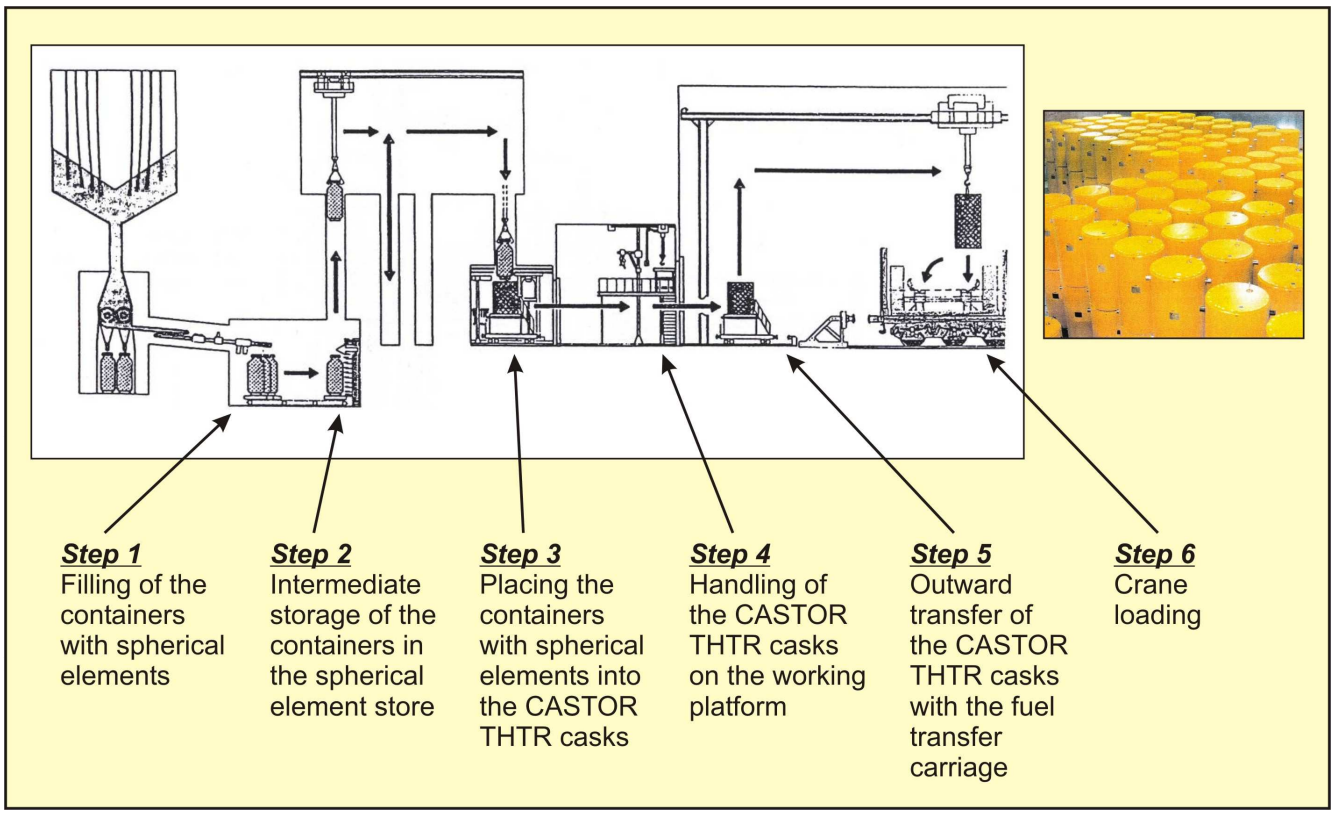

The core of the Dragon Reactor Experiment was prismatic with an effective diameter of 1.08 m and formed by 37 fuel elements arranged in a hexagonal array. The standard Dragon fuel element had an overall length of 2.54 m with both ends to contain reflector material and a 1.60 m middle section to contain the fuel. Held between the top block and bottom ring was a cluster of six driver fuel rods with each made up from 30 annular graphite fuel compacts within graphite sleeves, and a central rod that contained an experimental section. Helium coolant was flowing through the annular gap between graphite tube and fuel body. The fuel elements could be individually purged from fission gases. A total of 25 fuel element varieties for the DRE were developed during the course of Dragon operation (three examples shown in Fig. 7). The fuel was in form of coated particles originally suggested and patented by R. Huddle in 1957 and 1959, respectively.

A whole variety of types of fuel particles have been developed, fabricated, tested, and inserted into the Dragon core. They included kernels made of uranium monocarbide, uranium dicarbide, uranium dicarbide/thorium dicarbide, uranium monocarbide/zirconium monocarbide, or uranium dioxide, which were uncoated or coated either with pyrocarbon only or with a sequence of layers pyrocarbon/silicon carbide/pyrocarbon. Also the ratios of U/Th or U/Zr or U/C varied over broad

ranges. Furthermore process parameters during the fuel manufacture were changed to develop optimal designs. Fuel kernel diameters were ranging within allowable limits defined by the sieves employed. Therefore it is not possible to define a fixed set of characteristic data describing Dragon fuel as such.

Principal objective of the 1st charge loading was to irradiate fuel for the thorium cycle. The fuel was in form of a carbide with 93 % enriched uranium arranged in a two-zone core. The ten centrally located fuel element assemblies contained the fertile material thorium at a Th/U-235 ratio of ~10 with the remaining 27 fuel elements mainly serving to drive the reactor ("driver" fuel). For the purpose of reducing burnup, the uranium carbide (UC) was mixed with zirconium carbide as alloying diluent to form (U,Zr)C driver fuel with a Zr/U-235 ratio of ~8 [Price 1966]. By June 1964, a total of 18 driver elements with "releasing" type fuel (kernels coated with PyC only) were completed, right in time to achieve criticality in August (with 16 of the 18 elements of the outer ring). First charge production was completed in August 1966.

Already in May 1963, however, a decision was made by the Project to switch fuel design from the "emitting" type with kernels surrounded by just one PyC layer, to the "retaining" type fuel, which was used already in a part of the 1st charge.

For the initial charge, fuel particles with zirconium/uranium carbide and thorium/uranium carbide were embedded in a resin coated graphite powder matrix. Particle kernel used in driver fuel had a diameter between 251-422 µm (defined by passing through respective sieves), while they were sized between 353-500 µm for the fertile fuel. For experimentation, the center rods of three fuel element assemblies were used for the so-called Metallurgical Series I elements each containing 43 varieties of fuel (plus some 2000 graphite specimens). Fuel charge 1 was operated over 229 efpd.

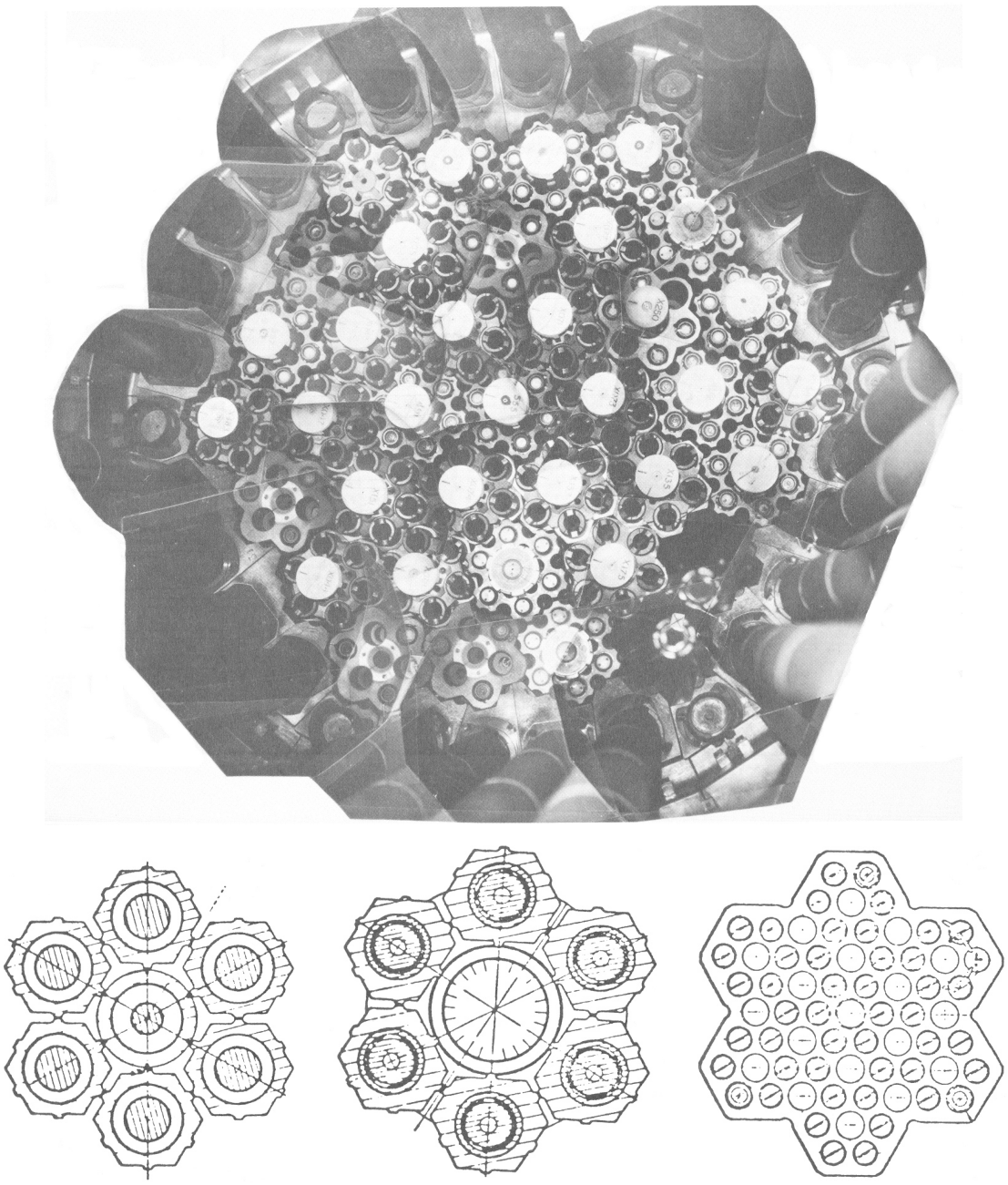

left: D4 with experimental fuel in the center rod;
middle: D9 with enlarged center rod to allow full-size German fuel spheres;
right: D22 as an integral block fuel element of US design

Figure 7 : Dragon reactor core (top) and some of the fuel element varieties (bottom) [Howard 1978]

For the 2nd charge, the Dragon core needed 32 new fuel element assemblies. Due to the aim of an unpurged fuel element design, a new type, D4 MK II, was developed where only the central rod as an experimental section remained purged, whereas the surrounding six "driver" fuel rods were unpurged. By January 1967, every fuel element was of this type. Also the new designed "UC-10" (UC_2 with excess carbon at a C/U-235 ratio of ~10-12) fuel kernel with a 420-572 µm diameter and a TRISO coating was applied in the driver zone. Furthermore the particles received a thick overcoating. The driver fuel considered the "Dragon Reference Particle" consisted of fuel particles with an 800 µm UO_2 kernel and a TRISO coating, bonded together in a carbonaceous matrix and pressed to compacts. Fuel charge 2 was operated over 262 efpd.

A significant portion of the 2nd charge was experimental fuel tested in a large-scale comparison of fuel compositions and coatings, and also for different irradiation times with the goal of extending fuel lifetime. They contained oxide or carbide mixed compounds, involving low enrichment uranium, thorium and plutonium, and with BISO or TRISO coatings. Also complete fuel spheres from the German programs could be irradiated in the central position (see also sections 3.2.1. and 3.2.2.).

Charge 2 included approximately 10 g of plutonium contained in TRISO coated fuel particles which were placed in cartridges. This amaount of Pu is about the same as was produced in charge 1 from neutron capture of the U-238 during operation [Price 1966a].

Also interest shifted from the thorium cycle to a LEU fuel cycle in a heterogeneous core with the first such fuel available for irradiation in 1967. Furthermore, fuel work was almost exclusively dedicated to porous uranium oxide fuel.

In the 3rd charge starting in July 1968, 13 new fuel elements with introduced, with them 26 of the 37 being of the D5 type, where the center rod and the surrounding driver rods were independently replaceable. Following the new fuel concept, by far most of the driver fuel was oxidic: UO_2/10C, UO_2/5C, UO_2/33C, UO_2/18C. Total production of this oxide fuel was around 650 kg of coated particles used in 43,000 compacts of various types and dimensions, of which some 33,000 compact were the "standard D13 type fuel". With charge 3, a cyclic mode of operation was pursued, which allowed the variation of residence times for the experimental fuel unlike the once-through character of the charges 1 and 2. Cycling was made by exchanging 20 % of the driver fuel every 30 efpd [Howard 1978].

The pin-in-block design for fuel elements, which was already tested with the earlier fissile-fertile fuel system to avoid high stresses in the main structural components of the core, was also later employed for the LEU fuel tested in the D14 and D16 type fuel elements.

With beginning of charge 5, the first integral multi-hole graphite block fuel element (type D22) was introduced into the Dragon core investigating the block design as was used for the US Fort St. Vrain HTGR.

By 1974, the Dragon was used for the irradiation of about 250 fuel elements, comprising 75,000 compacts and $8*10^8$ coated particles. In addition, more than 60 major experiments were conducted in various European MTRs [] (see also section 3).

Table 7 : Characteristics of the Dragon fuel

1st charge coated particle fuel with single PyC layer (left) and with SiC interlayer between PyC (right) 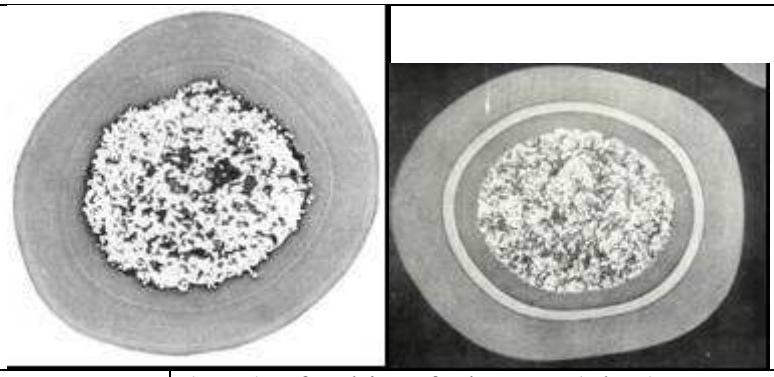	
Kernel composition	(Zr,U)C for driver fuel, (Th,U)C
Kernel density [kg/m^3]	9100
Kernel diameter [µm]	500-710 250-500
Enrichment [U_{235} wt.%]	93 %
PyC coating thickness (emitting type) [µm]	~ 75
U-contamination of HTI	$(1.03 \pm 0.15)*10^{-3}$
TRISO coating thicknesses [µm]	
1. layer (PyC)	20-30
2. layer (SiC)	20-30
3. layer (PyC)	70-100
2nd charge coated particle fuel TRISO coating with modified inner PyC, most driver fuel of D13 type 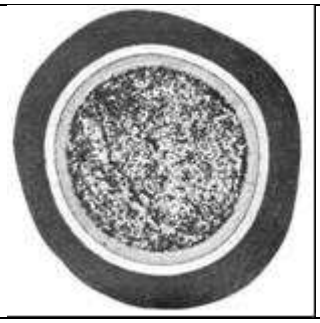	
Kernel composition	UC-10 (UC_2 + 10C) for driver fuel
C/U ratio	10-12
Kernel density [kg/m^3]	60-70 % theor. density
Kernel diameter [µm]	600
Enrichment [U_{235} wt.%]	93 %
Coating thicknesses [µm]	
Porous + inner HDI PyC	~ 75
SiC	30-35
Outer PyC	45

3rd charge coated particle Fuel of LEU UO_2 TRISO reference design	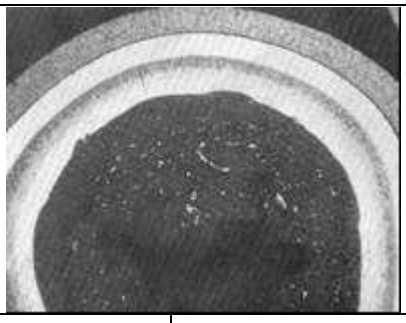 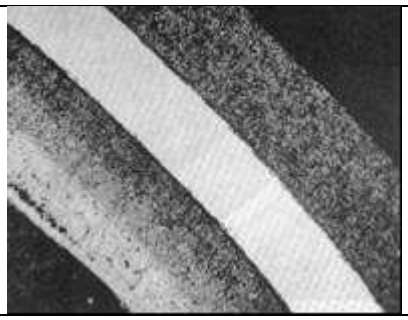
Reference Particle LEU	
Kernel composition	UO_2 + 10C
Kernel density [kg/m^3]	
Kernel diameter [µm]	700-800
Enrichment [U_{235} wt.%]	
Coating thicknesses [µm]	
Porous + inner HDI PyC	
SiC	33-46
total	150-190
U-contamination surface	< 1*10-6
Fuel Element compact	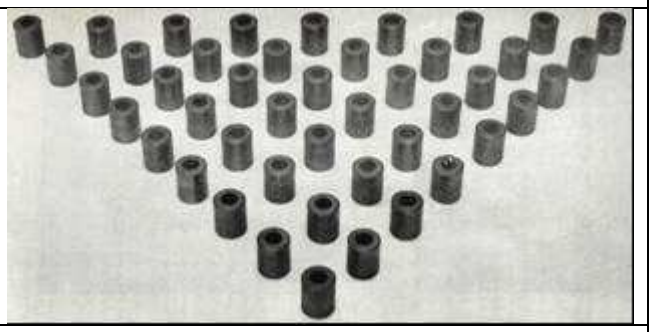
No. of fuel element clusters	37
No. of fuel rods per cluster	7
Distance across cluster [mm]	190
Overall length of fuel rod [m]	2.5
Fueled zone [m]	1.6
Type	
Diameter [mm]	
Matrix material grade	
Density [kg/m^3]	
Weight [g]	
Heavy metal loading [g/FE]	
Number of coated particles per FE	
Volume packing fraction in fuel zone [%]	
Free uranium	

2.3.3 *Unloading of the Dragon Fuel after Reactor Shutdown*

A movable shielded flask was used to withdraw spent fuel elements from the pressure vessel. From there they were transferred into fuel element canisters in a nitrogen atmosphere and sealed. Typical leak rate was in the order of 10^{-6} atm cm^3 s-1 [Howard 1978].

2.3.4 *Spent Fuel Management for the Dragon Reactor*

The Dragon reactor is presently held in the state of care and maintenance and will be presumably until 2035. All fuel has been removed from the reactor and placed into mild steel containers stored on-site in the Dragon fuel store. After it became obvious that corrosion could potentially affect the container integrity for long-term storage, UKAEA required sorting and repackaging of the Dragon fuel into stainless steel containers to be then relocated to Harwell [11]. Total number of containers is 85. Shipment of the material is planned to start in 2004 and be concluded by 2005/06.

In 1998, UKEA developed a strategy to decommission the majority of the nuclear liabilities on the Winfrith site. RWE NUKEM was awarded the multidisciplinary "Winfrith Operations Maintenance and Decommissioning" (WOMAD) project starting in March 2000 and with an 8 years duration. Final decommission will focus on the core, primary and secondary containment. The end state to be reached by 2020 will be a cleared site ready for remediation and delicensing [10].

Following defueling of Dragon, 75,000 fuel compacts were stored untreated in storage containers (see Fig. 8) and were subsequently repackaged in stainless steel cans in 1998. These waste packages contain fuel consisting of uranium and uranium/thorium oxide and carbide kernels, graphite and some ZrC, covered with carbon and SiC layers to give 0.1-0.25 mm particles. The fuel particles are mixed with graphite and compressed into compacts and some of the fuel has disintegrated. Chemically, the composition of the packages can be summarised as follows :

- ~95% graphite/pyrocarbon
- ~5% heavy metal oxides and carbides (U/Th/Zr)
- ^{14}C - graphite and pyrolytic carbon
- Th - Thorium oxide & thorium carbide (ThC & ThC_2)
- U - Uranium oxide and uranium carbide (UC & UC_2)
- Pu - Plutonium oxide and plutonium carbide (PuC)

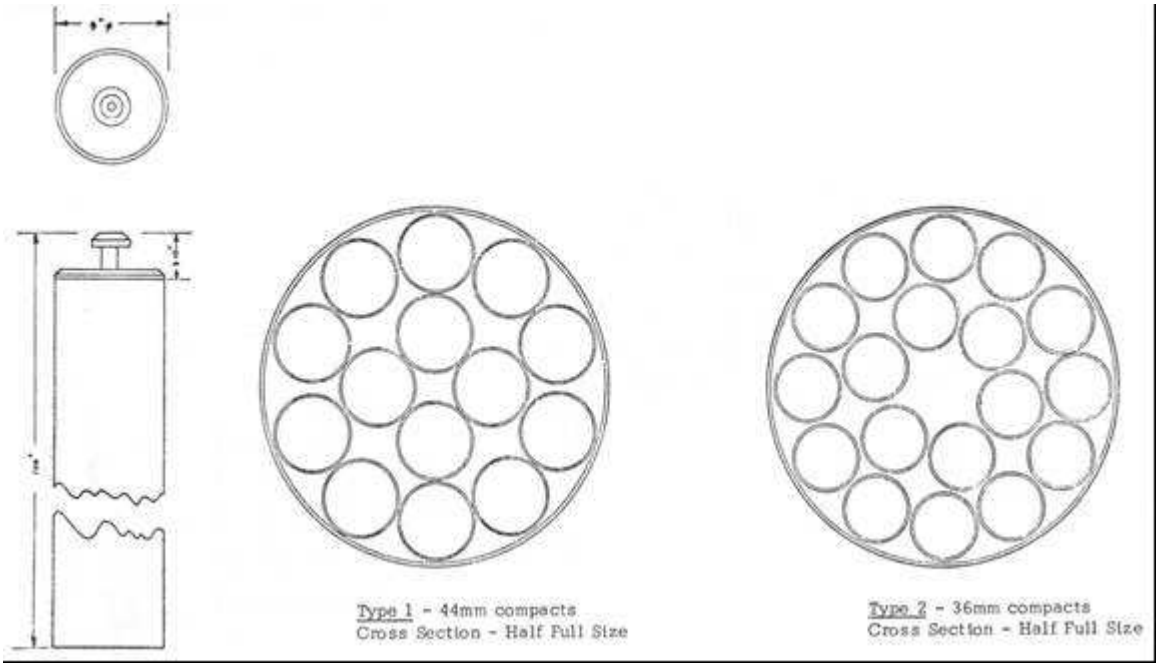

Figure 8 : Dragon irradiated fuel storage container

There is no detailed publically available experimental characterisation or inventory data for the Dragon waste packages, and published inventories are based on calculations using inventory codes. The Dragon waste packages are the property of the Nuclear Decommissing Authority (NDA), and are classified in the UK as ILW as their heat generation rates are low enough not to require engineered cooling [DEFRA 2005]. The situation with regard to the Dragon spent fuel is untypical because of the low heat generation rates as, in general, fuel waste streams arising from the treatment of spent HTR fuel would be classified as HLW.

3 CHARACTERIZATION OF SPENT HTGR FUEL

The characterization of HTGR fuel is done by the application of quality assurance and quality control methods during the manufacture process and by testing the fuel in MTRs under the conditions of future operation and even beyond. Apart from smaller-scale production during the fuel development phase, e.g., proof test fuel, also mass production and mass irradiation testing are important. Therefore, despite the lack of information on individual fuel elements, the large-scale testing in real HTGRs is an essential complement to MTR testing.

When fuel spheres were inserted into the reactor, they lost their identity such that after discharge, the operation history of an individual ball was not traceable. However, the operational gamma spectrometric measurements of each sphere gave hints on burnup and fuel type, and in PIE, the fuel type (and in most cases the reload charge number) of a discharged sphere could be identified according to the special groove pattern marked on the sphere surface. Distinction of the different fuel spheres could also be made by the different weights (see Fig. 3). Therefore statistical statements on the irradiation history of the different fuel types can be given.

The advantages of testing fuel in a real HTGR are :

- mass fuel production;
- mass fuel irradiation testing;
- exposition to mechanical stresses in a flowing pebble bed;
- running through real fueling and discharge procedures;
- PIE on spheres at different stages of fluence/burnup;
- PIE on a larger number of spheres allowing better statistical statements.

3.1 Characteristics of Unirradiated HTGR Fuel

3.1.1 AVR Fuel Properties

Free Uranium

Uranium contamination in fresh fuel elements for the AVR was specified to not exceed the limit of $5*10^{-4}$. It was measured by leaching and etching. Table 8 summarizes the acquired data for different fuel types.

In the first production of GO spheres (AVR reload charge 5-2), agglomerations of uranium were identified in the inner PyC coating layer. This effect, which was called “pepita”, was finally considered insignificant because of the small amount concentrated in these spots compared to what was normally homogeneously distributed in this PyC layer [AVR 1971b].

For the later oxide fuel production GO-3, a change was made in the coating process. This new coating called “noble BISO” resulted in a reduced contamination level in the outer coating layer and thus in the matrix material to $< 10^{-4}$ of U_{free}/U_{total}.

Table 8 : Average uranium contamination in fuel elements of different types [Wimmers 1977]

Fuel type	Reload charge	Fraction of uranium contamination [10^{-4} U_{free}/U_{tot}]	Final heat treatment [°C]
UCC	First core	4.7(1)	1450
T	1	0.7 ± 0.5	1450
GK	3-5	9.6(1)	1800
GO	5-2, 6-1	1.0(1)	1800
GO	6-1, 7	1.0(1)	1900
GLE-1	6	7.0 ± 7	1900
GLE-2	6	11.9 ± 7	1900
GFB-1	8	2.6 ± 7	1900
GFB-2	8	1.6 ± 1.6	1900
GO-THTR-1	9	4.8 ± 0.6	1900
GO-THTR-2	10, 11	2.7 ± 0.6	1950
GO	12	2.9 ± 0.5	1950
GLE-3	19	0.49(2)	1950
GLE-4	21	0.46(2)	1950
	21-2	0.078(2)	1950

(1) calculated from comparative measurements
(2) [Nabielek 1990], see also next Table 8

For the thorium contamination of particle coating and matrix material, no upper limit was specified. Measured data were

for GO-1: $0.2\text{-}0.4*10^{-4}$ Th/Th_{tot}
for THTR: $0.1\text{-}0.2*10^{-4}$ Th/Th_{tot}

The relatively high contamination for BISO fuel compared to TRISO is due to the manufacturing process where the final heat treatment at high temperatures expels the heavy metal from the kernel into coating and matrix material.

For the UCC type fuel elements, one specification of the coated particles was not fulfilled, the level of uranium in the PyC coating was higher than originally required. But it was finally deemed acceptable because of the good irradiation behavior of the UC_2 specimens tested. The specification was modified such that only 2 % of the examined particles were allowed to have uranium migrated further than 20 µm into the coating.

With the production of LEU TRISO fuel (GLE-3 and GLE-4), the high quality level of German HTGR fuel production could be proven. From the approximately 24,600 GLE-3 fuel spheres (reload charge 19), 70 were taken for quality control. Results are given in Fig. 9 showing that the U_{free}/U_{total} ratios were observed to be integer multiples of a coated particle inventory ($1/16400 = 0.61*10^{-4}$), meaning that the free uranium is mainly from particles with a defective SiC coating. It

demonstrated thus the extremely low contamination level of the matrix material with U-235 basically originating from natural contamination of the graphitic raw materials.

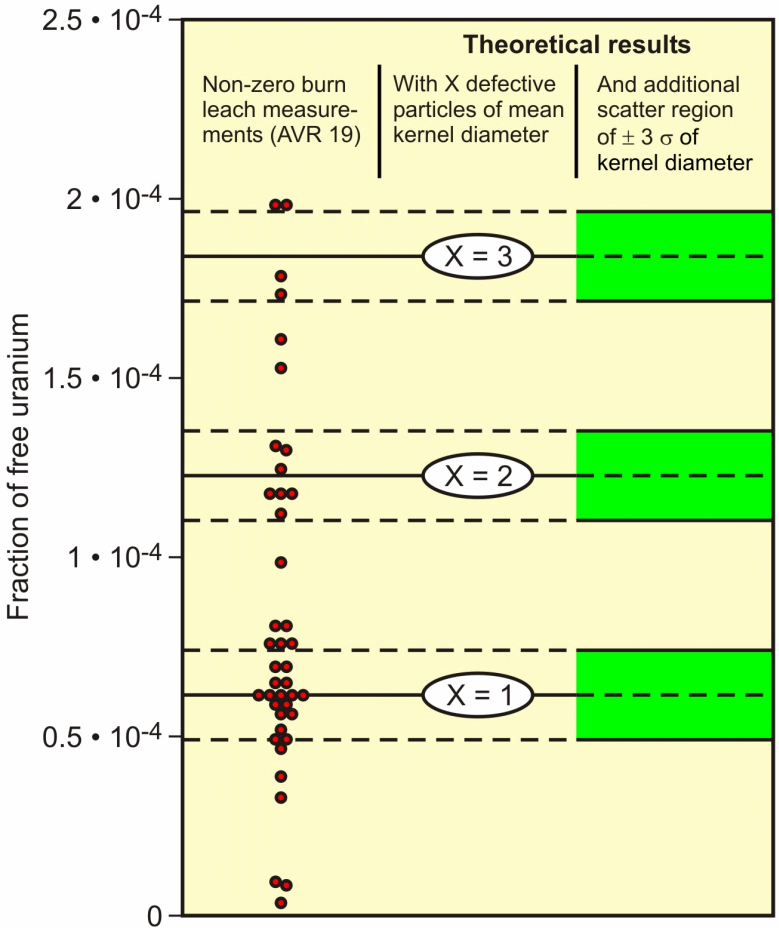

Figure 9 : Free uranium measurements from burn-leach tests on GLE-3

Later productions of HTGR (LEU TRISO) fuel representing the state-of-the-art of German pebble fuel development resulted in a further improvement of the statistics. Table 9 summarizes the results of the quality examination comparing GLE-3 (AVR reload charge 19) and GLE-4 (AVR reload charges 21 and 21-2) with the proof test fuel (= German reference) produced in 1988 on a small scale.

Table 9 : Evaluation of free uranium and defective SiC in German UO_2 Triso fuel elements [Nabielek 1990]

Free uranium and defective SiC in German LEU UO_2 TRISO fuel elements					
Designation of Fuel Element (FE) population	LEU Phase I	AVR 19	AVR 21	AVR 21-2	Proof test fuel
Production year	1981	1981	1983	1985	1988
No FEs produced	<100	24,600	20,500	14,000	<200
^{235}U enrichment	9.8%	9.8%	16.7%	16.7%	10.6%
Number of particles/FE	16,400	16,400	9,560	9,560	14,600
Evaluation of free uranium from burn-leach measurements					
Number of FEs tested in burn-leach	5	70	55	40	10
No. FEs with 0 part. defects	3	31	42	38	8
No. FEs with 1 part. defects	1	26	8	1	1
No. FEs with 2 part. defects	1	9	2	1	1
No. FEs with 3 part. defects	0	4	2	0	0
No. FEs with 4 part. defects	0	0	0	0	0
No. FEs with 5 part. defects	0	0	0	0	0
No. FEs with 6 part. defects	0	0	1	0	0
No. FEs with >= 7 part. defects	0	0	0	0	0
Total number of defective particles observed	3	56	24	3	3
Total number of measured particles	82,000	1,148,000	525,800	382,400	146,000
Measured free uranium fraction	$3.7*10^{-5}$	$4.9*10^{-5}$	$4.6*10^{-5}$	$7.8*10^{-6}$	$2.1*10^{-5}$
Upper 95 % confidence limit of U_{free}	$9.5*10^{-5}$	$6.1*10^{-5}$	$6.4*10^{-5}$	$2.0*10^{-5}$	$5.3*10^{-5}$
Average number defective particles per FE		0.64		0.12	

Mechanical Behavior

Crushing strength is the strength required to crush a sphere between two parallel steel sheets, vertical or parallel to its equator plain. Respective measurements are shown in Fig. 10.

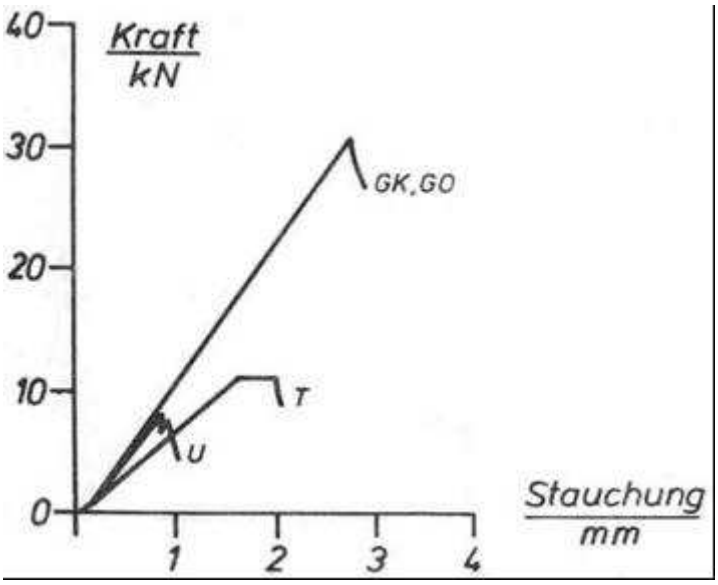

Figure 10 : Crushing strength vs. compression length during a crushing test [Wimmers 1977]

The drop survival ability is the number of drops survived from a height of 4 m onto a densely packed pebble bed of graphite balls. Specification of the drop stability is that with 95 % probability, at least 99.5 % of the spheres must survive at least 50 drops.

The corrosion resistance is measured in a standardized test, where spheres are exposed over 10 h to flowing helium – formerly (up to AVR reload charge 4) argon – containing 1 vol% of H_2O at a temperature of 900°C and 1000°C, respectively. Specification limits are mean values of 1.5 mg/(h cm^2) at 1000°C and 0.4 mg/(h cm^2) at 900°C. Results of measurements at 1000°C showed that the number of balls found with a higher corrosion rate than specified decreased significantly, reload charge 3: 20 %; reload charge 4: 17 %; reload charge 5: 0.5 %; all GO variants: 0.005 % [Wimmers 1977].

Measurements for the above properties of the different fuel element types are given in Table 10.

Table 10 : Mechanical characteristics of unirradiated AVR fuel spheres [Wimmers 1977]

Fuel type	Corrosion rate at 900/1000°C [mg/(cm^2 h)]	Drops survived from 4 m height onto pebble bed	Crushing strength || / _|_ [kN]
UCC	0.025 / 0.3	551	
T	0.12 / 0.3	660	
GK	0.34 / 1.44	543	21.8 / 24.2
GO	0.26 / 1.18	703	23.5 / 24.9
GLE-1	0.22 / 1.2	346	21.7 /
GLE-2	0.22 / 1.2	230	18.9 /
GFB-1	0.1 / 0.95	380	21.2 / 22.0
GFB-2	0.1 / 0.95	319	19.9 / 21.1
GO-THTR-1	0.15 / 1.07	470	23.5 / 24.8
GO-THTR-2	0.12 / 1.02	~ 470	~ 24 / ~ 25

3.1.2 THTR Fuel Properties

Free Uranium

Due to the manufacture procedure for THTR fuel, the fraction of uranium outside the particle kernels is comparatively high. From fuel quality control measurements on 770 fuel elements (see Fig. 11), the contamination of the A3-3 matrix material was derived to have an average fraction of $3.0*10^{-4}$ of the total inventory with a standard deviation of $0.7*10^{-4}$ [Röllig 1991].

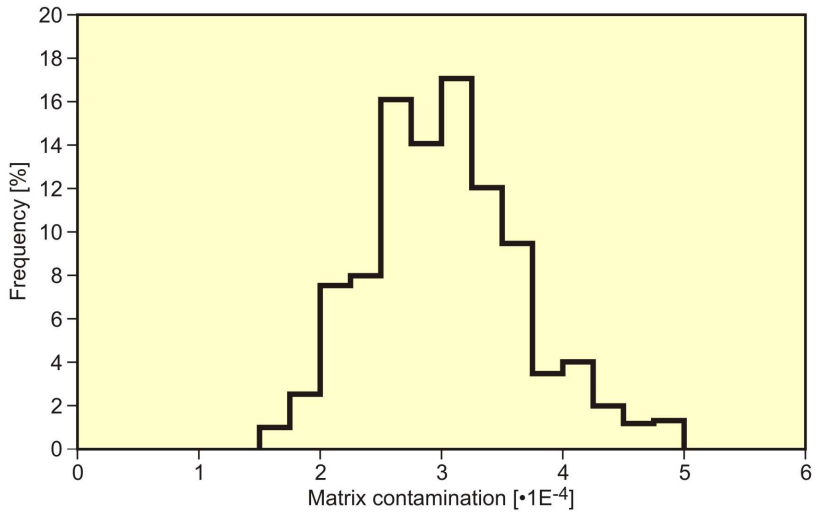

Figure 11 : Uranium contamination measured on 770 fresh THTR fuel spheres [Röllig 1991]

The U contamination in the outer PyC is $1*10^{-3}$; the fraction of manufacture-induced defective coated particles is $< 2*10^{-5}$ [Huschka 1978].

Crushing Strength

Measurements of the crushing strengths of unirradiated THTR fuel elements is presented in Fig. 12 showing a normal distribution around a mean value of 23 kN. For comparison, the results of irradiated AVR spheres are also shown. This parameter was of particular concern for the THTR due to its 42 control rods penetrating directly the pebble bed.

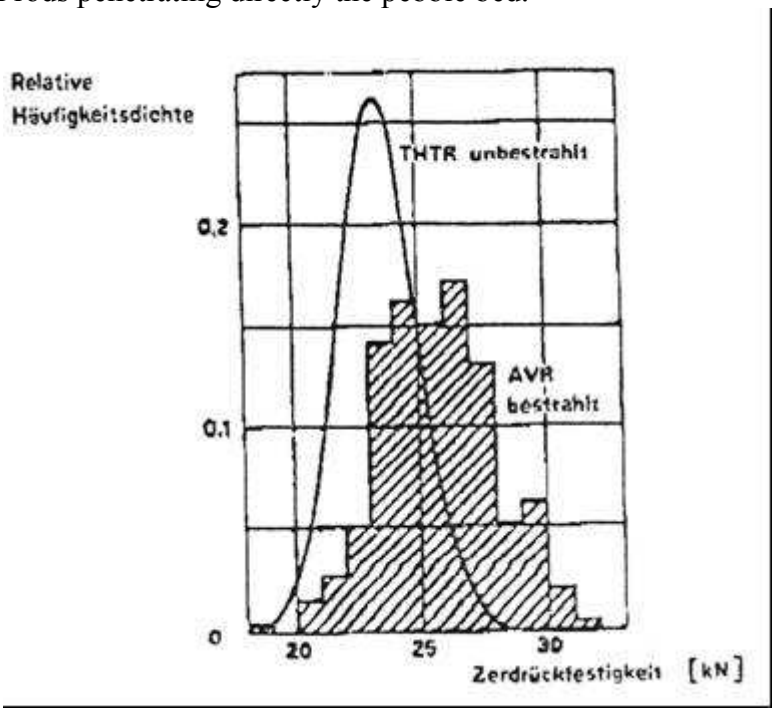

Figure 12 : Comparison of crushing strength distribution of irradiated AVR fuel elements with unirradiated THTR fuel elements [Kleine-Tebbe 1988]

3.1.3 Dragon Fuel Properties

Free Uranium

Fig. 13 shows clearly the tendency of decreasing fraction of free uranium in the Dragon fuel with growing experience with the fabrication [Howard 1978]. One method which led to a reduction in the U_{free} level was to sieve out under-sized particles (with incomplete coatings). Fig. 14 shows for early fuel production inclusions of free uranium in the pyrocarbon coating [Lefevre 1969].

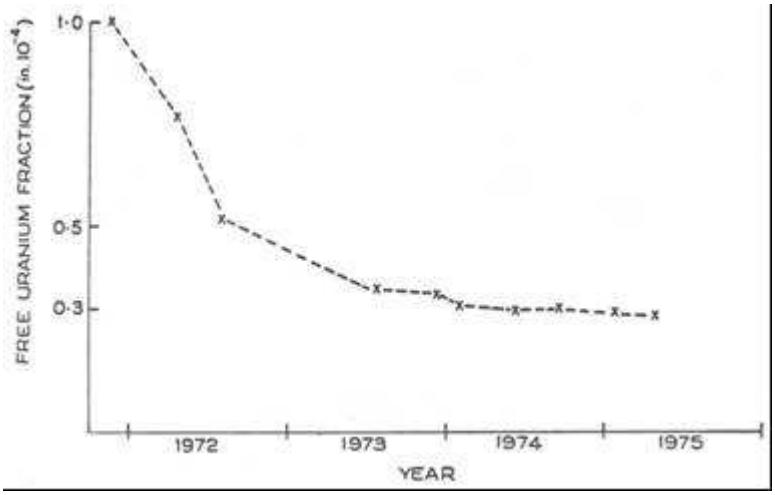

Figure 13 : Free uranium fraction in Dragon driver fuel [Howard 1978]

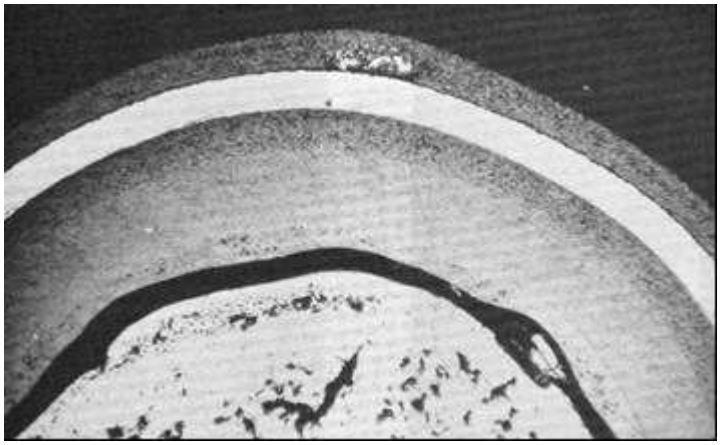

Figure 14 : Uranium contamination of the outer PyC layer

Corrosion Resistance

Corrosion testing with Dragon fuel was conducted by heating some 1000 loose particles to 1000°C and exposing them to an argon atmosphere containing typically 8000 vpm of water vapor, and inspecting them afterwards. Tests have shown that type and degree of corrosion attack on the oPyC varied for different coating batches, whereas an intact SiC layer demonstrated its superior ability of protecting the kernel against corrosion. The type of attack was first a discoloration of the outer surface, then pitting (see Fig. 15), before finally a disintegration of the particle occurred. An example of corrosion rates is given in Fig. 16 for particles from the so-called “Fourth Saclay Series” exposed to argon containing 8000 vpm of water vapor [Pollitt 1968].

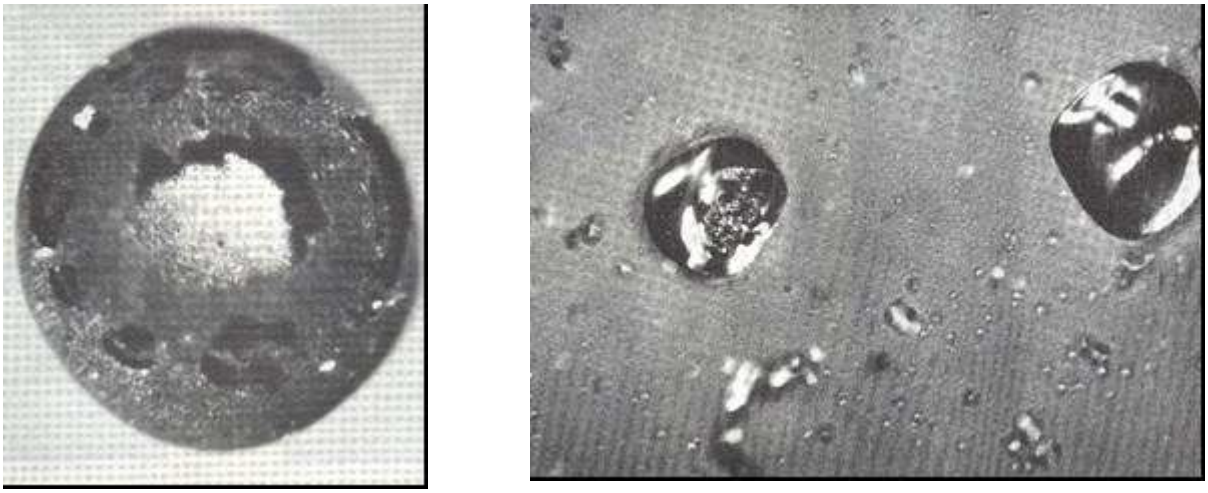

Figure 15 : Corrosion effects on particles
[Pollitt 1968] pitting with still intact SiC underneath (left), fragmentation (right)

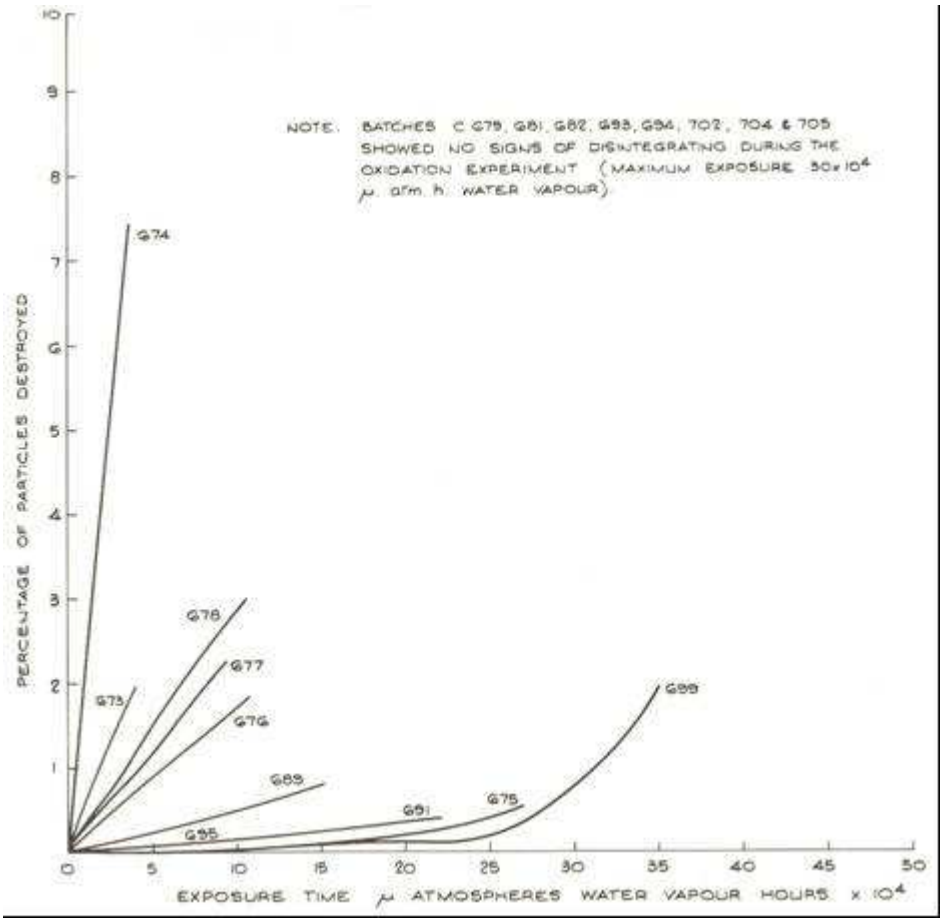

Figure 16 : Particles destroyed by oxidation vs. time of exposure to argon containing 8000 vpm of water vapor (particles from the so-called "Fourth Saclay Series")
[Pollitt 1968]

3.2 Operation Performance of HTGR Fuel

3.2.1 HTGR Fuel Performance in the French Irradiation Program

Overview of the Irradiation Program

Some irradiation tests are summarized in Table 11 . The program objectives were to study :

- the behavior of the particle, compact or fuel block under irradiation,
- fission product migration under normal and accidental operating conditions,
- specific properties including graphite creep.

The CEA reactors used were [Ballagny 1976] :

- SILOE (Grenoble) pool type thermal power : 35 MW
- OSIRIS (Saclay) pool type thermal power : 70 MW
- RAPSODIE (Cadarache) fast neutrons thermal power : 40 MW
- PEGASE (Cadarache) pool type thermal power : 30 MW

With respect to the GF experiments in SILOE, an initial irradiation campaign (GF1, GF2 and GF3) was performed at the beginning of 1975 [Blanchard 1978] with the following aims :

- Obtain more precise information about the performance limit pf the UC_2 TRISO particle ;
- Qualify both TRISO and BISO particles with $(U,Th)O_2$ and ThO_2 kernels, respectively ;
- Assess methods for inhibiting fission product release ;
- Qualify the French HTR fuel fabrication technology.

GF4 irradiation began with UC_2 TRISO particles in April 1975 and ended 15 months later after reaching high burnup (nearly 75 % FIMA). GF5 irradiation lasted 12 months under operating conditions comparable to those of GF4 (burnup), but with UC_xO_y TRISO particles. The GF6 experiment [Blanchard 1980a] began in June 1977 to qualify the fuel composed of fissile UC_xO_y TRISO and fertile ThO_2 particles. A burnup of nearly 75 % FIMA was obtained for the fissile materials. GF7 irradiation [Blanchard 1980b] ended in October 1979 with a burnup of nearly 70 % FIMA with UO_2 TRISO particles.

The CORAIL experiments were carried out in SILOE (1 and 2), OSIRIS (3 and 4) and finally in a fast reactor, RAPSODIE, (5 to 7). CORAIL 6 and 7 [Janvier 1973] were performed to evaluate the mechanical strength of heavily irradiated coated particles as a function of the deposition parameters. Coated particles were irradiated between 800 and 1200°C.

Table 11 : Irradiation experiments in France

Reactor	Irradiation	Kernel	Particles	Compacts	Temperature [°C]	Burnup [% FIMA]
OSIRIS	Corail 3	UO_2	8150	No	1100 - 1300	5.5
OSIRIS	Corail 4A	UO_2	8000	No	1090 - 1245	7.4
OSIRIS	Corail 4B	UO_2	8000	No	1090 - 1245	2
OSIRIS	RHT 0		6500		850 - 1100	2.26
OSIRIS	RHT 1		4410		1250	7.1
OSIRIS	RHT 3		11000		850 - 1250	10
OSIRIS	RHT 4		2800		1000 - 1330	
RAPSODIE	Corail 5	UO_2	3100	No	930 - 1300	0.13
RAPSODIE	Corail 6 A/B	UO_2	12500	No	800 - 1200	1.05
RAPSODIE	Corail 7	UO_2	12480	No	800 - 1200	0.5
SILOE	Corail 1	UO_2	1000	No	1000	6.1
SILOE	Corail 2	UO_2	950	No	>1400	4.5
SILOE	GF0	UO_2	2500	15	1050	1.7
SILOE	GF1	$(U,Th)O_2$ ThO_2	Yes	6	1250	9.7
SILOE	GF2	$(U,Th)O_2$ ThO_2	Yes	6	1050 to 1250	7.6
SILOE	GF3	$(U,Th)O_2$ ThO_2	Yes	6	1100	11.4
SILOE	GF4	UC_2 UC_xO_y	Yes	6	1100	75.5
SILOE	GF5	UC_2 UC_xO_y	Yes	6	1050 - 1250	74.6
SILOE	GF6	UO_2 $(U,Th)O_2$ UC_xO_y	Yes	4	1250 - 1500	75
SILOE	GF7	UO_2 $(U,Th)O_2$	Yes	8	1050 - 1300	70
SILOE	INDIGO	(UO2 + C) ThO_2	10800	6	1150	

The data reviewed here concern the physical and chemical evolution of HTR fuel that could potentially impact the long-term behavior of packages in a nuclear waste repository. They are based mainly on the results of experimental irradiations, post-irradiation examinations, and specific studies by the Centre d'Etudes Nucléaires de Grenoble, CENG in the experimental reactors SILOE and SILOETTE, in some cases jointly with General Atomics. The results concerning the behavior and evolution of the fuel under irradiation were of particular interest for the experimental part of the present study, for which a few of the remaining irradiated sample lots were transferred to Atalante in December 2006.

Dimensional Variations

In the reactor, the compacts, particles and kernels were subject to dimensional variations, of variable sign and amplitude depending on the irradiation conditions, especially the neutron fluence and temperature. Contraction of the compacts is generally observed at the beginning of irradiation. Various contributions to this phenomenon have been identified related to the irradiation behavior of the graphite matrix, the porosity, and the particles.

During experiments GF1, GF2 and GF3 carried out at CENG on compacts containing fissile particles (mainly $(U,Th)O_2$ or occasionally UCO) and fertile particles (ThO_2), the following phenomena were observed concerning the graphite matrix of the compacts [Kovacs 1980]:

- strong dependence on the neutron fluence;
- large contraction, reaching a maximum for fluence levels below $4*10^{25}$ m^{-2} (at 1100°C);
- contraction to a lesser extent when the compact contained only TRISO particles (compared with compacts containing both TRISO and BISO particles).

The variation of the compact volume V is given by the following relation according to the diameter D and length L:

$$\frac{\Delta V}{V} = \frac{2\Delta D}{D} + \frac{\Delta L}{L}$$

The diameter and length variations are not the same due to the anisotropy and its evolution under irradiation. The maximum reached at a fluence of $3.5*10^{25}$ m^{-2} for a TRISO-only compact was about:

$\Delta L/L$ = –1.1 %
$\Delta D/D$ = –1 %
i.e., $\Delta V/V$ = –3.1 %

Irradiating HTR-10 pebbles containing particles with enriched UO_2 kernels, resulted in diametral variations [Tang 2006] of –0.58% perpendicular to and –0.7% parallel with the direction of press compaction for a neutron fluence of $1.3*10^{25}$ m^{-2} at an irradiation temperature of 1000°C. The shrinkage was greater when the irradiation temperature was increased to 1200 and 1250°C. These variations are consistent with the data from the GF experiments in SILOE, at comparable fluence values. Fig. 17 taken from [Kovacs 1980], shows the variations measured during post-irradiation examinations on capsules GF1, GF2 and GF3.

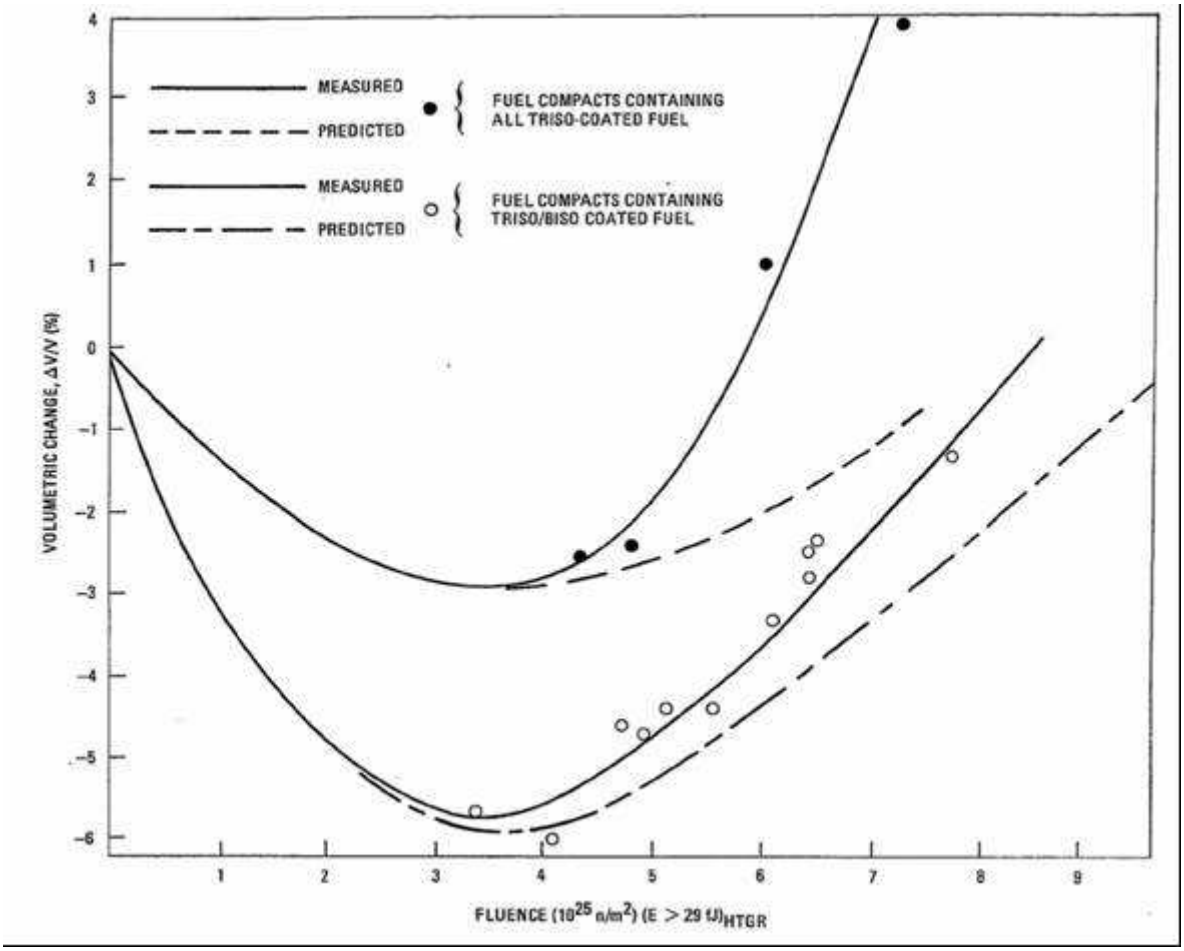

Figure 17 : Predicted and measured volume variations in compacts versus neutron fluence [Kovacs 1980]

At higher neutron fluence values, the graphite matrix expands, with relative volume variations exceeding 1 % for a fluence higher than $6*10^{25}$ m^{-2}. These variations are attributable mainly to elongation of the compacts.

During the GF4 experimental irradiations, a fast neutron fluence of $11*10^{25}$ m^{-2} was reached at an irradiation temperature of 1100°C. Two types of compacts were tested :

1. fissile UC_2 VSM TRISO particles and fertile ThO_2 TRISO particles
2. fissile UC_2 WAR TRISO particles and fertile ThO_2 BISO particles

The dimensional measurements results reported in [Blanchard 1977] are indicated in table 12.

Table 12 : Dimensional variations of GF4 compacts under neutron irradiation

Type of compact	Longitudinal variations $\Delta L/L$ [%]	Diametral variations $\Delta D/D$ [%]	Volume changes $\Delta V/V$ [%]
1 (TRISO/TRISO)	+0.61	–0.57	–0.53
1 (TRISO/TRISO)	+0.81	–0.44	+0.07
2 (TRISO/BISO)	–0.67	–1.46	–3.59
2 (TRISO/BISO)	–2.51	–3.04	–8.59

The dimensional variations were similar, but both the contraction and expansion were smaller than for the GF1, GF2 & GF3 experiments at the same neutron fluence. The main differences were:

- the nature of the fissile particle kernels,
- the fissile particle burnup ranging from 5 to 11.4 % FIMA for the initial GF experiments and reaching a mean value of 70 % FIMA for irradiation GF4.

The volume reduction of the TRISO coated particles was also maintained over the entire fluence range from 3 to $9*10^{25}$ m^{-2}, and reached –3 to –4 % for irradiation at 1100°C. The contraction was much larger for BISO particles, up to –18 % for equivalent fluence and temperature values. The graphite matrix behavior is thus the only component capable of accounting for the expansion of the compacts.

Kernel Volume Expansion

Under irradiation, fissile nuclei exhibit solid swelling due to fission reactions producing two nuclei, as well as to the formation of gas bubbles. This phenomenon has been widely investigated in UO_2 and MOX PWR fuel. The extent of the changes is primarily a function of the burnup which produces significant changes in HTR fuel.

The TANGO experiments in the SILOE reactor were carried out to investigate this phenomenon according to the burnup, the irradiation temperature, and the initial porosity. The experiments were carried out with UO_2 kernels with 25 % U-235 enrichment for burnup values between 2 and 6 % FIMA, at temperatures ranging from 400 to 700°C. The results are described briefly in [Bruet 1980]. The volume expansion and porosity data in Table 13 correspond to samples with an initial porosity of 4.7 %.

Table 13 : Volume expansion of irradiated UO_2 kernels

Burnup [GWd/t_{iHM}]	Irradiation temperature [°C]	Volume expansion [%]	Porosity [%]
15	700	1.1	5.6
15	500	1.3	5.8
15	360	1.3	5.9
30	770	2.8	7.2
30	610	2.8	7.3
30	460	3	7.4

Increased porosity was systematically observed, apparently related to the increasing burnup.

The in-reactor solid swelling can be estimated at about 0.09 % per 1 GWd/T_{iHM}, or nearly 1 %/ % FIMA. It may also be noted that the volume expansion was inversely proportional to the initial porosity. A kernel with an initial porosity of 1.6 % was subject to 3.4 % bulk swelling after irradiation to a low burnup of 3 % FIMA at 770°C. The porosity also increased to a greater extent, reaching about 4.8 %. The irradiation temperature appears to have a very limited role, at least below 1000°C. Most of the fission gases are concentrated in bubbles that take part in swelling only when they have grown to sufficient size.

These values are in good agreement with the experimental results reported in [Petti 2002]. In these experiments, LEU particles with UO_2 kernels enriched to 8 % were compared with UCO kernel particles enriched to 93 %. Their volume expansion ranged from 0.6 to 1.5 % per 1 % FIMA because of intergranular fission gases bubbles. Theoretical estimations by Olander as part of this study indicated a volume expansion of only 0.3 to 0.45 % per 1 % FIMA. For a burnup of 20 % FIMA, the kernel volume increase under irradiation in the reactor could reach as much as 30 %.

Figure 18 :18 shows the mean kernel volume expansion versus burnup. The volume expansion results in a gas overpressure in the particle. At high burnup, the volume expansion reduces the free volume in the internal pyrocarbon layers, increasing the risk of direct interaction between the kernel and the SiC coating and thus the potential risk of rupture.

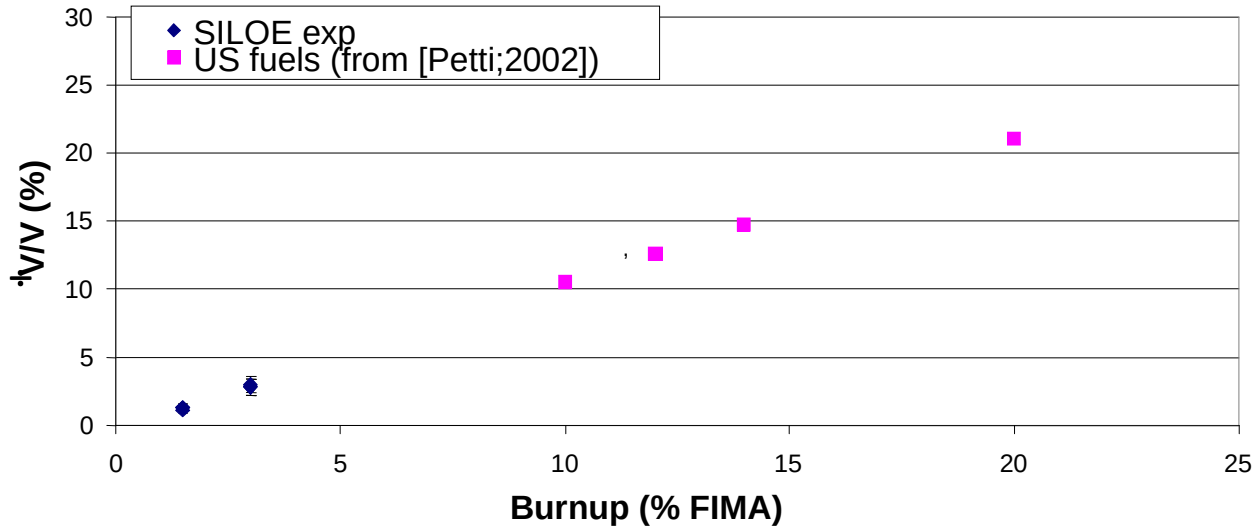

Figure 18 : Mean UO_2 kernel volume expansion versus burnup

Migration of Fission Products

After irradiation, some migration of solid and gaseous fission products is also systematically observed in the internal PyC layers. The SiC layer then systematically retains all these elements inside the particle [Millet 2001, Chapelot 2001]. Nevertheless, the nature of the fission products in the internal layers and their migration depends to a considerable extent on the type of fissile kernel.

The CEA conducted irradiation campaigns as part of the CORAIL experiments on particles containing UO_2 kernels with a burnup of 6 % FIMA and a low-level fast fluence ($0.9*10^{25}$ m^{-2}) at an irradiation temperature of 1250°C. Electron microprobe analysis revealed significant cesium migration to the SiC layer, whereas the other volatile fission products (Xe, Mo, Ba, Nd, I) were stopped by the internal pyrocarbon layer [DMG 1973, DMECN 1978]. Fig. 19 shows the profiles obtained along a particle radius. Although the proportion of some solid fission products that migrated outside the kernel was limited (but nevertheless represented several percent of the inventory formed under irradiation), the fission gases were almost entirely released in the particle at burnup exceeding 70 GWd/t, resulting in substantial overpressure in the particle. This was also the case for iodine and cesium.

Similarly, analysis of irradiated HTR-10 fuel [Tang 2006] showed high Cs mobility in the internal pyrocarbon layers extending to the SiC layer. For a burnup of 10 % FIMA and an irradiation temperature of 1000°C, however, the cesium inventory outside the kernel represented only 1.5 % of the total inventory created by irradiation in the kernels.

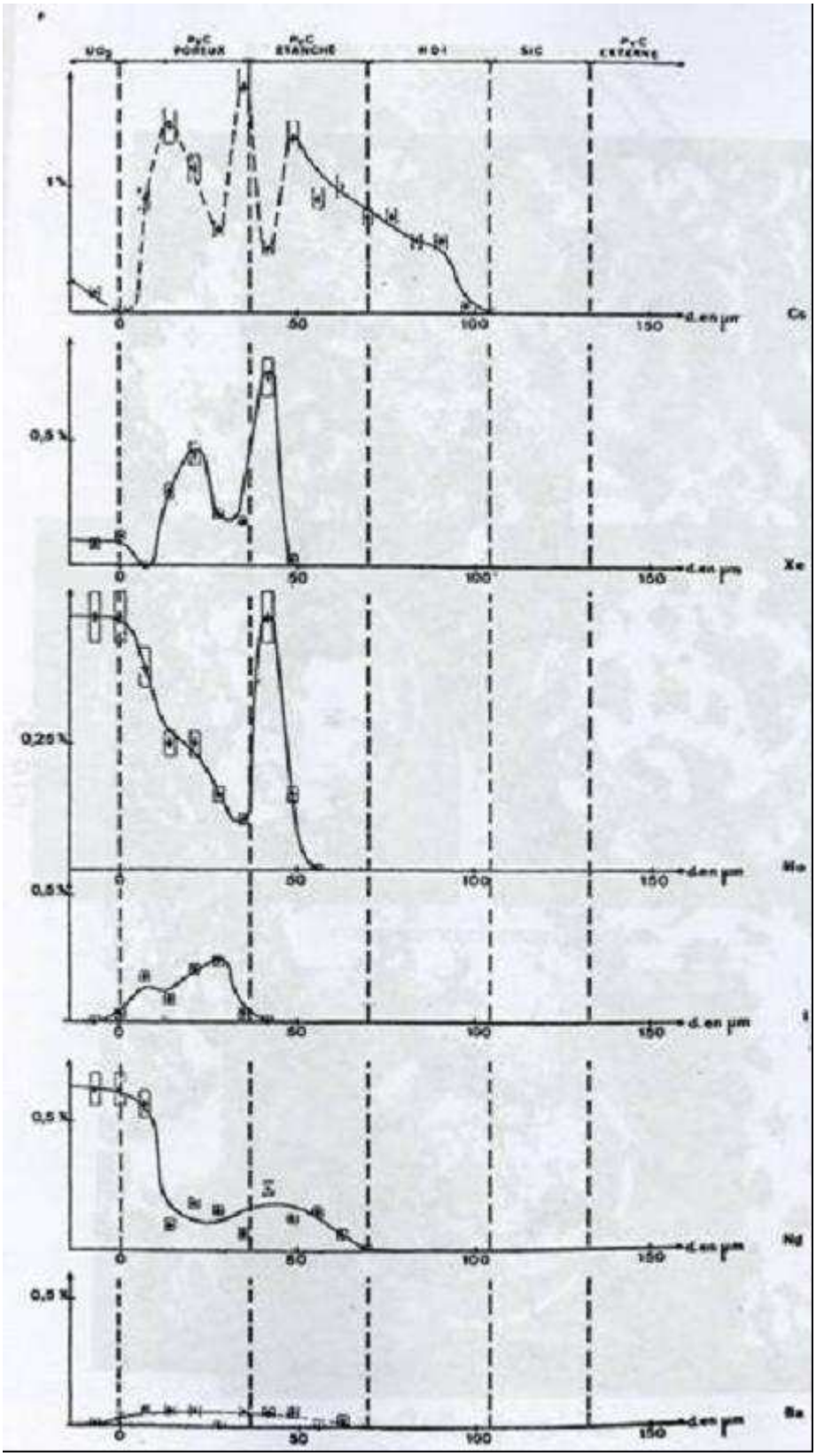

Figure 19 : Fission product release in coating layers surrounding the UO_2 kernel (CEA CORAIL experiments)

The work described in reference [Förthmann 1975] compares the behavior of fission products under irradiation in different kernels: oxide (TRISO UO_2 particles) or carbide (BISO UC_2 particles). As shown in Fig. 20, taken from that article, the major solid fission products exhibited high mobility in particles containing a UO_2 kernel, and their behavior with respect to the different layers was similar. The rare earth elements are in a different chemical state in the case of a carbide kernel, and exhibit a high release rate. In that study, however, the irradiation conditions were very severe, with a burnup of 50 % FIMA at a temperature of 1300°C.

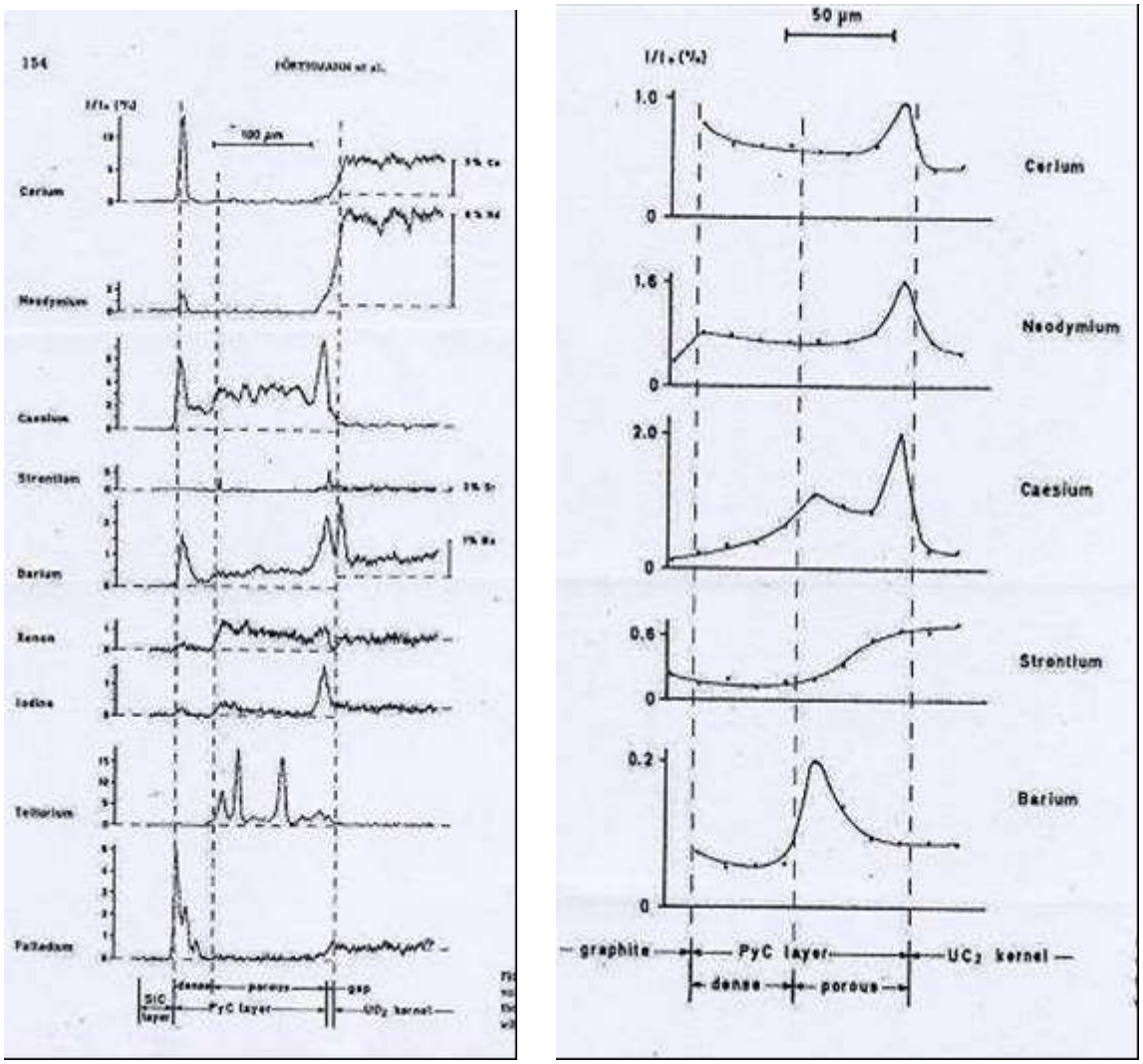

Figure 20 : Comparison of fission product release between carbide kernel and oxide kernel particles [Förthmann 1975]

The behavior of particles with mixed oxide kernels $(U,Th)O_2$ was also studied in the course of the GF1, GF2 and GF3 experimental irradiations in SILOE. According to [Kovacs 1980], this type of particle generally exhibited better fission product retention, apparently trapped in the high porosity created in the kernel under irradiation.
Carbide UC_2 or UCO kernels were also studied during these experimental irradiations and compares with mixed oxide $(Th,U)O_2$ kernels. The greater mobility of metal fission products

toward the pyrocarbon and SiC layers was confirmed. The following conclusions can be drawn from these experimental irradiations :

- Most of the volatile FP (especially Cs) systematically migrate, making the SiC layer necessary for use in the reactor ;
- The oxide kernels (UO_2) and carbide kernels (UC_2 and UCO) exhibit increased migration of metal FP, which reach the IPyC/SiC interface ;
- No migration was observed with carbide UC_2 and mixed oxide $(8Th,U)O_2$ kernels (amoeba effect).

For some fission products such as palladium, migration leading to interactions with the SiC layer can result in the formation of corrosion zones at the irradiation temperatures, embrittling the coating by local thinning. This phenomenon was reported in [Förthmann 1975] with oxide and carbide kernels as shown in Fig. 20. Modeling the impact on the failure rate [Miller 2006] showed that corrosion of the SiC layer by fission products results in local thinning with little effect on the resistance of the layer to overpressure, all other conditions being equal, especially with regard to the dense pyrocarbon layers.

Fission Gas Behavior

Fission gas behavior in the particles was a subject in the past of investigation and experimental irradiations by the CEA. The results obtained are in good agreement with published data and suggest that fission gas release depends mainly on the burnup. Virtually all fission gas is released above 8 % FIMA as shown in Fig. 21 which summarizes various tests on HTR fuel with different burnup values [Blanchard 1972]. Fig. 22 reflects this trend in terms of the partial pressure at room temperature. Under these experimental conditions, for burnups higher than 12 % FIMA, the partial pressure may reach about 8 MPa.

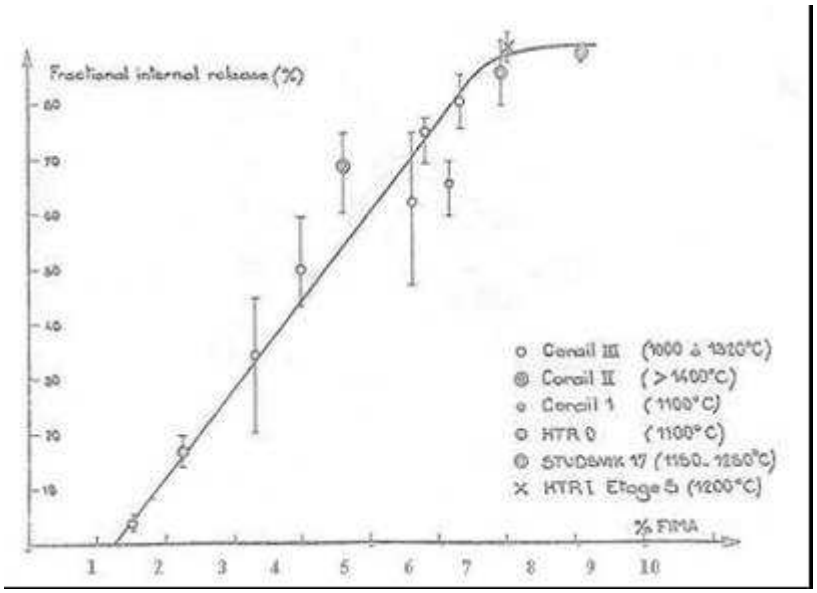

Figure 21 : Fission gas release versus burnup
[Blanchard 1972] (Abscissa is from 0 to 10 % FIMA)

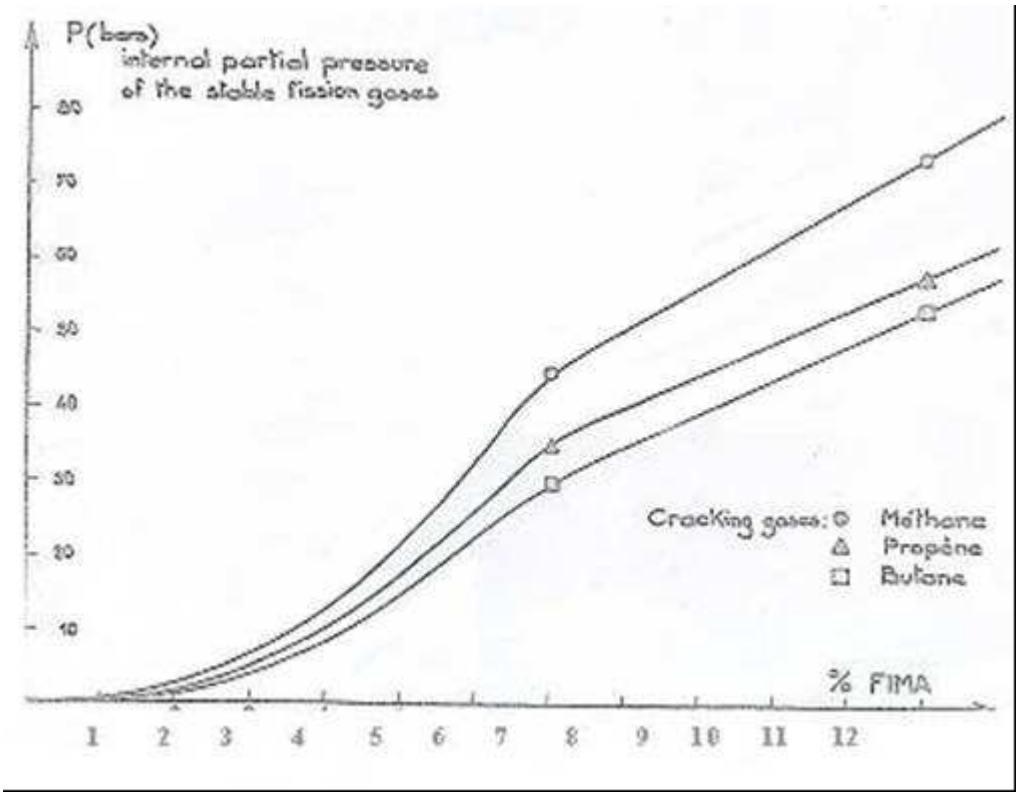

Figure 22 : Fission gas partial pressure in HGTR particles [Bruet 1972] (Abscissa is from 0 to 12 % FIMA)

Another study [Chénebeau 1972] showed that the initial kernel porosity can potentially have a major effect on the fission gas fraction released inside the particle in the reactor. UO_2 kernels with initial porosity values of 5, 16 and 20% were compared, and the release was found to be related both to the fission density and to the specific surface area. The temperature (between 700°C and 1400°C) did not appear to affect the results.

Moreover, because of the presence of graphite inside the UO_2 kernel fuel particles, fissions result in the formation of CO and/or CO_2. Thermodynamic calculations indicate that this production can be significant, leading to overpressure values exceeding those due to fission gases [Gossé 2006]. This production depends on the burnup and on the irradiation temperature.

Nevertheless, experimental studies and CO analyses to date have yielded substantially lower gaseous CO balances. Fig. 23 shows the CO partial pressure in a particle containing a UO_2 kernel 500 µm in diameter with 10 % enrichment, based on the thermodynamic data in [Petti 2002]. This variation with the irradiation temperature was calculated for burnup values near 100 GWd per ton of initial heavy metal. An overpressure exceeding 8 MPa will quickly be reached with this type of particle fuel. Moreover, above 1400 K, this phenomenon is accompanied by an amoeba effect resulting in the displacement of the kernel toward the SiC coating. However, experimental studies do not give values as high as those predicted by thermodynamic calculation.

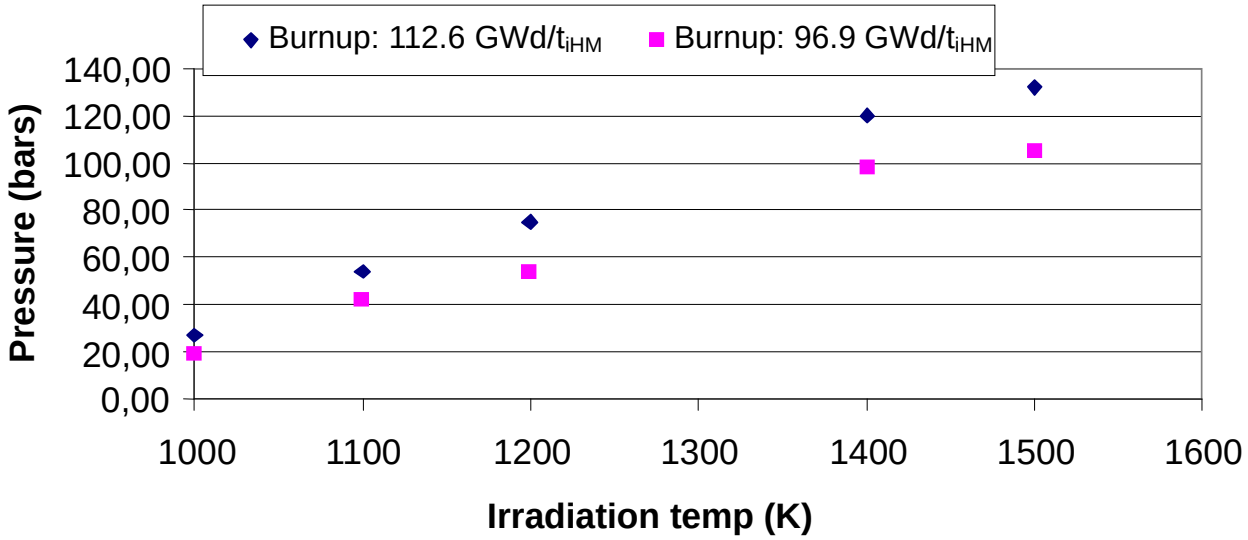

Figure 23 : CO partial pressure in a UO_2 kernel particle versus temperature [15]

According to the same author, in carbide fuel with UCO kernels, the CO production remains very low, less than 20 kPa for a burnup of 200 GWd/t and a temperature of 1400 K (computed for a UCO kernel with 200 µm diameter and a density of 10,500 kg/m^3).

In addition, no amoeba effect was observed during the SILOE irradiation campaigns (GF experiments), nor in the literature for kernels of this type. During the CORAIL experiments, CO pressures below 0.1 MPa were measured at a temperature of 1500°C in unirradiated UO_2 kernel particles with 20 % enrichment [DMG 1973, DMECN 1978].

Particle Failure Rate

Examinations on removal from the reactor generally show only a very small fraction of particles damaged or ruptured under neutron irradiation, resulting in very limited fission gas release [Millet 2001]. Various types of fuels and particles were tested during the GF1, GF2, GF3, GF4 and GF5 irradiation campaigns in the SILOE reactor at CEN Grenoble. The failure rates were inferred from measurements of fission gas release (Kr and Xe). Comparisons are generally established between direct measurements during irradiation and re-irradiation at high temperature and are based on laser analyses of failed particles. The analyses generally concern Kr-85m, a short-lived isotope of krypton, and are expressed as an R/B ratio.

The first three series of experiments concerned free particles and compacts with mixed oxide $(U,Th)O_2$ kernels. The irradiation conditions were very similar, with a burnup of between 7 and 11 % FIMA at temperatures between 1000 and 1250°C. The principal results obtained in [Kovacs 1980] show that the best performance was obtained with the smallest kernels (400 µm in diameter) or with a thicker buffer (more than 100 µm). The particle failure fraction in the compacts under these conditions was less than 1.8 % for TRISO fissile particles.

For the GF4 irradiation tests with free particles containing TRISO UC_2 or UCO kernels [Blanchard 1977], no failures were observed in any of the lots of 1280 units. These irradiations were carried

out at 1100°C in a high neutron flux with a burnup near 70 % FIMA, for a fluence of $11*10^{25}$ m^{-2}, but the particles had small-diameter kernels (300 µm).

Irradiation GF6 [Blanchard 1980a] was performed under extreme temperature and burnup conditions (60 % FIMA at 1500°C and 75 % FIMA at 1250°C) on particles with a UCO kernel of 300 µm in diameter. The failure fraction was nevertheless very low, less than 0.23 %. Conversely, major and more frequent deterioration of the external PyC layer was observed (5 % failure fraction at 1500°C).

Irradiation GF7 [Blanchard 1980b] involved UO_2 particles with a 780 µm diameter kernel and a thin (35 µm) porous layer. The burnup reached 70 to 80 % FIMA at 1300°C. A very high failure rate was obtained under these very unfavorable conditions, and was nearly systematic for certain lots (five with 93 % failure fraction). Given the nature and diameter of the kernel, and the irradiation conditions, major fission gas and CO/CO_2 production inside the particles also contributed to this high failure rate. The failure fraction was observed to be dependent on the irradiation temperature in these experiments.

More recently, HTR-10 fuel showed improved behavior and a very satisfactory ultimate tensile strength for irradiated particles [Tang 2006] consisting of a 500 µm UO_2 kernel combined with a 95 µm porous layer; the irradiations were carried out between 1000 and 1200°C with a burnup not exceeding 95 GWd/t. The failure fraction was estimated at 0.1 % rapidly increasing to 6 % for temperatures above 1600°C.

3.2.2 AVR Fuel during Operation

Qualification

An essential step of fuel qualification is irradiation testing of graphite, coated particles, and fuel elements. For the early German HTGR fuel production, the tests were conducted to investigate the mechanical strength of the spheres and particle failure rates under design operating conditions. The goals were to show that [Huschka 1978]:

- relative dimensional changes (diameter) are less than 2 % (or 1.2 mm);
- crushing strength remains above specification (lower limit: 18 kN);
- R/B of Xe-133 averaged over all temperatures and powers remains below $6*10^{-5}$.

The first core fuel of the AVR of UCC type, a US product, was irradiation tested in Oak Ridge. The test with three spheres finished in March 1965 at a burnup of 5.1 % FIMA revealed a release fraction of long-lived fission gases of $< 2*10^{-4}$ which was lower than the required limit of $5*10^{-4}$. PIE of two of the three balls did not show a coating defect in the examined 173 and 176, respectively, examined particles. Another test finished in February 1966 was done with loose particles at 1300°C to a burnup of 10.1 % FIMA. The measured R/B of Kr-88 was $4.7*10^{-5}$.

The first reload charge for the AVR, the wall paper (T) fuel elements of German production, was irradiation tested in the Dragon reactor. Seven fuel spheres were irradiated over 100 efpd and reached 7 % FIMA burnup and $1.2*10^{25}$ m^{-2}, E>0.1 MeV, fast neutron fluence, respectively. A 3 %

failure fraction of the coated particles was observed presumably due to a strong shrinkage of the binder in the matrix material. This is why only a limited number of T-type fuel elements was allowed to be given into the AVR core.

First testing of the pressed-type fuel concept was done in the Material Test Reactors (MTR) at Studsvik (R2) and at Dragon. MTRs offer the possibility of accelerated testing under well defined conditions typically at or even beyond maximum design operating conditions. The tests R2-K1 and DR-K2 with carbidic fuel (GK) were dedicated to qualifying German fuel of the pressed type to be compared with the wall paper type and different annular gap variants. The pressed type balls appeared to be the economically and technically most promising type resulting in the insertion of 2 pressed spheres in the experiment R2-K1 for the purpose of irradiation to the AVR design limits of 11 % FIMA burnup and $2.2*10^{25}$ m^{-2}, E>0.1 MeV, fast neutron fluence. Details on these tests are summarized in Table 10. Main result was that no damage was observed neither to the particles nor to the fuel balls. In addition, fission gas release remained very low (see Table 14).

Maximum bouncing force of a ball is the force when bouncing in a free fall from a height of 1 m onto a steel sheet. From the height to which the ball is bouncing back, the elasticity module can be estimated.

After these successful tests, the production of ~ 50,000 GK fuel elements to follow the UCC and T sphere types was initiated [Ragoss 1975]. For all later irradiation testing, the AVR reactor itself became test bed for the different variants developed such as oxidic fuel (GO), LEU cycle fuel (GLE), fissile/fertile particle systems (GFB) as well as the original THTR fuel design.

Operation

The AVR reactor was an indispensable mass test facility for all development steps of spherically shaped HTGR fuel. Table 15 gives the achievements in terms of burnup and fast neutron fluence for the different fuel types and variants, respectively. Burnup data are based on measurements or best estimates. The corresponding fast fluences have been derived from Fig. 24 showing the calculated relationship between burnup and fast neutron fluence.

Table 14 : Irradiation testing of pressed fuel spheres for AVR [Ragoss 1975]

Test	Date	Irr. time [efpd]	Max. irr. temperature [°C]	Burnup [% FIMA]	Fast fluence [10^{25} m^{-2}, E>0.1 MeV]	Max. power [kW]	Fuel composition	Kernel diameter [µm]	Number of cp
DR-K2 (8 balls)	Jan 67 – Mar 68	224	1170 (surface)	5.1-8.2	0.8-1.5		$(Th,U)C_2$	~ 400	76,500
R2-K1/1	Mar 68 – Sep 68	111.4	1250	10.3	2.1	3.0	$(Th,U)C_2$	~ 400	6000
/2		111.4	1250	10.8	2.2	3.1	$(Th,U)C_2$	~ 400	6000

Table 15 : Irradiation achievements of the AVR fuel

Fuel			Begin insertion	Burnup [% FIMA]		Burnup [GWd/t]		Fast neutron fluence(3) [10^{25} m^{-2}, E>0.1 MeV]	
Type	Variant	Reload charge		Average	Maximum	Average	Maximum	Average	Maximum
1. HEU (5 g Th)	UCC	First core	Jul 1966	13.6(1)	23	124	210	3.1	7.8
	T	1-1, 1-2	Oct 1968 - Aug 1973	13.6(1)	22	124	200	3.1	7.3
	GK	3, 4, 5-1	Apr 1969 - Apr 1973	13.6(1)	25	124	230	3.1	9.0
	GO-1	5-2, 7, 6-1, 12, 14	Dec 1971 - Nov 1976	13.6(1)	23	124	210	3.1	7.8
	GO-2	15 20	Feb 1981 Oct 1985	16.0 7.5	19 11	146 68	173 100	4.0 0.8	5.7 1.8
	GO-3	18	Jul 1981	16.0	18	146	164	4.0	5.1
	GFB-3/4/5	13	Dec 1977 - Jul 1980	18.2(2)	20	166	183	5.3	6.3
2. HEU (10 g Th)	GFB-1/2	8	May 1974	10.0	12.5	91	114	3.8	5.5
	GO-THTR	9, 10, 11 22	Sep 1974 Sep 1986	10.0 2.0	12.5 -	91 18	114 -	4.0 0.4	5.7 -
3. LEU (20 g U)	GLE-1	6-2	Dec 1973	6.7	8.0	60	71	2.2	3.0
4. LEU (10 g U)	GLE-3	19	Jul 1982	8.5	10.0	76	89	2.2	3.0
5. LEU (6 g U)	GLE-4	21 21-2	Feb 1984 Oct 1987	11.0 3.5	14.0 -	9.8 31	125 -	1.7 0.3	2.6 -

(1) Average in retrospect deduced from the reactor integral power production
(2) For the bulk of this variant removed with the later accurate sphere measurement
(3) Deduced from calculated relations in Fig. 12

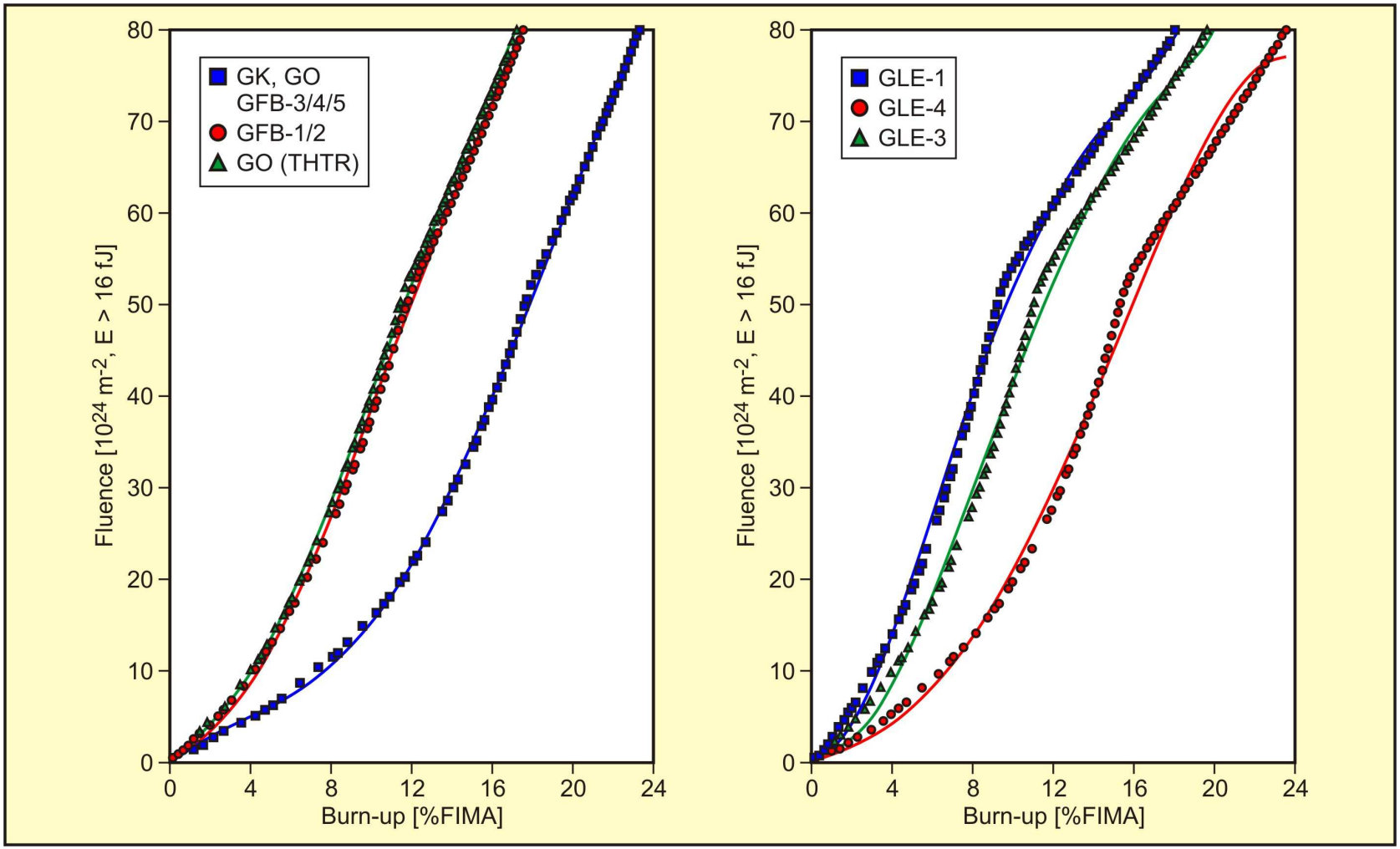

Figure 24 : Calculated fast neutron fluence vs. burnup for the AVR fuel element variants GK, GO, GFB (top) and GLE (bottom) [Werner 1984]

AVR Coolant Temperatures

Due to the flow direction of the coolant from the core bottom upwards, the strongest temperature load on the fuel was at the beginning after insertion into the core. Direct measurements of the coolant temperature, however, were only locally possible with usual techniques. Average coolant temperatures could be derived from coolant flow rates and power of the steam generator.

In order to measure the temperature of the coolant as directly exiting from the pebble bed, temperature monitoring balls were prepared and inserted into the core to flow with the pebble bed. In 1970, one fuel sphere and 16 graphite spheres were fabricated with melting bodies introduced in bore holes in both radial and tangential direction. The analysis showed surprisingly that the maximum helium temperature was at least 1000°C [AVR 1971a]. In 1972, 80 more monitoring balls were added to the core, 40 for gas and 40 for fuel temperature measurements. Drawback of these early tests was the difficulty to obtain individual core passage information for these monitor spheres and hints on where the temperatures were measured.

The experiment HTA-8 of September 1986 was also designed as a “melting wire test”. The specifically prepared A3 matrix spheres were fabricated in the same size of the fuel spheres, in which a set of 20 quartz capsules was inserted each containing a metal wire of a different metal alloy and expected to melt if a certain temperature were exceeded (see Fig. 25). A total of 190 of those monitoring spheres were added to the core, 102 of which through the central tube and 22 through either of the four outer tubes. At the time of insertion, the AVR was operated at full power and an average coolant outlet temperature of 950°C. They were x-rayed after discharge.

The results are shown in Fig. 26 revealing that from all inserted monitoring spheres, about 20 % had seen an unexpectedly high temperature of > 1280°C (where all wires melted). For most spheres added to the inner core, the maximum (coolant) temperature was around 1070°C. For spheres passing through the outer core zone, two distinct temperature levels could be identified: one at around 1100°C and another one at > 1200°C [Gottaut 1990].

Since it is possible to obtain the individual core passage information for each sphere, a more detailed evaluation in terms of coolant temperature profiles was conducted in the meantime, details of which will be published separately.

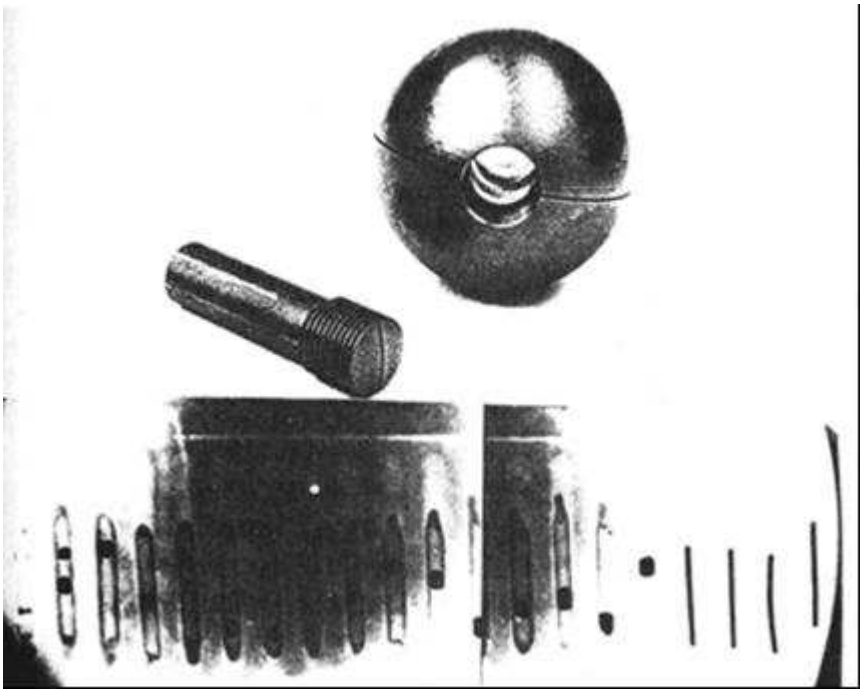

Figure 25 : Temperature monitoring sphere prepared for the HTA-8 experiment [Derz 1990]

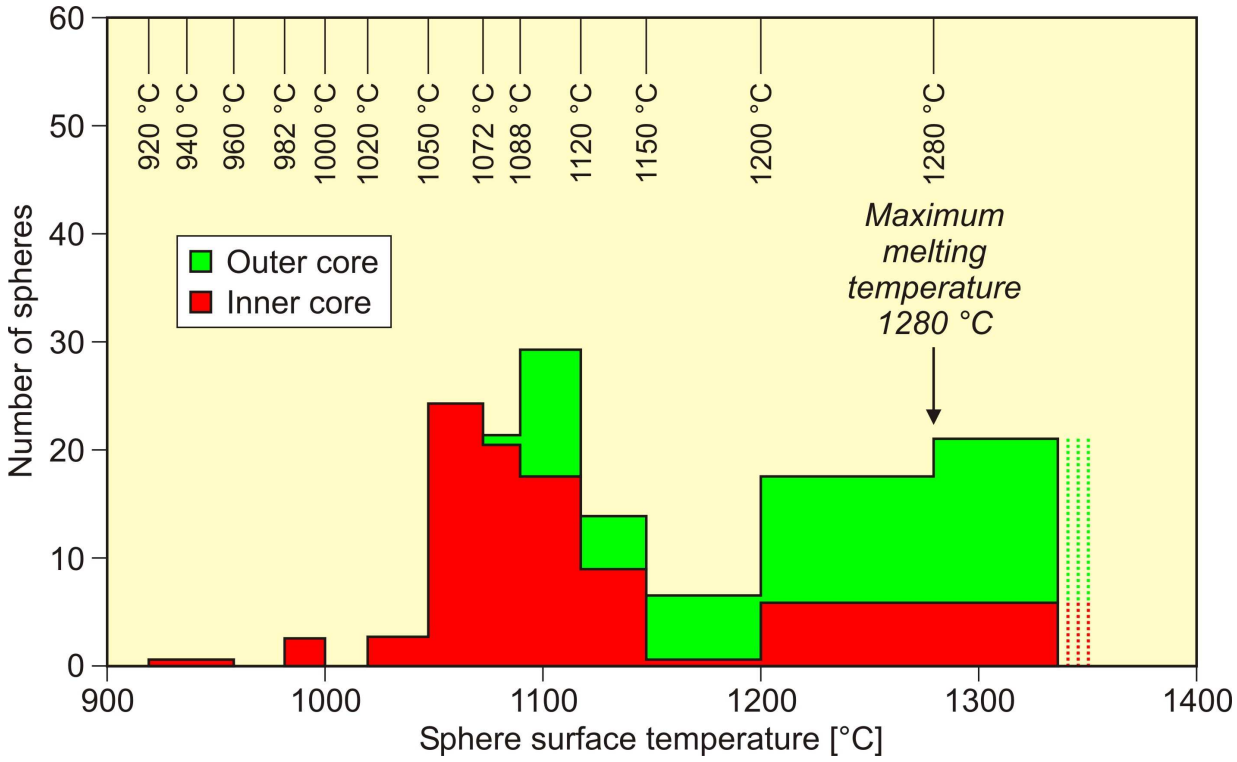

Figure 26 : Coolant temperature histogram measured with monitoring spheres in the experiment HTA-8 of September 1986

The shape of the thermal neutron flux profile in the core showing strong radial gradients is influenced by the side reflector graphite blocks, the two-zone core with more fissile material in the outer zone, and the control rod guiding noses. Together with the loading strategy, it influences the power density which has a direct effect on the fuel temperature distribution. Respective results calculated with the HTR2000 code are shown in Fig. 27. The agreement with the experimental results of HTA-8 is currently disputed.

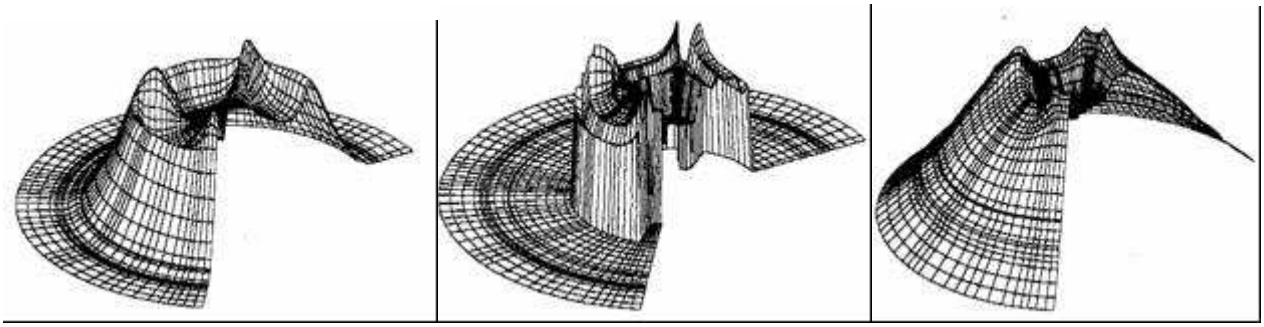

Figure 27 : Calculated distribution of thermal neutron flux (left), power density (middle), and temperature (right) in the AVR core

AVR Coolant Activities

The activity in the cooling gas was continuously measured. Its origin was mainly the heavy metal contamination in the matrix material of the fuel elements whose level has changed significantly over the long operation time of the AVR. BISO fuel exhibited with ~10^{-3} a comparatively high level of matrix contamination. The measured coolant activities in the early years of AVR operation were around 1100 GBq (30 Ci). The testing of TRISO coated fuel in the AVR started as early as 1974 with the fissile particles contained in the GFB-2 variant and, at a larger scale, in 1977 with the GFB-3/4/5 variants. The insertion of mixed oxide TRISO fuel began in 1981 (GO-2), finally followed by the modern LEU TRISO fuel (GLE-3, GLE-4) since 1982.

The first TRISO fuel contamination showed already a lower level of ~10^{-4}. Modern TRISO fuel reduced this level further to the range of contamination with natural uranium (~10^{-5}) making the fraction of fissile material as low as ~10^{-7}. This improvement was verified as one of the reasons for the particularly low coolant activity measurements on the level of 740 GBq (20 Ci) in the final years of operation (see Fig. 28).

Fission gas (Xe and Kr isotopes) activity was measured and recorded regularly at various in-reactor positions (coolant samples, VAMPYR test loop, cold gas filter). But also solid fission products were measured both in the hot and cold gas. They were typically deposited on the fuel element surfaces and partially remobilized as dust and transported through the primary circuit.

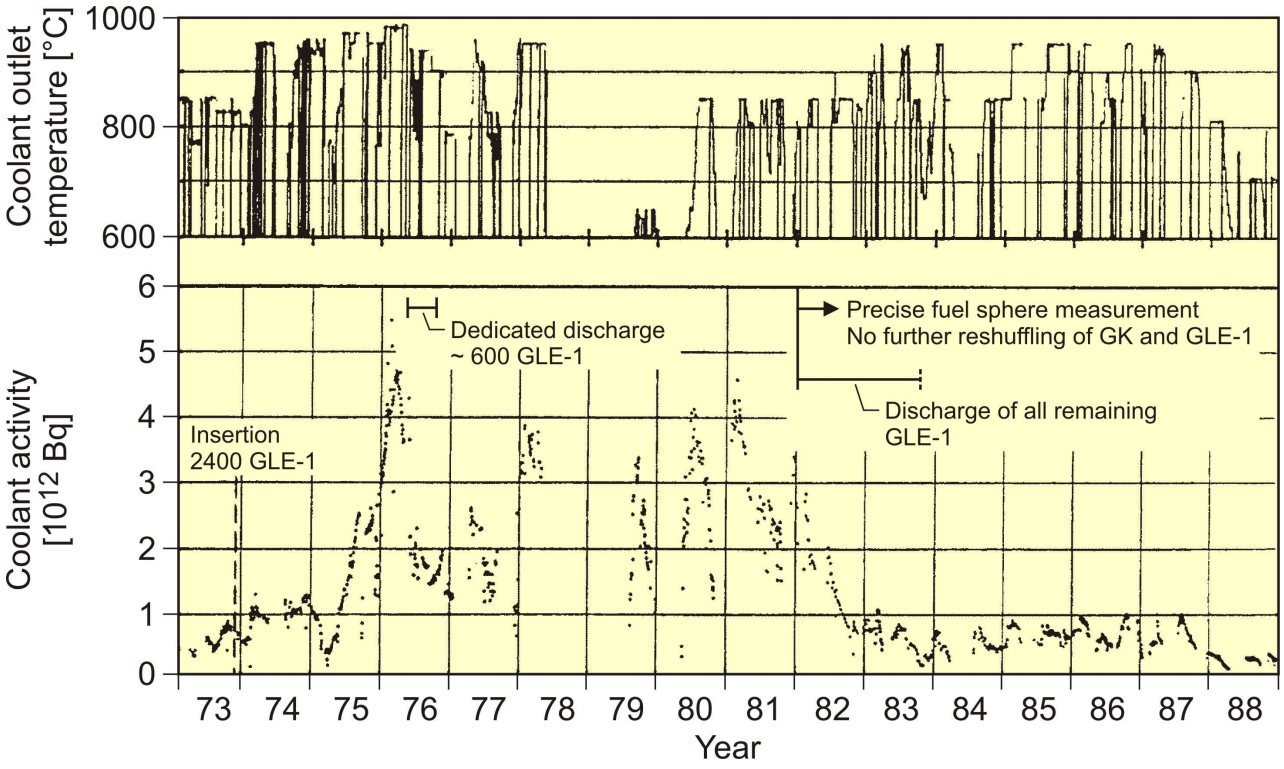

Figure 28 : Coolant activity measurements and coolant outlet temperature during the AVR operation history

After raising the average coolant outlet temperature to 950°C, fission gas activity stabilized at a level of 1100-1500 GBq (30-40 Ci) or 30 GBq/MW (0.8 Ci/MW) [Wimmers 1977]. Activity concentrations valid for full-power stationary AVR operation at 950°C, as were measured in the time period 1984-87 are listed in the following Table 16. The increase of liberated activity with increasing average helium exit temperatures is shown in Fig. 29.

Table 16 : Coolant activity concentrations in the AVR during stationary operation at 950°C [Gottaut 1990]

Radionuclide	Activity concentration [Bq/m^3]
H-3	$3.7*10^7$
C-14	$1.9*10^7$
I-131	$5.2*10^2$
Cs-137	$3.0*10^2$
Sr-90	$2.0*10^2$
Ag-110m	$4.9*10^1$
Co-60	$1.0*10^1$
Total fission gases	$4.6*10^8$

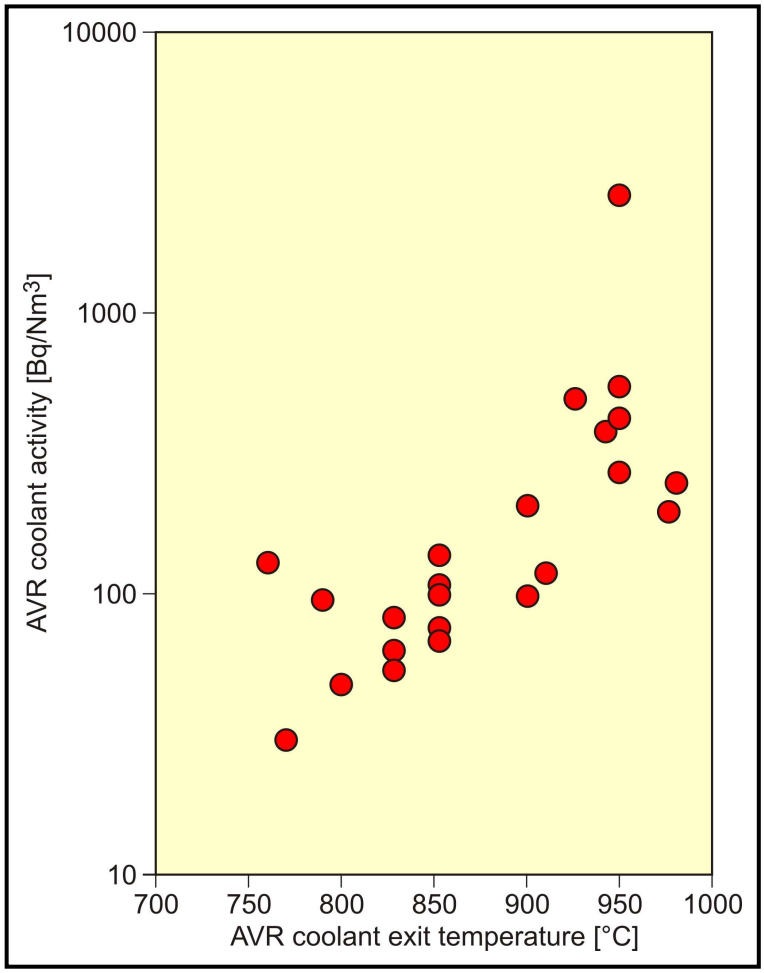

Figure 29 : AVR coolant activity vs. medium coolant exit temperature

Activities of metallic fission products released into the primary circuit of the AVR vs. operation time are shown in Fig. 30. A first major increase in the coolant activity can be identified in the beginning of 1974 traced back to enhanced Sr release from carbidic fuel (GK). The coolant activity increase observed from mid 1975 was presumed to originate from particle failure. Heating tests with all fuel types eventually identified the GLE spheres as being responsible for the enhanced activity release. Due to its high fuel content, the maximum operation temperature was estimated to be 1200-1280°C, from today's perspective even beyond 1400°C. During PIE heating at temperatures < 1200°C, no failures were observed. The failure rate, however, increased significantly if heated at temperatures above 1250°C. When reaching 1500°C, even more than 25 % of the particles were found destroyed [Wimmers 1977]. As a consequence, it was decided to remove all GLE-1 fuel from the core. The trial not being perfect, however, the circulation strategy was changed so not to re-circulate GLE-1 spheres to the outer core with its higher temperatures. The bulk of this variant was not removed until 1982. The effect of the complete removal on the coolant activities can clearly be seen from Fig. 28.

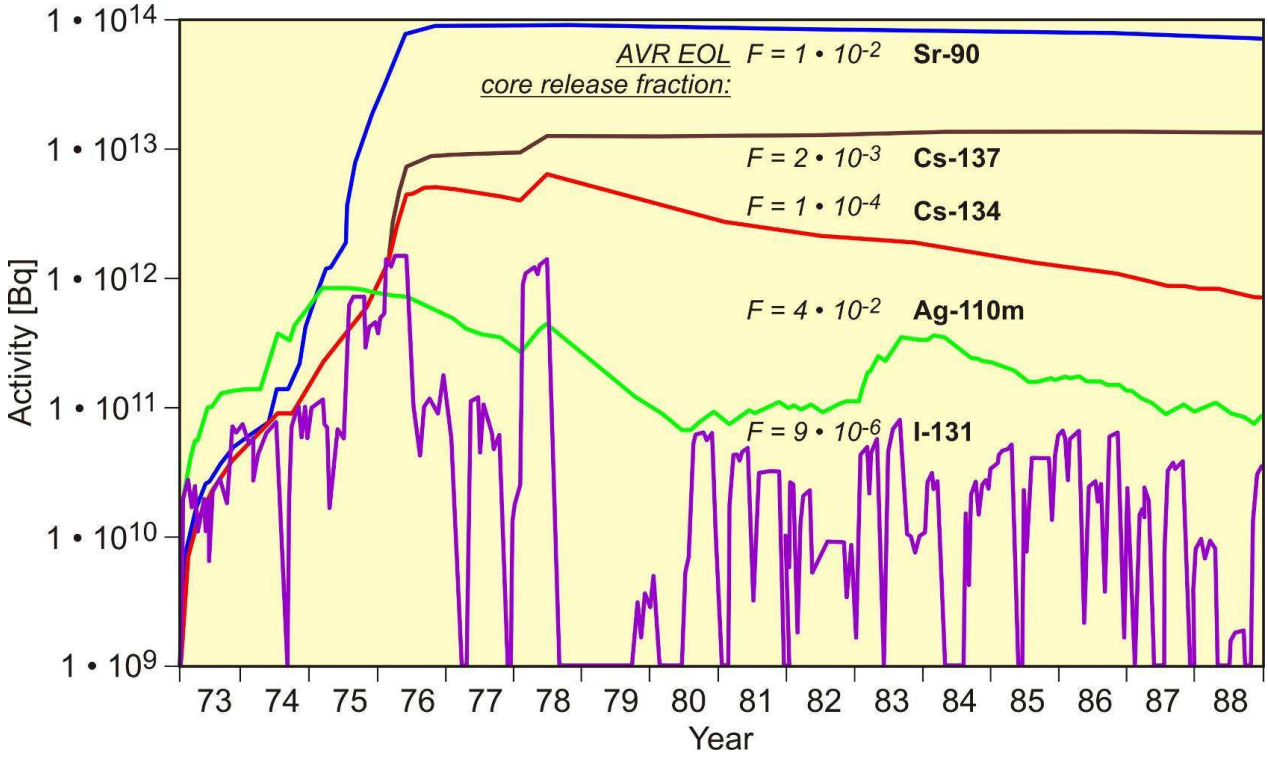

Figure 30 : Activities of different radionuclides accumulated in the AVR primary circuit over operation time [Gottaut 1990]

The following Table 17 lists the fractional release of AVR fuel at EOL.

Table 17 : End-of-Life fractional release of metallic fission products and iodine from AVR fuel

Radionuclide	EOL fractional release from AVR core
Cs-137	$2*10^{-3}$
Cs-134	$1*10^{-4}$
Sr-90	$1*10^{-2}$
Ag-110m	$4*10^{-2}$
I-131	$9*10^{-6}$

Dust Production

Dust in a pebble bed reactor is primarily of graphitic nature, mainly resulting from mechanical erosion of the circulating spheres, particularly in the fuel handling system. Other sources of dust are breakage of spheres and other mechanical damages such as notches, spallings, pitting (see next section 3.3.2.). It is transported in the coolant and partially deposited in low-flow regions and adhesively bonded on metal surfaces.

Total dust inventory in the primary circuit has been estimated to be about 90 kg, when the operation was terminated at the end of 1988, excluding the dust in the storage cans with the crushed elements. Particular dust sources of the AVR were the different generations of graphite fuel spheres with varying corrosion behavior and, resulting from a corrosive attack after an air ingress in 1971, the so-called peeling effect (see next section 3.3.2.), which may have contributed an estimated 8 kg [Wimmers 1977]. A size distribution of the dust particles as was measured in one of the VAMPYR tests is given in Fig. 31. The number-weighted size distribution reveals an average size of 0.6 µm, whereas the volume-weighted distribution has an average size of 5 µm.

Dust concentrations in the coolant varied over several orders of magnitude with peak values achieved when dust was remobilized at inforced coolant flow shortly after reactor shutdown (Fig. 32). Because of its large specific surface area, dust particles are able to bond a significant amount of activity. Being aware of major uncertainties concerning production, deposition, and interaction with gas-borne or plated out fission products, specific activities were estimated as given in Table 18. Variations in the data of the table refer to dust sampling at different locations and times. A fraction of 8 % for Cs-137 and 11 % of Sr-90 of the totally released activity was assessed to be bound to dust.

Table 18 : Estimated dust-borne activities in the AVR [Gottaut 1990]

Nuclide	Activity in AVR dust [GBq/kg]
Cs-137	2 - 96
Cs-134	0.7 - 27
Sr-90	19 - 363
Sr-89	0.6 - 42
Ag-110m	0.1 - 43
I-131	0 - 3
Co-60	0.2 - 8

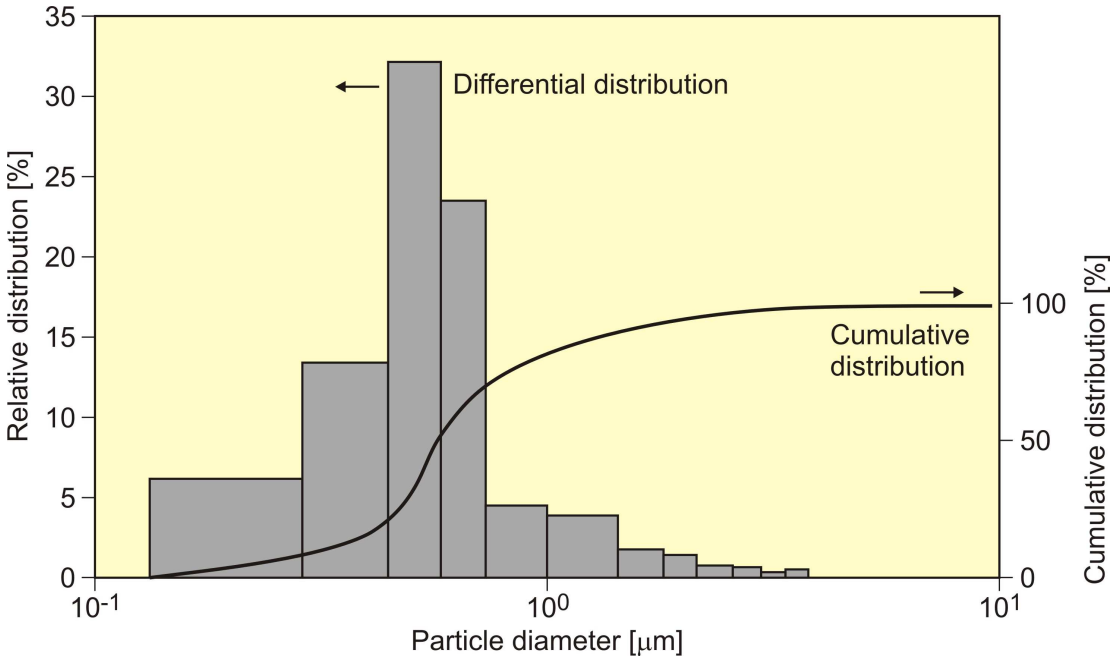

Figure 31 : Typical number-weighted distribution of dust particle sizes in the AVR coolant as measured in one of the VAMPYR tests
[Gottaut 1990]

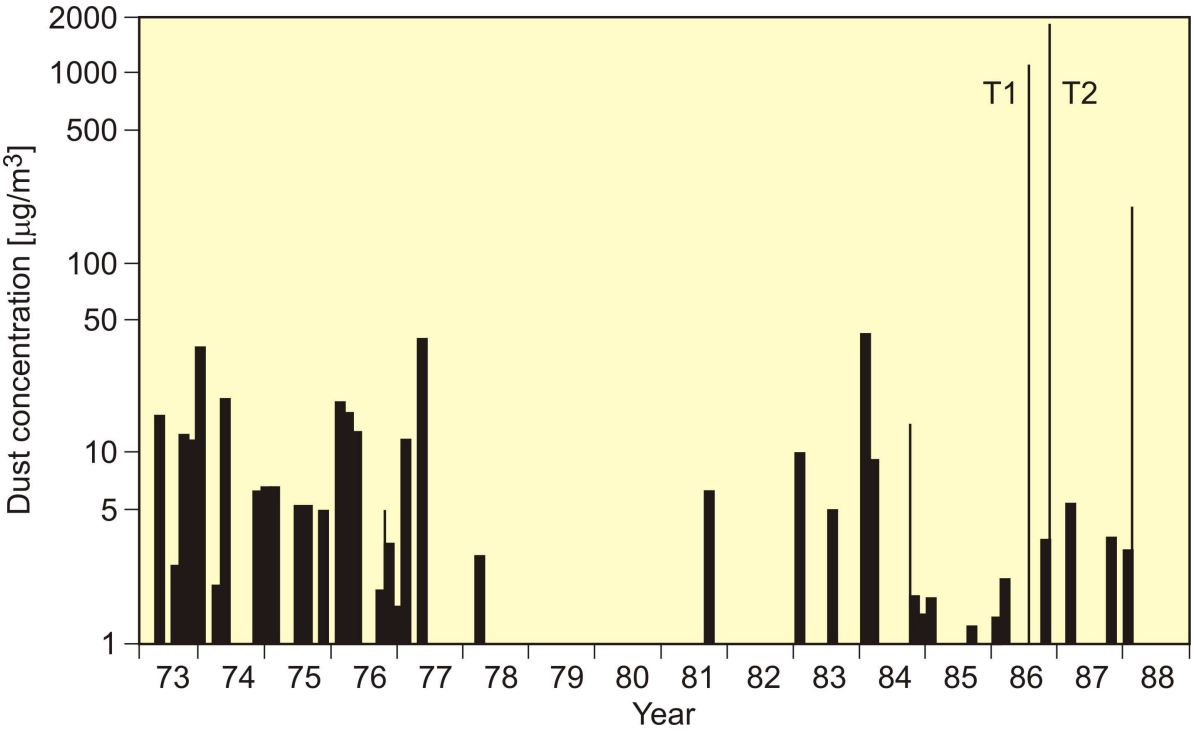

Figure 32 : Measured dust concentrations in the AVR coolant during steady state operating conditions, T1 and T2 were tests with the shutdown reactor
[Von der Decken 1990]

3.2.3 THTR Fuel during Operation

Qualification

Table 19 summarizes the operational requirements which fuel was expected to be exposed to during THTR operation.

Table 19 : Operational requirements for THTR fuel [Ragoss 1977]

Parameter	Average value	Maximum value
Fuel temperature [°C]	650 (time average)	1000 (s), 1200 (c)
Operation time [efpd]	600	600
Fast neutron fluence [10^{25} m^{-2}, E>0.1 MeV]	4.5	6.3
Heavy metal burnup [% FIMA]	11.6	14.1
Fuel element power [kW/sphere]		3.8

Maximum values for burnup and fast fluence were assessed to be reached by less than 10^{-4} of the fuel spheres; the maximum temperature of 1200°C was expected to be seen in not more than 10^{-3} of the lifetime of the fuel spheres [Ragoss 1977].

Irradiation tests were dedicated to qualifying fuel for the first THTR core. They also included specimens with carbidic fuel used as a fall-back position in case of too poor performance of the oxidic fuel. Testing of the THTR fuel concept was done in the MTRs at Studsvik (R2) and as long-term testing at Dragon (see Table 20). A first experiment, R2-K2, was conducted with fuel produced on a laboratory scale. Goal of the follow-on test R2-K3 was to move on to the easier and more economic production of oxidic fuel, however, with still one capsule filled with a carbidic fuel ball as backup solution to assure to have with a high certainty an appropriate fuel element for the THTR. Also fuel production was made using a 3 kg coater to prepare for large-scale production. Furthermore one sphere was filled with a THTR representative volume fraction of particles, which had, however, a lower power (smaller kernel compensated by thicker buffer, higher Th/U-235 ratio) to avoid the risk of failure. Finally two capsules were filled with representative coated particles (GO 105 f), except for the Th/U-235 ratio and for the lower number. The R2-K3 test included also short-term temperature cycles to simulate load changes. The corresponding long-term test to R2-K3 was DR-K4 in the Dragon reactor [Ragoss 1977].

Results from the R2-K3 experiment have shown that fission gas (Xe-133) release from the oxidic fuel remained below the upper limit specified, whereas significant irradiation-induced damage of the carbidic fuel coatings was observed. Crushing strength of the irradiated sphere No. 2 was unexpectedly low compared to the average of 20 unirradiated spheres (- 15.6 %), but with 19.4 kN still above the specified limit. All results of R2-K3 favored the choice of the oxide fuel in capsules 1 and 3 to become the reference for THTR fuel mass production [Ragoss 1977].

Table 20 : Irradiation testing of pressed fuel spheres for THTR [Ragoss 1975, Groos 1977]

Test	Date	Irrad. time [efpd]	Max. irrad. temp. [°C]	Burnup [% FIMA]	Fast fluence [10^{25} m^{-2}, E>0.1 MeV]	Max power [kW]	Fuel	Kernel diameter [µm]	Number of cp	Fractional release		
										Cs-137	Sr-90	Ag-110m
Qualification for THTR first core												
DR-K3 (25 balls)	7/68 – 1/72	719	1100 (s)	8.0-15.1	2.2-5.1	~ 4	$(Th,U)O_2$	~ 400	44,000			
DR-K4 (15 balls) (10 balls)	3/70 – 1/74	742 742	1050 (s) 1050 (s)	9.4-14.6 10.1-15.1	3.4-7.8 3.7-7.8	~ 4 ~ 4	$(Th,U)O_2$ $(Th,U)C_2$	414 407	52,000 63,000			
R2-K2/2 /3 /4	4/69 – 9/70	275.1 275.1 275.1	1150 1250 1250	16.2 16.7 15.3	6.3 6.5 4.6	3.5 3.1 3.1	$(Th,U)O_2$ $(Th,U)O_2$ $(Th,U)C_2$	~ 400 ~ 400 ~ 400	6000 6000 9500			
R2-K3/1 /2	2/70 – 4/71	278.6 278.6	1250 1250	15.0 7.1	6.2 7.7	4.8 4.4	$(Th,U)O_2$ $(Th,U)O_2$	414 302	7000 45,000	$5.6*10^{-5}$ $1.0*10^{-4}$	$3.5*10^{-6}$ -	- -
/3 /4	2/70 – 3/71	267.6 267.6	1250 1250	16.8 15.3	7.5 6.0	3.9 3.6	$(Th,U)O_2$ $(Th,U)C_2$	414 407	4400 7400	$5.1*10^{-4}$ $5.5*10^{-5}$	$5.6*10^{-6}$ $4.6*10^{-6}$	- -
R2-K9/1 /2	1/72 – 4/73	345.0 345.0	1250 1250	14.7 16.2	7.0 8.7	3.3 3.4	$(Th,U)O_2$ $(Th,U)O_2$	410 410	5300/ 32,500 4000	$1.1*10^{-4}$ $1.7*10^{-4}$	$2.6*10^{-5}$ $2.9*10^{-5}$	$5.0*10^{-2}$ $3.8*10^{-2}$
/3 /4	1/72 – 2/73	299.5 299.5	1250 1250	15.2 13.0	7.1 4.6	3.2 3.0	$(Th,U)O_2$ $(Th,U)O_2$	410 410	4000 8000	$8.4*10^{-5}$ $4.0*10^{-5}$	$1.6*10^{-5}$ -	$3.4*10^{-2}$ $2.4*10^{-2}$

Table 20 (cont'd): Irradiation testing of pressed fuel spheres for THTR [Ragoss 1975, Groos 1977]

Test	Date	Irrad. time [efpd]	Max. irrad. temp. [°C]	Burnup [% FIMA]	Fast fluence [10^{25} m^{-2}, E>0.1 MeV]	Max power [kW]	Fuel	Kernel diameter [µm]	Number of cp	Fractional release		
										Cs-137	Sr-90	Ag-110m
Qualification for THTR reload charges (and follow-on plants)												
R2-K4/1	4/69	261.8	1300	6.8/12.5	6.5	4.4	$(Th,U)O_2$	623/427	9000	-	-	-
/2	–	261.8	1300	7.9	8.0	4.2	$(Th,U)O_2$	427	12,000	$4.8*10^{-5}$	$7.5*10^{-6}$	-
/3	9/70	261.8	1250	14.0	7.9	3.8	$(Th,U)O_2$	623	1650	-	-	-
R2-K7/1		417.9	1250	13.6	7.3	3.3	$(Th,U)O_2$	415	6000	$2.1*10^{-5}$	$3.5*10^{-6}$	$9.8*10^{-3}$
/2		417.9	1250	15.3	9.2	3.7	$(Th,U)O_2$	415	4500	$7.0*10^{-6}$	$3.9*10^{-6}$	$4.9*10^{-2}$
/3		417.9	1250	15.9	9.4	3.3	$(Th,U)O_2$	415	4200	$4.0*10^{-6}$	$1.0*10^{-5}$	$2.5*10^{-2}$
/4		417.9	1250	14.0	6.6	2.8	$(Th,U)O_2$	415	6000	$2.0*10^{-6}$	$5.0*10^{-6}$	$7.6*10^{-3}$

Fig. 33 shows, as an example, for test R2-K9, the dependence of the gas release process of some Kr isotopes on the irradiation temperature, which was stepwise varied to simulate cycle operation. The curves were found to show no long-term change [Röllig 1977].

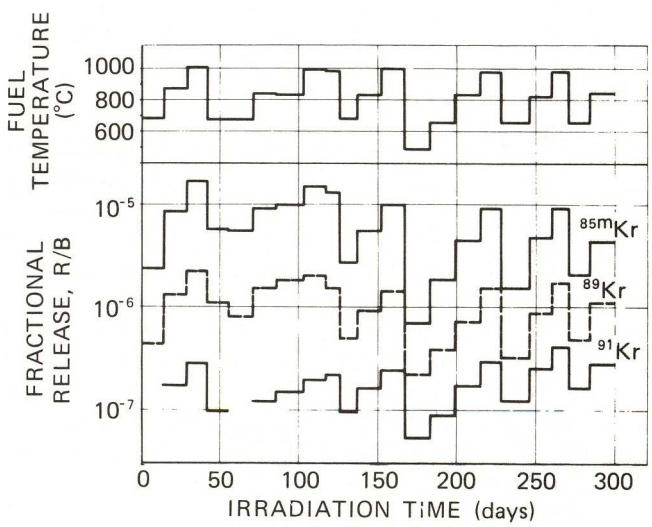

Figure 33 : In-pile release from irradiation test R2-K9, capsule 3 [Röllig 1977]

From irradiation testing of THTR fuel, the irradiation induced failure fraction was estimated to be $2*10^{-3}$ at the end of life of a fuel element, i.e., having reached a burnup of about 11.5 % FIMA and accumulated a fast neutron fluence of $4.5*10^{25}$ m^{-2}, E>0.1 MeV [Röllig 1991]. Fig. 34 shows the experimentally covered ranges of fluence and burnup compared to the design limits for THTR and AVR.

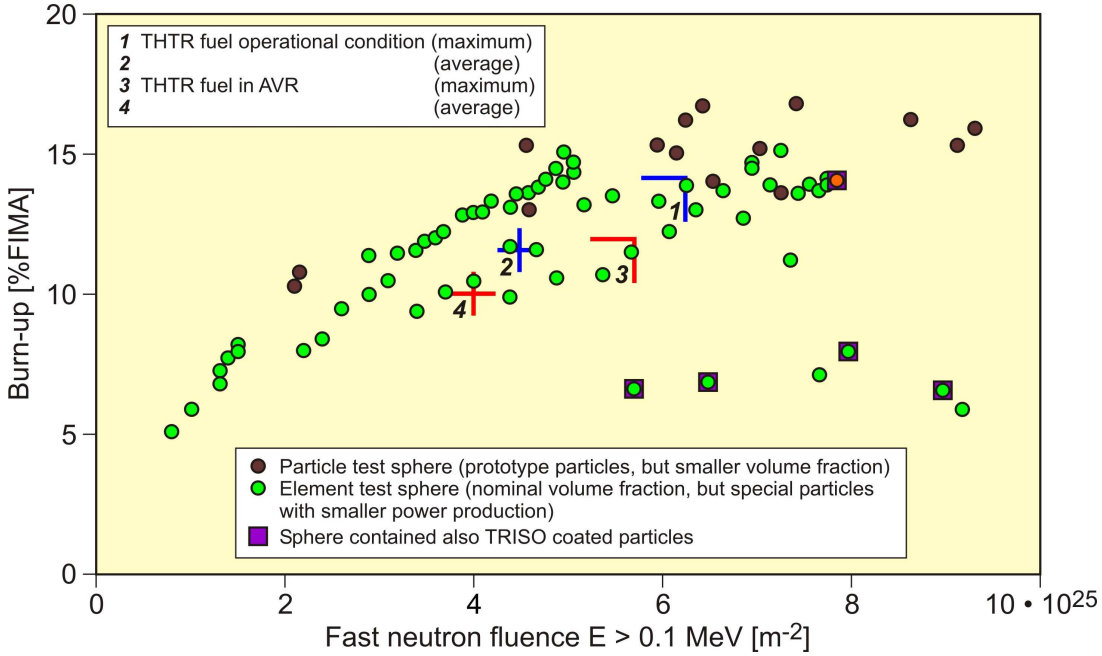

Figure 34 : Fast fluence vs. burnup diagram for THTR fuel irradiation testing [Ragoss 1975] compared with the ranges for the GO-THTR fuel variant achieved in the AVR

Other MTR tests, R2-K4, -K7, and DR-K5, were focusing on fuel for THTR reload charges (and partially already for follow-on HTGRs). Details on all THTR fuel tests in MTRs are also summarized in Table 16. After this four years testing period in MTRs, the AVR reactor was used for further irradiation testing.

Main results from the irradiation testing of THTR fuel were [Ragoss 1975] :

- The requirement of stability of dimension is fulfilled by the pressed-type A3 standard matrix fuel elements. Neutron-induced dimensional changes were as expected from isothermal tests with pure matrix specimens. Also the dimensional changes were observed to be smaller for those test spheres which contained TRISO coated particles.
- The specifications of mechanical strength were met. Crushing strength measurements revealed no clear relationship to the neutron fluence. It appeared to be not significantly influenced by the neutron irradiation.
- Coated particles embedded in a sphere showed the tendency of a better irradiation performance compared to loose particles, because swelling tends to close gaps developed between coating and overcoating and to support the particle structure.
- Coated particle integrity during irradiation could be confirmed for all mixed oxide particles with PyC coating, however, with a limit for methane-derived PyC at about $7\text{-}10*10^{25}$ m^{-2}, E>0.1 MeV.
- Gaseous and metallic fission product release during irradiation was mainly due to the presence of free uranium outside intact coatings which is both natural contamination of the graphite with U and imported contamination from the high enrichment during the manufacture process.

Based on the good results of the R2-K9 irradiation experiment (see Fig. 35), the production of the first core loading for the THTR-300 was recommended [Ragoss 1975].

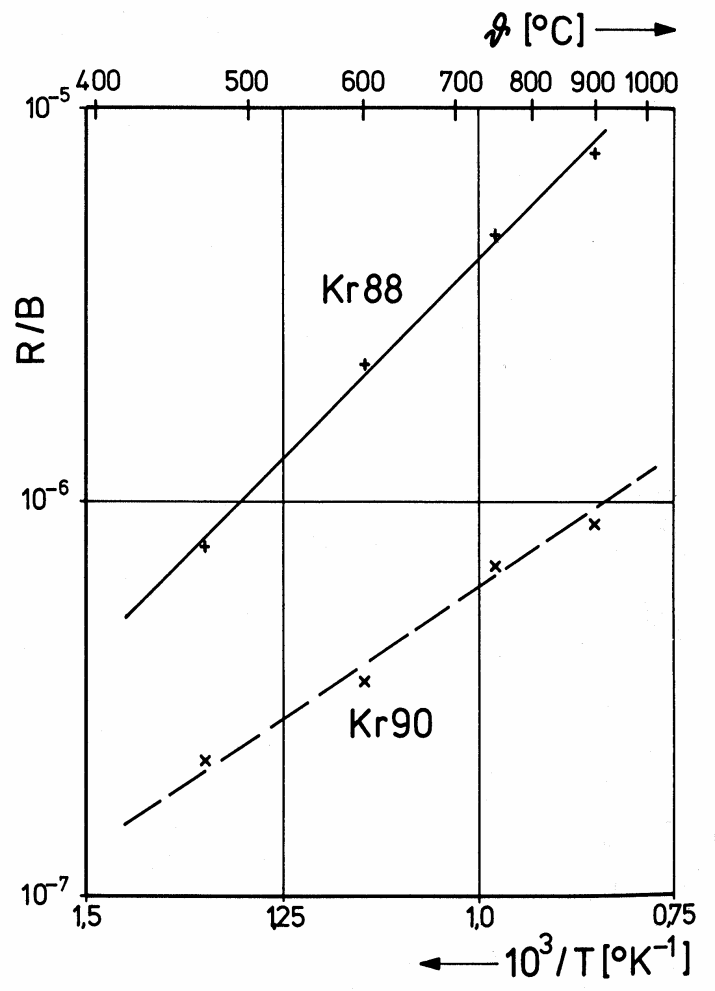

Figure 35 : R/B of Kr-88 and Kr-90 for sphere 2 in irradiation experiment R2-K9 [Ragoss 1975]

THTR Coolant Activities

During THTR operation, the coolant activity was continuously monitored by beta counting devices to control the fuel quality and detect immediately relative changes, and in more detail by gamma spectroscopy of gas samples. Fig. 36 gives an example for the gas release of short-lived Xe and Kr isotopes into the primary circuit at partial load operation and the comparison with respective calculations.

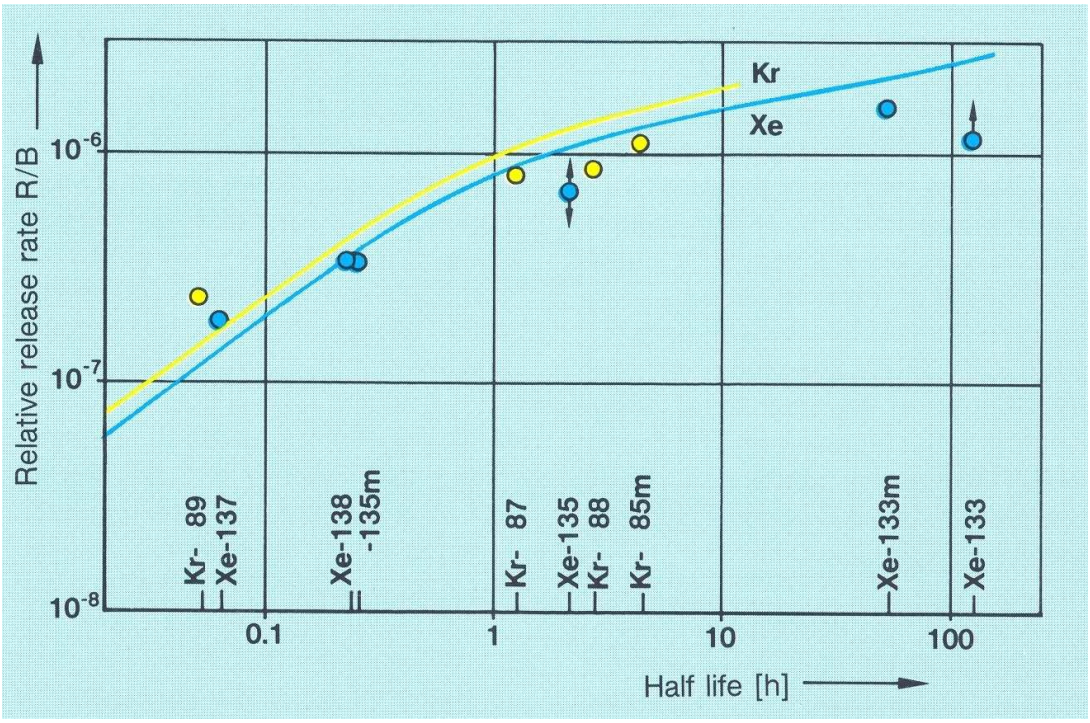

Figure 36 : Calculated and measured inert gas release in the THTR-300 at 40 % load [HKG 1989]

Measurements of the specific coolant activity as the sum of 9 noble gas nuclides, covering an estimated 90 % of the total activity, over the total operating time is shown in Fig. 37. A steep rise can be recognized at about 100 efpd (marked with "SWKP") which was found to coincide with a very high occurrence of damaged fuel elements and a fracture of many BISO coated particles, respectively [Röllig 1991]. Still the measured activity is generally considered to be in good agreement with respective model predictions, not significantly affected by the comparatively high fraction of broken balls.

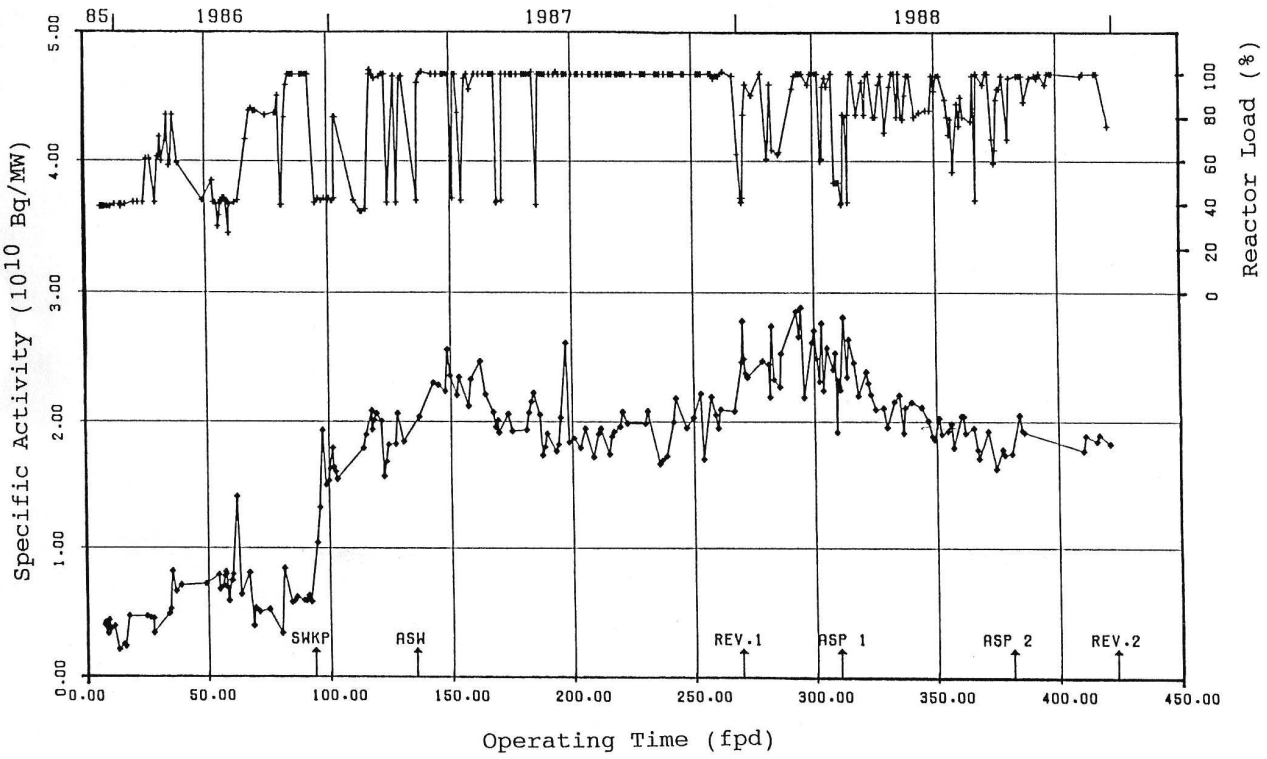

Figure 37 : Specific coolant activity (sum of 9 noble gas nuclides) in the THTR-300 [Röllig 1991]

The presence of oxygen impurities leading to corrosion was estimated to have resulted in a total loss of 65 kg (both operating elements and core internals), which is small compared to the total inventory of about 728 t [Bäumer 1991].

3.2.4 Dragon Fuel during Operation

Qualification

Irradiation testing of the original "releasing" type of fuel was carried out in the late 1950s and early 1960s. The testing program was defined with respect to the investigation of both the mechanical performance of the fuel and its fission product retention capability. Apart from the Dragon reactor itself, various irradiation facilities in Europe were used applying different kinds of rigs such as hermetically sealed capsules, vented capsules, swept capsules, or engineering loops.

With the transition of the fuel design to the "retaining" (TRISO) coated particle fuel, irradiation testing continued in Harwell (Pluto), Studsvik, and Risoe (HTD) with standard (Th,U)C2 fuel to be inserted into the central core region of charge 1. Irradiation times were between 40-173 days in the temperature range of 700-1700°C with burnups achieved of 0.3-12 % FIMA.

Table 21 gives an overview of the irradiation test series conducted at various facilities.

Table 21 : Summary of fuel irradiation experiments in MTRs [Price 1967]

Charge	Date	Fuel	Coating	Temperature	Burnup [% FIFA]	Xe-133 R/B
1	28.12.1961-03.03.1962	Powdered UC_2/C comp	None	1100	4	$1*10^{-1}$
2	04.06.1962-13.08.1962	Powdered UC_2/C comp	Fuel box	1150-1200	2.2	$7*10^{-1}$
3	21.11.1962-18.03.1963	UC_2 sintered kernels	PyC	1200	8.7	$2*10^{-3}$
4	29.04.1963-08.07.1963	UC_2/ThC_2 sintered kernels	PyC-SiC-PyC	1400	4.3	$6*10^{-5}$
5	22.08.1963-05.10.1963	UC/ZrC sintered kernels	None	1380	4.4	$\sim 1*10^{-1}$
6	10.12.1963-26.01.1963	UC/ZrC sintered kernels	None	1380	4.8	$1.5*10^{-1}$
8	27.02.1964-30.09.1964	UC_2/ThC_2 sintered kernels	PyC-SiC-PyC	1400	14.4	$8*10^{-6}$
15	1965-66 (150 d)	UC_2/ThC_2	PyC	1500	~ 4.5	$2*10^{-4}$
16	1966 (50 d)	UO_2/ThO_2 loose particles	PyC	1400	~ 4.5	$2*10^{-6}$

Due to the initial focus on a thorium cycle, the irradiation programs for Dragon fuel were concentrating on the identification of a fissile-fertile particle system.

Irradiation testing of the 1st charge driver fuel (UC-10) was conducted in swept capsule tests in the R2 reactor, Studsvik, and at Würenlingen, as well as in static capsule tests in the Dragon High Power Density (HPD) Rig of the DR3 reactor, Risoe, and the Pluto Loop at Harwell, and, of course, in the experimental sections of the Dragon reactor itself. Particularly the positive results from eight irradiation tests in the PLUTO Loop facility with the coated fuel particles paved the way for their insertion into the Dragon core [Howard 1978].

In the DIDO 4V series, three capsules were used each containing a ~ 6 inch long section of a Dragon fuel rod where coated particles of the "emitting" type were inserted. The Pluto Loop experiment at AERE Harwell was designed to simulate a single channel of the Dragon fuel specimen in full size radius and 40 % of the length. $(Th,U)C_2$ fuel with SiC interlayer was tested in #8 over 180 days up to 6 % FIMA at ~ 1400°C with no evidence of damage and a Xe-133 release of $< 10^{-5}$ [Huddle 1966]. The DIORIT reactor in Würenlingen was able to irradiate full-size fuel rods in six independent capsules.

Table 21 summarizes some of the irradiation test data. Main results achieved from the irradiation program was that

- SiC coated particles clearly proofed to be superior to plain PyC coated particles in terms of higher stability and lower release;
- the introduction of a porous buffer layer was of great advantage;
- contamination level of oxide fuel was lower than that of carbide fuel.

Also Xe-133 R/B measurements, e.g. from sampling primary gas at the 37 individual purge connections, revealed the enormous difference for SiC coated particles compared to those of the "emissive" type. The fact that the equilibrium was rapidly reached, indicated the released fission products to originate mainly from recoil and coating contamination rather than diffusion from the kernel.

Analyzing the purification system at the end of charge 1, the R/B of Xe-133 for the whole core was estimated to be ~ 10^{-4}. Since this was about the normal operation limit in the primary circuit, it has shown that a cleaning-up of the primary circuit would actually not have been necessary. The above figure translates into a coolant concentration of $1.7*10^{5}$ µCi/cm^3 of Xe-133 activity [Price 1966a].

The analysis of surfaces of one heat exchanger and the circulator have led to estimated release fractions for cesium (from cartridges) of $5*10^{-6}$ and $1*10^{-5}$ for strontium (whole core) [Price 1966a].

Regarding plutonium, the experience is very limited ; a few particles have been irradiated in the experimental DRAGON reactor and reached a burnup of 750 GWd/t of heavy metal or ~ 80 % FIMA. Specimens of Pu fuel were also irradiated in an HPD capsule in Risoe. Two complete fuel rods prepared in the Belgonucleaire/CEN Laboratory at Mol were inserted in the central positions of two Dragon fuel elements.

First irradiation tests with LEU fuel were carried out in the DR3 reactor and the R2 reactor. A DR3 test at 1600°C with 5.5 % FIMA revealed first fuel particle failures after 200 efpd due to kernel migration (amoeba effect). A test with some 10^7 particles in Dragon over 85 efpd at 950-2000°C showed no major failure below 1600°C, but progressive amoeba attack above 1800°C [Howard 1978]. Irradiation of LEU oxide fuel was conducted using the irradiation facilities in Studsvik, Risoe, Petten, Mol, Saclay, Cadarache, and Dragon. Main LEU fuel testing was done in the Dragon reactor with 3rd and 4th charge as well as with MET IV and MET V. Results achieved [Howard 1978] :

- Successful in pressing compacts with high fuel loading (> 50 %) ;
- LTI PyC survived much higher fast neutron doses ;
- Performance limiting features were amoeba effect depending on temperature and temperature gradient, PyC cracking depending on fast neutron dose, temperature, and PyC type, and pressure vessel failure depending on geometry and burnup ;
- Upper temperature limit was seen at 1250-1300°C ;
- TRISO coating became transparent for Ag-110m at about 1250°C and for Cs and Sr at higher temperatures (~ 1600°C).

Dragon Coolant Temperatures

The mean coolant temperatures were 360°c at the core inlet and 810°C at the core outlet. The hottest channel had a maximum temperature of 926°C. The mean heating rate of a fuel rod was 482.6 W/cm, and the peak fuel temperature in a mean channel was about 1250°C.

Dragon Coolant Activities

Helium samples were taken from the primary circuit for gas analysis, initially Xe and Kr isotopes. The purge system, in the first core applied to all fuel rods, but later only to the central rods with the experimental fuel, served initially the purpose to keep the coolant clean. With the employment of retaining coated particle fuel, it became more or less obsolete, but served then as a diagnostic means to monitor fission gas release from the fuel experiments and individual fuel specimens, respectively. Later Dracule probe monitoring of coolant borne activities and helium purge from the individual fuel elements; was a sampling device for both hot gas from the core and cold gas downstream a heat exchanger.

With the insertion of the 2nd charge fuel in the Dragon reactor starting in April 1967 and due to the fact that now ~70 % of the fuel remained unpurged, the quantity of gas-borne activities rose to an equilibrium level of 56 GBq [Price 1967]. Table 22 shows the measured R/B for fuel (via purge) and for coolant (via primary circuit) of some fission gas isotopes. The mean purge factor is the ratio of both R/B values.

Table 22 : Fission gas activities in the Dragon reactor [Price 1967]

	Isotope	R/B Fuel	R/B Coolant	Mean Purge Factor
1st charge	Xe-133	$1.22*10^{-4}$	$1.8*10^{-6}$	65
	Xe-135	$1.10*10^{-4}$	$1.5*10^{-6}$	72
	Kr-85m	$0.65*10^{-4}$	$1.2*10^{-6}$	53
2nd charge	Xe-133	$8.81*10^{-6}$	$3.75*10^{-6}$	2.4
	Xe-135	$7.31*10^{-6}$	$2.34*10^{-6}$	3.1
	Kr-85m	$2.81*10^{-5}$	$6.97*10^{-6}$	4.0

Iodine release from Dragon fuel elements could not be identified directly due to condensation in the sampling lines. But from MTR testing, a similar release behavior between xenon and iodine could be deduced, i.e., no significant holdup in the matrix material.

Fig. 38 shows the R/B of Xe-133 measured via the purge system for an experimental fuel rod which was operated at 1800°C, much higher than the nominal fuel temperature of 1250°C. Under these severe conditions, the increase in the gas release was relatively slow [Graham 1974].

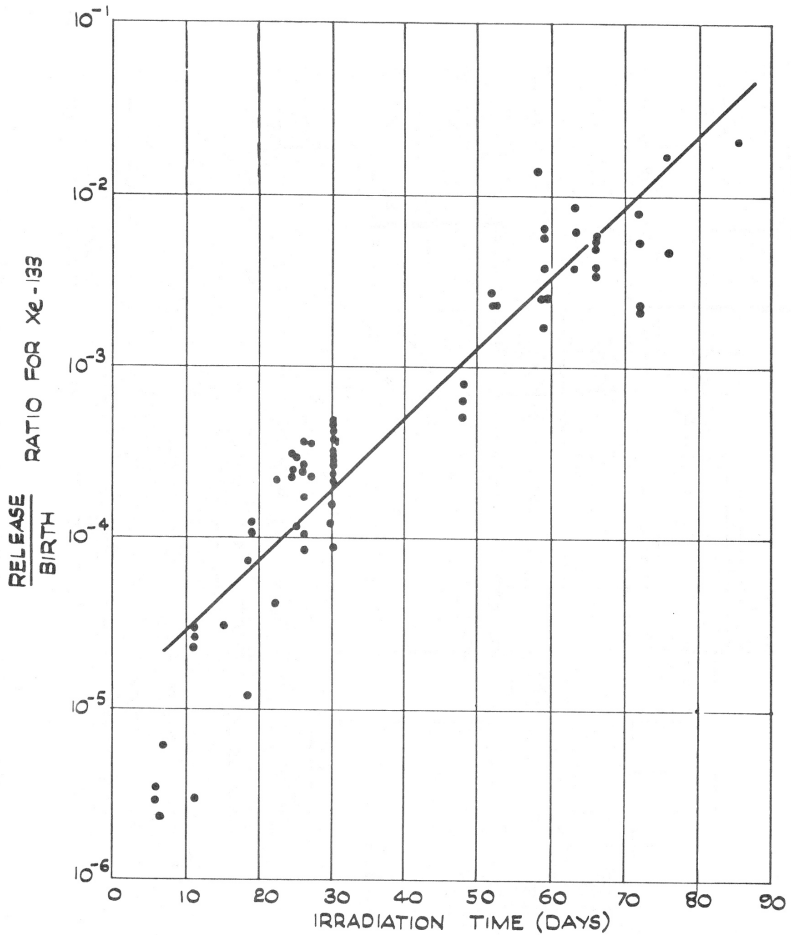

Figure 38 : Xe-133 R/B for experimental fuel operated at 1800°C [Graham 1974]

In Fig. 39, the fractional release of Ag-110m is shown for different fuels of the MET II series in Dragon as a function of the parameter D't with D't = 0.055*exp{-25,650/T}t and T in [K], t in [s]. D* is defined as D_{SiC}/d_{SiC}^2 with the diffusion coefficient D in [m^2/s] and the SiC layer thickness dSiC in [m]. The general trends that could be concluded from the figure are that silver release is higher from BISO than from TRISO coated particles, and also higher from carbide than from oxide fuel. The findings also apply to cesium and strontium [Nabielk 1977].

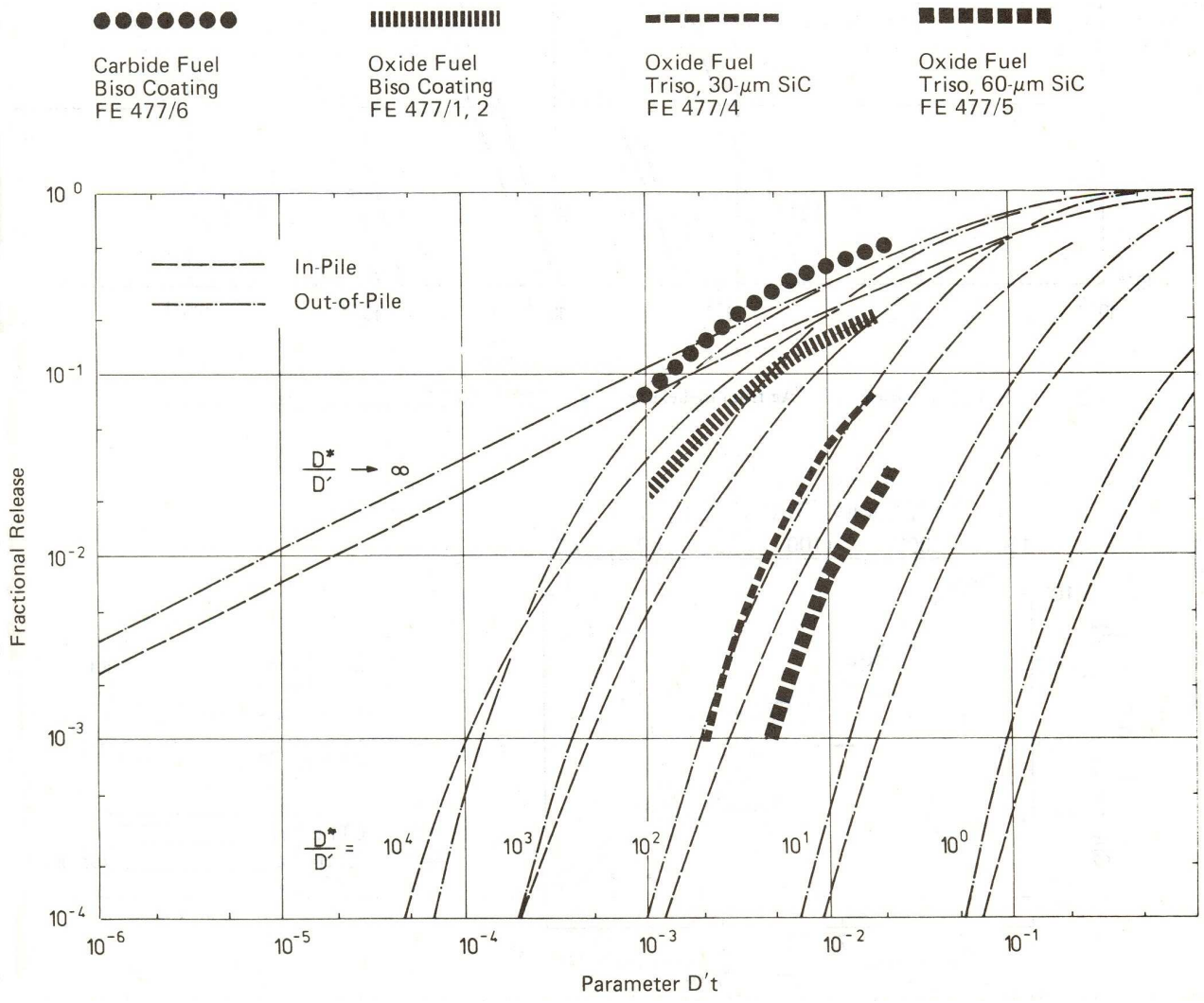

Figure 39 : Ag-110m fractional release from (Th,U)C_2 fuel (MET II series) [Nabielek 1977]

3.3 Postirradiation Examination of AVR Fuel

PIE was mainly conducted in the Hot Cells at FZJ. Both random and especially selected fuel element samples from the AVR were taken and separated during removal from the core (Table 23).

Table 23 : Dates of discharge of AVR fuel specimens for potential PIE

Fuel sample	Date of discharge	Fuel sample	Date of discharge	Fuel sample	Date of discharge
1		32		63	04/1981
2		33		64	02/1982
3		34		65	02/1982
4		35		66	11/1982
5		36		67	12/1982
6	04/1970	37	09/1974	68	06/1983
7	08/1970	38	09/1974	69	06/1983
8	12/1970	39	09/1974	70	06/1983
9	06/1971	40	04-06/1975	71	01/1984
10	09/1971	41	10-11/1975	72	
11	02/1972	42	02-03/1976	73	02/1985
12		43		74	02/1985
13	10/1972	44		75	
14		45		76	10/1985
15		46	05-12/1976	77	10/1985
16		47	10/1976	78	09/1986
17		48	05-12/1976	79	09/1986
18		49	05-12/1976	80	09/1986
19		50	11/1977-03/1978	81	10/1986
20		51	11/1977-03/1978	82	10/1986
21		52	11/1977-03/1978	83	
22		53		84	
23		54		85	07/1988
24		55	04/1978	86	07/1988
25		56		87	
26		57		88	12/1988
27	10/1973	58	05-06/1980	89	01/1989
28	10/1973	59	05-06/1980	90	01/1989
29		60	05-06/1980	91	01/1989
30		61	05-06/1980	92	01/1989
31		62	04/1981		

Guidelines were established according to which a specific PIE program was executed. It included

- measurements of Xe-133 and Kr-85 equilibrium release from single fuel elements during heating tests at constant temperatures of 1050 and 1250°C, respectively, used as indicator for coated particle failure;
- measurements of burnup;
- measurements of concentration profiles of solid fission products in the fuel-free zone;
- metallographic investigations to study the integrity of particles.

3.3.1 General Results from AVR Operation

Fuel and Fission Product Inventories in AVR Spheres

The decrease of the U-235 inventory in a fuel sphere vs. burnup and the corresponding buildup of U-233 (from the thorium) and Pu isotopes was calculated for the different fuel types and is plotted in Fig. 40.

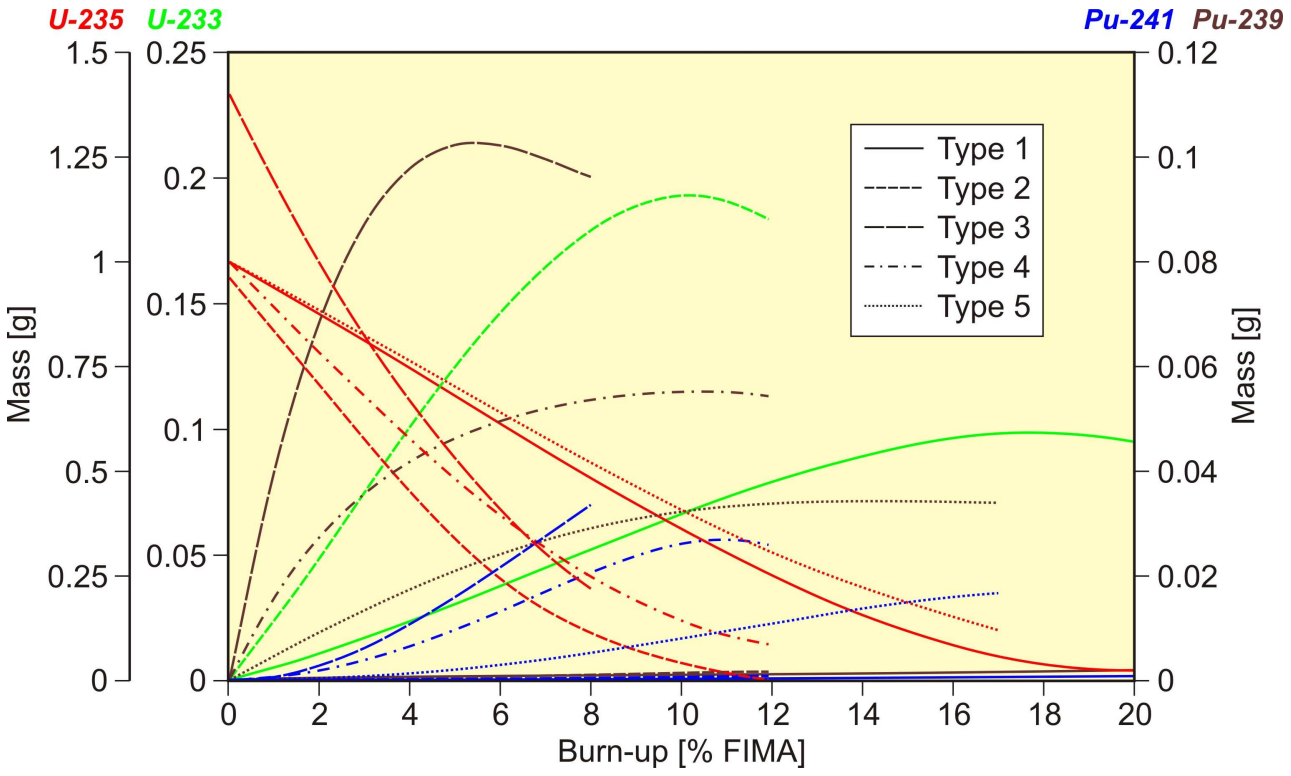

Figure 40 : Fissile material as a function of burnup

The research center Seibersdorf, Austria, investigated experimentally the heavy metal and fission product contents of five spent fuel spheres from the AVR [Falta 1993]. Respective specimens were prepared by disintegration of the spheres, isolating coated particles, mechanical separation of particle kernels and coatings. Table 24 lists some characteristics of the spheres examined and the measured inventories of uranium and plutonium isotopes as well as some fission products. From

the table, it can be figured that each of the GO-1 spheres contain at EOL more α-activity (mainly from the Pu isotopes) than the GLE-3, but only ~ 7 % of the total plutonium contents. A smaller Cs-137 inventory than expected from the burnup was found with decreasing kernel weight indicating its mobility (release from kernel) in contrast to the stationary elements U, Pu, Am, Cm, Nd [Falta 1993].

Table 24 : Measured inventories of heavy metal and fission products for five fuel spheres [Falta 1993]

	GO-1		GLE-3	GLE-4	
	79/12	**90/28**	**89/22**	**86/20**	**92/03**
Operation time [efpd]	3854	4700	2386	1618	1794
Burnup [% FIMA]	18.5	18.7	9.6	10.6	11.6
Decrease U-235 enrich. [%]	93 → 9-10		9.8 → 1.7	16.7 → ~7	
Nuclide	**Inventories at end-of-life [mg]**				
U-233	95.5	96.2			
U-234	22.41	23.39	4.21	6.30	6.06
U-235	38.2	30.7	157.	368.1	352.6
U-236	146.3	140.6	139.2	107.1	113.8
U-238	59.2	52.1	8790.	4822.	4806.
Σ	361.5	343.0	9090.	5303.	5278.
Pu-238	4.84	5.73	3.55	0.87	1.49
Pu-239	1.42	1.45	48.7	37.6	37.6
Pu-240	0.877	0.901	35.6	17.2	20.3
Pu-241	0.444	0.480	18.5	8.7	11.8
Pu-242	0.627	0.719	15.9	2.8	5.2
Σ	8.21	9.28	122.2	67.1	76.4
Am-241	0.02	0.10	4.17	2.13	2.59
Am-242m	0.	0.	0.02	0.01	0.01
Am-243	0.11	0.14	1.96	0.20	0.46
Cm-244	0.18	0.24	2.01	0.11	0.34
Cm-245	0.004	0.01	0.06	0.004	0.01
Cm-246	0.004	0.004	0.01	0.	0.004
Cs-134	2.55	2.25	1.95	0.92	1.11
Cs-137	33.8	33.7	35.2	21.4	22.5
Ce-144	-	-	2.77	2.92	3.30
Ru-106	-	0.02	0.23	0.12	0.15
Sb-125	0.09	0.08	0.10	0.07	0.07
Eu-154	0.30	0.31	0.28	0.13	0.16

Pu Buildup

The investigation of AVR fuel elements in terms of isotope composition was made for validation purposes of a respective computer model (HTROGEN) to be applied to the characterization of spent fuel spheres with LEU fuel. This became particularly important with the conversion of the AVR from a HEU to a LEU core which made the fuel to a significant Pu source. In the test, five GLE-4 fuel spheres were loaded onto the still pure HEU/Th inner core. Five of those having passed the core once through the center were then discharged. The characterization of these LEU fuel spheres was conducted by way of deconsolidation of the balls and gamma scanning of the coated particles. Sets of particles of each sphere were mechanically cracked with the kernels being weighed and chemically dissolved. Various isotopes could then be identified by means of the isotope dilution method and subsequent mass spectrometry. The experimental results and comparison with HTROGEN calculations are given in Table 25 showing that the Pu vector is in good agreement with the computer model [Werner 1997].

Table 25 : Comparison of measured and calculated burnup and U and Pu isotope inventories in AVR GLE-4 fuel elements [Werner 1997]

	Measurement (averaged over 5 spheres)	Calculation
Burnup [% FIMA]		
by Nd isotopes	3.48 ± 0.03	3.8
by gamma spectroscopy	3.57 ± 0.11	3.8
Inventory [mg/sphere]		
U-234	7.68 ± 0.12	7.77
U-235	761.17 ± 12.34	744.10
U-236	44.41 ± 0.87	47.30
U-238	4912.47 ± 51.99	4921.10
Pu-238	0.0184 ± 0.0003	0.02081
Pu-239	18.5 ± 0.4	17.79
Pu-240	4.04 ± 0.05	3.909
Pu-241	0.73 ± 0.02	0.657
Pu-242	0.056 ± 0.001	0.0559

For disposal purposes, spent fuel needs to be characterized in terms of fissile and fertile materials still left in the fuel. The computer code HTR-2000 developed at FZJ was applied to estimate these masses by simulating the physical behavior of the AVR reactor determining the neutron flux, power, and temperature distributions in the core. The fissile and fertile materials contained in 281,000 fuel elements discharged from the core were calculated as indicated in the following Table 26 [Wolf 1993].

Table 26 : Calculated HM contents of the fuel discharged from the AVR reactor [Wolf 1993]

Contents in total AVR fuel [kg]						
U-233	**U-235**	**U-238**	**Th-232**	**Pu-238**	**Pu-241**	**Pu-total**
19.1	57.	424.	1262.	2.75	0.95	6.81

3.3.2 Mechanical Behavior of Fuel Spheres

Strength

The fuel element diameter was found to slightly decrease with fast neutron fluence (see Fig. 41) amounting to an approximately 0.5 mm smaller diameter compared to the nominal value at the end of life.

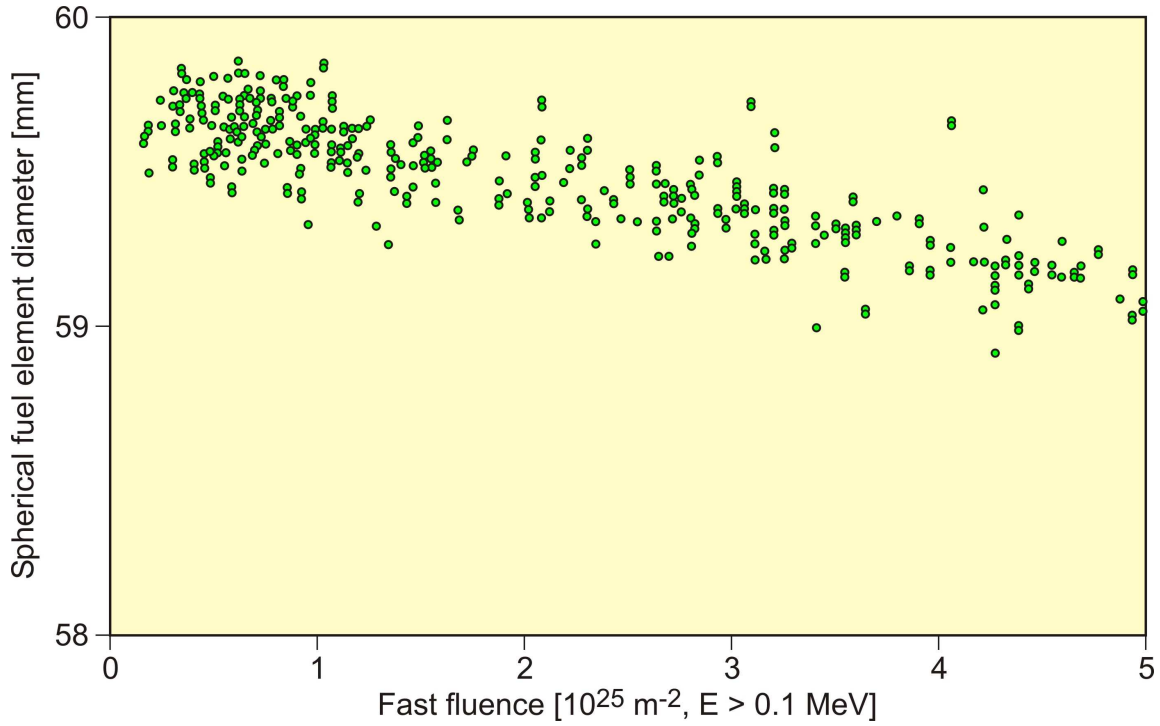

Figure 41 : Measured fuel sphere diameter vs. fast neutron fluence [Pohl 2001]

The mechanical strength of fuel spheres slightly improves at lower fluences compared to the unirradiated state, since neutron radiation raises the density of the matrix material (decreasing diameter, see previous figure) resulting in a somewhat higher crushing strength, a larger number of drops survived, and a steep increase of the E-module of the matrix material. In contrast corrosion during reactor operation, which enlarges the matrix porosity, has a strength decreasing effect. The experience from AVR operation is that, as a rule, no loss of mechanical strength compared to the manufacture specifications is expected after irradiation. Crushing strength of the spheres was found to be principally unaffected by neutron irradiation (up to ~ $5*10^{25}$ m^{-2}, E>0.1 MeV) (see Fig. 42) [Rebmann 1988, Ziermann 1997]. Table 27 lists the experimental data of drop tests for both unirradiated and irradiated fuel spheres [Wimmers 1977].

Table 27 : Number of drops survived for unirradiated and irradiated fuel spheres [Wimmers 1977]

Fuel type	Unirradiated spheres Drop from 4 m height onto a pebble bed		Irradiated spheres Drop from 2 m height onto steel sheet		
	No. drops survived	No. of measurements	No. drops survived	No. of measurements	Fast neutron fluence
UCC	540 + 260	97	97 + 28 12 + 7	4 44	0. 1.6 – 2.8
T	660 + 220	120			
GK	540 + 190	230	269 + 62	83	0.2 – 2.0
GO	690 + 150	265	213 + 50 356 + 58	5 17	0. 0.2 – 0.6

Crushing strength is influenced by the temperature, the degree of corrosion, and the fast neutron fluence. For unirradiated fuel, the crushing strength is increasing with temperature, for instance, 30% from room to reactor operating temperature. It was also observed that for fuel elements irradiated up to $3.5*10^{25}$ m^{-2}, E>0.1 MeV, the crushing strength was higher compared to unirradiated spheres. Finally crushing strength decreases with increasing degree of corrosion. In summary, it can be stated that under operating conditions, the crushing strength does not fall below the values for fresh fuel at room temperature [Kleine-Tebbe 1988]. Fig. 42 shows crushing strength measurements on the AVR fuel with 6 g of heavy metal (GLE-4) with no tendency of decrease with fast neutron fluence [Ziermann 1997].

The behavior of irradiated fuel spheres and coated particles under a pressure load were experimentally investigated using a crushing facility which allowed to impose pressures of up to 30 MPa. The failure of particles was identified by measuring the liberated tritium and Kr-85 gases. The examination covered 12 fuel spheres of the types GO-1, GO-3, GLE-3, GFB-4 consisting of A3-3 (GO-1) or A3-27 matrix material and BISO and/or TRISO coated particles as well as particles taken from a deconsolidated GO-1 (16 % FIMA) and GLE-3 (5.8 % FIMA) sphere, respectively. Highest coated particle failure was observed when crushing GFB-4 fuel spheres, whereas for both GO and GLE balls, none or only few failures ($\leq 7*10^{-4}$) occurred. Furthermore particle damage was observed to begin at pressures $\geq$ 15 MPa [Rebmann 1988].

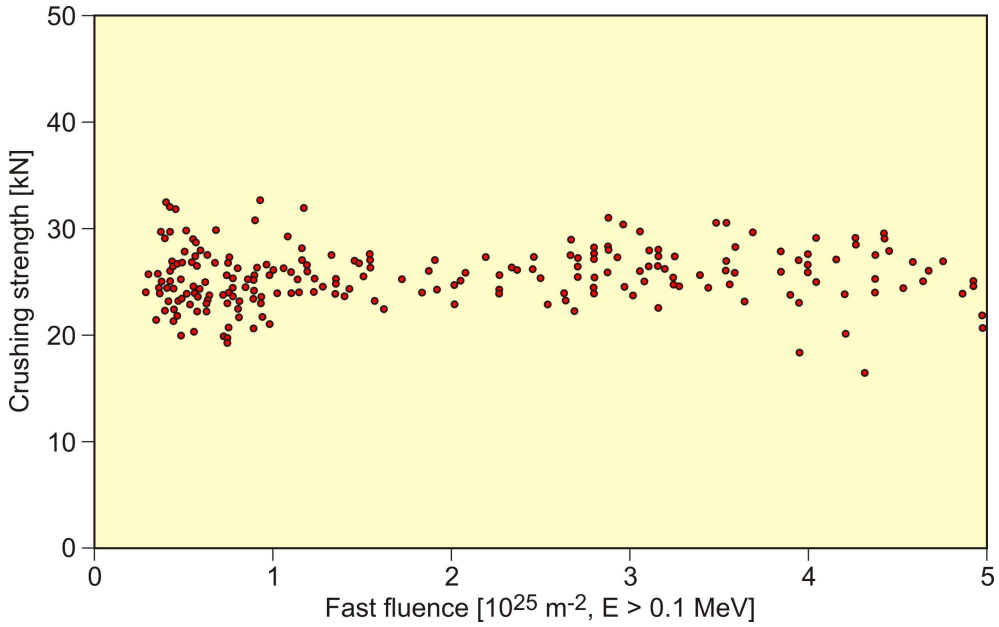

Figure 42 : Measured crushing strength vs. fast neutron fluence for GLE-4 fuel elements [Pohl 2001]

Corrosion

The pore system of A3 matrix material changes under neutron irradiation as is shown in Fig. 43. It is of relevance, if the fuel element is exposed to a corrosive environment.

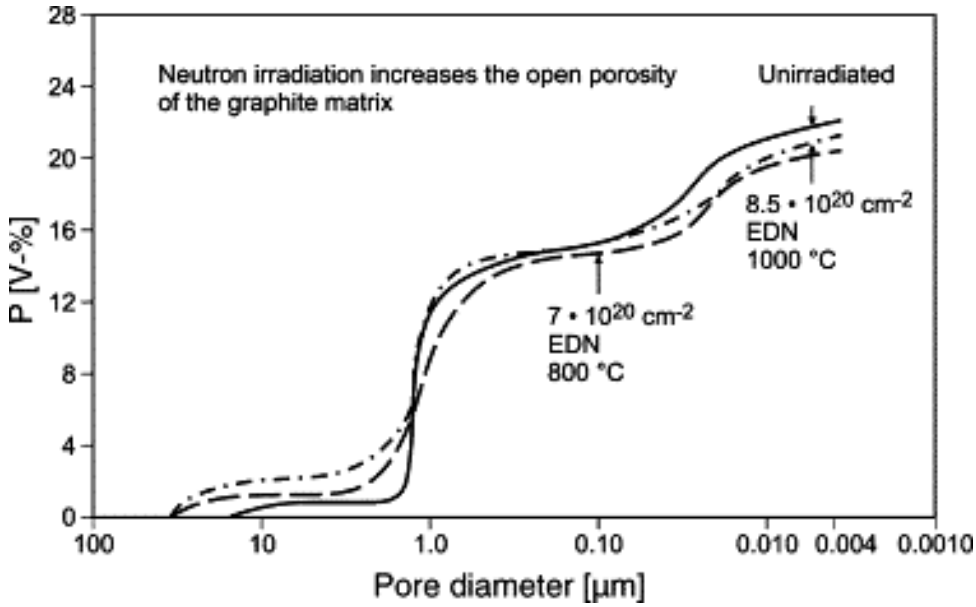

Figure 43 : Comparison of pore diameter distributions for unirradiated and irradiated A3 matrix material [Fachinger 2006]

Oxidation of fuel graphite can occur due to the presence of water in the core. Rates are negligible at partial pressures $P_{H2O} \leq 0.05$ Pa and $0.5 \leq P_{CO2} \leq 3$ Pa. Concentrations of oxidizing atmospheres in the AVR core were sometimes higher, e.g., when the primary circuit had to be opened for repair works. The control of graphite oxidation was made regularly in a standardized procedure with random fuel samples by weight measurements. They indicated an average weight loss of 0.8 g or 0.4 wt% during the lifetime of the fuel sphere [Burck 1977]. Slightly lower data for mean weight loss due to corrosion are given in [Wimmers 1977]:

0.7 ± 0.1 g for GK fuel spheres
0.6 ± 0.15 g for GO fuel spheres

The former value of 0.8 g seems to include also weight losses from abrasion and smaller notches. There were also indications that the corrosion effect was catalyzed at the presence of strontium, barium (mainly from the GK fuel after the coolant exit temperature was raised to 950°C), or iron (from failed thermocouples). Furthermore it was observed that a significant weight loss occurred during the first two runs through the core, while corrosion losses do not increase with increasing burnup. This was also confirmed by standard corrosion testing on irradiated fuel spheres [Wimmers 1977]. There was, however, some dependence on the time of conducting the tests correlated with the ingress of oxidizing atmospheres or other impurities (see sections on pitting and peeling effect).

Measurements are plotted in Fig. 44 revealing a general increase in the corrosion rates after the helium outlet temperature was raised to 950°C. Reasons identified are the high releases of Sr, Ba, Eu from the carbidic fuel acting as a catalyst for the oxidizing reaction [Ziermann 1997].

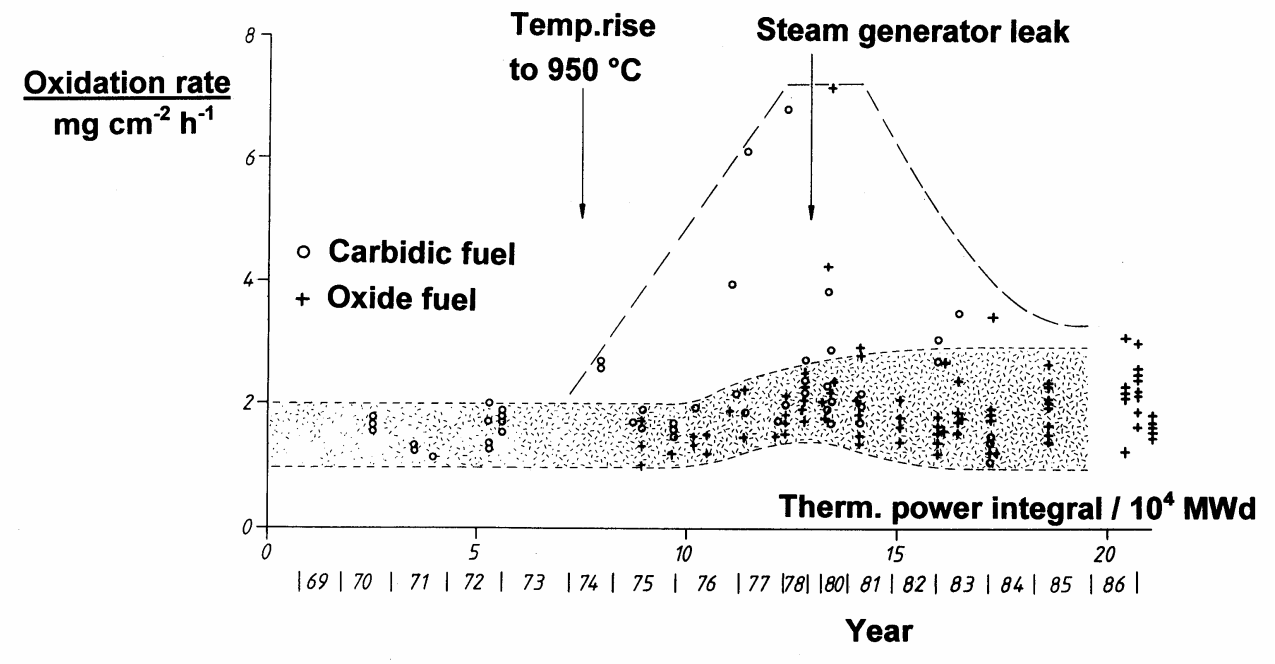

Figure 44 : Measured oxidation rates on spent AVR fuel spheres [Pohl 2001]

The examination of five AVR fuel spheres, four with carbidic (GK), one with oxidic fuel (GO), after the water ingress event in the AVR in May 1978, where 25 m^3 of water were flowing through a leak in the steam generator into the core and fuel elements were under water for about 30 days, has shown moisture levels of up to 2.6 g or 1.3 wt% of H_2O [Burck 1978]. Sphere surfaces contained iron-compound impurities which presumably originated from the corrosion of parts of the fuel handling system, which also were in contact with the water. The strength of the wet balls was found to be significantly reduced, but gained back their previous strength after drying. Corrosion rates were measured to be enhanced by a factor of 2 at 900°C and a factor of 7 at 800°C, respectively, compared to the "typical" values. The results confirmed corresponding data obtained on moist balls from storage containers.

Surface Defects and Breakage of Fuel Spheres

Small damages at the sphere surfaces, apart from scratches, mainly showed up in form of notches and cutting traces or of spalling of parts off the graphite shell. It is a local effect on – as a rule – not more than 1 % of the sphere's surface (see Fig. 45).

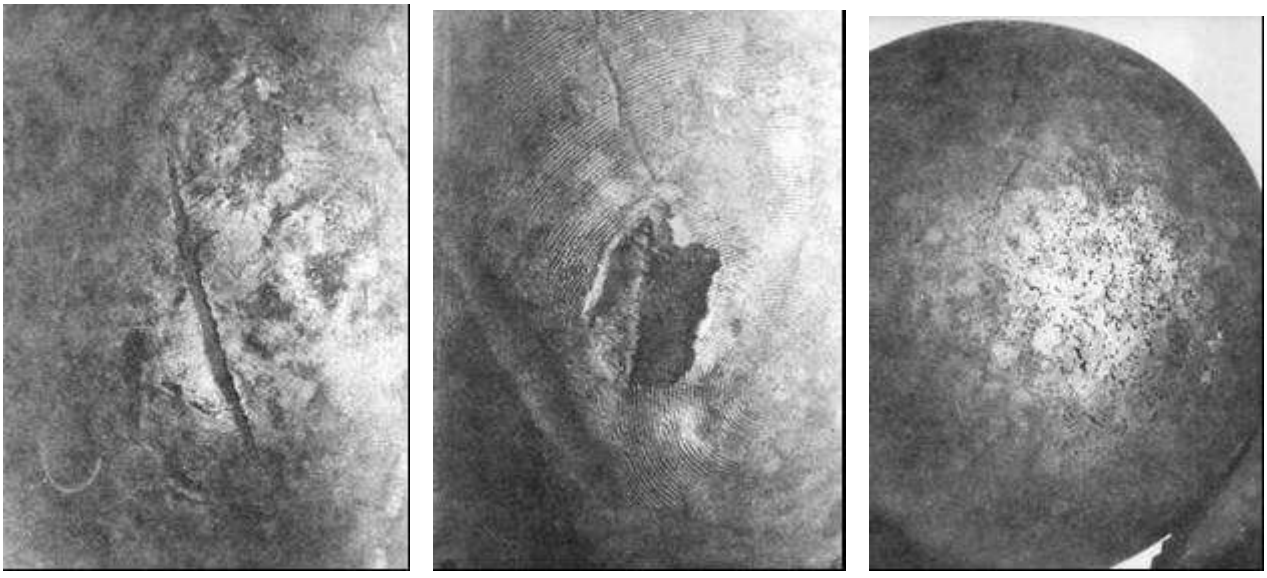

Figure 45 : Fuel element surface damages
notch (left), spalling (middle), pitting (right)

Fractured balls were collected separated. The fact that still intact coated particles were found in the debris, indicated that breakage did not occur in the core, but rather at the core exit prior to (or when) reaching the singulizer. This indication is supported by the finding of a relatively low drop stability of the UCC elements and the strong increase of the fracture rate for UCC with irradiation time. The crushing strength of UCC was found to be reduced to 4 kN at the end of life most probably due to a different shrinkage of graphite shell and fuel zone leading to gap formation.
As of 1977, fracture rate of pressed type balls was determined to be $1.4*10^{-4}$ or 14 balls per cycling of the complete pebble bed [Wimmers 1977]. An overall value for the fraction of broken fuel

spheres of the pressed type was given to be < $2*10^{-5}$, i.e., 1-2 spheres out of 100,000 cycled spheres [Pohl 2001]. A total of 220 broken pebbles were identified, many of them of the shell type UCC or T (see Figs. 46 and 47).

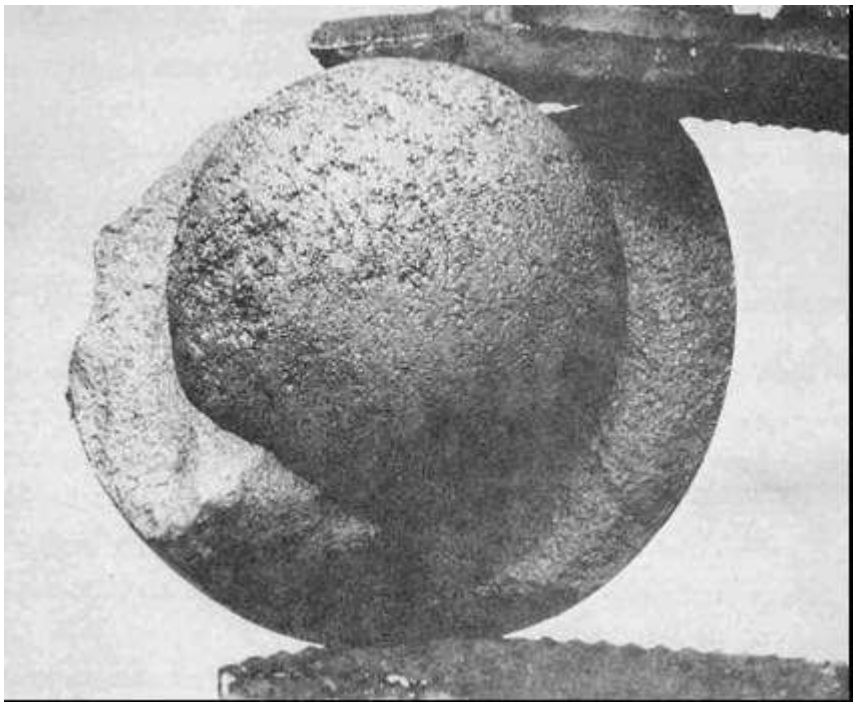

Figure 46 : Broken UCC type fuel sphere
[Wimmers 1977]

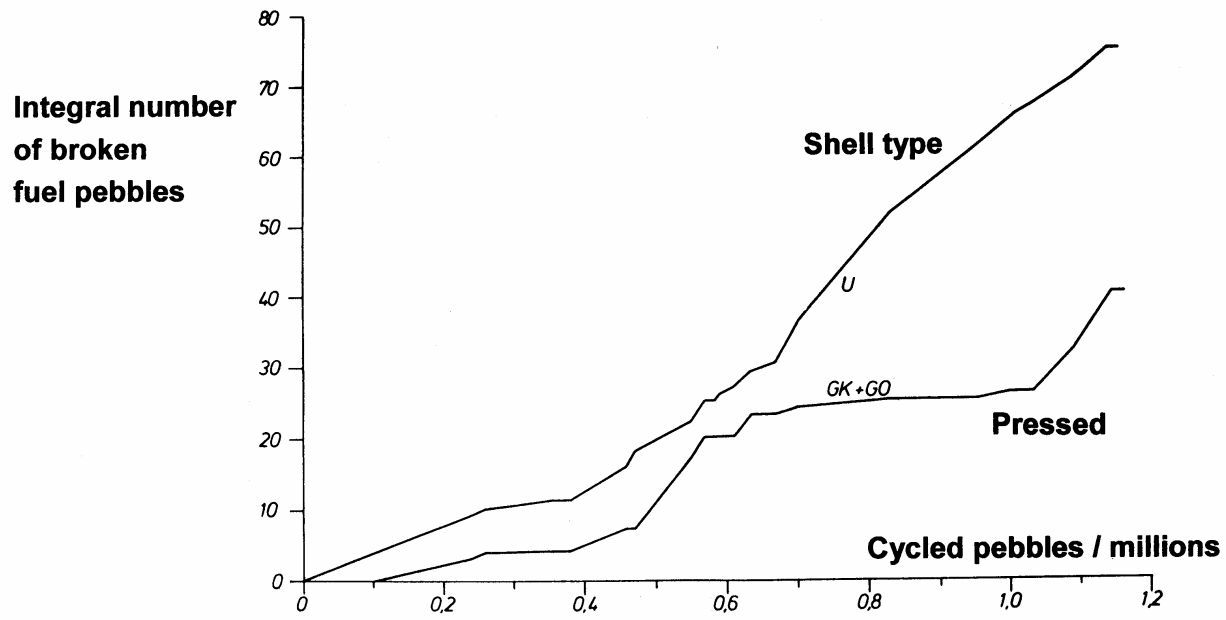

Figure 47 : Fuel breakage in the AVR
[Pohl 2001]

Peeling Effect

It was in 1972 that for the first time a peeling effect was observed (see Fig. 48), but only on the surfaces of carbidic fuel spheres (GK) which had a burnup of > 6% FIMA. These large-area peels had a thickness of 0.1-0.3 mm and an average weight of 2.7 ± 0.2 g, however, with large variations up to 10 g [Wimmers 1977]. The crushing strength of the balls, however, remained approximately the same. The frequency of balls found with peeling effect was 6 % in 1972, rising to 10 % by 1974 and then gradually decreasing again. The origin of the peeling effect was eventually presumed in an air ingress of estimated 100 m^3 that occurred in May 1971 leading to an oxidation reaction which made the sphere surface soft and porous and, with increasing fast neutron fluence, i.e., shrinkage of the matrix, eventually led to a peeling. An estimated 4500 spheres were identified as peeling balls and gradually removed from the core [Burck 1977].

Figure 48 : Peeling effect observed on AVR fuel sphere surfaces [Burck 1977]

3.3.3 *Irradiation Damage*

The typical effects in coated particle fuel from neutron irradiation are kernel swelling, pressure buildup, densification of buffer layer, gap forming layer disconnection, reduction of SiC tensile strength, all of which may increase the probability of a particle failure. For the property SiC tensile strength, most experimental data were achieved for particle batches in the unirradiated state. It was only one batch up to now, EO 1607, for which the change in the Weibull statistical distribution of SiC strength was measured (see Fig. 49).

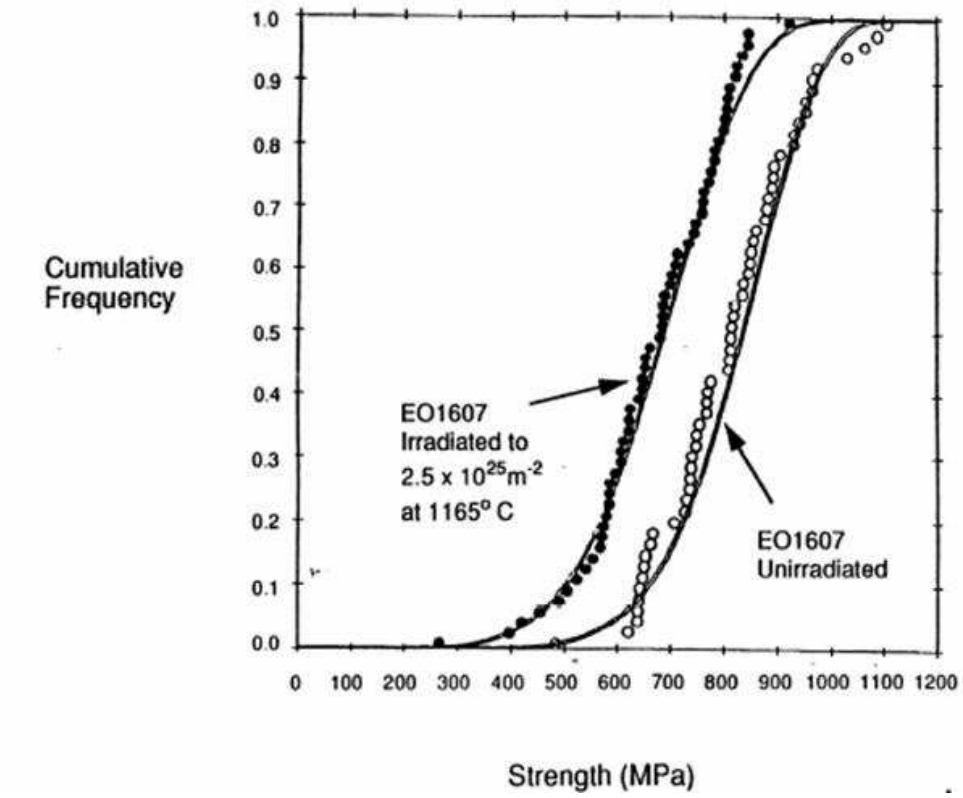

Figure 49 : Weibull distribution of silicon carbide strength measured for particle batch EO1607 before and after irradiation

Ceramography of Coated Particles from AVR Fuel Elements

According to ceramographic cuts of coated particles from the UCC type fuel element, first damages of the inner pyrocarbon (buffer) layer could be observed after short irradiation already (see Fig. 50), later expanding also to the outer, dense PyC layer. However, a complete penetration was never observed [Cautius 1974].

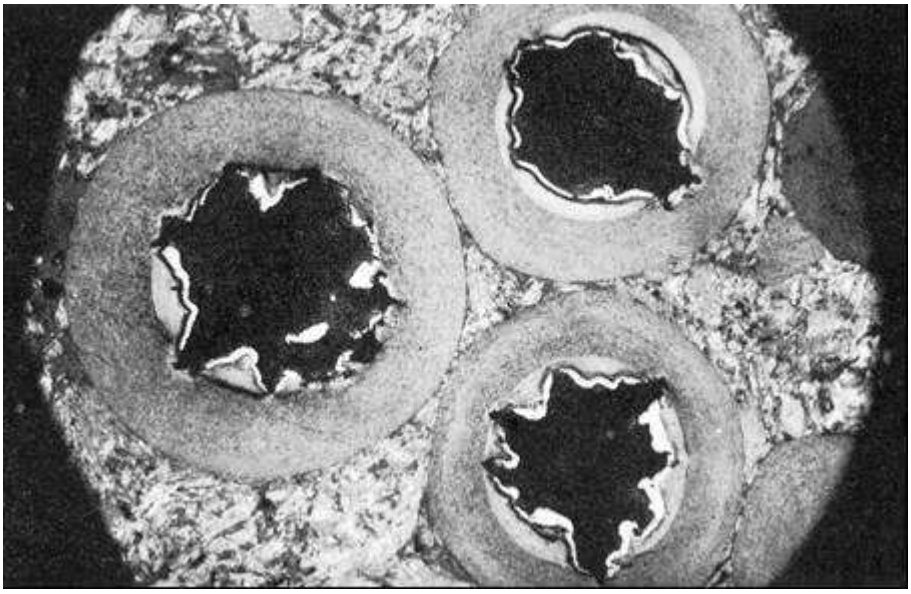

Figure 50 : UCC, 14 % FIMA
[Cautius 1974]

The carbidic particles produced for the T spheres showed a better irradiation behaviour with no damage observed up to a burnup of 14 % FIMA, only a regular shrinkage of the inner PyC layer and gas bubble formation in the kernel (see Fig. 51) [Cautius 1974].

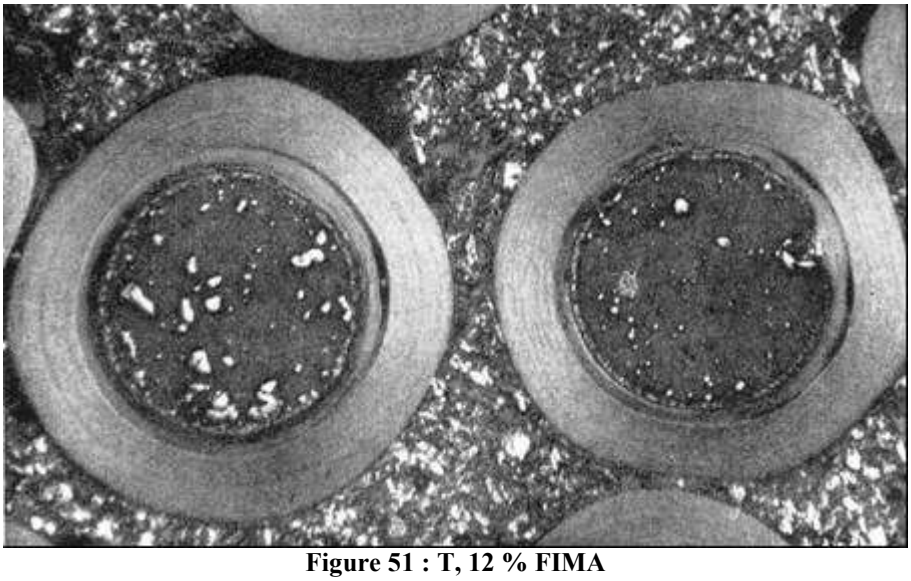

Figure 51 : T, 12 % FIMA
[Cautius 1974]

The investigation of 31 GK type fuel elements taken from 19 random samplings demonstrated a very good irradiation behavior with only minor irradiation-induced damages to the coated particles. At burnups > 10 % FIMA, fission gas bubbles in the kernels could be observed. At > 14 % FIMA, gaps between buffer and HDI layer developed. Radial shrinkage cracks were discovered in only three of the examined particles and never was a destruction of the HDI layer observed. Some examples of ceramographic cuts are shown in Fig. 37 [Gontard 1984a].

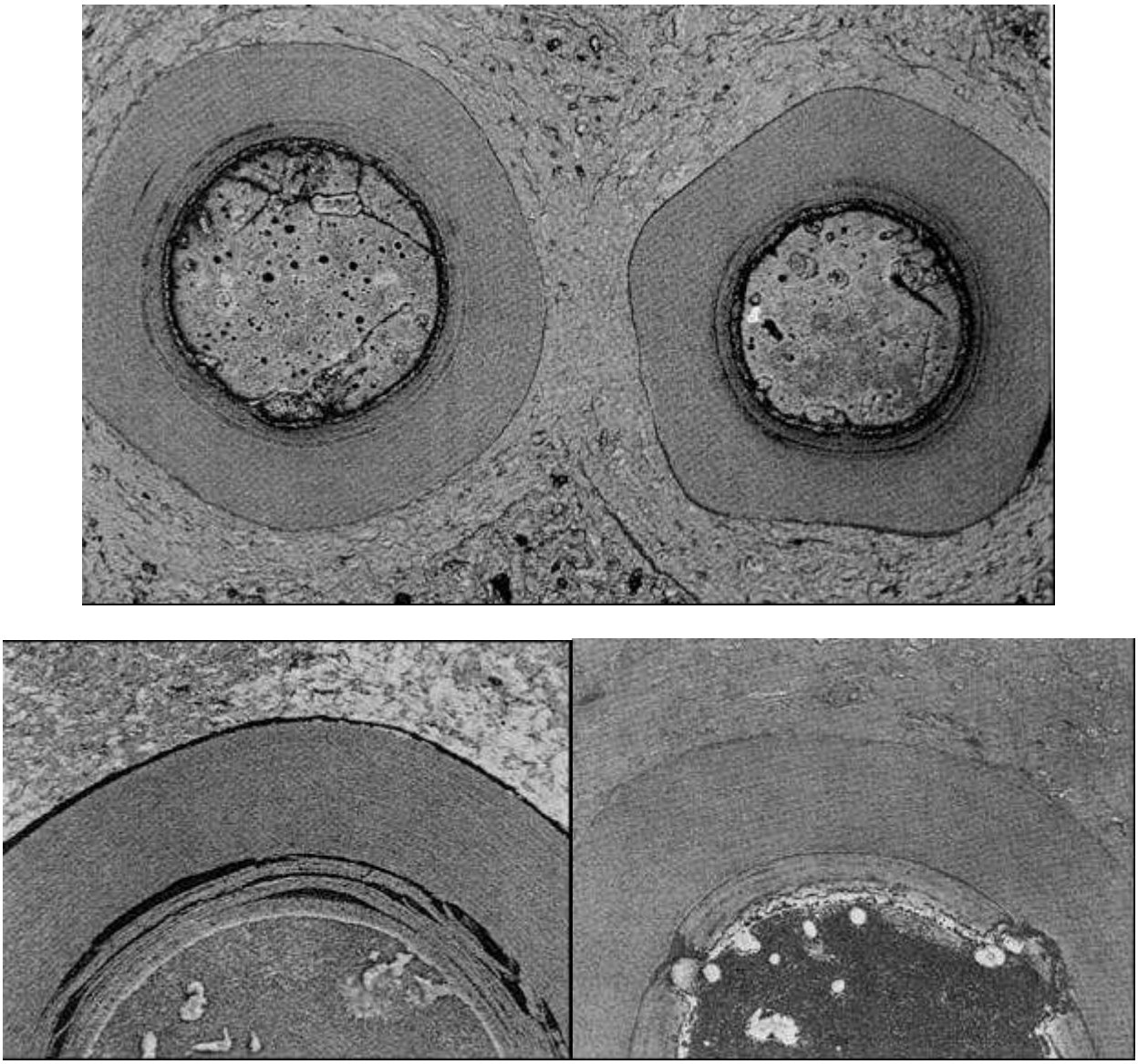

Figure 52 : GK
[Gontard 1984a]
top: 40/56, 15.3 % FIMA, bottom left: 50/29, 17.4 % FIMA, bottom right: 64/15, 18.4 % FIMA

The investigation of 37 GO type fuel elements taken from 22 random samplings has shown that up to a burnup of 6 % FIMA, only slight irradiation-induced changes to the fuel occurred. At higher burnups, 10-15 % FIMA, shrinkage cracks between buffer, sealing, HDI layer, and overcoating developed. It was also observed that the buffer densified with radial cracks into which kernel material has penetrated due to swelling. At burnups above 15 % FIMA, kernels showed numerous pores and larger voids. Gaps between particle and overcoating reached a width of up to 20 µm. Some examples of ceramographic cuts are shown in Fig. 53 [Gontard 1984b].

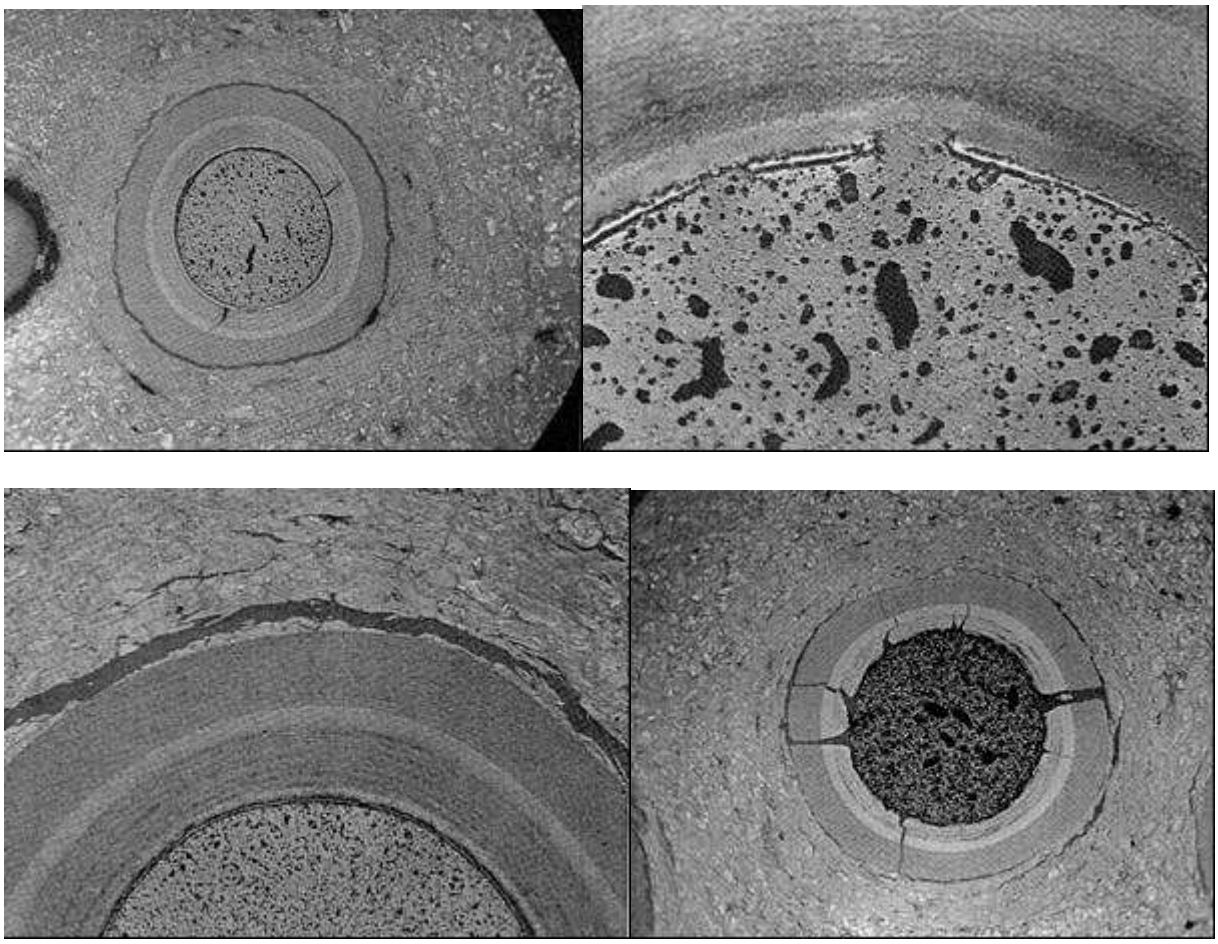

Figure 53 : GO-1
[Gontard 1984b]
top left: 55/34, 15.3 % FIMA, top right: 58/28, 14.6 % FIMA
bottom left: 63/31, 15.4 % FIMA, bottom right: 69/11, 17.4 % FIMA

From the GO-THTR-1 sphere 72/26 (Fig. 54) with 9.3 % FIMA burnup, 13 BISO particles were examined. There is a narrow gap (3 µm) of kernel-buffer interaction, but both sealing and HTI layers appear intact. A decoupling of the overcoating was observed all around the particle with a gap of up to 10 µm.

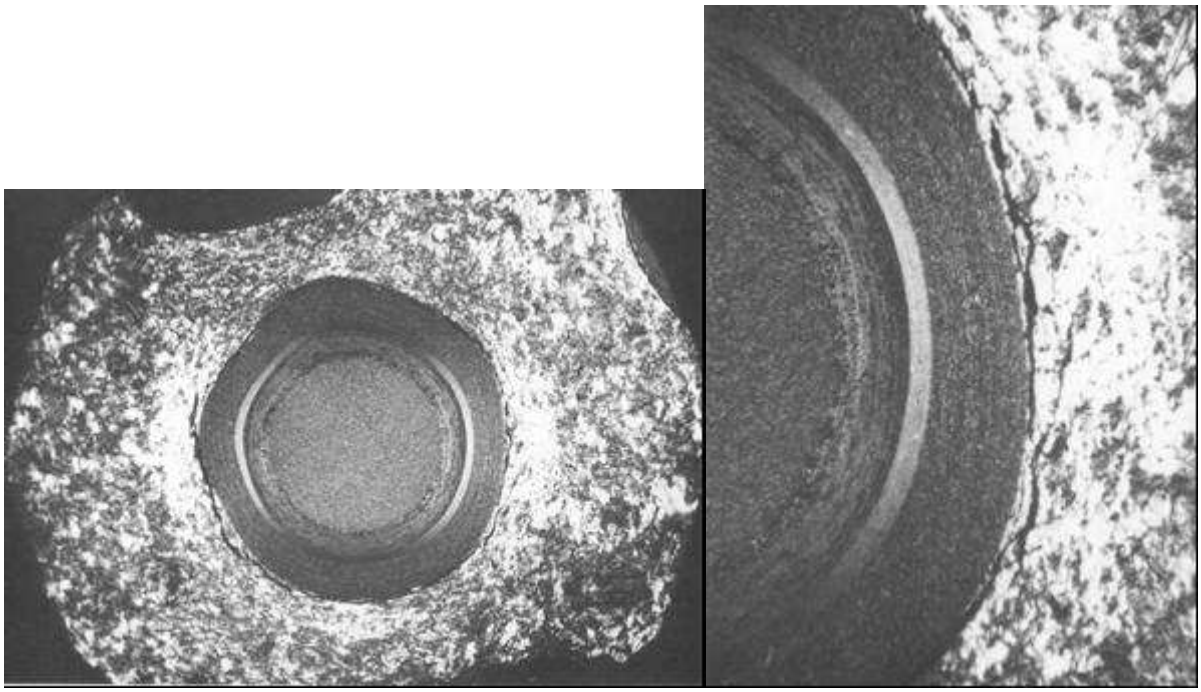

Figure 54 : GO-THTR-1 (72/26), 9.3 % FIMA burnup
[Flossdorf 1985]

Also for the other GO-THTR sample sphere 71/32 of the variant 2 (Fig. 55) with the same burnup of 9.3 % FIMA, sealing and HTI layers were found intact. They show a 3 µm zone of kernel coating interaction (white areas), a buffer which is densified in its inner part, whereas both sealing and HTI layers are still intact. Furthermore decoupling of the overcoating was observed to create a gap up to a width of 20 µm.

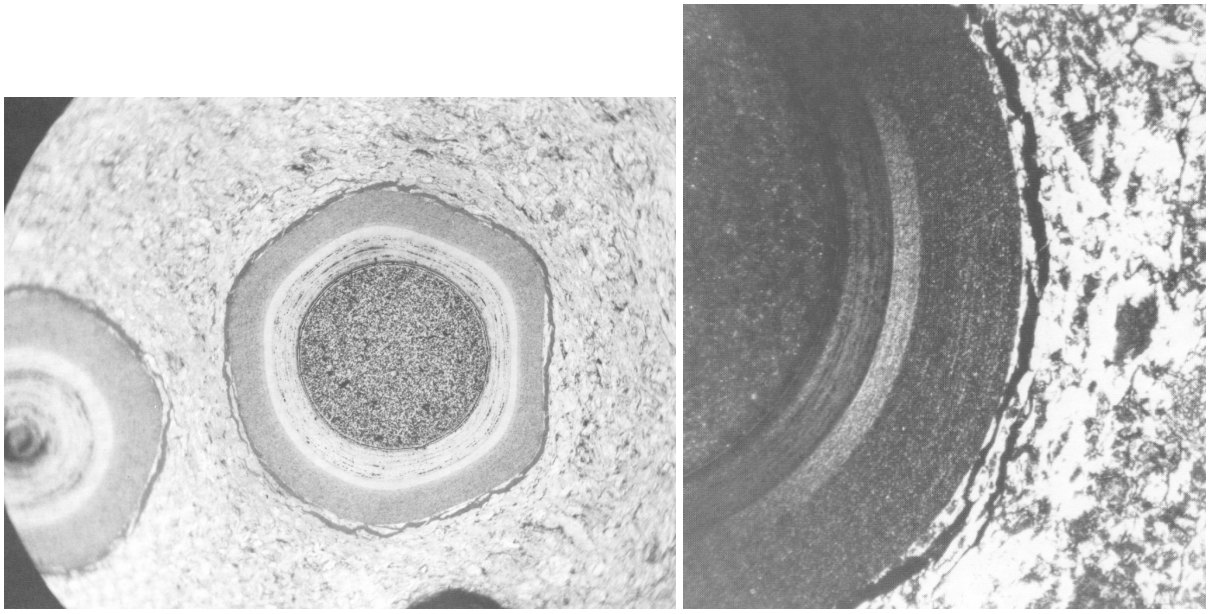

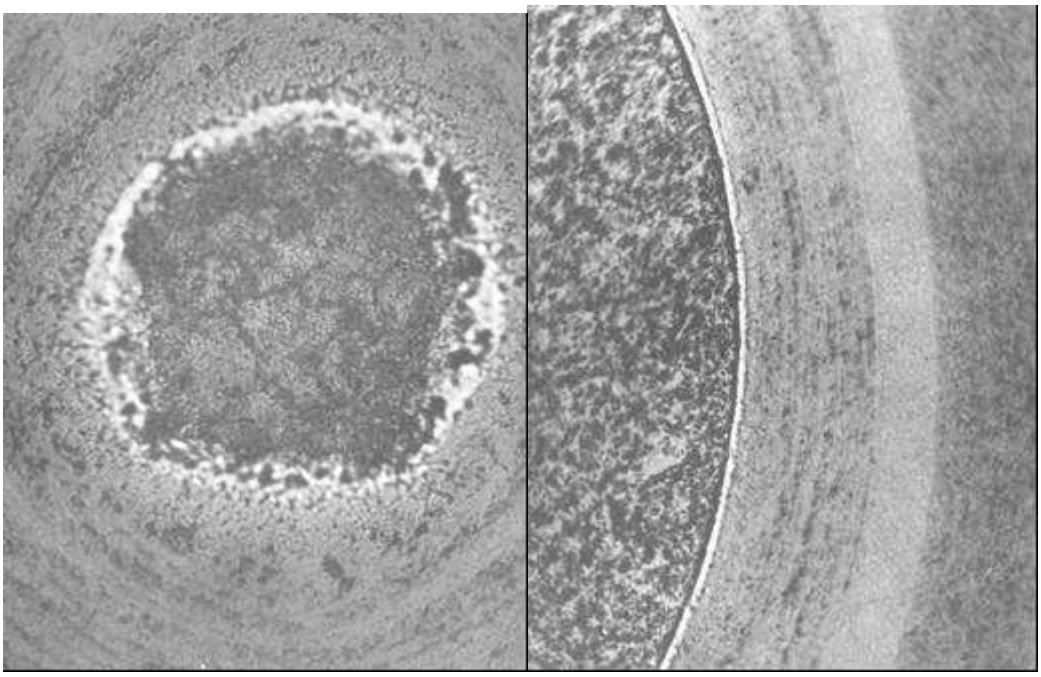

Figure 55 : GO-THTR-2 (71/32), 9.3 % FIMA burnup
[Flossdorf 1985]

Observations for the GO-3 sphere 72/4 with a burnup of 8.4 % FIMA (Fig. 56) were similar to the THTR balls with a small reaction zone between kernel and buffer, intact sealing and HTI layers and decoupled overcoatings.

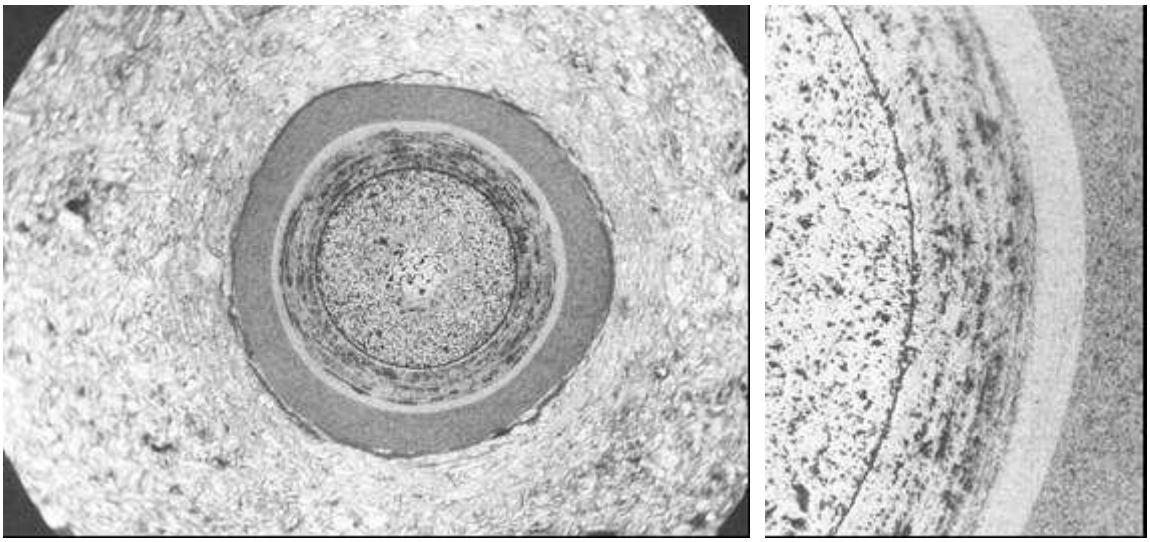

Figure 56 : GO-3 (72/4), 8.4 % FIMA burnup
[Flossdorf 1985]

The GLE-3 sphere 71/26 (Fig. 57) examined containing LEU TRISO coated particles had a burnup of 3.2 % FIMA. Ceramography revealed debonding both of buffer and inner PyC layer in some particles, and partially of outer PyC and overcoating.

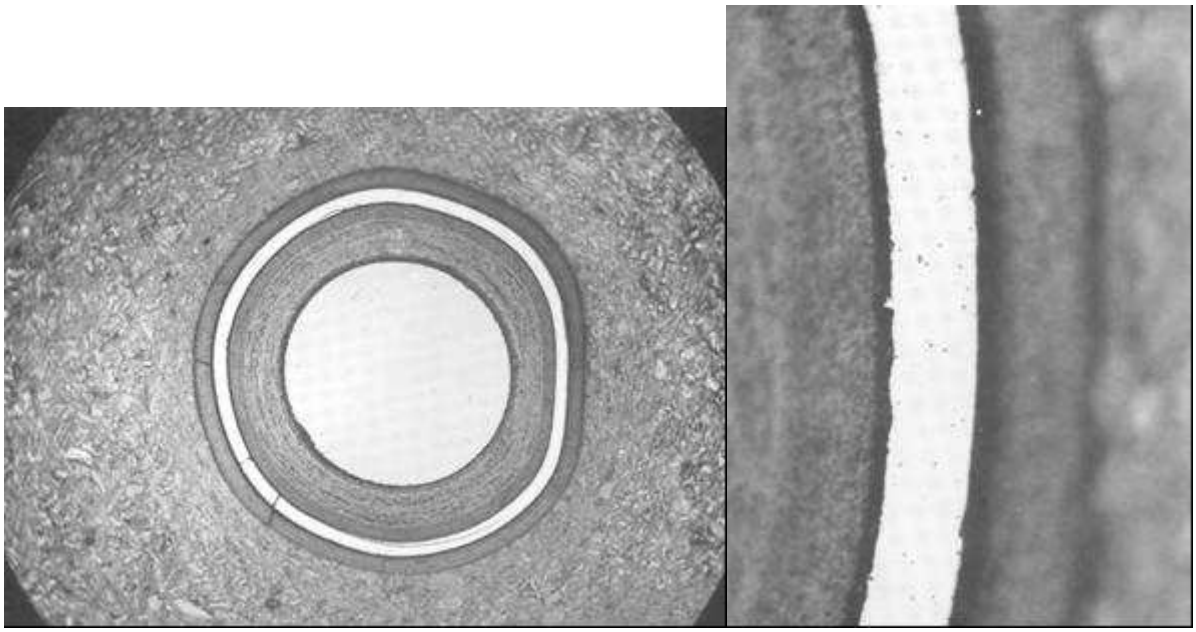

Figure 57 : GLE-3 (71/26), 3.2 % FIMA burnup
[Flossdorf 1985]

For sphere 71/18 of GFB-2 type with fissile TRISO and fertile BISO particles and a burnup of 10.0 % FIMA (Fig. 58), large fission gas bubbles in the fissile kernels were identified as well as local swelling in all particles. Some particles developed radial cracks through both buffer and inner PyC, whereas the outer PyC remained intact. In 90 % of the examined fertile particles, debonding occurred between buffer and HDI layer with tangential gaps of up to 20 µm width.

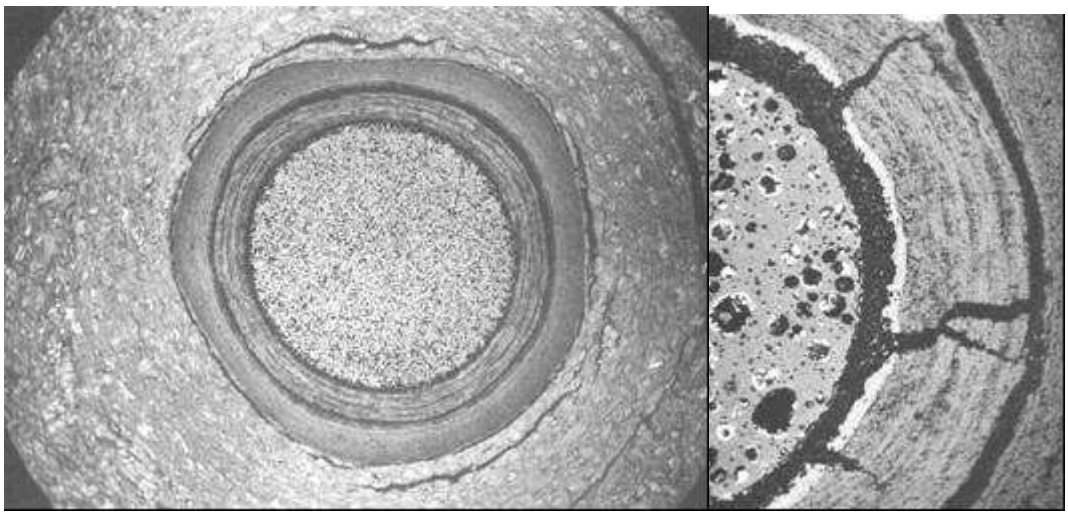

Figure 58 : GFB-2 (71/18), 10.0 % FIMA burnup

Sphere 72/18 of GFB-3 type with carbidic fissile TRISO and fertile BISO particles had a burnup of 11.1 % FIMA (Fig. 59). Kernels showed again large gas bubbles and an up to 15 µm wide carbon deposition layer with local kernel swelling. Buffer-HDI layer debonding was found in all fissile particles. While the HDI layer in the fertile particles remained intact, it debonded with a 10-15 µm from the overcoating.

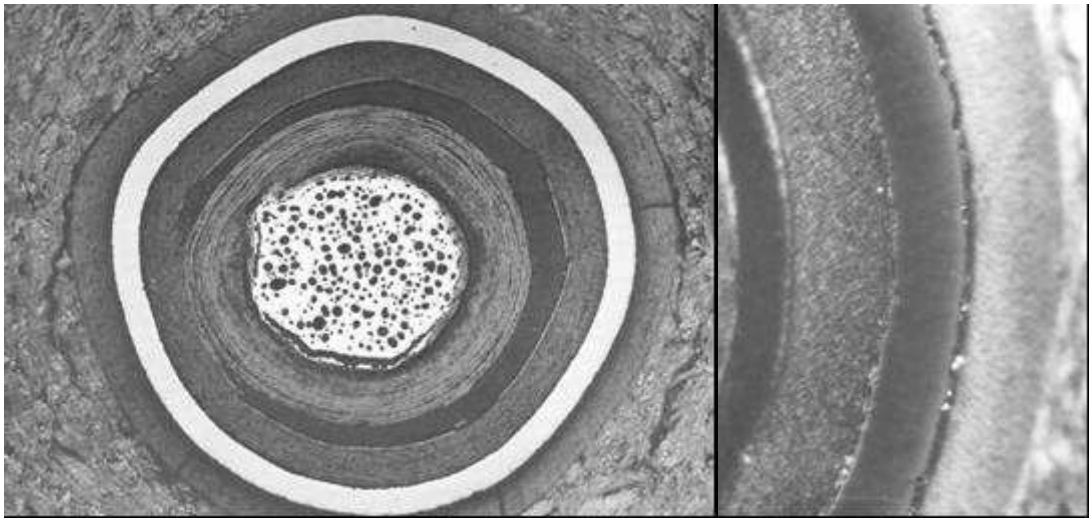

Figure 59 : GFB-3 (72/18), 11.1 % FIMA burnup

Observations on sphere 72/13 of GFB-4 type with 10.1 % FIMA burnup (Fig. 60) were similar to those of the previous GFB-3 ball.

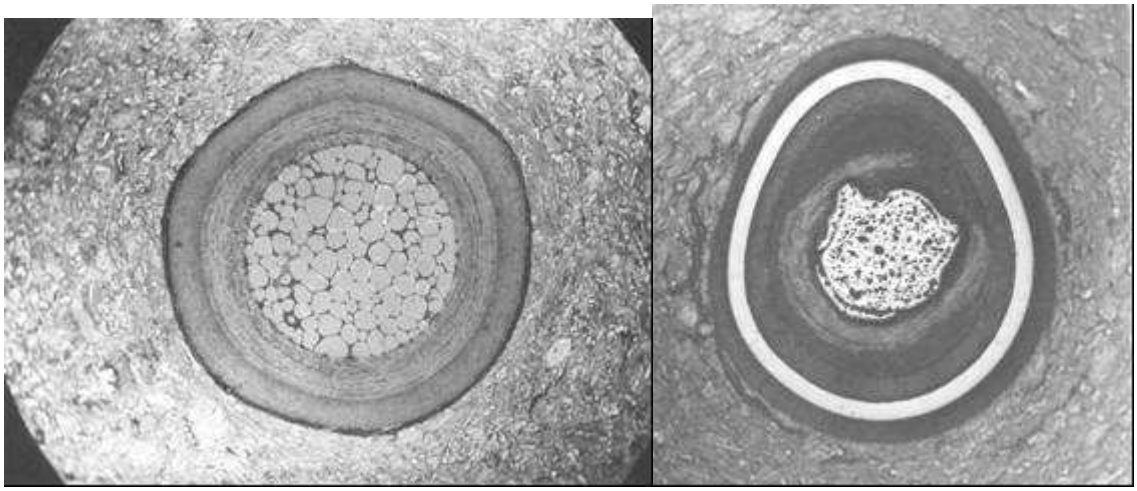

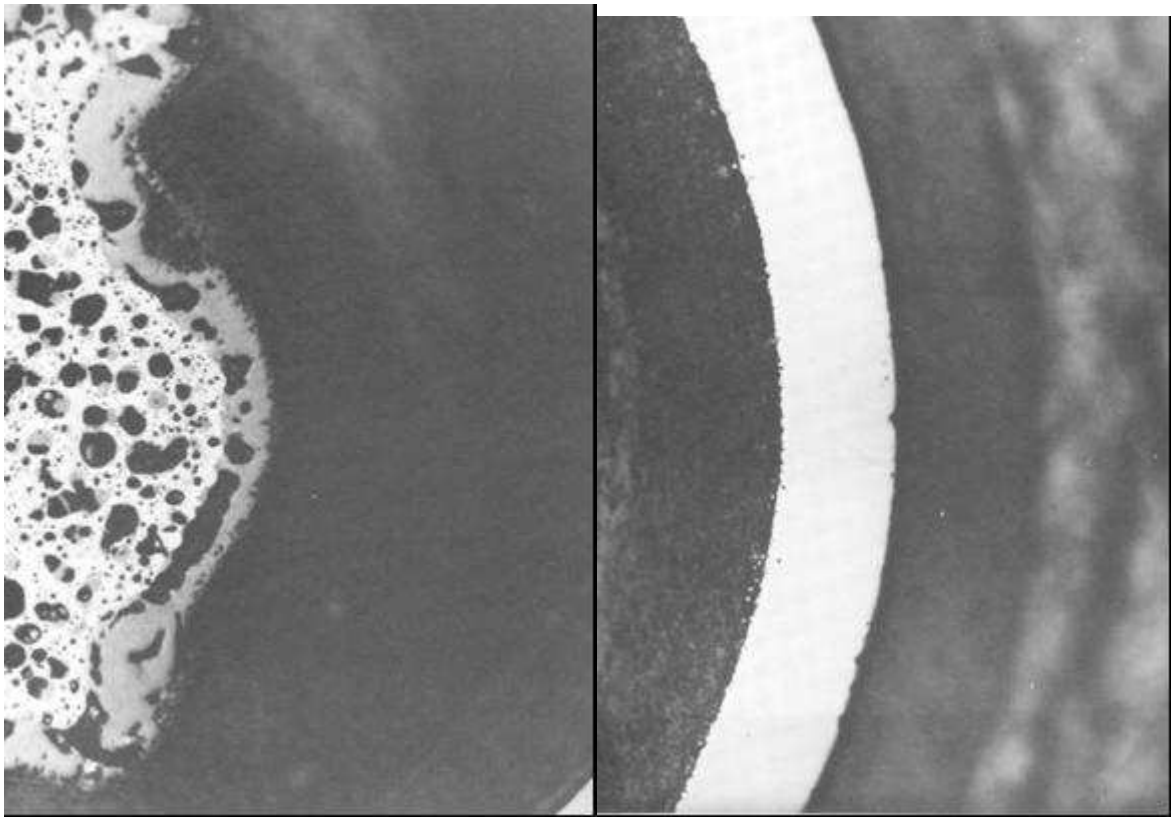

Figure 60 : GFB-4 (72/13), 10.1 % FIMA burnup

The GFB-5 variant with all-TRISO fissile and fertile particles, sample sphere 72/8 with 11.7 % FIMA (Fig. 61), revealed debonding of buffer and inner PyC in all particles. SiC layers remained intact. The kernels had large gas bubbles and massive metallic fission product precipitation as well as a 10-15 µm wide reaction zone with the buffer.

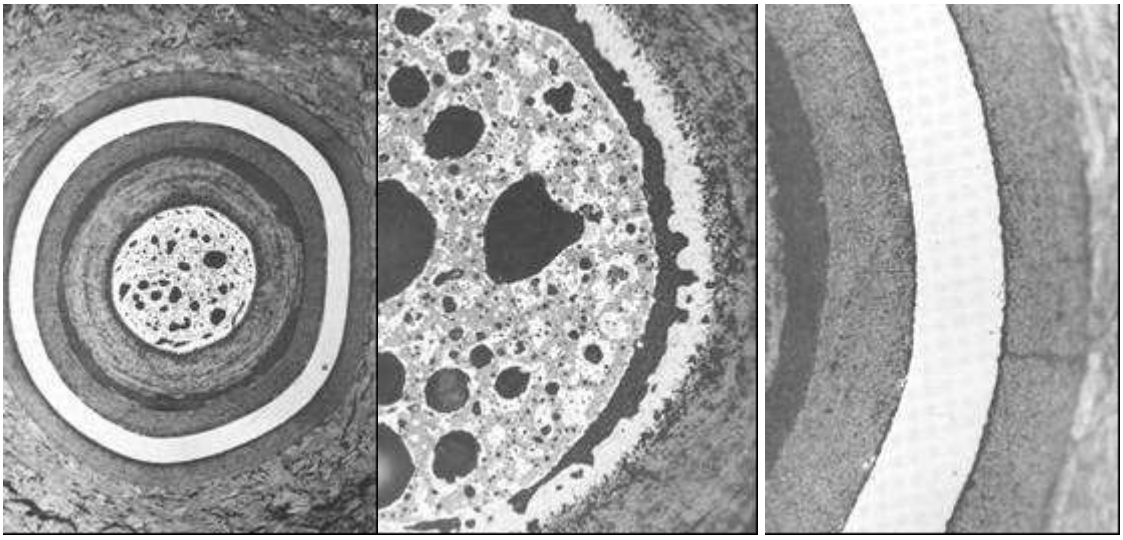

Figure 61 : GFB-5 (72/8), 11.7 % FIMA burnup
[Flossdorf 1985]

Spearhead Attack

The spearhead attack was first observed at Dragon reactor fuel. It is a form of cracking of the PyC layer next to the kernel (buffer) attributed to fission fragments and high temperature chemical interaction between kernel and coating (amoeba attack). The name originates from the typical conical shape observed for the cracks in the buffer layer (see Fig. 62). It was later also observed during PIE of the first UCC and T type fuel elements taken from the AVR; the effect, however, was limited to the buffer and did not influence the outer layer.

The effect was eventually overcome by modification of the buffer manufacture procedure adopting a low-density, low modulus acetylene-derived buffer layer.

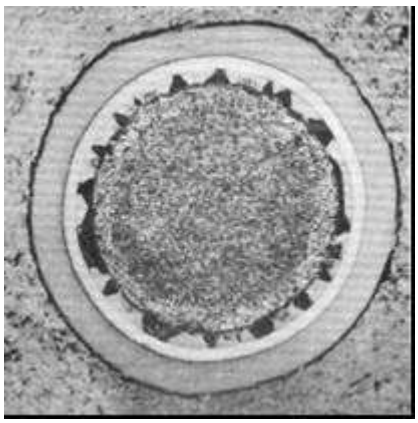

Figure 62 : Metallographs of an irradiated (Th,U)C_2 fuel particle designed to show spearhead attack
(5.2 % FIMA at 1200°C, 30 % porosity)
[Huddle 1969]

3.3.4 Fission Product Release Behavior

After removal from the AVR core, measurements with individual fuel spheres were possible. During operation of the reactor, neither single fuel spheres nor a single fuel element type can be individually analyzed. Only integral statements on the fuel performance over the total core can be given via coolant activity measurements.

The investigation of 45 fuel elements of the UCC type discharged between August 1968 and January 1969 revealed

- no irradiation induced change of graphite;
- insignificant mechanical damage;
- the formation of a 0.1 mm gap between matrix and graphite shell leading to a strong variation of the balls' crushing strength;
- corrosion rates still meeting the specifications of unirradiated material;
- surface contamination of 10^{-3} Ci/sphere mainly due to activation products such as Sc-46, Hf-181, and Co-60;
- low activity release of $< 5*10^{-4}$ (Xe-132) during operation;
- "spearhead" attack on the inner PyC layer.

Crush tests with irradiated fuel spheres have shown occasionally spontaneous Kr-85 release bursts indicating failing particles. The failure fraction, however, was not higher than 10^{-3} for both BISO and TRISO particles [Brinkmann 1990].

Strontium and Cesium Contamination of the AVR Core

In 1974, after raising the average coolant outlet temperature from 850 to 950°C, a relatively high level of strontium contamination was identified in the AVR core, which has caused a maintenance problem since. The AVR was even quoted as having "the worst beta contamination of any nuclear installation in the world" [Nucleonics Week 2002]. The origin of this strontium could be traced back to enhanced release from carbidic fuel with $(Th,U)C_2$ HTI BISO coating (UCC, T, GK) and at temperatures > 900°C having reached a maximum burnup of 17 % FIMA [Ziermann 1997].

While strontium was mainly released from the carbide fuel, the origin of the cesium is particularly from the poor-quality GLE-1 type fuel elements.

The "Irradiated Microsphere Gamma Analyzer", IMGA, is a PIE system to characterize the performance of a large population of coated particles measuring radioisotope inventories of individual coated particles by detecting γ radiation. Among the fuel spheres examined at the ORNL with the IMGA method was the AVR irradiated GLE-3 sphere 76/20 used as a control sphere (vs. irradiated and heated spheres). From the electrolytically deconsolidated AVR ball, some 5000 individual coated particles were given to the IMGA system. The main result was characteristic of no particle failure. No statistical evidence of cesium release from the individual particles and no significant particle-to-particle variation in fission product retention was observed [Baldwin 1990].

Fission Product Profiles in the Fuel-Free Zone

The fuel-free zone of spheres was examined with respect to the long-lived isotopes of cesium, strontium, silver, and others. The procedure of profile measurement was usually such that a 6 mm wide groove was made over the whole circumference of the sphere in 10 steps of 0.4 mm each. Activities for these single graphite powder specimens were then measured and calculated back to the date of discharge from the reactor.

Fig. 63 shows for the nuclide Cs-137 the profiles discovered in GLE-1 spheres with (top curve) and without (bottom curve) defective / failed particles. Concentrations at the surface are generally higher (for normal particle performance) than further inside the ball. Activity transported with the coolant was obviously deposited on the fuel element surfaces in colder core areas. In contrast, a high concentration level well inside the ball indicates the presence of defective / failed particles having released part of their radionuclide inventory into the matrix material.

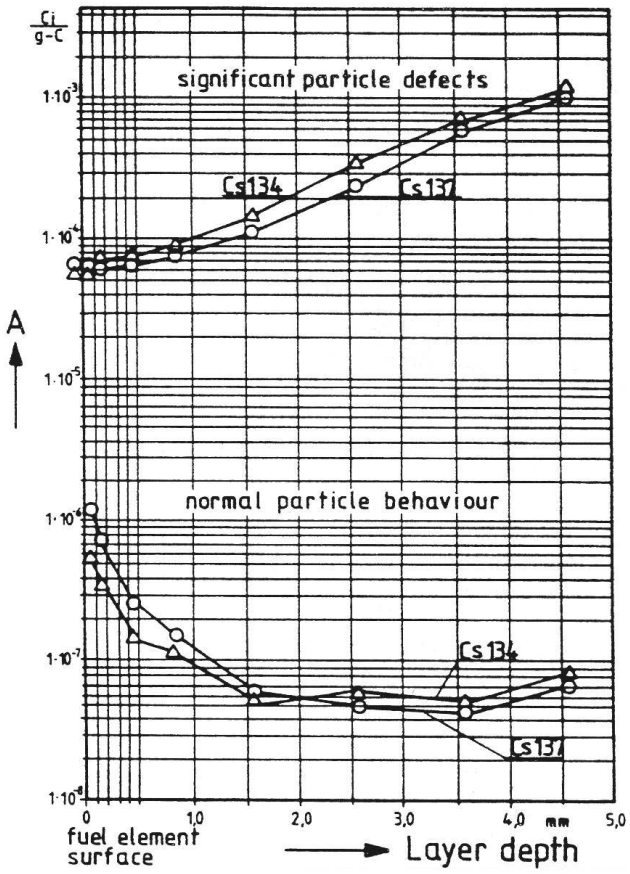

Figure 63 : Cesium profiles in the fuel-free zone of AVR fuel elements with and without failed coated particles [Wawrzik 1985]

The Ag-110m profiles were found to be strongly varying for different spheres with sometimes high, sometimes low activities. No burnup dependence on the release behaviour was observed.

The above profiles were also observed in other fuel types [El-Masry 1989]. Measurements of fission product profiles on various fuel spheres and a moderator (graphite) ball transformed into activity ratios (surface over depth of 3.9 mm) are summarized in Table 28. The typical profiles were even observed for a moderator sphere (see Fig. 64). Deviations were only found for silver.

Table 28 : Activity ratios in the fuel-free zone of different fuel types [El-Masry 1989]

Fuel element	Burnup [%FIMA]	Cs-137			Cs-134	Ag-110m
		surface	3.9 mm depth	ratio	ratio	ratio
		[10^{13} atoms/g graphite]				
GO-1	9.0	11	6.7	1.6	5.0	-
GO-1	9.3	9.8	2.7	3.6	1.6	44.0
GO-1	10.5	8.7	2	4.4	1.9	39.7
GO-THTR-2	8.8	37	10	3.7	3.7	3.2
GO-THTR-2	8.8	12	5.4	2.2	1.3	0.8
GO-THTR-2	9.6	24	4.8	5.6	4.0	0.8
GFB-2	10.8	18	1.9	9.5	4.3	15.5
GFB-2	11.1	19	13	1.5	1.0	20.0
GLE-3	3.9	19	3.3	5.8	3.2	36.5
Moderator	-	14	2.8	5	2.5	5.5

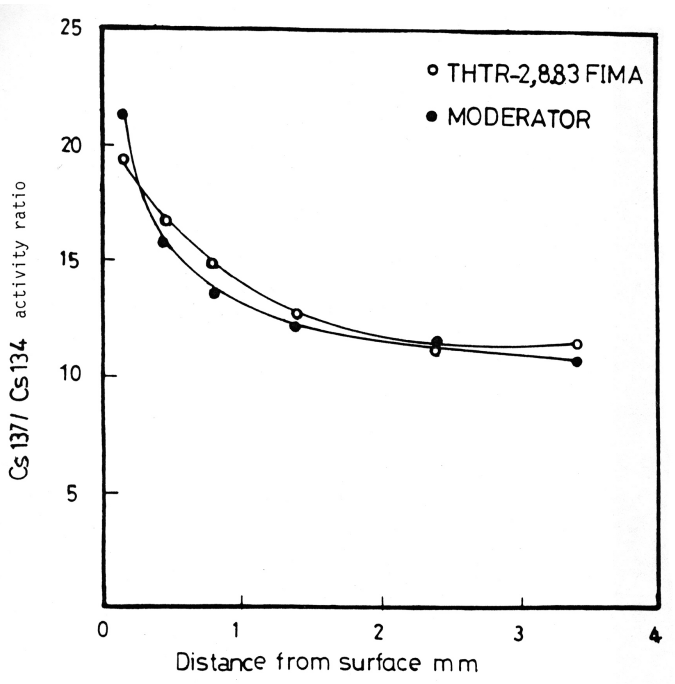

Figure 64 : Comparison of activity ratios Cs-137/Cs-134 between a GO-THTR sphere and a moderator graphite sphere [El-Masry 1989]

The principal sources of C-14 in HTR fuel elements are the nuclear reactions :

N-14	(n,p)	C-14
C-13	(n,γ)	C-14
O-17	(n,α)	C-14

C-14 production rates in AVR fuel elements during operation were estimated from the contents of the above sources, respectively, of AVR spheres with the following results [AVR 1977] :

82 Bq ($2.2*10^{-9}$ Ci)/efpd of C-14	from C-13 contained in a 200 g graphite sphere
140 Bq ($3.8*10^{-9}$ Ci)/efpd of C-14	from 1 ppm of N-14 impurity in the ball

Depending on its lifetime, a fuel element can accumulate a C-14 inventory of up to $5*10^{6}$ Bq, from which a nitrogen contents in the ball of 15-30 ppm can be assessed contributing by around 75% to the C-14. In contrast, the contribution from the coated particles is very small meaning that in a potential head-end, i.e., the step of separating the graphite from the heavy metal, most of the C-14 will be removed [Schmidt 1979].

Since 1980, integral measurements of C-14 were conducted every 3 months. For the period 1980-1983, an activity of 126 GBq (3.4 Ci)/yr ± 40% with decreasing tendency was observed. Furthermore a strong correlation between C-14 release and graphite corrosion rates was identified. The measured C-14 profiles shown in Fig. 65 have a nearly constant level at 37,000 Bq (1 µCi)/g of graphite inside the sphere with increasing values near the surface [Röllig 1984].

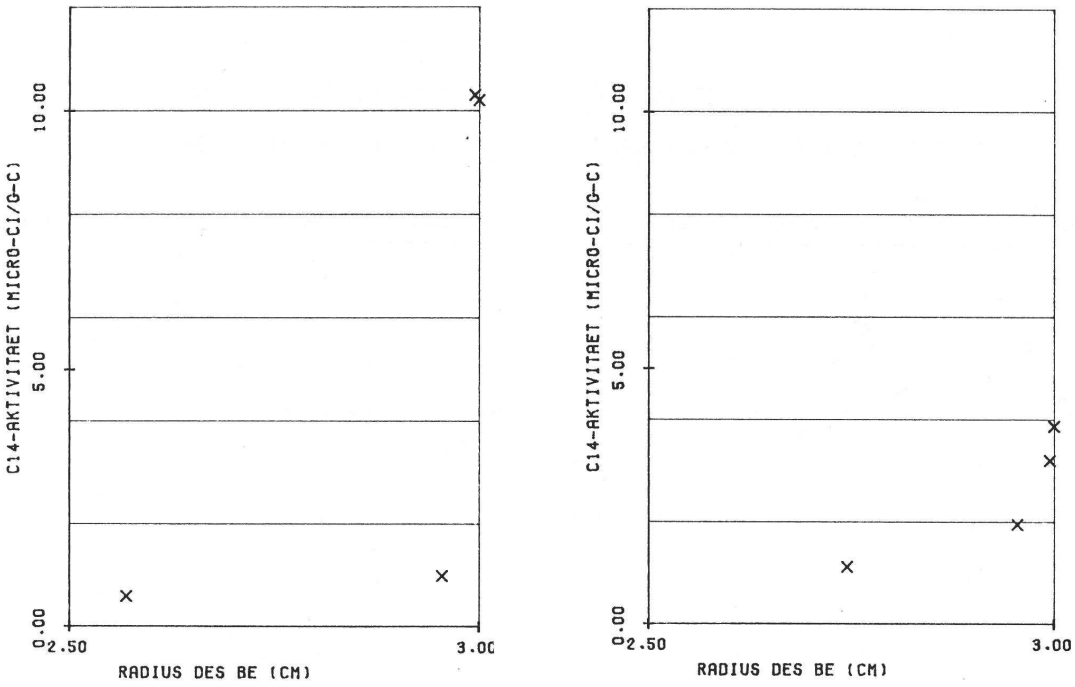

Figure 65 : C-14 profiles in the fuel-free zone of GK fuel elements from the AVR left: 57/26 (14.8 % FIMA), right: 59/23 (14.4 % FIMA) [Röllig 1984]

The increase in concentration towards the surface is mainly from air getting access to the sphere during the manufacturing process after the heat treatment. Other sources are impurities in the helium due to, e.g., air ingress or ammonia injection for testing purposes.

3.4 Postirradiation Examination of THTR Fuel

Unlike the AVR reactor, the THTR-300 was fueled with only one type of fuel element and coated particle design (see Table 5 in section 2.2.2.). Also fuel temperatures were lower than in the AVR under normal operating conditions with the average coolant temperature being 750°C at the steam generator inlet.

Apart from the experience gained from THTR operation, the investigation of the irradiation behavior of THTR fuel elements was done in respective experiments in MTRs and, as a mass test, in the AVR reactor. The THTR reactor itself was not designed for an intentional discharge of fuel elements for testing purposes. Correspondingly, PIE work was conducted on those spheres tested in the MTRs and on random samples of THTR-type fuel taken from the AVR. There were never fuel elements discharged from the THTR taken for further post-irradiation examination.

The calculated contents of heavy metal contained in 617,606 fuel elements discharged from the THTR core are given in the following Table 29 [Niephaus 2000].

Table 29 : Calculated HM contents of the fuel elements discharged from the THTR reactor [Niephaus 2000]

Contents in total THTR fuel [kg]						
U-233	**U-235**	**U-238**	**Th-232**	**Pu-238**	**Pu-241**	**Pu-total**
104.	239.	-	6110.			2.2

3.5 Postirradiation Examination of German HTGR Fuel from MTR Irradiation Tests

Apart from mass testing in the AVR, also MTRs were taken for irradiation testing in order to qualify the fuel. Table 30 gives an overview of the irradiation tests performed.

Table 30 : German irradiation experimental program with HTGR fuel

Old LEU 1972-1976	**HEU program for PNP and HHT 1977-1981**			**LEU program 1982-1993**	**Test goal**
UO_2 TRISO UO_2 BISO	Variant 1 $(Th,U)O_2$ BISO	Variant 2 $(Th,U)O_2$ TRISO	Variant 3 UC_xO_y TRISO ThO_2 TRISO	UO_2 TRISO	
Tests with coated particles					
HFR-M5 DR-S6	BR2-P24	BR2-P25	BR2-P23	HFR-P4 SL-1	Particle Performance
DR-S4	FRJ2-P22	FRJ2-P23	FRJ2-P24	FRJ2-P27	FP transport in intact particles
	FRJ2-P25	FRJ2-P25	FRJ2-P25	FRJ2-P28	Release from kernel
FRJ2-P16			HFR-P3	HFR-P5	Chemical effects
Tests with fuel elements					
DR-K5	HFR-K1	R2-K12 R2-K13	R2-K12	HFR-K3	Fuel element performance
		FRJ1-K11	FRJ2-K10	FRJ2-K13 FRJ2-K15	FE fission product transport
AVR 6	AVR 14	AVR 15	AVR 13	AVR 19 AVR 21 AVR 21-2	Large-scale demonstration
				HFR-K5 HFR-K6	Proof tests

AVR, Jülich, Germany
FRJ2, Jülich, Germany
DR, Dragon, Winfrith, United Kingdom
HFR, Petten, The Netherlands
R2, Studsvik, Sweden
BR2, Mol, Belgium
SL, Siloe, Grenoble, France

While in an early phase of LEU TRISO fuel testing, the fuel was exposed to isothermal conditions in order to demonstrate the suitability of the particle design, it was in later tests subjected to temperature cycles typical for the HTR-Modul and other thermal transients expected during operational events. Table 31 provides more detailed data on the irradiation testing of HEU and LEU TRISO fuel.

Table 31 : Parameters and results from irradiation testing with modern TRISO particles

Experiment	Fuel	Specimen	No. of cp	Irradiation time [efpd]	Center temperature [°C]	Burnup [% FIMA]	Fast fluence [10^{25} m^{-2}, E>0.1MeV]	EOL Kr-85m R/B	EOL Cs-137 fractional release	EOL Ag-110m fractional release
HFR-P4/1	UO_2 LEU	12 spheres	19,600	351	940-1008	11.1-14.7	5.5-8.0	$8.0*10^{-8}$	$5*10^{-6}$	
HFR-P4/3		12 spheres	19,600		1010-1082	10.9-14.7	6.1-8.0	$8.0*10^{-9}$	$2*10^{-5}$	
SL-P1	UO_2 LEU	12 spheres	19,600	330	743-794	8.6-11.3	5.0-6.8	$1.2*10^{-6}$	$5*10^{-6}$	
HFR-K3/1	UO_2 LEU	1 FE	16,400	359	1200	7.5	4.0	$1*10^{-7}$	$9.1*10^{-6}$	$2.2*10^{-3}$
HFR-K3/2		1 FE	16,400		920	10.0	5.8	$1*10^{-7}$	$1.7*10^{-5}$	$4.5*10^{-4}$
HFR-K3/3		1 FE	16,400		920	10.6	5.9	$1*10^{-7}$	$1.7*10^{-5}$	$1.6*10^{-4}$
HFR-K3/4		1 FE	16,400		1220	9.0	4.9	$3*10^{-7}$	$1.4*10^{-5}$	$1.8*10^{-2}$
FRJ2-K13/1	UO_2 LEU	1 FE	16,400	396	1125	7.5	0.2	$2*10^{-8}$	$1.4*10^{-5}$	$1.9*10^{-2}$
FRJ2-K13/2		1 FE	16,400		1150	8.0	0.2	$2*10^{-8}$	$1.8*10^{-5}$	$2.0*10^{-2}$
FRJ2-K13/3		1 FE	16,400		1150	7.9	0.2	$7*10^{-9}$	$6.1*10^{-6}$	$1.7*10^{-2}$
FRJ2-K13/4		1 FE	16,400		1120	7.6	0.2	$7*10^{-9}$	$6.4*10^{-6}$	$3.9*10^{-2}$
FRJ2-P27/1	UO_2 LEU	3 comp.	7340	232	880-1080	7.2-8.4	1.4	$1.6*10^{-6}$	$4.7*10^{-5}$	$1.8*10^{-2}$
FRJ2-P27/2		3 comp.	7340		1220-1320	8.0-9.0	1.7	$1.0*10^{-5}$	$1.5*10^{-4}$	$8.2*10^{-3}$
FRJ2-P27/3		3 comp.	7340		1080-1130	7.2-8.1	1.3	$1.2*10^{-7}$	$1.6*10^{-4}$	$2.0*10^{-2}$
FRJ2-K15/1	UO_2 LEU	1 FE	9600	533	970	14.1	0.2	$1*10^{-8}$	$1.1*10^{-6}$	$7.5*10^{-4}$
FRJ2-K15/2		1 FE	9600		1150	15.3	0.2	$5*10^{-9}$	$9.5*10^{-7}$	$3.2*10^{-3}$
FRJ2-K15/3		1 FE	9600		990	14.7	0.1	$3*10^{-9}$	$4.3*10^{-7}$	
HFR-K5/1	UO_2 LEU	1 FE	14,580	565	923	7.8	4.0	$1.6*10^{-7}$		
HFR-K5/2		1 FE	14,580		909	10.1	5.8	$3.1*10^{-7}$		
HFR-K5/3		1 FE	14,580		903	10.3	5.9	$3.1*10^{-7}$		
HFR-K5/4		1 FE	14,580		921	9.3	4.9	$3.5*10^{-7}$		
HFR-K6/1	UO_2 LEU	1 FE	14,580	634	1090	8.3	3.2	$1.5*10^{-7}$		
HFR-K6/2		1 FE	14,580		1130	10.6	4.6	$4.4*10^{-7}$		
HFR-K6/3		1 FE	14,580		1140	10.9	4.8	$4.4*10^{-7}$		
HFR-K6/4		1 FE	14,580		1130	9.9	4.5	$1.2*10^{-6}$		
		Total LEU Σ	357,460							

Table 31 (cont'd): Parameters and results from irradiation testing with modern TRISO particles

Experiment	Fuel	Specimen	No. of cp	Irradiation time [efpd]	Center temperature [°C]	Burnup [% FIMA]	Fast fluence [10^{25} m^{-2}, E>0.1MeV]	EOL Kr-85m R/B	EOL Cs-137 fractional release	EOL Ag-110m fractional release
R2-K12/1 R2-K12/2	$(Th,U)O_2$ HEU	1 FE 1 FE	10,960 10,960	308	1100 1280	11.1 12.4	5.6 6.9	$3*10^{-7}$ $2*10^{-7}$	$2.4*10^{-5}$ $1.7*10^{-5}$	$3.3*10^{-2}$ $1.4*10^{-2}$
R2-K13/1 R2-K13/4	$(Th,U)O_2$ HEU	1 FE 1 FE	19,780 19,780	517	1170 980	10.2 9.8	8.5 6.8	$7*10^{-8}$ $5*10^{-8}$	$1.1*10^{-5}$ $3.2*10^{-6}$	$3.9*10^{-2}$ $2.7*10^{-3}$
BR2-P25	$(Th,U)O_2$ HEU	12 spheres	17,880	350	1043	13.9-15.6	6.2-8.1	$1*10^{-6}$	$4*10^{-4}$	
		Total HEU Σ	79,360							
		Total TRISO Σ	436,820							

Fig. 66 is, as an example, the record of R/B measurements for various fission gases in one of the three FRJ2-K15 capsules showing an extremely low release level. The spikes in R/B have been measured during +200°C temperature transients. The slow increase in R/B is an artifact of the birthrate calculation for 16.7% enriched uranium, while the actual release is from uranium contamination of natural enrichment.

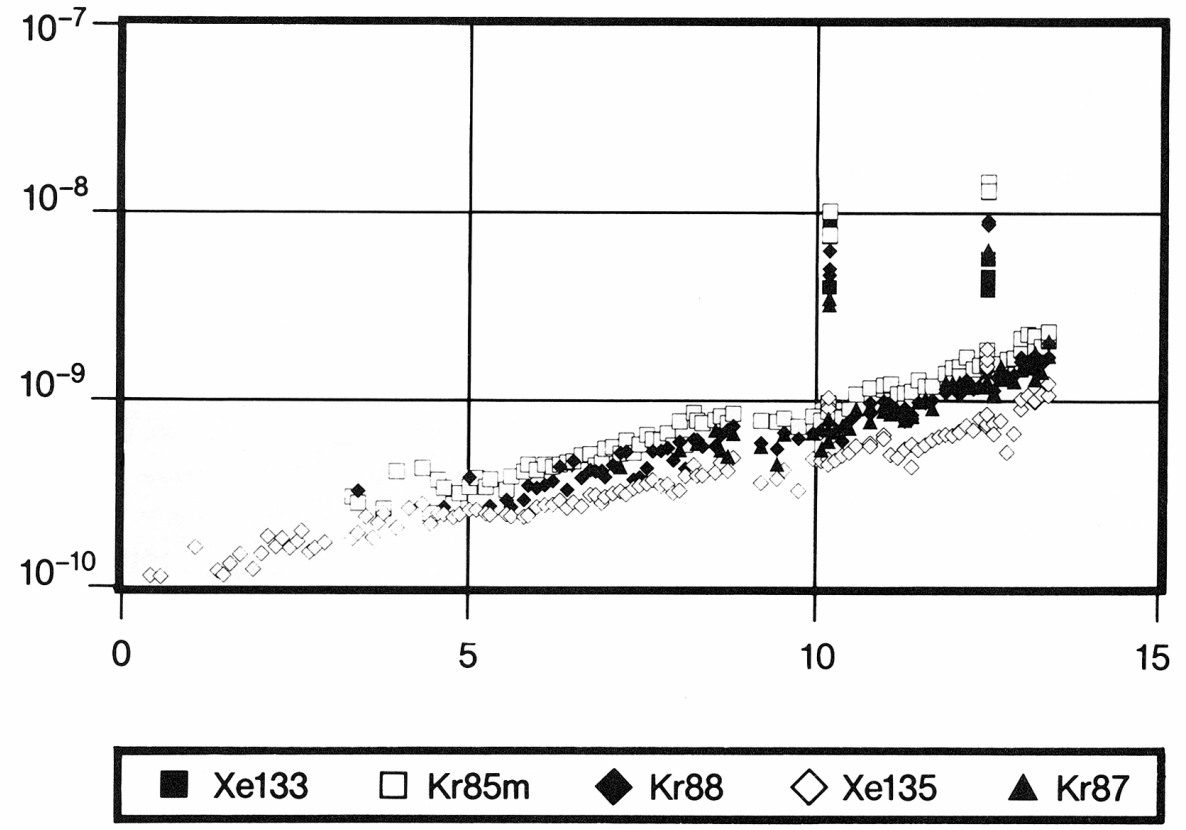

Figure 66 : R/B measurements in cell 3 of the FRJ2-K15 irradiation test

During the irradiation program with LEU UO_2 TRISO fuel, a particle failure during irradiation was never observed.

Coating quality is demonstrated by the retention of solid fission products. The diagram in Fig. 67 summarizes the EOL values of Cs-137 and Ag-110m release as a function of irradiation temperatures for various tests, but ignoring the differences in irradiation times, which varied between 230-530 efpd. It shows that particularly silver is easily migrating through intact (irradiated) SiC layers at temperatures above 1000°C.

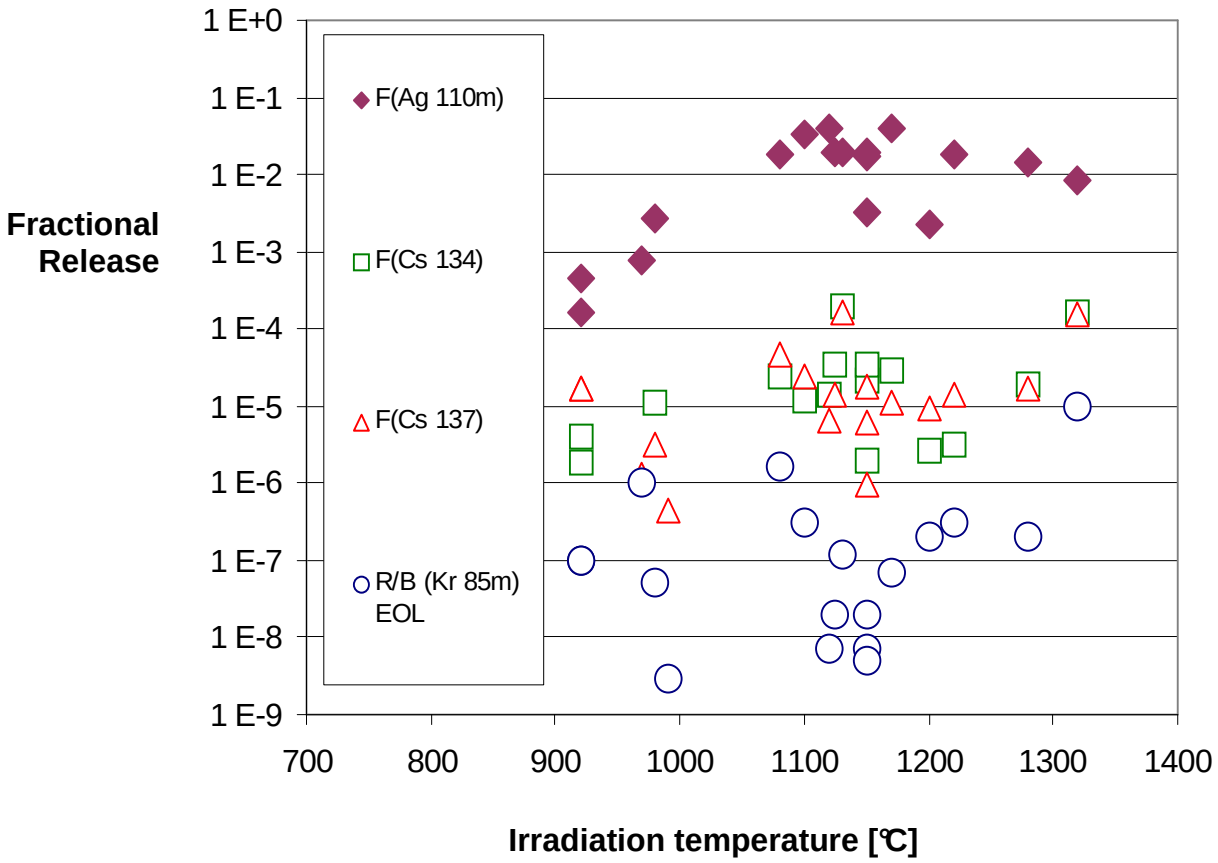

Figure 67 : Fission product release fraction and R/B after irradiation of TRISO coated fuel

More details on the THTR fuel elements containing (Th,U)O_2 BISO coated particles (see HEU program, variant 1 in previous table) were tested between 1968 and 1980 in various irradiation experiments as listed in Table 32.

Table 32 : Irradiation experiments for (Th,U)O_2 HEU BISO coated fuel [Burck 1988]

Irradiation Test	Fuel	Irradiation time [efpd]	Irradiation temperature [°C]	Burnup [% FIMA]	Fast fluence [10^{25} m^{-2}, E>0.1 MeV]
FRJ2-P22	12 compacts 1: 3000 cp 2: 3000 cp 3: 4700 cp 4: 4700 cp	189	 1050 av 1130 av 1360 av 1200 av	 9.3 11.3 11.1 10.1	 1.0 1.3 1.3 1.0
FRJ2-P25	12 compacts 1% def. cp 1: 000 cp 2: 000 cp 3: 00 cp 4: 00 cp	189	 900-1030 980-1050 980-1050 1070-930	 13.3 10.7 10.8 53.2	 1.5 max
BR2-P24	12 „small s.“ 31,800 cp	259	940-1050 av	11.2-13.2	1.5-2.3
R2-K3	4 FE 1: 7000 cp 2: 3: 4000 cp 4:	 278 278 267 267	Cycled 1280-1200 c 1280-1180	 15.0 16.8	 6.2 7.5
R2-K7	4 FE 3: 4200 cp	418	cycled	 15.9	 9.4
R2-K9	4 FE 1: 2: 4000 cp 3: 4000 cp 4: 8000 cp	 345 345 300 300	cycled 750-1150 c	 16.2 15.2 13.0	 8.7 7.1 4.6
R2-K10	4 FE 1: 5600 cp 2: 3500 cp 3: 3500 cp 4: 9100 cp	106	870-910 s	 5.3 6.4 6.0 4.1	 3.2 3.6 3.4 2.6
DR-K3	25 FE 36,500 cp/FE	719	900-1200 s 1050-1480 c	8.0-15.1	2.2-5.1
DR-K4	15 FE 42,000 cp/FE (+15 FE with carb. fuel)	742	550-1050 s	9.4-14.6	4.3-7.6
HFR-K1	4 FE 1: 18500 cp 2: 18500 cp 3: 18500 cp 4: 18500 cp	334	 1100-1220 1130-1240 910-1060 980-1030	 13.8 15.0 15.0 13.3	 6.1 6.7 5.9 4.9

3.6 Postirradiation Examination of Dragon Fuel

Postirradiation examination of Dragon fuel included among various other investigation methods metallography, annealing tests, radiochemical analysis.

A first serious threat of the fuel program was given by the observation of fission fragment damage or "spearhead attack", which gave rise to the so-called Metallurgical Series I Experiment (MET I) with experimental fuel specimens introduced in three fuel elements of the 1st charge.

Fig. 68 shows ceramographic cuts of (Zr,U)C particles of the 1st charge after irradiation in the HPD rig in Risoe. The particle on the left-hand side reveals spearhead attack in the inner PyC layer, whereas the other does not. A difference, which may have had an influence, was given in the thermal treatment of the oPyC (1600°C in the former, 1800°C in the latter case) [Price 1966].

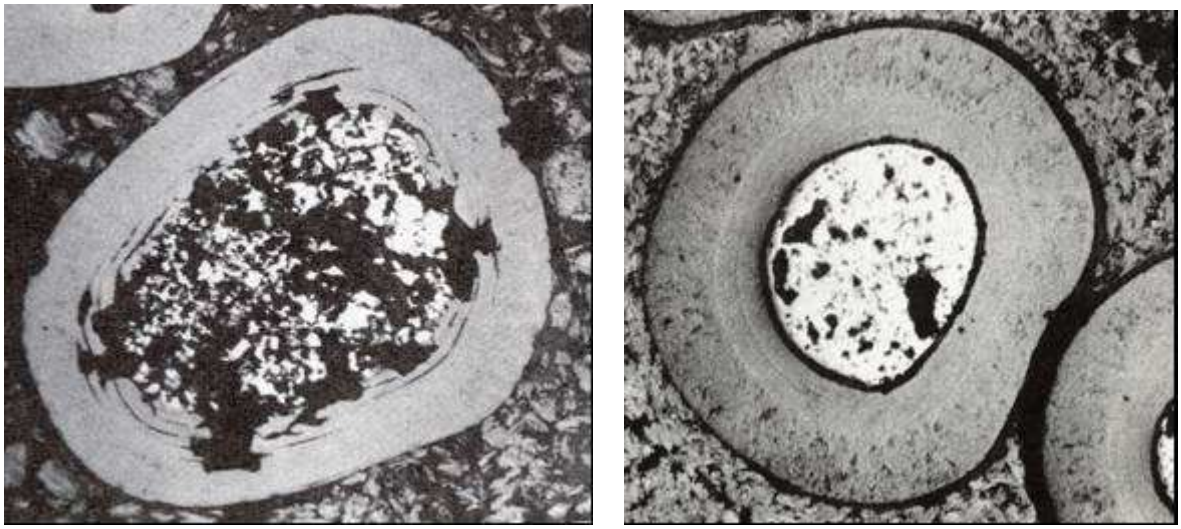

Figure 68 : Irradiation results on (Zr,U)C coated particle fuel
[Price 1966]
left: HPD-5 with 1056 efpd @ 1300-1750°C and 2.5 % FIMA of burnup achieved
right: HPD-6 with 1055 efpd @ 1130-1475°C and 3 % FIMA of burnup achieved

Other typical coated particle fuel with SiC layer after irradiation is shown in Fig. 69. Most irradiation damage observed was limited to the inner PyC. The SiC layer did not breach up to burnups of 12 % FIMA at temperatures up to 1600°C. Only at higher temperatures (~ 1900°C) at a burnup of 3.2 % FIMA in a Studsvik test, particle failure occurred due to kernel-coating interaction. Xe-133 R/B levels were in the range of 10^{-4} - 10^{-5} between 1000-1500°C with no clear temperature dependence. There was, however, a burnup dependence with release values higher by one order of magnitude from particles with burnups beyond 4 % FIMA [Rose 1966].

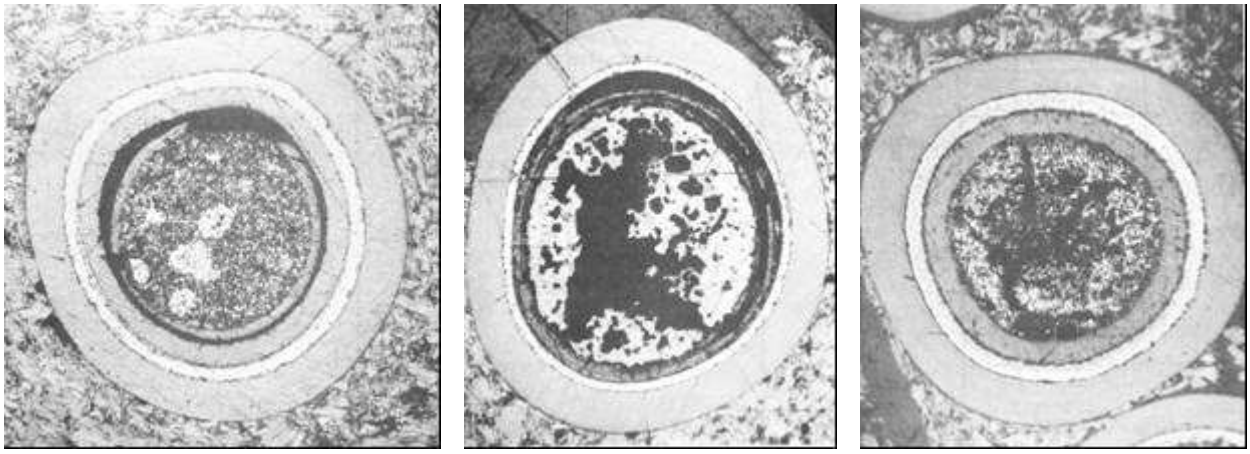

Figure 69 : Irradiation results on coated particle fuel with SiC interlayer [Huddle 1966]
left: Pluto-8 with ~240 days @ 1400°C and 23 % FIFA of burnup achieved
middle: LTHPD with 144 days @ 1300°C and 27 % FIFA of burnup achieved
right: HPD-15 with 44 days @ 1350°C and 26 % FIFA of burnup achieved

The Metallurgical Series II with three fuel elements of the D3 type were carried out for the purpose of comparing plain PyC coated vs. TRISO coated particles and $(U,Th)O_2$ vs. $(U,Th)C_2$ kernels. The operation histories of these fuel elements are listed in Table 33.

Table 33 : Operational parameters of the three fuel elements of MET II [York 1974]

Fuel Element	Total Core Days [MW]	Mean Fuel Temperature [°C]	Peak Fuel Temperature [°C]	Mean Burnup [% FIMA]	Peak Fast Fluence [10^{25} m^{-2} EDN]
311	1869	1290	1350	1.4	0.53
474	8567	1243	1390	5.3	2.1
477	11,135	1124	1385	7.2	2.8

Fig. 70 shows the profiles of fractional release of Cs-137 and Ag-110m from two of the three fuel elements indicating an excellent performance for the high burnup and fast neutron fluence achieved. Particles with TRISO exhibit the much better retention capability than those with a plain PyC coating. Silver release is up to 10 % for fuel with only PyC coating and is varying much stronger than cesium. Furthermore it was observed that UO_2 kernels have a high retention effect for strontium [York 1974].

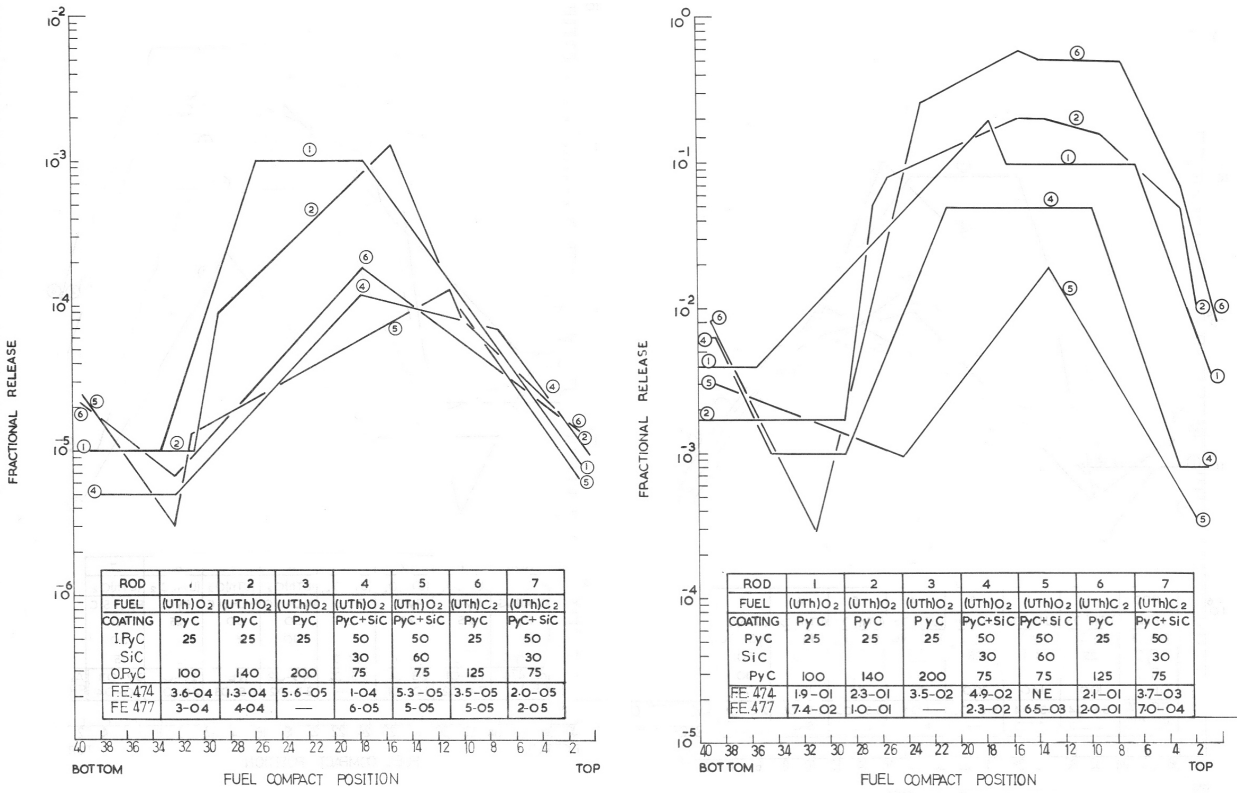

ROD	1	2	3	4	5	6	7
FUEL	$(UTh)O_2$	$(UTh)O_2$	$(UTh)O_2$	$(UTh)O_2$	$(UTh)O_2$	$(UTh)C_2$	$(UTh)C_2$
COATING	PyC	PyC	PyC	PyC+SiC	PyC+SiC	PyC	PyC+SiC
I.PyC	25	25	25	50	50	25	50
SiC				30	60		30
O.PyC	100	140	200	75	75	125	75
FE.474	3.6-04	1.3-04	5.6-05	1-04	5.3-05	3.5-05	2.0-05
FE.477	3-04	4-04	—	6-05	5-05	5-05	2-05

ROD	1	2	3	4	5	6	7
FUEL	$(UTh)O_2$	$(UTh)O_2$	$(UTh)O_2$	$(UTh)O_2$	$(UTh)O_2$	$(UTh)C_2$	$(UTh)C_2$
COATING	PyC	PyC	PyC	PyC+SiC	PyC+SiC	PyC	PyC+SiC
PyC	25	25	25	50	50	25	50
SiC				30	60		30
PyC	100	140	200	75	75	125	75
FE.474	1.9-01	2.3-01	3.5-02	4.9-02	NE	2.1-01	3.7-03
FE.477	7.4-02	1.0-01	—	2.3-02	6.5-03	2.0-01	7.0-04

Figure 70 : Fractional release profiles of cesium (left) and silver (right) from MET II fuel [York 1974]
(Last line of table in figures are average fractional release values)

4 FINAL DISPOSAL OF HTGR FUEL

4.1 Nuclide Inventory of Spent Fuel

Most of the activity of spent fuel is existing in a solid, non-releasable form. From the gaseous fission and activation products, only the long-lived isotopes are of importance with regard to spent fuel storage. During transfer of spheres from the small to the larger storage canisters, fuel specific data (type, burnup) were collected to know about the exact amounts of fuel and radioactivity contents in the dry storage. H-3, C-14 and Kr-85 have been identified as the only considerable contributors to radioactive release from spent HTGR fuel at inert storage conditions [Krumbach 2004]. Fig. 71 shows the radioactive inventory of a spent fuel sphere after two years [Duwe 1980].

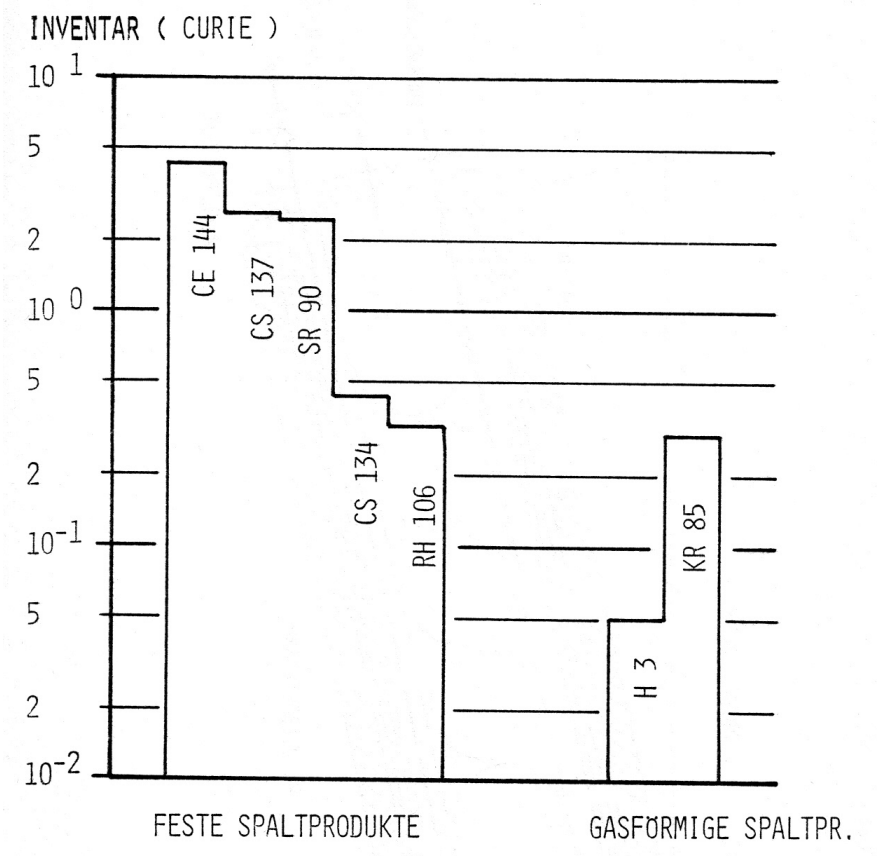

Figure 71 : Inventories of solid and gaseous fission products in a spherical fuel element after 2 yrs of decay time [Duwe 1980]

The origin of tritium is mainly from B and Li contamination in the matrix and from He-3 activation. A small fraction from fission mainly remains inside the fuel particles. A dry fuel element can take up 50 mg of water. For a wet fuel sphere, water contents can be up to several grams. Hydrogen atoms in the water may be substituted by tritium leading to HTO molecules

accounting for 95 % of the tritium inventory in the storage container. In combination with radiolysis, HT or T_2 gas will be formed. The Kr-85 is a fission product and mainly contained in the fuel particles. Its amount is directly related to the uranium contamination in the matrix and the number of failed particles.

A H-3 inventory of 0.53 GBq per sphere spent was calculated with the ORIGEN-S 2 code for THTR fuel elements for a target burnup of 11.4 % FIMA and 3 years of cooling time [Niephaus 2000]. For the tritium activity inventory in a HEU fuel element from the AVR, an upper limit has been estimated to be 2.5 GBq with about 20 % inside the coated particles and 80 % inside the matrix material. A respective value for the Kr-85 inventory in a HEU fuel element, considered as an upper limit for all AVR fuel spheres, was assessed to be 17.3 GBq, almost all inside the coated particles. The estimated figure for C-14 in the matrix material is 0.045 GBq [Niephaus 2000].

After shutdown of both German HTGRs, a more detailed analysis has been made to estimate the realistic radioactive inventory of all spent fuel. With respect to the AVR fuel with its different types, it is wise o further subdivide fuel types into burnup classes to avoid a calculation based on an inappropriate averaging of the burnup and allow for a more precise assessment of the single nuclide activities. For this purpose, 12 reference fuel elements have been defined representing all spent AVR fuel [Pohl 2003a]. Table 26 summarizes the results listing for each reference group the total activity (sum of all individual activities > 10^6 Bq from fission and activation products and actinides) as of the year 2003 as well as for a selection of nuclides their relative contribution to the total activity [Pohl 2003b].

The results of a respective study for the spent THTR fuel are shown in Table 35. Activity data are here based on the year 1998 corresponding to a 10-years cooling period [Niephaus 2000].

Fig. 72 shows an upper limit prediction of the total activity from the AVR and THTR fuel for a 50 yrs period up to 2038. The data are based on real burnup values (see Tables 34 and 35). The AVR fuel curve is here based on calculations considering five fuel types, which reveal a total activity value of $7.5*10^{16}$ Bq for the year 2003. This is to be compared with the figure of $8.4*10^{16}$ Bq (in Table 34) as the result of the reference group approach.

Table 34 : Predicted total activity of AVR spent fuel for the year 2003 [Pohl 2003]

Fuel type	No. fuel elements (rounded)	Burnup [%FIMA]	Operation time [yrs]	Total activity [Bq]	Fraction of total activity [%]							
					H-3	Kr-85	C-14	Sr-90	Cs-134	Cs-137	Pu-238	Pu-241
AVR HEU-1		(av. 14.9)										
1.1	90,000	13.6	5.0	$2.35*10^{16}$	0.3	1.1	0.004	24.0	0.03	25.2	0.6	0.3
1.2	24,400	21.0	13.6	$9.39*10^{15}$	0.2	0.9	0.006	24.1	0.04	24.8	1.2	0.3
1.3	42,000	18.2	9.7	$1.63*10^{16}$	0.3	1.3	0.004	24.0	0.2	24.5	0.9	0.4
1.4	11,400	7.5	2.4	$1.78*10^{15}$	0.6	1.6	0.002	24.2	0.1	24.7	0.1	0.2
1.5	28,300	16.0	7.9	$9.57*10^{15}$	0.3	1.3	0.004	24.0	0.2	24.5	0.7	3.3
AVR HEU-2		(av. 6.7)										
2.1	21,100	10.0	8.8	$7.60*10^{15}$	0.2	1.2	0.003	24.4	0.1	24.6	0.7	0.2
2.2	15,200	2.0	1.4	$1.15*10^{15}$	0.1	1.6	0.003	24.1	0.05	24.5	0.006	0.1
2.3	2000	12.0	13.0	$9.40*10^{14}$	0.2	1.3	0.004	24.3	0.2	24.5	0.8	0.3
AVR LEU-3	2400	8.0	7.7	$1.29*10^{15}$	0.2	0.7	0.002	16.2	0.03	22.3	0.5	20.4
AVR LEU-4	24,600	8.5	5.5	$7.45*10^{15}$	0.3	1.1	0.002	19.2	0.2	23.4	0.3	11.9
AVR LEU-5		(av. 8.6)										
5.1	8700	3.5	0.8	$6.30*10^{14}$	1.1	1.5	0.001	22.8	0.05	23.9	0.03	2.6
5.2	20,400	11.0	3.7	$4.71*10^{15}$	0.4	1.3	0.002	21.1	0.1	23.7	0.2	7.6
Σ	**290,700**			**$8.43*10^{16}$**	**0.3**	**1.2**	**0.004**	**23.3**	**0.1**	**24.5**	**0.7**	**2.0**

Table 35 : Predicted total activity of THTR-300 spent fuel for the year 1998 [Niephaus 2000]

Fuel type	No. fuel elements (rounded)	Burnup [%FIMA]	Operation time [yrs]	Total activity [Bq]	Fraction of total activity [%]							
					H-3	Kr-85	C-14	Sr-90	Cs-134	Cs-137	Pu-238	Pu-241
THTR HEU-2	617,606	5.0		$1.31*10^{17}$	0.6	2.0	0.002	22.9	0.5	23.1	0.1	0.2

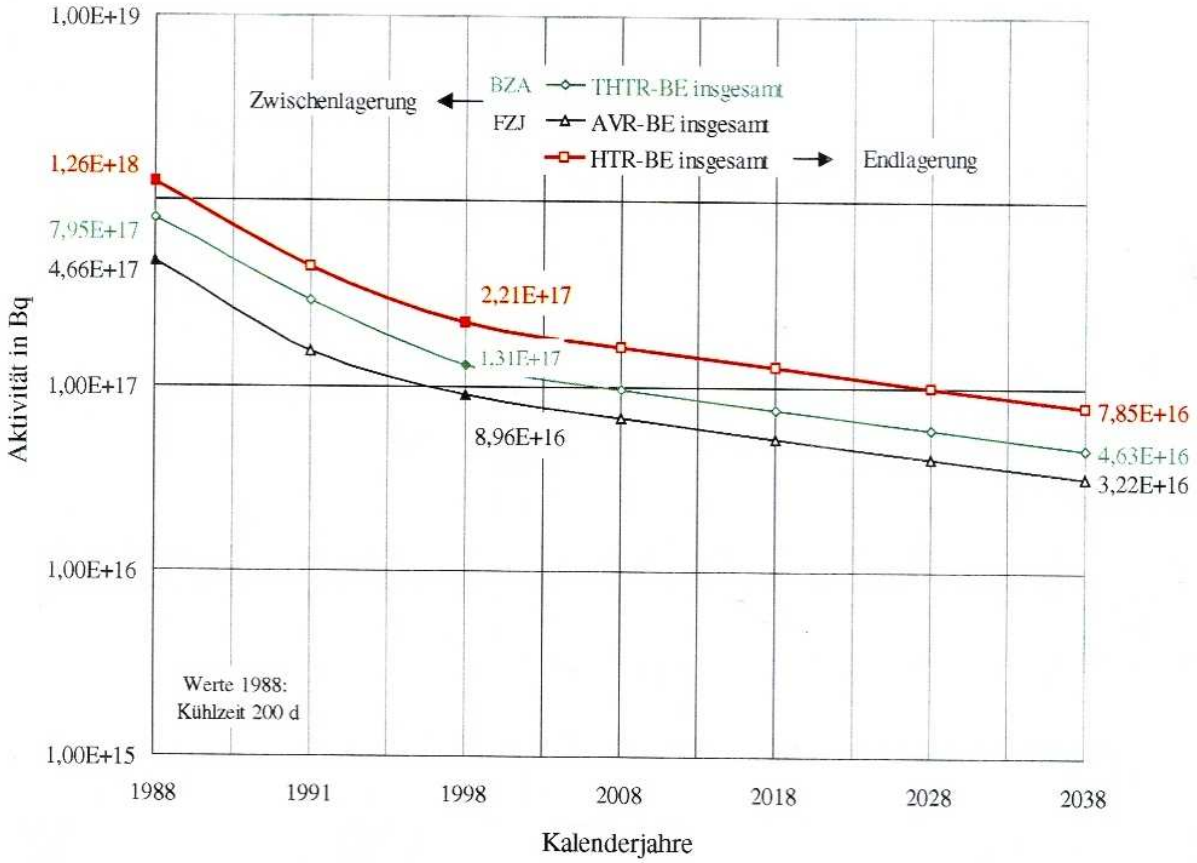

Figure 72 : Prediction of thermal power production (top) and total activity (bottom) over 50 years for the German spent HTGR fuel [Niephaus 2000]

With respect to the predecessor generation of gas-cooled reactors, four GCR at Marcoule, Chinon, Saint Laurent, and Bugey with a total of nine units were shut down in the meantime. The total amount of graphite accumulated is 16,440 t. An assessment was made on selected radionuclide inventories in the Bugey GCR; values after 5 yrs cooling time (see Table 36).

Table 36 : Assessed values of selected radionuclides in the shut-down Bugey GCR

Nuclide	Inventory in the Reactor Graphite of Bugey (after 5 yrs of cooling) [Bq/g]
H-3	$6.9*10^6$
C-14	$3*10^5$
Co-60	$1.8*10^6$

4.2 Heat Production from Spent Fuel

FZJ conducted an experimental program to test the storage behavior of spent AVR fuel measuring activities and decay heat production of 17 spheres with a burnup ranging between 4-16 % FIMA and decay periods of 150-1700 d (see Fig. 73) showing good agreement with respective ORIGEN predictions [Brinkmann 1980].

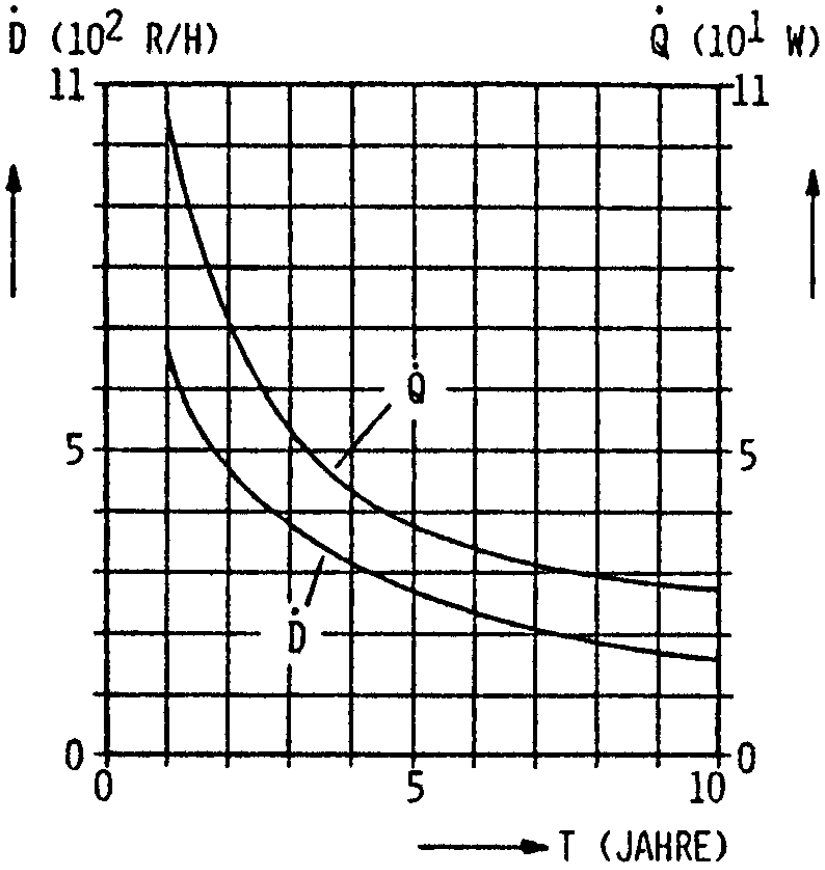

Figure 73 : Estimated decay heat and dose rate of a 950 ball capacity storage canister [Brinkmann 1980]

The decay heat production in spent AVR fuel elements calculated as a function of burnup is shown in Fig. 74 for decay times between 150 d and 3 yrs.

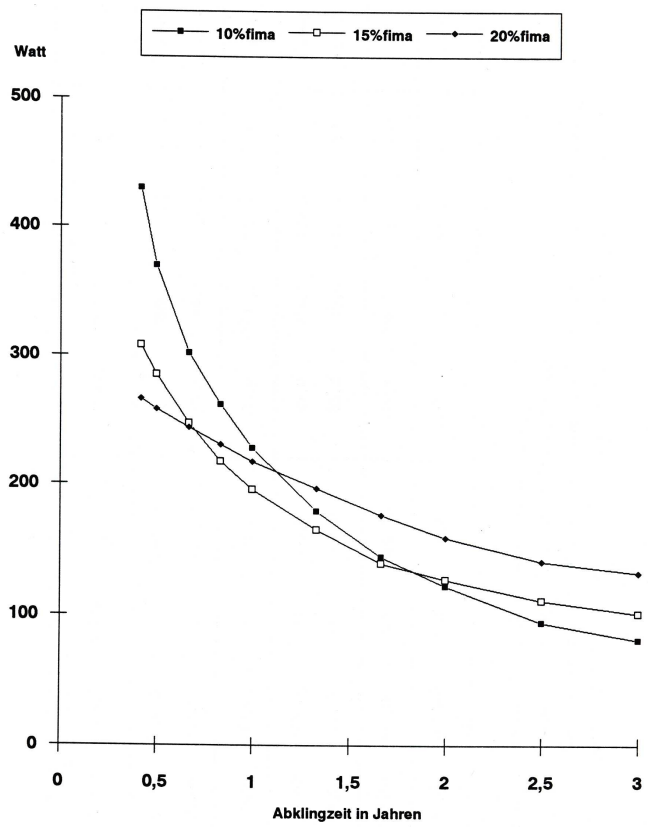

Figure 74 : Decay heat production rate during the first three years of 1900 fuel elements as a function of burnup [Duwe 1993b]

Calculations of thermal power production were made with the ORIGEN-S 2 code for the CASTOR casks for THTR fuel elements within the frame of the licensing process for the storage and transport casks. Assuming a canister for damaged fuel filled with 2320 THTR fuel spheres, calculations were made for an average target burnup[1] of 11.4 % FIMA as a conservative coverage of all casks and compared with the case of an average burnup of 5.3 % FIMA measured with the SMR for the discharged fuel. The results after 3 years of cooling given in Table 37 showed an acceptable level [Niephaus 2000].

Table 37 : Thermal power produced in a CASTOR cask filled with 2320 damaged fuel elements [Niephaus 2000]

Cooling time [yrs]	Thermal power			
	for average burnup 5.3 % FIMA		for average burnup 11.4 % FIMA	
	[W/fuel sphere]	[W/cask]	[W/fuel sphere]	[W/cask]
1	$196*10^{-3}$	455	$266*10^{-3}$	617
2	$87*10^{-3}$	202	$152*10^{-3}$	353
3	$51*10^{-3}$	118	$106*10^{-3}$	246

[1] Target burnup is the burnup, for which the generated isotopes U-233, Pu-239, Pu-241 reach maximum values.

The predicted transient decay heat production of the total spent fuel from AVR and THTR for the 50-years period between 1988 and 2038 is shown in Fig. 75 [Niephaus 2000].

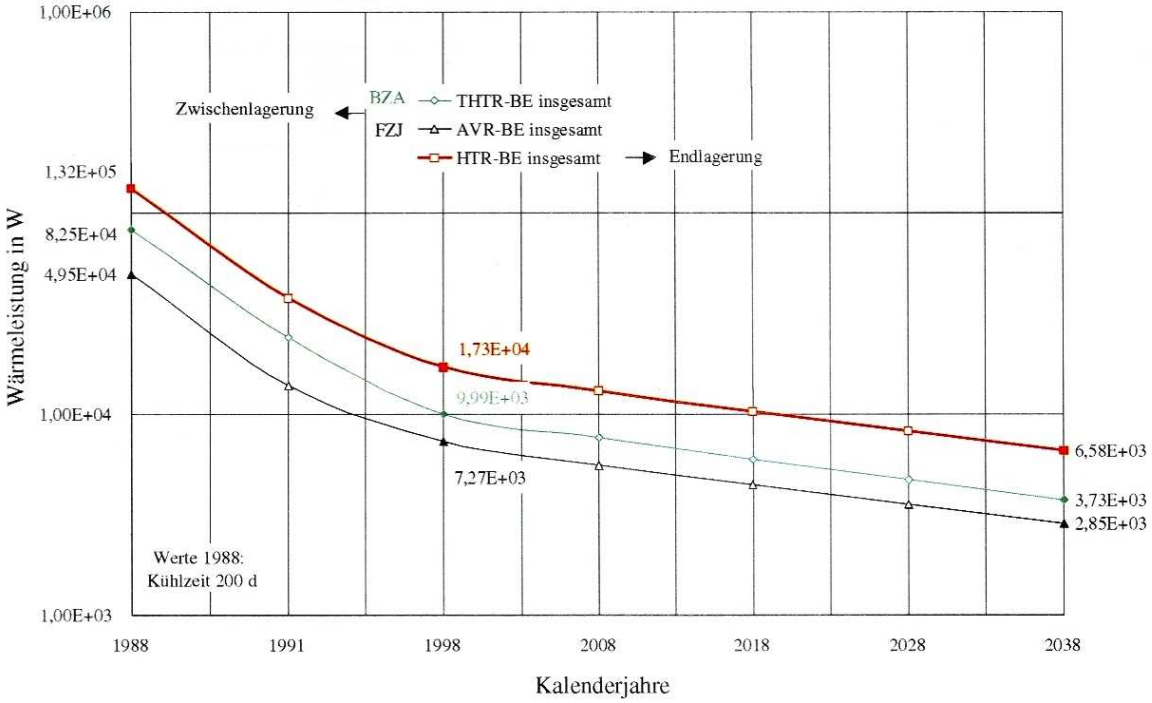

Figure 75 : Prediction of thermal power production (top) and total activity (bottom) over 50 years for the German spent HTGR fuel [Niephaus 2000]

4.3 Activity Release from Spent Fuel

First measurements on AVR spent fuel were conducted in the 1970s in a facility simulating dry storage conditions [Duwe 1980]. It consisted of a furnace with a capacity of 5 spheres and two gas-tight storage containers which could take up 20 spheres each. These were connected to a sweep gas circuit including traps for the gaseous species. The furnace could be heated up to 400°C, while the two containers were kept at temperatures of 140°C (maximum temperature at dry storage) and 40°C (nominal operating temperature of disposal site), respectively. Fuel types investigated were UCC with 16.7-18.0 % FIMA burnup for testing carbide fuel and GO-THTR with 5.1-6.5 % FIMA for testing oxide fuel [Duwe 1980].

4.3.1 Release of H-3 and Kr-85

Tritium was found to be released at rates independent of the fuel type explained by the fact that its origin is mainly from He-3 and impurities in the graphite. A repetition of these measurements a few weeks later exhibited reduced rates, a depletion effect showing that only a part of the tritium adsorbed on the pore surfaces is available for release. The activities released into the containers were found to show no significant further increase after 50 d at 40°C and after 10 d at 140°C,

respectively, (see Fig. 76) due to the depletion of the inventory and increasing partial pressure in the void volume [Duwe 1980].

The isotope Ra-226 can be neglected under interim storage conditions. Unlike the H-3, Kr-85 release rates into the container were observed to significantly increase during the investigation time (see Fig. 76). The depletion effect was not observed for Kr-85.

Furthermore measurements on the release of H-3 and Kr-85 were made using two specially prepared canisters. One canister is filled with GK type (average burnup 15 % FIMA), the other one with GO type fuel balls (12.4 % FIMA), with all fuel discharged from the AVR end of 1976. The canisters were equipped with valves to allow sampling of the inside gas atmosphere. The void volume of the canisters is 118 l initially consisting of normal air (at 25°C) with a relatively high moisture content (10-20 mg of H_2O per liter of air) which originated from the former interim storage in a water basin.

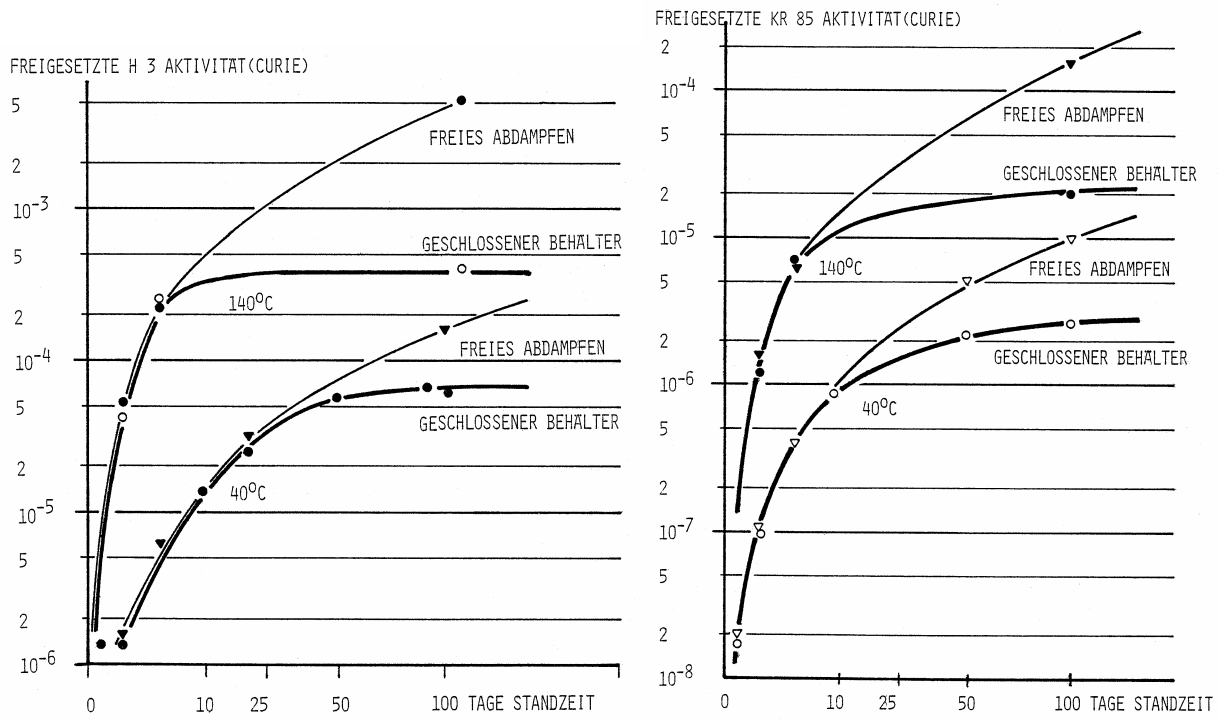

Figure 76 : H-3 (left) and Kr-85 activity released from 20 GO fuel elements in open and closed container (7 l void volume) [Duwe 1980]

Fig. 77 shows the tritium activity (top) and Kr-85 activity (bottom) measured during storage over several years. For the first three years, the observed increase in H-3 activity corresponds to an average of $7.4*10^{-3}$ GBq/yr for both GO and GK, whereas for Kr-85, the average release rate was $3.7*10^{-3}$ GBq/yr for GO and $1.9*10^{-3}$ GBq/yr for GK [Duwe 1986].

The Kr-85 inventory for a THTR fuel element was calculated with the ORIGEN-S 2 code based on a target burnup of 11.4 % FIMA and 3 years of cooling time with a value of 17.3 GBq per sphere [Niephaus 2000].

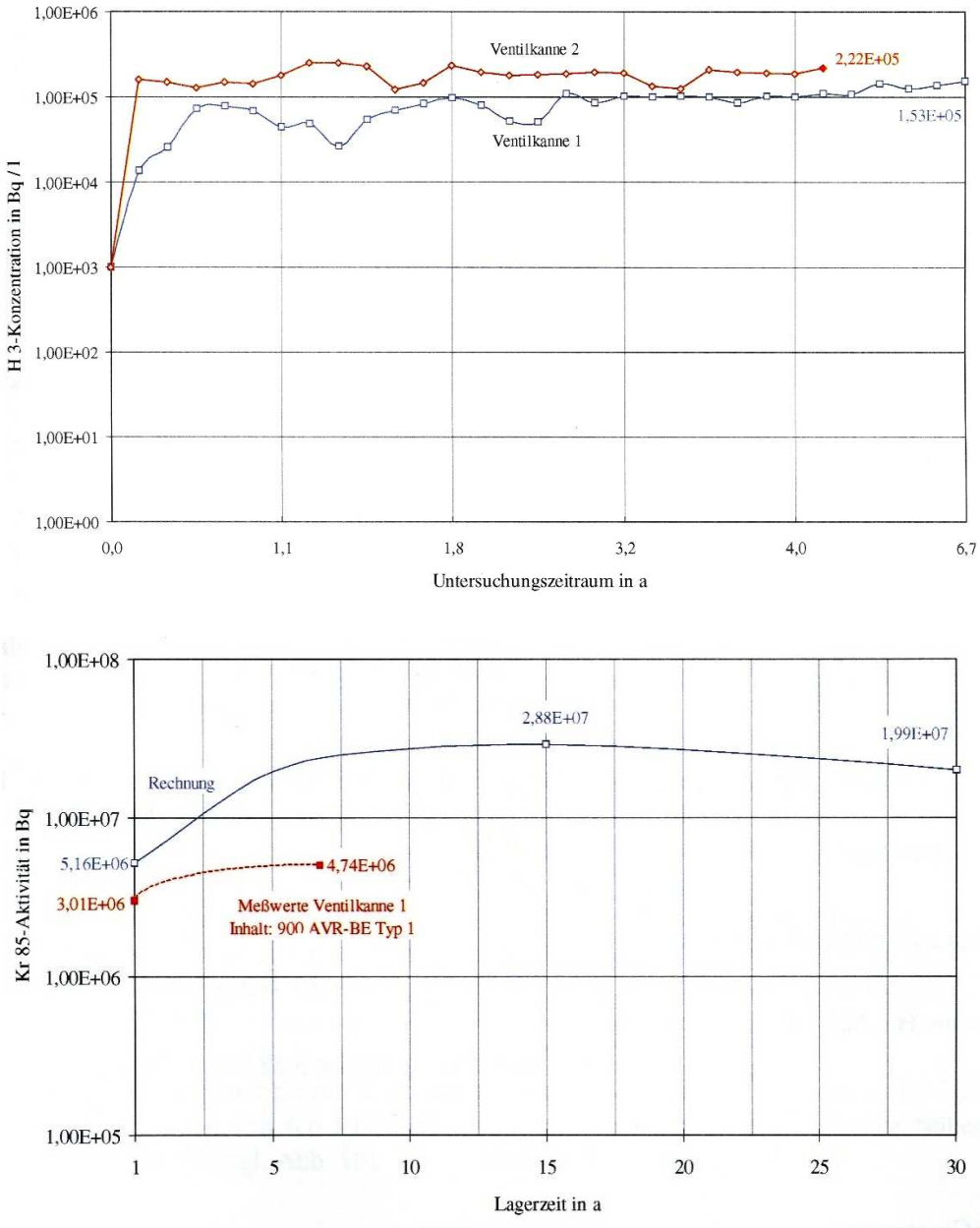

Figure 77 : Release of H-3 (top) and Kr-85 (bottom) activity into the canister atmosphere [Niephaus 2000]

Activity release rates from AVR spheres into the canister gas atmosphere are shown in Fig. 78 in an Arrhenius-type diagram for H-3 and Kr-85.

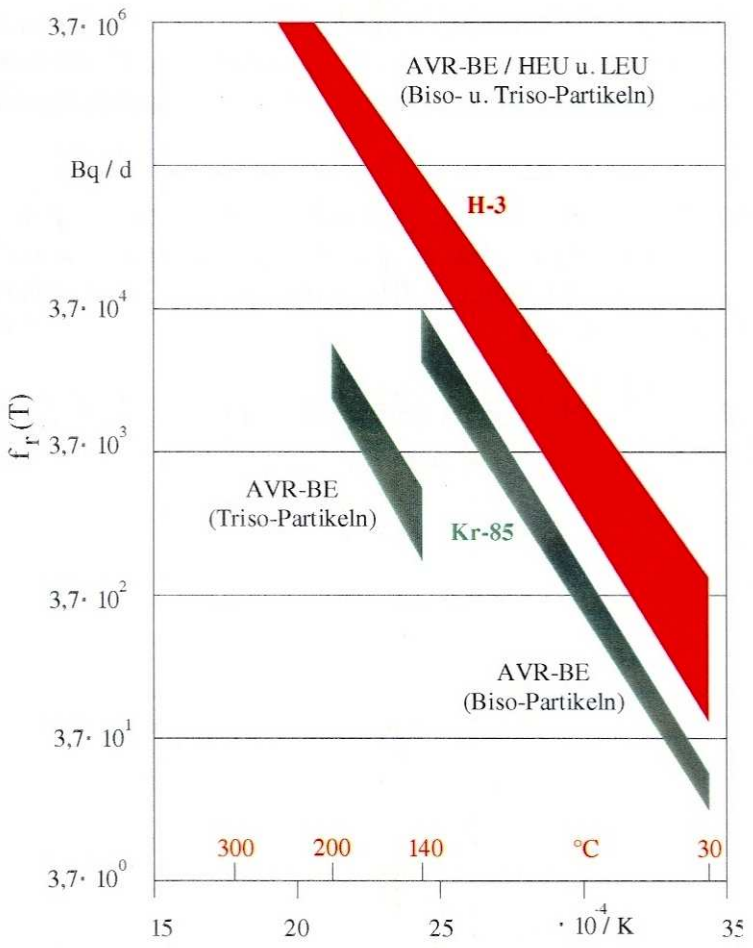

Figure 78 : Arrhenius diagram of H-3 and Kr-85 release rates from experimental data [Niephaus 2000]

4.3.2 Release of C-14

With regard to C-14, an activation product from N-14 and C-13, high concentration values are typically found near the sphere surface resulting from coolant deposition. It can be released as CO_2 during oxidation processes. The C-14 is bound to the binder material in the matrix graphite and, at presence of moisture in the storage container, is liberated as gaseous CO_2 during corrosive reactions.

For the C-14 activity measurements conducted on the same two canisters in the time 1986-89, the fractions of O_2 and CO_2 and the C-14 concentrations are listed in Table 38.

Table 38 : C-14 concentrations and O_2 and CO_2 fractions in the canister gas atmosphere for GK and for GO fuel elements [Röllig 1989]

GK fuel elements				GO fuel elements			
Time [yrs] (0=Oct 83)	O_2 [vol%]	CO_2 [vol%]	C-14 [Bq/ml]	Time [yrs] (0=Sep 82)	O_2 [vol%]	CO_2 [vol%]	C-14 [Bq/ml]
0	21.	0	0	0	21	0	0
2.7	10.2	5.7	n.m.	3.8	7.4	7.0	n.m.
3.8	6.6	7.8	129	4.9	6.1	8.5	72
4.1	6.3	8.6	137	5.2	5.7	8.6	81
4.6	6.0	8.9	166	5.7	5.0	9.2	99
5.3	4.2	10.9	228	6.4	4.3	9.2	108

The decreasing amount of O_2 and the concomitant increase of CO_2 show the corrosive origin of the C-14. The accumulated CO_2 corresponds to a carbon loss of averaged 7.7 mg per GK sphere (after 5.3 yrs) and 6.5 mg per GO sphere (after 6.4 yrs). Considering an averaged C-14 inventory of $5.5*10^6$ Bq per fuel sphere, the fractional release rate of C-14 into the canister atmosphere is $8.6*10^{-4}$/yr. It is a conservative figure used for the first 10 years. For longer times, the depletion of oxygen in the container atmosphere can be taken into account [Röllig 1989].

To judge upon the C-14 activity in the storage canisters of THTR fuel, the experimental data gathered with the stored AVR fuel is taken and transferred to the conditions of THTR fuel. For a fuel lifetime of 1000 efpd in the THTR core, the C-14 inventory is 0.015 GBq per fuel sphere (to be seen as an upper limit). With a void volume of 206 l in the (one) canister initially consisting of a helium-air atmosphere (at 200°C), the C-14 activity in the canister gas accumulates to 0.27 GBq after 10 yrs of storage time. This is conservative with respect to the smaller amount of oxygen available to each fuel element in the THTR canister [Röllig 1989]. A C-14 inventory of 0.004 GBq per spent THTR fuel was calculated with the ORIGEN-S 2 code based on a target burnup of 11.4 % FIMA and 3 years of cooling time [Niephaus 2000].

Since 1988, also C-14 activities of the gas atmosphere inside the CASTOR cask for the AVR spheres, but outside the two canisters are being measured. These values, however, are much lower because of the low leakage rates of the canisters [Röllig 1989].

4.4 Disposal in Salt Mine

Visco-plastic behaviour in rock salt will eventually close gaps/voids, so-called convergence, around the storage arrangement and imposes a hydrostatic pressure buildup according to the depth of the disposal location which, after all gaps are closed, corresponds to the total mountain pressure. Convergence is enhanced with increasing temperature. For a depth of 800-1000 m and a maximum temperature of 200°C, a temporarily and locally limited maximum pressure of about 30 MPa has to be taken into consideration [Rebmann 1988].

If there are gaps between coating layers or between particle and overcoating, they may interrupt the transfer of the pressure load from the outside to the particle. Convergence was measured in the ASSE salt mine at a rate of about 0.3 mm/yr. The annular gap around the waste barrels in a bore hole is expected to be closed after approximately 200 yrs [Rebmann 1988].

In the 1970s, an in-situ demonstration test of direct final storage with about 100,000 AVR fuel elements in 100 canisters was planned and prepared at the Asse salt mine in Germany. The retrievable canisters with 950 spheres each were intended to be placed into four 36 m deep bore holes at the 750 m level of Asse [Wolf 1975]. Before starting the experiment, however, the project was stopped in 1978 for political reasons (Merz1993).

Resuming respective works in 1983, the project MHV (MAW and HTR Fuel Element Test Storage in Bore Holes) was started focusing on the retrievable in-situ disposal for demonstrating respective handling techniques. Five 1 m diameter bore holes with a depth of 10 m were drilled in the Asse salt mine (Fig. 79). One hole was considered to contain four gas-tight stainless steel canisters with 950 spent AVR fuel elements each (see Table 39).

Table 39 : Characterization of the AVR fuel to be test-disposed [Buttler 1987, Duwe 1993b]

Canister	AVR fuel type	Burnup [%FIMA]	Decay heat [W] (1.11.82)	Activity [Ci] (1.11.82)	U_{tot} [g]	U-233 [g]	U-235 [g]	Th [kg]
1	GO	12.6	93.0	847,300	403.4	88.0	123.3	4.56
2	GK	17.4	89.3	758,500	403.3	87.9	123.3	4.56
3	GO	13.9	91.0	804,750	403.0	87.6	123.3	4.56
4	GK	17.6	88.4	758,500	403.4	88.0	123.3	4.56

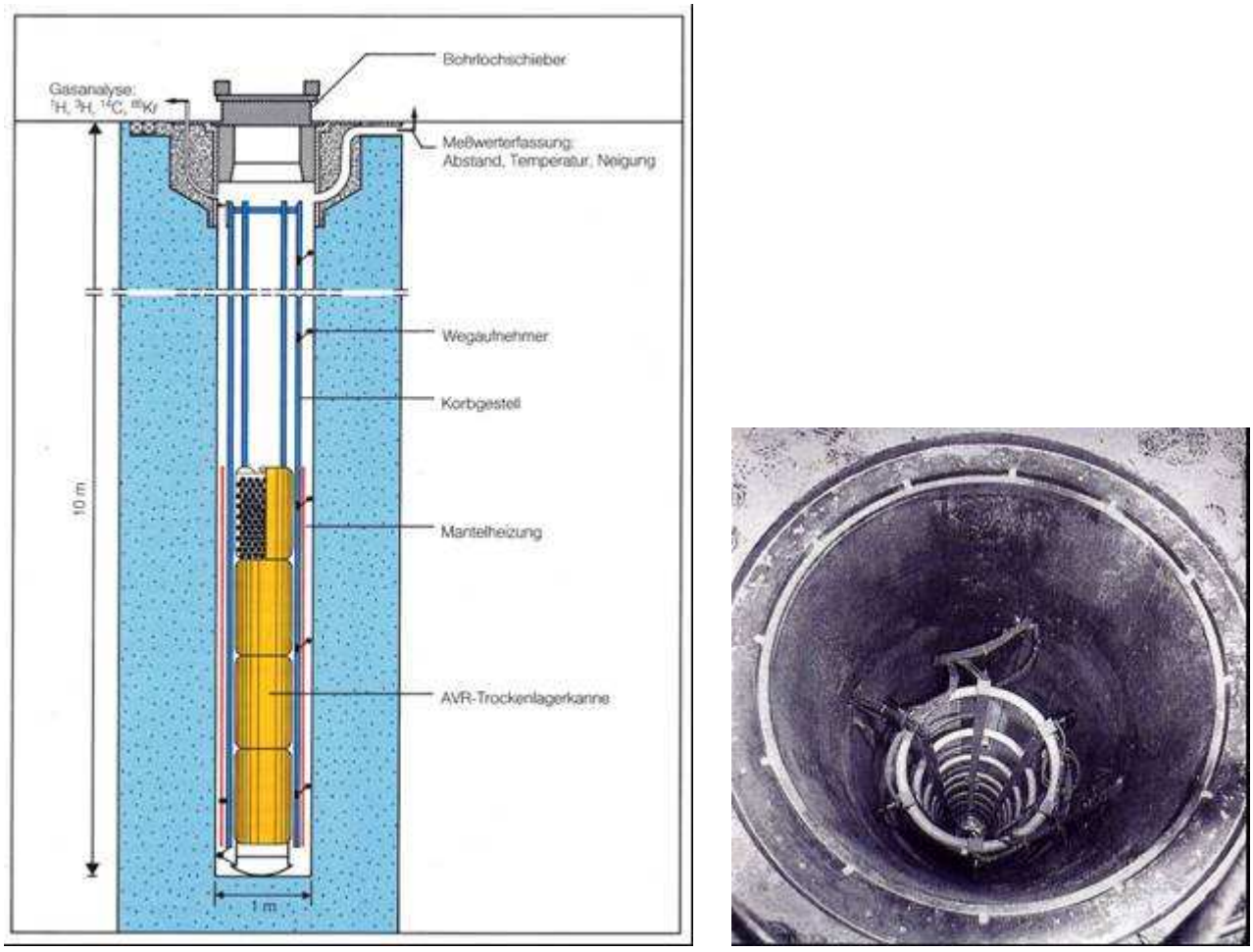

Figure 79 : Planned demonstration test for final disposal of spent HTGR fuel spheres

The material to be controlled according to IAEA standards were 444 "effective g", where "effective grams" for enriched uranium are defined as the U_{tot} (in grams) multiplied by the square of the enrichment (which was 52.4 %). Therefore the test site was classified as "location outside facilities", which can handle < 1 "effective kg", the lowest level of IAEA control [Buttler 1987].

The project also included an electrical heating to keep the temperature at a level of 70°C and comprehensive devices for measuring geo-mechanical parameters, gas release and heat development. The test was planned for a duration of 5 yrs [Kirch 1990]. This project, however, was also discontinued for financial reasons, the demonstration storage test never did materialize.

The same canisters were later used in a demonstration test program for the verification of two designs of a transport and storage cask, the TN-AVR-2, and the GNS-CASTOR-AVR [Duwe 1993b]. The former cask contained canisters No. 1 and 2 (see Table 40), the latter cask contained canisters 3 and 4. Fig. 80 shows the radiation field at the surface of the unshielded canisters and in a distance of 1 and 2 m. Canisters No. 2 and 4 (GK fuel) show the higher dose rates because of the higher burnup and Cs inventory, respectively.

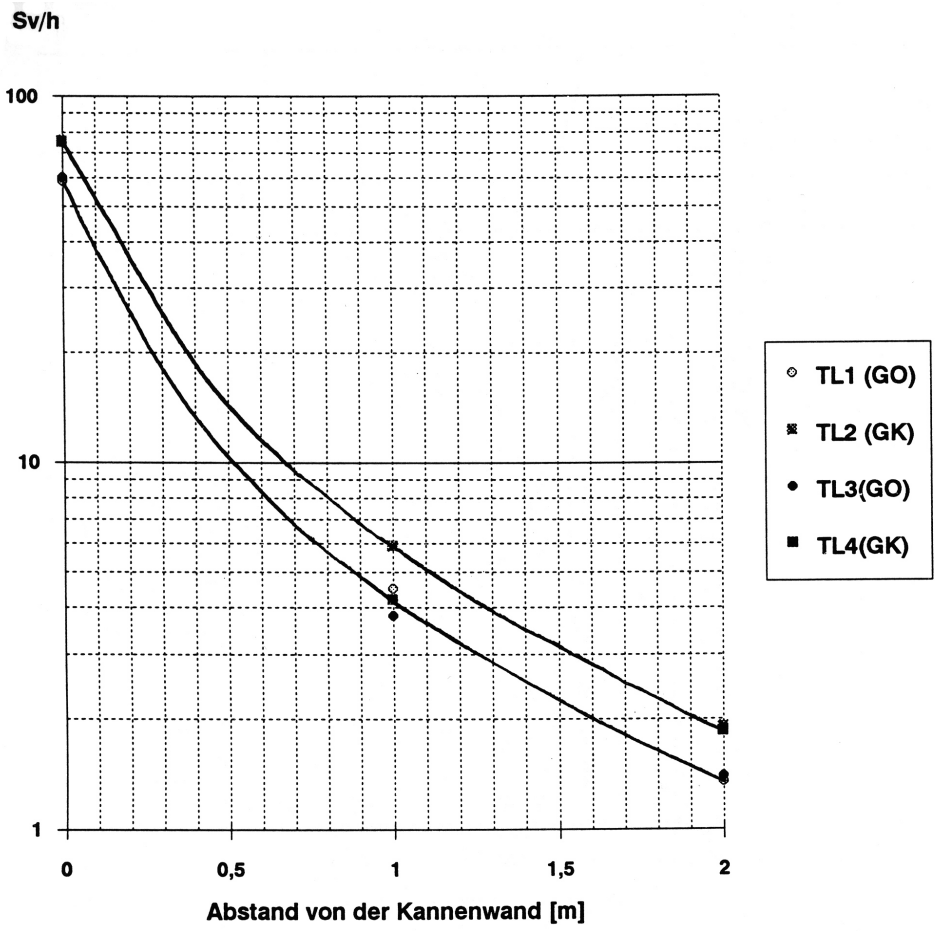

Figure 80 : Gamma-radiation field of the unshielded canisters [Duwe 1993b]

Also the release from the two AVR canisters inside a CASTOR cask into the cask atmosphere was experimentally investigated. Between 1987-1992, one CASTOR THTR/AVR cask and one TN-AVR 2 cask were externally heated up to 55°C. The higher temperature resulted in the release of moisture and thus of tritium in form of HTO. The released activities after six months are given in Table 31 [Niephaus 2000].

Table 40 : Comparison of activity release into container atmosphere for two different casks [Niephaus 2000]

Cask containing two canisters with a total of 1900 fuel spheres	Activity released into cask atmosphere [Bq]		
	H-3	C-14	Kr-85
CASTOR THTR/AVR	$1.7*10^5$	$8.5*10^3$	$6.6*10^3$
TN-AVR 2	$8.1*10^4$	$1.4*10^4$	$1.5*10^4$

Due to the fact that leakage rates from a cask lid are by three orders of magnitude lower than those from a canister plug, activity release from CASTOR casks, which are closed with two lids, into the environment is expected to be negligibly low.

After loading the canisters into the two casks, measurements of the temperature at various positions revealed a difference between outside wall and room temperature of around 1 K and were later discontinued. In Fig. 81, the γ dose rate profiles measured at the casks' surface after 1 yr of decay time (top) and about 7 yrs later (bottom) are plotted. The curve after 1 yr of decay time shows lower values for the two canisters with GK fuel despite the higher burnup compared to GO. This is due to the fact that fuel with lower burnup contains more short-lived nuclides, here Ce-144 and Pr-144. Fuel with higher burnup, in turn, contains more long-lived nuclides, here Cs-137. Thus, after short decay times, the lower burnup fuel is more active. This changes with growing decay times, when the higher burnup fuel becomes more active.

4.5 Long-Term Behavior of HTGR Fuel in Salt Environment

An accident scenario to be considered for final storage of spent fuel is the event of a water ingress into the salt mine, where the evolving salt brine would start corroding the waste package and may reach the fuel particles. Since for intact coatings, no corrosion effect has been observed, coated particles are assumed to have excellent long-term chemical resistance. A release of activity from leaching is only possible with defective particles. In an experimental series, single bare fuel kernels – HEU $(U,Th)O_2$ of 12.1 % FIMA irradiated at 900°C, LEU UO_2 of 10.7 % FIMA at 1000°C, unirradiated UO_2 – were leached with a saturated brine at pressures of ambient/13 MPa and temperatures of ambient/90°C. The results for the higher temperature and pressure (see Fig. 82) reveal a nuclide specific leachability with Cs, Sb, or Eu being well mobilized in contrast to Ru or Am. A rapid release of activity was observed for UO_2 with almost all inventory within 100 d, and for $(U,Th)O_2$ a 30-50 % fraction within 1-2 yrs. In contrast, $(Th,U)O_2$ kernels release about 10 % within a year. Under these storage typical conditions, some of the kernels had partly disintegrated and released a large portion of their inventory [Brodda 1988].

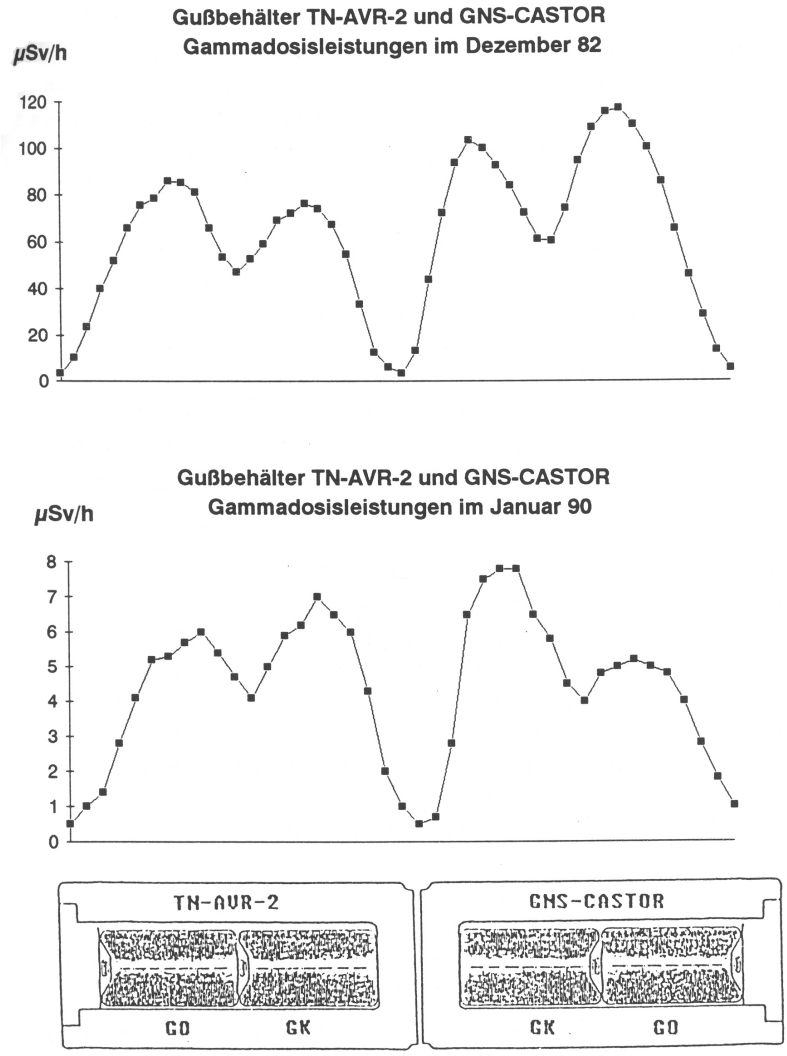

Figure 81 : γ radiation profiles at the cask wall surface [Duwe 1993b]

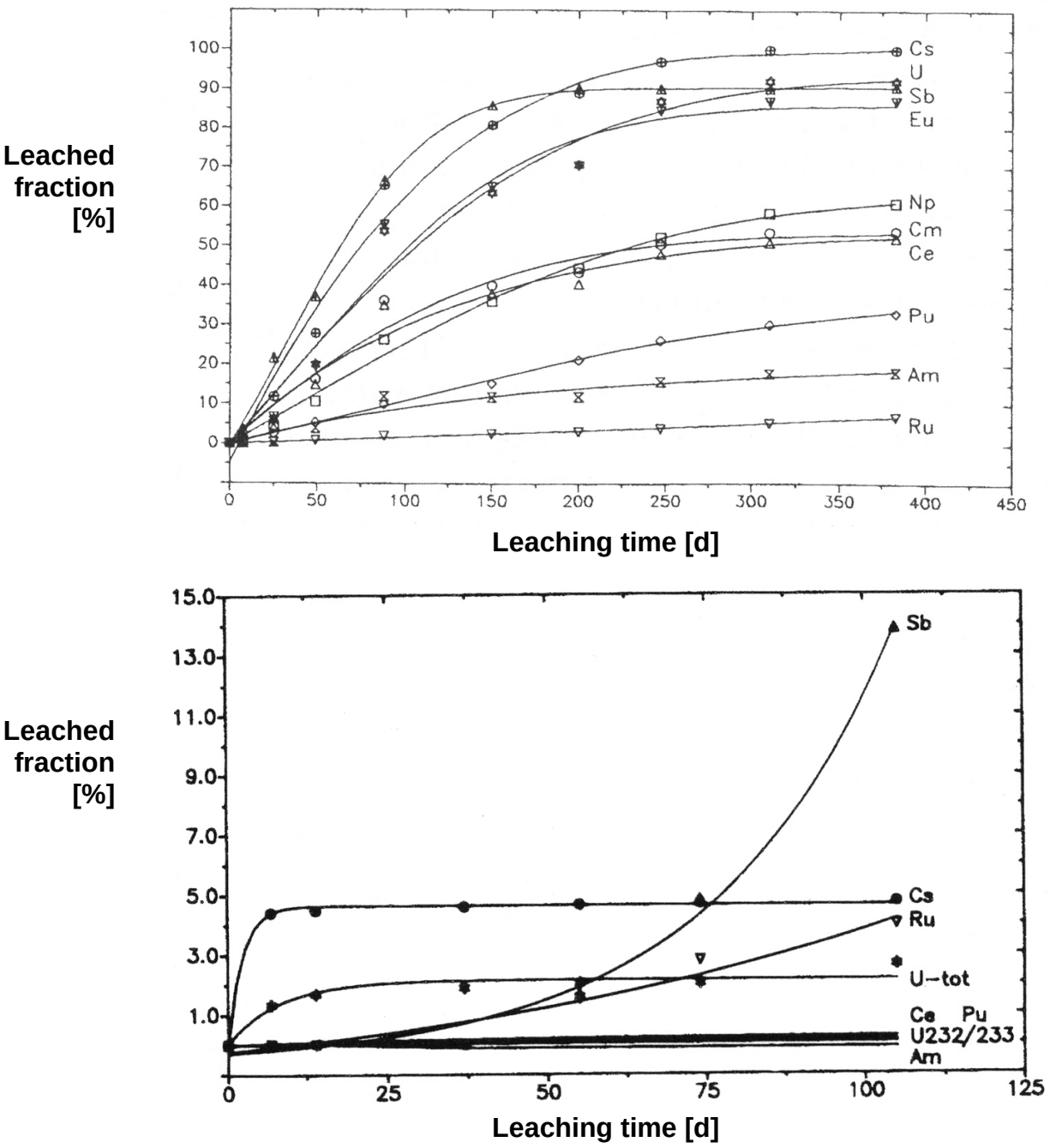

Figure 82 : Radionuclide leaching from irradiated $(U,Th)O_2$ (top) and UO_2 (bottom) kernels at 13 MPa pressure and 90°C temperature [Brodda 1988]

The leak resistance of complete spent AVR fuel spheres of different types and also one of the non-heated spheres of the HFR-K3 experiment in a salt brine was experimentally investigated at pressures up to 30 MPa and temperatures up to 150°C over up to 1230 days. Leached activities were mainly given by Cs-137, Cs-134, Sr-90, Ce-144, Ba-133, Eu-154, Co-60. The tests have revealed a gradual release of the matrix contamination into the brine, for Cs about 10 – 20 % of its inventory in the matrix. Fig. 83 shows the Cs-137 release rate under final storage typical conditions revealing lower figures for TRISO fuel. The total release fraction is $< 10^{-4}$ after more than four years. Release from defective particles is by orders of magnitude higher. Long-term relevant nuclides like I-129, Tc-99, Np-237, are expected to exhibit much lower release rates [Ganser 1987].

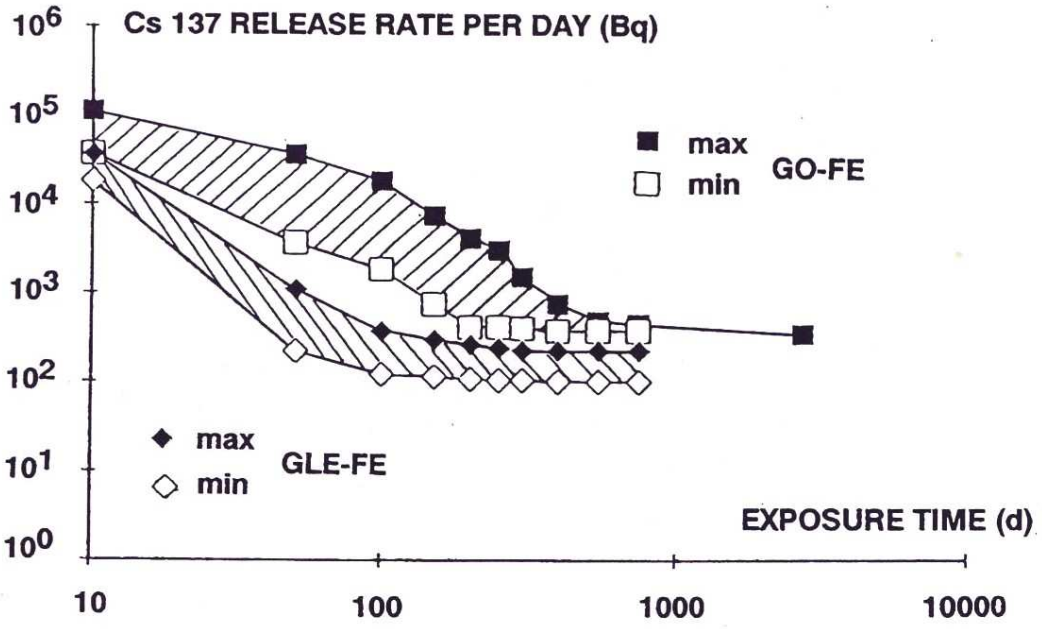

Figure 83 : Cesium release in leach tests with irradiated AVR fuel elements at 13 MPa pressure and 90°C temperature [Kirch 1990] GO: BISO coated (U,Th)O2 fuel; GLE: TRISO coated UO2 fuel

An aqueous solution can penetrate the A3 matrix graphite of a fuel element through its open pore system (see previous section). Under normal conditions, a sphere takes up about 8 ml. Under pressurized conditions and dissolution of the pore gases in the liquid, this amount raises to conservatively estimated 23 ml [Fachinger 2006].

The release behaviour of HTR fuel elements under final disposal conditions was experimentally examined for spent AVR fuel spheres which were given into a saturated quinary alkaline solution (Q-brine) representative of salt repository conditions [Duwe 1993a]. Table 41 lists some features of the fuel spheres investigated. Prior to the leaching process, activity profile measurements in the fuel-free zone were conducted by carving grooves (3 times 0.3 mm and 4 times 1 mm) and measuring the activity in the collected graphite dust (see Fig. 84).

Table 41 : Irradiated fuel spheres exposed to leaching process

Fuel type	Number	Coating	Burnup	End of life	Begin leaching
GO-1	AVR 65/7	BISO	12.4	Feb 1982	Oct 1983
GLE-3	AVR 79/18	TRISO	9.0	Sep 1986	Jan 1988
	AVR 80/17		8.8	Sep 1986	Jan 1988
	HFR-K3/2		10.1	Oct 1981	Sep 1984

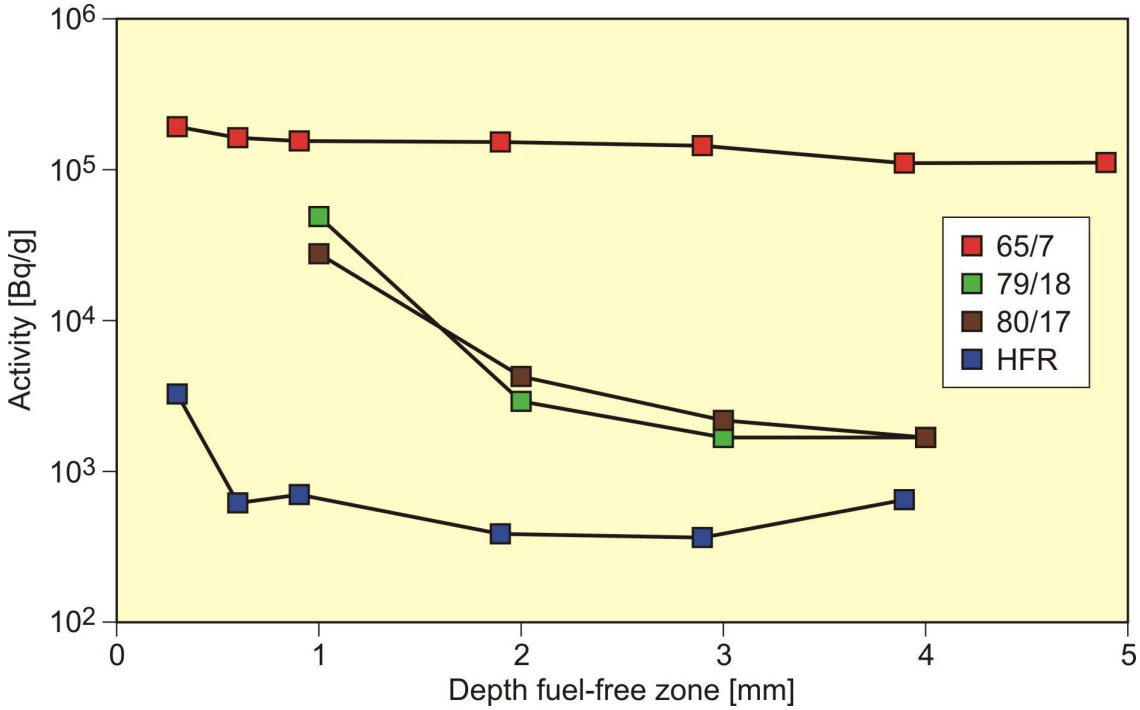

Figure 84 : Cs-137 activity profiles in the fuel-free zone prior to leaching [Duwe 1993a] (0 = sphere surface)

The leaching process at 90°C temperature and 13 MPa pressure exhibited two distinct phases: removal of surface activity on a short-term (~ weeks), and removal of activity from uranium contamination and defective/failed particles on a longer term. The experiments have shown that leaching rates did not significantly differ from those at higher pressures (30 MPa) in previous tests. Major differences in the release behaviour were given between BISO-coated and TRISO-coated fuel (see Fig. 85). TRISO fuel with the lower uranium contamination of the matrix showed a respective lower long-term release [Duwe 1993a].

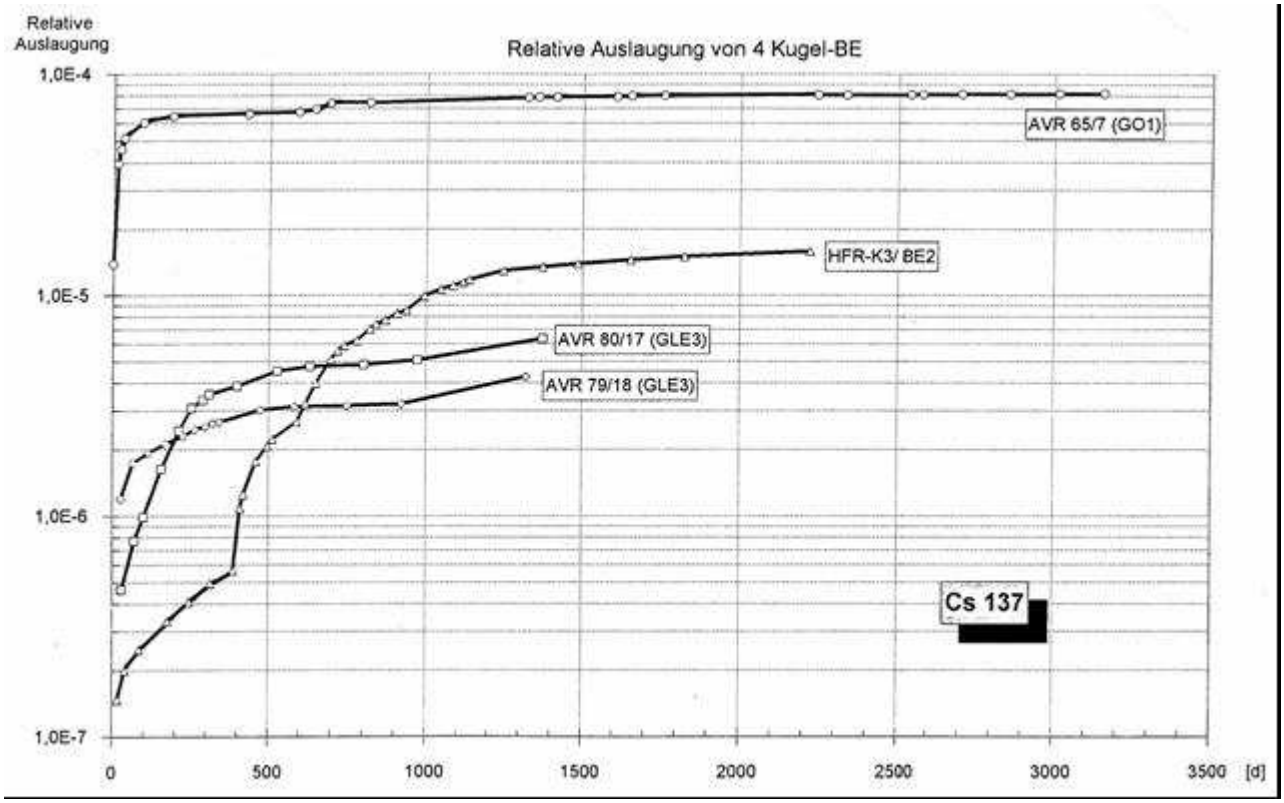

Figure 85 : Cs-137 fraction leached in Q-brine
[Duwe 1993a]

Apart from the above "integral" tests, further investigations are also concentrating on the understanding of the behaviour of the single components under respective conditions. These included the measurements of corrosion rates of the fuel materials matrix, pyrocarbon, silicon carbide, as well as the leaching of uranium and thorium from particle kernels. Table 42 summarizes the results from the corrosion experiments under various conditions based on an investigation time of 40 d. They show that corrosion rates for A3 matrix are higher at the presence of oxygen. The significant increase in an argon atmosphere under γ-radiation is due to the generation of radiolysis products. Respective results for pyrocarbon are similar to those for matrix material. Corrosion rates for silicon carbide were found to be strongly related to the corrosive environment and the temperature. Leaching tests with different types of unirradiated kernels in Ar at 90°C for more than one year exhibited lower dissolution rates for $(Th,U)O_2$ kernels by one to two orders of magnitude compared to UO_2 kernels [Fachinger 2006].

Table 42 : Corrosion rates of A3 matrix, pyrocarbon, and silicon carbide in aqueous solutions [Fachinger 2006]

Atmosphere	γ-radiation	Aqueous solution	Corrosion rate at 90°C [g/m²/d]			
			A3 matrix	Pyrocarbon	Non-irradiated silicon carbide	Irradiated silicon carbide
Argon	no	Brine	$1.7*10^{-8}$	$1.4*10^{-8}$		
		Water	$7.4*10^{-8}$			
Oxygen	no	Brine	$2.2\text{-}6.3*10^{-7}$	$9.3*10^{-8}$		
		Water	$1.3*10^{-6}$	$4.7*10^{-7}$		
Air	no	Brine	$1.8\text{-}2.8*10^{-7}$	$2.2*10^{-7}$	$1.7*10^{-5}$	$2.3*10^{-5}$
		Water	$6.2*10^{-7}$	$3.4*10^{-7}$	$9.6*10^{-6}$	$2.8*10^{-5}$
	?	Clay pore			$1.1\text{-}3.7*10^{-5}$	$8.3*10^{-5}$
Argon	yes	Brine	$6.2\text{-}12.8*10^{-6}$	$2.6*10^{-5}$		
		Water		$1.0\text{-}1.3*10^{-6}$		

5 CONCLUSIONS

5.1 Conclusions from the French Program

In a waste disposal condition, as an initial period of intrinsic evolution in a closed system, we usual consider 10,000 years to obtain an envelop value of the source term to take into account for the water ingress. Corrosion by water and the environment must then be assessed for the HTR particles or the graphite in the compacts. This will result in the rapid release of a fraction of radioelements directly or rapidly accessible to water, followed by progressive dissolution of the fissile compounds. In the case of HTR fuel, the radionuclide fraction likely to be released depends first of all on the particle integrity, i.e, mainly the SiC layer, and then on the corrosion mechanisms liable to damage it. Given the time scale involved, the potential consequences of changes within the particles likely to modify the source term must be evaluated between the moment of disposal and the initial water ingress. The main phenomena that must be considered are initially the stress changes on the SiC layer, then the possibility of additional diffusion in the internal layers together with physical and structural changes in the kernels. These stages are shown schematically in Fig. 86 with the objective of estimating the lifetime of the SiC layer and the changes that occur during this period in the internal layers.

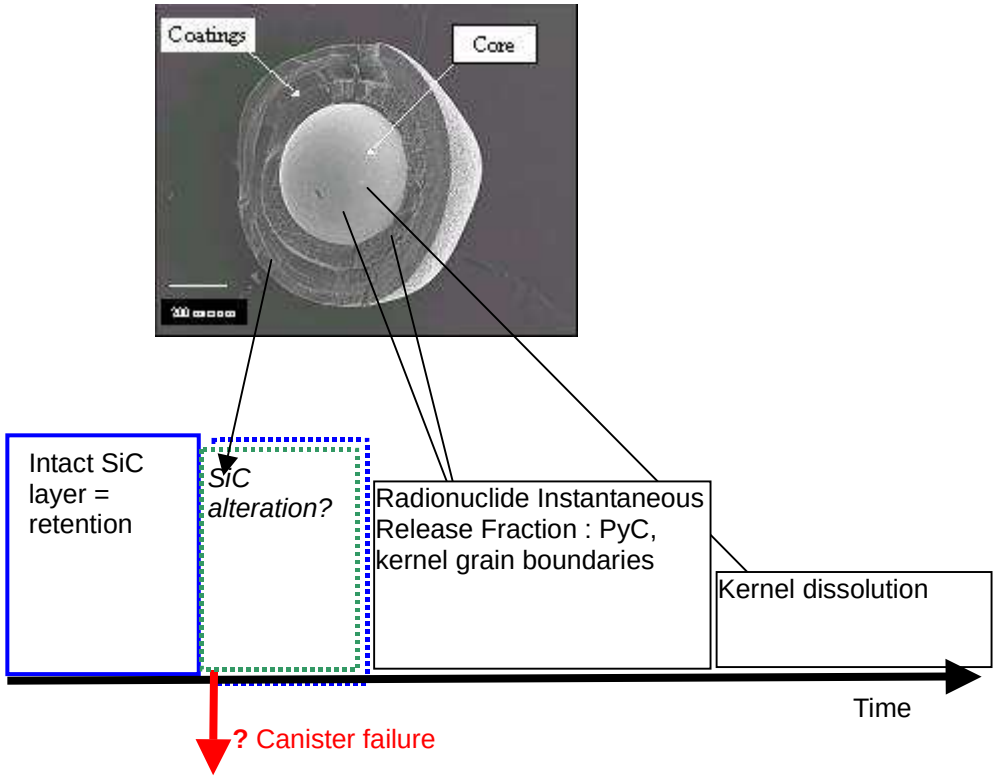

Figure 86 : Contributions to radionuclide release

5.2 Conclusions from the German Program

In Germany, two high temperature reactors were operated, the AVR test reactor in Jülich and the prototype reactor THTR – 300 in Hamm-Uentrop. Both were shut down, but considerable experience has been gained during their operating period.

The AVR reactor which was operated over 21 yrs until 1988 served particularly the purpose to test and qualify HTGR pebble fuel. In the course of operation, more than 290,000 spherical fuel elements of 15 different types and variants (carbide/oxide, BISO/TRISO, HEU/LEU) with more than 6 billion coated fuel particles were inserted into the core. The continuous measurements of coolant activities over the years has provided profound information on the performance of the various fuel types and particularly allowed the identification of failing coated particles and, in combination with comprehensive PIE on selected and randomly discharged fuel element specimens, the identification of poorer-quality fuel charges like GLE-1, which were responsible for an extremely high contamination level during their residence time in the core and beyond. On the other hand, the measurements also showed the steady improvement of fuel quality, e.g., the lower level of heavy metal contamination of 10^{-5} for the modern TRISO fuel (GLE-3/4) compared to the 10^{-3} level of the older BISO fuel.

In contrast, the THTR-300 was operated over 423 efpd based on one type of fuel with high-enriched uranium and BISO coated particles. Unlike AVR, the THTR operation was not designed for discharging fuel elements for the purpose of dedicated PIE. The information needed to characterize THTR fuel in terms of spent fuel has been achieved from the fuel element variant GO-THTR tested on a large scale in the AVR.

All fuel from both AVR and THTR has been stored in CASTOR casks (approx. 2000 balls each) and given to interim storage sites. In Germany, the spent HTGR fuel treatment of intermediate dry storage before transfer to a deep-mined salt dome repository, is presently the only accepted concept.

The total spent fuel from the two German HTGRs amounts to approximately 910,000 spheres with 32 % being from the AVR and 68 % from the THTR-300. The total activities for the year 2003 amount to $7.5*10^{16}$ Bq for the spent AVR fuel and $1.1*10^{17}$ Bq for the spent THTR fuel. The corresponding decay heat production is 6.2 kWt from all AVR fuel and 8.4 kWt from all THTR fuel.

A particular problem to be solved in connection with direct disposal of HTGR fuel is the C-14 activity requiring a decent and licenceable long-term concept. Methods need to be developed to treat the vast amounts of contaminated graphite.

Burnup analyses which have been extensively conducted with AVR fuel both in experimental and in simulation studies, allow specific statements on the inventories of heavy metal and transuranium isotopes, which then may lead to optimized boundary conditions for fuel cycles and the development of new fuel compositions for future HTGRs. It will help minimize the jeopardizing potential of spent fuel to be disposed. HTGR fuel allows very high burnups where, at some point, most of the fissionable material is transformed without further reprocessing. Furthermore the

investigation of partitioning methods will help to develop alternatives to direct disposal with the goal of reducing lifetime of the radioactive waste and reducing the proliferation risk.

Spherical fuel elements and coated particles, respectively, were also - and still are - investigated with respect to the conditions of disposal in salt mines. An excellent long-term chemical resistance was found for intact coated particles, whereas activity release from leaching in a brine is only possible from particles with defective coatings. Further and more precise efforts are also needed to investigate the long-term behaviour of the various HTGR fuel materials under the given geochemical conditions of a salt mine – or even other types of repositories not considered so far – in terms of dissolving processes and transformation to new phases with different properties and retention capabilities. Apart from experimental works, studies should also include efforts to simulate the spent fuel behaviour under long-term storage conditions.

Since a national infrastructure is no longer available, German activities need to be done in an international frame.

6 REFERENCES

AVR, AVR Atomversuchskraftwerk, 1. Quartalsbericht 1971 (1.1.1971 – 31.3.1971), Arbeitsgemeinschaft Versuchsreaktor, Düsseldorf, Germany (1971a).

AVR, AVR Atomversuchskraftwerk, 4. Quartalsbericht 1971 (1.10.1971 – 31.12.1971), Arbeitsgemeinschaft Versuchsreaktor, Düsseldorf, Germany (1971b).

AVR, AVR Atomversuchskraftwerk, 4. Quartalsbericht 1977 (1.10.1977 – 31.12.1977), Arbeitsgemeinschaft Versuchsreaktor, Düsseldorf, Germany (1977).

Bäumer R., Kalinowski I., Decommissioning Concept for the High Temperature Reactor THTR-300, Kerntechnik 56 (1991) No. 6 362-366 (1991b).

Bäumer R., Dietrich G., THTR Commissioning and Operating Experience, Energy 16 (1991) No. 1/2 59-70.

Ballagny A., Irradiation d'Éléments Combustibles pour Réacteurs à Haute Température, NT SECMRG/76/31 (1976).

Barr P., Everett M. R., Graham L. W., The Role of Irradiation Experiments in the Development of High Temperature Reactors, Dragon Report D.P. 794, Winfrith, UK (1972).

Baldwin C.A., Kania M.J., IMGA Examination of Set #4 Fuel under Project Work Statement FD-20, Report DOE-HTGR-88381 and ORNL/TM-11455, Oak Ridge National Laboratory, USA (1990).

Blanchard R., Cuerq A., Mesures des Gaz de Fission Contenus dans les Particules HTR, CR DMG n° 86/72, Département des Matériaux de Grenoble (1972).

Blanchard R., Guéguen A., Prouvé M., Expérience GF.4. Résultats des Examens Visuels et des Métrologies. CR DMG n°DR 06/77, Département des Matériaux de Grenoble (1977).

Blanchard R., et.al., Rapport de synthèse des irradiations GF1, GF2, GF3. Rapport DMG-DR-34/78 (1978).

Blanchard R., et.al., Experience GF6, Examen des Échantillons après Irradiation, CR DMG n° 120/80, Département des Matériaux de Grenoble (1980a).

Blanchard R., et.al., Experience GF7, Examen des Échantillons après Irradiation, CR DMG n° 136/80, Département des Matériaux de Grenoble (1980b).

Brinkmann U., et.al., Entsorgung des AVR-Versuchskraftwerks und Untersuchungen an abgebrannten Brennelementen für trockene Zwischenlagerung, Proc. Jahrestagung Kerntechnik, March 25-27, 1980, Berlin, Germany (1980) 497-500.

Brinkmann H.U., et.al., Contributions towards the Development of a Packaging Concept for the Final Disposal of Spent HTGR Pebble Bed Fuel, Nucl Eng Des 118 (1990) 107-113.

Brodda B.G., Merz E.R., Leachability of Actinides and Fission Products from Spent HTR Fuel, Radiochimica Acta 44/45 (1988) 3-6.

Bruet M., Thèse CNAM, Conservatoire National des Arts et Métiers (1972).

Bruet M., et.al., IAEA Specialist Meeting on Water Reactor Fuel Element Performance Computer Modelling, England, (1980).

Burck W., Engelstädter R., Untersuchungen von Oberflächenschäden (-Pelleffekt-) an bestrahlten kugelförmigen HTR-Brennelementen, FZJ Internal Report KFA-IRW-IB-22/77, Research Center Jülich, Germany (1977).

Burck W., Nachuntersuchungen an feuchten und verunreinigten AVR-Brennelementen, FZJ Internal Report KFA-IRW-IB-19/78, Research Center Jülich, Germany (1978).

Burck W., Krautwasser P., Datensatz zum Bestrahlungsverhalten von hochangereicherten (Th,U)-Mischoxid-Brennstoffteilchen mit HTI-Pyrokohlenstoffschicht (HTI-BISO-Partikeln), FZJ Internal Report KFA-IRW-IB-10/88, Research Center Jülich, Germany (1988).

Buttler R., Kernmaterialüberwachung beim rückholbaren Einlagerversuch mit verbrauchten AVR-Brennelementen, Proc. Status Seminar on „MAW- und HTR-BE-Versuchseinlagerung in Bohrlöchern“, held at Jülich, Germany, December 10-11, 1986, FZJ Report Jül-Conf-60, 187-200.

Cahier des Connaissances sur les Combustibles pour Réacteur Haute Température. Compte Rendu DMG n°DR 33/73, Département des Matériaux de Grenoble (1973).

(Cahier), Les Expériences d’Irradiation Française de Combustible HTR à Uranium Faiblement Enrichi (U.F.E.)” DMECN HTR 78-1304, France (1978).

Cautius W., et.al., Der Betrieb des Versuchskraftwerks AVR und die HTR-Entwicklung, ATW 19 (1974) 444-450.

Chapelot P., CEA past experience on high temperature reactors, NT SERI/LCSI/01/4038 (2001).

Chénebeau P., Pointud M.L., Instantaneous Fission Gas Release from UO_2 Kernels, 5th Meeting of the Dragon Project Quality Control Working Party at A.E.E, Oct 11-12, 1972, CR N° 81/72 (1972).

DEFRA, The 2004 UK Radioactive Waste Inventory, Defra Report DEFRA/RAS/05.002, Nirex Report N/090, (2005).

Derz H., et.al., Experiment HTA-8 the Determination of the Maximum Coolant Temperatures in the AVR Core, FZJ Internal Report KFA-HTA-IB-3/90, Research Center Jülich, Germany (1990).

Dietrich G., Hochtemperatur-Kernkraftwerk GmbH, Hamm, Germany, Personal Communication (2006).

DMECN, Les expériences d'irradiation française de combustible HTR à uranium faiblement enrichi, rapport DMECN HTR 78/1304, (1978).

DMG, Cahier des connaissances sur les combustibles pour réacteur haute température, CR DMG DR 33/73, (1973).

Duwe R., Münstermann H., Experimentelle Untersuchungen zum Freisetzungsverhalten von HTR-BE unter Trocken-Lagerbedingungen, FZJ Internal Report KFA-IRW-IB-7/80, Research Center Jülich, Germany (1980).

Duwe R., Müller H., Begleitende Messungen im AVR-Trockenlager – Freisetzung gasförmiger Radionuklide – Temperaturverlauf, FZJ Internal Report KFA-IRW-IB-3/86, Research Center Jülich, Germany (1986).

Duwe R., Schröder R., Auslaugverhalten von HTR-Brennelementen und -Brennstoffteilchen in Salzlauge, FZJ Internal Report KFA-IWE-IB-1/93, Research Center Jülich, Germany (1993a).

Duwe R., Schröder R., Temperatur und Dosisleistung abgebrannter HTR-Brennelemente in Transport- und Lagerbehältern (GNS-Castor, TN-AVR-2), FZJ Internal Report KFA-IRW-IB-2/93, Research Center Jülich, Germany (1993b).

Eichenbaum C., Interviews d'experts des combustibles HTR, NT DER/STR/LCFR/01/006 (2001).

El-Masry M.A.A., El-Sayed A.A., Distribution on Fission Products in the Fuel Free Zone of AVR Irradiated Fuel Elements, FZJ Internal Report KFA-IRW-IB-10/89, Research Center Jülich, Germany (1989).

Fachinger J., et.al., Behaviour of Spent HTR Fuel Elements in Aquatic Phases of Repository Host Rock Formations, Nucl Eng Des 236 (2006) 543-554.

Falta G., Strigl A., Zeger J., Untersuchung der Schwermetallgehalte an fünf abgebrannten AVR-Brennelementen, Report OEFZS-A-2749, Research Center Seibersdorf, Austria (1993).

Flossdorf T., Keramographische Nachuntersuchung an AVR-Brennelementen der Gruppen 71 und 72, FZJ Technical Note IRW-TN-57/85, Research Center Jülich, Germany (1985).

Fonquernie S. and al, CEA and AREVA R&D on HTR Fuel Fabrication & Presentation of the GAIA Experimental Manufacturing Line, HTR 2004, China.

Förthmann R., et.al., Chemical Behavior and Improved Retention of Fission Products in Irradiated HTGR Fuels, IAEA-SM-190/35 (1975).

Ganser B., et.al., FuE-Arbeiten zur Endlagerung von HTR-Brennelementen, Proc. Status Seminar about Works on High Temperature Reactor Fuel Elements, Graphite, and Disposal, held at Jülich, Germany, May 18, 1987, FZJ Report Jül-Conf-61, 147-160.

Gontard R., Keramographische Nachuntersuchungen an AVR-Brennelementen, Teil 1: Gepresste karbidische Brennelemente (GK-BE), Technical Note HBK-TN-19/84, Research Center Jülich, Germany (1984a).

Gontard R., Keramographische Nachuntersuchungen an AVR-Brennelementen, Teil 2: Gepresste oxidische Brennelemente (GO1, Original AVR-BE), Technical Note HBK-TN-19/84, Research Center Jülich, Germany (1984b).

Gossé S., Gueneau C., Chatillon C., Chatain S., Critical Review of Carbon Monoxide Pressure Measurements in the Uranium-Carbon-Oxygen Ternary System, J Nucl Mat 352 (2006) 13-21.

Gottaut H., Krüger K., Results of Experiments at the AVR Reactor, Nucl Eng Des 121 (1990) 143-153.

Graham L. W., et.al., HTR Fuel Development and Testing in the Dragon Project, Dragon Report D.P. 885, Winfrith, UK (1974).

Groos E., et.al., Fission product Release from Coated Particles Embedded in Spherical Fuel Elements for High-Temperature Reactors, Nuc Tech 35 (1977) 509-515.

HKG, The Commissioning of the THTR 300, A Performance Report, Publication No. HKG 002 89 E, Hochtemperatur-Kernkraftwerk GmbH, Hamm, Germany (1989).

Huddle R.A.U., Conde J. F. G., Graham L. W., High Temperature Reactor Materials, Proc. BNES Symposium on High Temperature Reactors and the Dragon Project, held in London, UK, May 24, 1966, Dragon Report D.P. 425 Part III, Winfrith, UK (1966), Paper 9.

Huddle R.A.U., Jones K.W., Mayr K., The Influence of Fabrication Parameters on the Incidence of Spearhead Attack in Coated Particle Fuel, Dragon Report D.P. 652, Winfrith, UK (1969).

Huschka H., Leischner E., Rind W., Freier Schwermetallgehalt in Hochtemperaturbrennelementen, Zielsetzung und erreichter Stand, Proc. Reaktortagung, April 4-7, 1978, Hannover, Germany (1978) 628-631.

Janvier J.C., et.al., The Behavior of Pyrocarbon Fuel Coatings at High Fast Neutron Dose, CR DMG n° 56/73, Département des Matériaux de Grenoble (1973).

Kirch N., Brinkmann H.U., Brücher P.H., Storage and Final Disposal of Spent HTR Fuel in the Federal Republic of Germany, Nucl Eng Des 121 (1990) 241-248.

Kleine-Tebbe A., Röllig K., Schmidt G., Bestimmung von Kugelbruchraten im THTR, HRB Technical Note (1988).

Knizia K., Der THTR-300 – Eine vertane Chance?, ATW 47 (2002) No. 2, 110-117.

Kovacs W.J., Blanchard R., Pointud M.L., Post Irradiation Examination of Capsules GF-1, GF-2, GF-3; - General Atomic Project 6400 (1980).

Krumbach H., Duwe R., Rödig M., Handling and Behaviour of AVR Fuel Elements for Interim Storage, HOTLAB 2004, Halding, Norway, September 2004.

Lefevre R., Contamination in the Coating of Fuel Particles, Dragon Report D.P. 633, Winfrith, UK (1969).

Marin F., Synthèse des Expériences Critiques César II et Marius III avec Combustible HTR, NT DER/SERSI/LECC/00/4022 (2000).

Marnet C., et.al., Decommissioning of the AVR Reactor Concept for the Total Dismantling, IAEA TCM on Gas Cooled Reactor Decommissioning, Fuel Storage and Waste Disposal, held at Jülich, Germany, September 8-10, 1997.

Merz E., Brücher H., Halaszovich S., Lösung der Entsorgungsfrage beim Hochtemperatur-reaktor, in: Fortschritte in der Energietechnik, Monographien des Forschungszentrums Jülich, Germany, Vol. 8 (1993) 336-348.

Miller G.K, et.al., An Evaluation of the Effects of SiC Layer Thinning on Failure of TRISO-Coated Fuel Particles, J Nucl Mat 355 (2006) 150-162.

Millet P., Combustible RHT – Connaissances CEA, NT SESC/01/001 (2001).

Morier F., et.al., Les Assemblages Critiques César et Marius, BIST n° 168 (1972).

Nabielek H., et al., Development of Advanced HTR Fuel Elements", Nucl Eng Des 121 (1990) 199-210.

Neubacher, Die Brennelementbilanz des AVR, Technical Note H6-N7, Arbeitsgemeinschaft Versuchsreaktor, Düsseldorf, Germany (1991).

Niephaus D., Referenzkonzept zur direkten Endlagerung von abgebrannten HTR-Brennelementen in CASTOR THTR/AVR Transport- und Lagerbehältern, FZJ Report Jül-3734, Research Center Jülich, Germany (2000).

Nucleonics Week, Decommissioning Costs for German Pebble Bed Reactor Escalating, Issue of July 4, 2002, p. 7.

Petti D.A., Homan F.J., Coated Particle Fuel Behavior under Irradiation, HTR Class, held at Cadarache, France, Nov 4-8, 2002.

Plätzer S., Mielisch M., Unloading of the Reactor Core and Spent Fuel Management of THTR-300, IAEA-TCM on Gas Cooled Reactor Decommissioning, Fuel Storage and Waste Disposal, held at Jülich, Germany, September 8-10, 1997.

Pohl P., AVR Decommissioning Achievements and Future Programme, IAEA TCM on Gas Cooled Reactor Decommissioning, Fuel Storage and Waste Disposal, held at Jülich, Germany, September 8-10, 1997.

Pohl P., Short Review of Lessons Learned from AVR Mass Fuel Testing, HTR-TN International HTR Fuel Seminar, Brussels, Belgium, February 1-2, 2001.

Pohl P., Betrachtung der aufgelaufenen Buchabweichungen nach Abschluss der bisherigen Brennelement- und Brennstoffbuchführung, Eine Geschichte der Brennelementerkennung am AVR, AVR Technical Note E-6509, Arbeitsgemeinschaft Versuchsreaktor, Düsseldorf, Germany (2002).

Pohl P., Endlagergerichtete CASTOR-Dokumentation: Bestimmung des Nuklidinventars der AVR-Brennelemente nach einem Referenzbrennelement-Verfahren, AVR Technical Note E-7562 (corrected version), Arbeitsgemeinschaft Versuchsreaktor, Düsseldorf, Germany (2003a).

Pohl P., Nuklidaktivitäten der bestrahlten AVR-Brennelemente zum Jahresende 2003, AVR Technical Note E-8039, Arbeitsgemeinschaft Versuchsreaktor, Düsseldorf, Germany (2003b).

Pollitt N., The Corrosion Behaviour of Coated Fuel Particles, Dragon Report D.P. 395, Winfrith, UK (1968).

Price M.S.T., Gough J. R. G., Horsley G.W., Fuel Element Fabrication for the Dragon Reactor Experiment, Proc. BNES Symposium on High Temperature Reactors and the Dragon Project, held in London, UK, May 24, 1966, Dragon Report D.P. 425 Part III, Winfrith, UK (1966), Paper 10.

Price M.S.T., Smith E., Safety Aspects of the Replacement Elements in the Second Charge of the Dragon Reactor, Dragon Report D.P. 489, Winfrith, UK (1966a).

Price M.S.T., Ashworth F.P.O., Graham L.W., Fuel Element Fabrication, Proc. Dragon-THTR Assessment Meeting, held at Brussels, Belgium, May 22-24, 1967, Dragon Report D.P. 475 Part II, Winfrith, UK (1967), Paper 3.2.

Howard R. M., Price M.S.T., Shepherd L.R. (Eds.), A Summary & Evaluation of the Achievements of the Dragon Project & Its Contribution to the Development of the High Temperature Reactor, Dragon Report D.P. 1000, Winfrith, UK (1978).

Ragoss H., Stand der Bestrahlungserprobung gepresster kugelförmiger Brennelemente, FZJ Internal Report KFA-IRW-IB-15/75, Research Center Jülich, Germany (1975).

Ragoss H., Bestrahlungsexperiment R2-K3, Referenzerprobung von Brennelementen für den THTR-300 MWel, Report EUR 5364, Kommission der Europäischen Gemeinschaften, Luxembourg (1977).

Rapport DMG DR 34/78, Département des Matériaux de Grenoble (1978).

Rebmann A., Duwe R., Das Belastungsverhalten von HTR-Brennelementen im salinären Endlager, FZJ Internal Report KFA-IRW-IB-3/88, Research Center Jülich (1988).

Röllig K., Release of Rare Fission Gases from Spherical Fuel Elements with Coated Fuel Particles, Nuc Tech 35 (1977) 516-523.

Röllig K., C14-Freisetzung des AVR, HRB Technical Note HBK-5125-BF-GHRA 000988 (1984).

Röllig K., et.al., Entsorgung von Hochtemperaturreaktoren, Proc. Status Seminar about Works on High Temperature Reactor Fuel Elements, Graphite, and Disposal, Jülich, Germany, May 18, 1987, FZJ Report Jül-Conf-61, Research Center Jülich, Germany (1987) 109-134.

Röllig K., C-14 Freisetzung von abgebrannten THTR-BE, HRB Technical Note 413-211-BF3521, Mannheim, Germany (1989).

Röllig K., The THTR Coolant Gas Activity, an Indicator of Fuel Performance Behaviour, Proc. IAEA Specialists' Meeting, Oak Ridge, USA, IWGGCR/25, International Atomic Energy Agency, Vienna, Austria (1991) 99-108.

Röllig K., THTR-300 Fuel Elements, Production and Operation Experiences, Proc 2nd Soviet/German Seminar on Fuel and Graphite for HTR, July 8-12, 1991, Jülich, Germany, Internal Report HTA-IB-3/91, Research Center Jülich, Germany, 435-448 (1991b).

Rose K.S.B., Hauser G.P., The Irradiaion Performance of Triplex Coated (Pyrocarbon/SiC/ Pyrocarbon) Fuel Particles, Dragon Report D.P. 400, Winfrith, UK (1966).

Schmidt P.C., Alternativen zur Verminderung der C-14-Emission bei der Wiederaufarbeitung von HTR-Brennelementen, FZJ Report Jül-1567, Research Center Jülich, Germany (1979).

Schröder G., et.al., Aspekte der Entsorgung des THTR-300, in: Fortschritte in der Energietechnik, Monographien des Forschungszentrums Jülich, Germany, Vol. 8 (1993) 301-308.

Tang C., et.al., Fuel Irradiation of the First Batches Produced for the Chinese HTR-10, Nucl Eng Des 236 (2006) 107-113.

Wawrzik U., Ivens G., Operational Monitoring of the Release Behaviour of the AVR Core, Proc. IAEA Specialists' Meeting on Fission Product Release and Transport in Gas-Cooled Reactors, Oct. 22-25, 1985, Berkeley, United Kingdom, Summary Report IWGGCR/13 (1985)15-26.

Werner H., Darstellung der Funktionen von Isotopenmengen/BE ausgewählter Isotope and Abbrand (fima) sowie Fluenz/BE und fima als Polynome, AVR Technical Note from May 23, 1984, Arbeitsgemeinschaft Versuchsreaktor, Düsseldorf, Germany (1984).

Werner H., Nuclear Build-up of Plutonium Isotopes in HTR Fuel Elements, A Comparison between Computed Prediction and Chemical Analysis, Nucl Eng Des 170 (1997) 147-164.

Wimmers M., Das Verhalten kugelförmiger HTR-Brennelemente bei der Massenerprobung im AVR-Reaktor, AVR Report, Arbeitsgemeinschaft Versuchsreaktor, Düsseldorf, Germany (1977).

Wolf J., Endlagerung verbrauchter Brennelemente aus dem AVR-Versuchskernkraftwerk im Salzbergwerk Asse, FZJ Report Jül-1163, Research Center Jülich, Germany (1975).

Wolf L., et.al., HTR-2000, Ein praxiserprobtes HTR-Anlagenmodell für den AVR-Reaktor, in: Fortschritte in der Energietechnik, Monographien des Forschungszentrums Jülich, Germany, Vol. 8 (1993) 355-364.

York J., Hick H., Metallic Fission Product Behaviour in Dragon Fuel Elements as Observed from Gamma-Spectrometric Examination, Dragon Report D.P. 874, Winfrith, UK (1974).

Ziermann E., Ivens G., Abschlussbericht über den Leistungsbetrieb des AVR-Versuchs-kernkraftwerkes, FZJ Report Jül-3448, Research Center Jülich, Germany (1997).